

SSC MASTER COPY

SSC-318

Executive Director
Ship Structure Committee
U.S. Coast Guard (G-MI/R)
2100 Second Street, SW
Washington, DC 20593-0000

**FATIGUE CHARACTERIZATION OF
FABRICATED SHIP DETAILS FOR DESIGN**



This document has been approved
for public release and sale; its
distribution is unlimited.

SHIP STRUCTURE COMMITTEE

1983

SHIP STRUCTURE COMMITTEE

The SHIP STRUCTURE COMMITTEE is committed to organize a research program to improve the hull structures of ships and other marine structures by an extension of knowledge pertaining to design, materials and methods of construction.

RADM Clyde T. Lusk, Jr., USCG (Chairman)
Chief, Office of Merchant Marine
Safety
U.S. Coast Guard Headquarters

Mr. J. G. Batts
Deputy Assistant Administrator for
Commercial Development
Maritime Administration

Mr. P. M. Palermo
Executive Director
Ship Design & Integration
Directorate
Naval Sea Systems Command

Mr. J. W. Gregory
Chief, Research & Development Staff
of Planning & Assessment
U.S. Maritime Survey

Mr. W. N. Hannan
Vice President
American Bureau of Shipping

Mr. Robert M. Allen
Chief Engineering Officer
Military Sealift Command

Lcdr D. B. Anderson, U.S. Coast Guard (Secretary)

SHIP STRUCTURE SUBCOMMITTEES

The SHIP STRUCTURE SUBCOMMITTEES assist the Ship Structure Committee on technical matters by providing technical consultation for the determination of goals and objectives of this program, and by evaluating and improving the results in terms of design, materials, construction and maintenance.

U.S. COAST GUARD

Mr. J. B. HEIK
Mr. J. W. BROWN
Mr. J. W. BROWN
Mr. J. W. BROWN

NAVAL SEA SYSTEMS COMMAND

Mr. J. W. BROWN
Mr. J. W. BROWN
Mr. J. W. BROWN
Mr. J. W. BROWN
Mr. J. W. BROWN
Mr. J. W. BROWN

MARITIME ADMINISTRATION

Mr. J. W. BROWN
Mr. J. W. BROWN
Mr. J. W. BROWN
Mr. J. W. BROWN

NATIONAL ACADEMY OF SCIENCES
COMMITTEE ON MARINE STRUCTURES

Mr. J. W. BROWN - CHAIRMAN
Mr. J. W. BROWN - VICE CHAIRMAN

SOCIETY OF NAVAL ARCHITECTS
MARINE ENGINEERS

Mr. J. W. BROWN - CHAIRMAN
Mr. J. W. BROWN - VICE CHAIRMAN

STEERING RESEARCH COUNCIL

Mr. J. W. BROWN - CHAIRMAN

INTERNATIONAL MARITIME ORGANIZATION

Mr. J. W. BROWN - CHAIRMAN

INTERNATIONAL MARITIME FEDERATION

Mr. J. W. BROWN - CHAIRMAN

INTERNATIONAL MARITIME SERVICE

Mr. J. W. BROWN - CHAIRMAN

INTERNATIONAL SHIP STRUCTURES CONGRESS

Mr. J. W. BROWN - CHAIRMAN

INTERNATIONAL SHIP STRUCTURE INSTITUTE

Mr. J. W. BROWN - CHAIRMAN

STATE UNIVERSITY OF NY MARITIME COLLEGE

Mr. J. W. BROWN - CHAIRMAN

U.S. COAST GUARD ACADEMY

Mr. J. W. BROWN - CHAIRMAN

U.S. MARINE ACADEMY

Mr. J. W. BROWN - CHAIRMAN

U.S. MERCHANT MARINE ACADEMY

Mr. J. W. BROWN - CHAIRMAN

SSC-318

Member Agencies:

*United States Coast Guard
Naval Sea Systems Command
Military Sealift Command
Maritime Administration
United States Geological Survey
American Bureau of Shipping*



An Interagency Advisory Committee
Dedicated to Improving the Structure of Ships

Address Correspondence to:

Secretary, Ship Structure Committee
U.S. Coast Guard Headquarters, (G-M/TP 13)
Washington, D.C. 20593

13 JAN 1984

SR-1257

This report presents a fatigue design procedure for ship details that should help to eliminate cracks in details. It is an important part of the Ship Structure Committee's overall program to provide information on sound and economical details for ship structures.

A handwritten signature in black ink, appearing to read 'Clyde F. Luscomb Jr.', is written over the typed name.

Clyde F. Luscomb Jr.
Rear Admiral, U.S. Coast Guard
Chairman, Ship Structure Committee

1. Report No. SSC-318		2. Government Accession No.		3. Recipient's Catalog No.	
4. Title and Subtitle Fatigue Characterization of Fabricated Ship Details for Design				5. Report Date August 1982	
				6. Performing Organization Code	
7. Author(s) W. H. Munse, Thomas W. Wilbur, Martin L. Tellalian, Kim Nicoll and Kevin Wilson				8. Performing Organization Report No. SR-1257	
				10. Work Unit No. (TRAIS)	
9. Performing Organization Name and Address Department of Civil Engineering University of Illinois at Urbana-Champaign 208 N. Romine Street Urbana, IL 61801				11. Contract or Grant No. DOT-CG-823889A	
				13. Type of Report and Period Covered Final Technical Report	
12. Sponsoring Agency Name and Address U.S. Coast Guard Office of Merchant Marine Safety Washington, DC 20593				14. Sponsoring Agency Code	
				15. Supplementary Notes Project sponsored by the Ship Structure Committee, Washington, D. C.	
16. Abstract <p>Fatigue cracking has for many years been responsible for extensive and costly ship repair work. This investigation provides a simple fatigue design procedure that will help to minimize such cracking in future ships. The design procedure provides for (a) a large variety of ship details, (b) the basic fatigue resistance of these various welded details, (c) a reliability factor (factor of safety) that accounts for the many uncertainties that exist in the fatigue data, the predicted loading history, and in the associated analyses and (d) the random nature of the loading history to which a ship may be subjected during its lifetime.</p>					
17. Key Words Fatigue, Ship Structure Details, Design, Reliability, Loading History, Random Loading, Fatigue Data, Fatigue Tests.			18. Distribution Statement Document is available to the U.S. public through the National Technical Information Service, Springfield, VA. 22161		
19. Security Classif. (of this report) Unclassified		20. Security Classif. (of this page) Unclassified		21. No. of Pages 207	22. Price

METRIC CONVERSION FACTORS

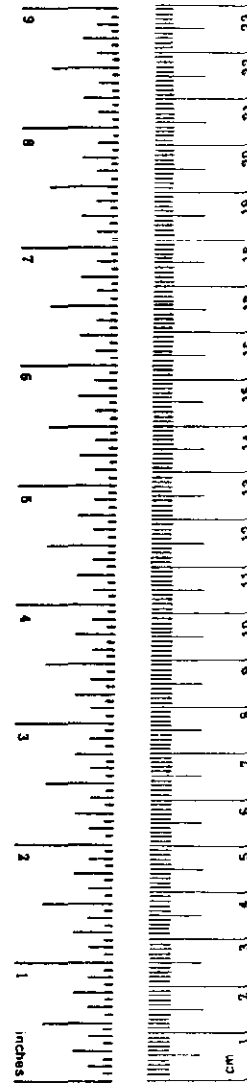
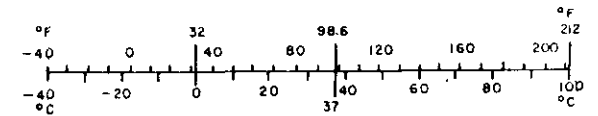
Approximate Conversions to Metric Measures

Symbol	When You Know	Multiply by	To Find	Symbol
LENGTH				
in	inches	*2.5	centimeters	cm
ft	feet	30	centimeters	cm
yd	yards	0.9	meters	m
mi	miles	1.6	kilometers	km
AREA				
in ²	square inches	6.5	square centimeters	cm ²
ft ²	square feet	0.09	square meters	m ²
yd ²	square yards	0.8	square meters	m ²
mi ²	square miles	2.6	square kilometers	km ²
	acres	0.4	hectares	ha
MASS (weight)				
oz	ounces	28	grams	g
lb	pounds	0.45	kilograms	kg
	short tons (2000 lb)	0.9	tonnes	t
VOLUME				
tsp	teaspoons	5	milliliters	ml
Tbsp	tablespoons	15	milliliters	ml
fl oz	fluid ounces	30	milliliters	ml
c	cups	0.24	liters	l
pt	pints	0.47	liters	l
qt	quarts	0.95	liters	l
gal	gallons	3.8	liters	l
ft ³	cubic feet	0.03	cubic meters	m ³
yd ³	cubic yards	0.76	cubic meters	m ³
TEMPERATURE (exact)				
°F	Fahrenheit temperature	5/9 (after subtracting 32)	Celsius temperature	°C

* 1 in = 2.54 (exactly). For other exact conversions and more detailed tables, see NBS Misc. Publ. 286, Units of Weights and Measures, Price \$2.25, SD Catalog No. C13.10.286.

Approximate Conversions from Metric Measures

Symbol	When You Know	Multiply by	To Find	Symbol
LENGTH				
mm	millimeters	0.04	inches	in
cm	centimeters	0.4	inches	in
m	meters	3.3	feet	ft
m	meters	1.1	yards	yd
km	kilometers	0.6	miles	mi
AREA				
cm ²	square centimeters	0.16	square inches	in ²
m ²	square meters	1.2	square yards	yd ²
km ²	square kilometers	0.4	square miles	mi ²
ha	hectares (10,000 m ²)	2.5	acres	
MASS (weight)				
g	grams	0.035	ounces	oz
kg	kilograms	2.2	pounds	lb
t	tonnes (1000 kg)	1.1	short tons	
VOLUME				
ml	milliliters	0.03	fluid ounces	fl oz
l	liters	2.1	pints	pt
l	liters	1.06	quarts	qt
l	liters	0.26	gallons	gal
m ³	cubic meters	35	cubic feet	ft ³
m ³	cubic meters	1.3	cubic yards	yd ³
TEMPERATURE (exact)				
°C	Celsius temperature	9/5 (then add 32)	Fahrenheit temperature	°F



METRIC CONVERSION FACTORS

TABLE OF CONTENTS

Chapter	Page
1. INTRODUCTION	1
1.1 Fatigue in Welded Ship Design	1
1.2 Objective and Scope of Investigation	1
1.3 References	3
2. STRUCTURAL FATIGUE	4
2.1 Laboratory Studies	4
2.2 Principal Fatigue Factors	4
Geometry	4
Stresses	7
Material	9
2.3 Fatigue S-N Relationships	9
2.4 References	11
3. FATIGUE BEHAVIOR OF WELDED DETAILS	13
3.1 Mean Fatigue Resistance - Fatigue Details	13
3.2 Effect of Mean Stress	16
3.3 Effects of Residual Stresses	18
3.4 Effect of Material	18
3.5 Evaluation of Variability in Fatigue Life	20
3.6 References	20
4. FATIGUE DESIGN	24
4.1 Current Fatigue Design Criteria	24
4.2 References	27
5. SHIP STRUCTURE - DETAILS AND ASSEMBLIES	29
5.1 Classification of Ship Details	29
5.2 Catalog of Welded Ship Structure Details and Assemblies	30
5.3 Local Fatigue Details	30
5.4 Fatigue Cracking in Ship Details	38
5.5 References	41
6. SHIP LOADING HISTORIES	42
6.1 Ship Loads	42

TABLE OF CONTENTS (continued)

Chapter	Page
6.1.1 Low Frequency Wave-Induced Loading (Quasi-Static)	42
6.1.2 High Frequency Loading (Dynamic)	43
6.1.3 Still Water Loading	43
6.1.4 Thermal Loading	46
6.2 Measurement of Ship Response	46
6.3 Ship Loading Stress Histories	46
6.3.1 Low Frequency Wave-Induced Load Histories	46
6.3.2 Complete Stress Histories	50
6.4 Selection of Probability Distributions to Describe Ship Loading Histories	50
6.4.1 Probability Distributions	54
6.4.2 Comparison of Probability Distributions with Long-Term Loading Histories	57
6.5 References	62
7. DEVELOPMENT OF SHIP STRUCTURE FATIGUE DESIGN CRITERIA	64
7.1 S-N Relationships	64
7.2 Uncertainty - Coefficient of Variation	65
7.3 Reliability Factor	69
7.4 Variable Loading - Random Load Factor	75
7.5 Design Procedure - Examples	85
7.6 References	92
8. SUMMARY AND CONCLUSIONS	96
9. ACKNOWLEDGEMENTS	97
APPENDICES	
A. CATALOG OF SHIP DETAILS AND ASSEMBLIES	99
References	126
B. FATIGUE PROPERTIES OF LOCAL FATIGUE DETAILS	127
C. EXAMPLES OF CRACKING IN SHIP STRUCTURE DETAILS	153
References	167
D. DETERMINATION OF WEIBULL DISTRIBUTION TO FIT SL-7 SCRATCH GAGE DATA	169
D.1 Determination of Weibull Parameters k and w	170
D.2 Estimation of S_{10-8} for Weibull Distribution	173
E. DERIVATION OF $E(S^m)$ AND ξ	175
E.1 Weibull Distribution	176

TABLE OF CONTENTS (continued)

Chapter	Page
E.2 Exponential Distribution	178
E.3 Rayleigh Distribution	178
E.4 Shifted Exponential Distribution	179
E.5 Lognormal Distribution	182
E.6 Beta Distribution	185
E.7 References	186
F. REPORT OF FATIGUE TEST, DETAILS 21, 30A, 51 AND 52	187

LIST OF TABLES

Table	Page
3.1 MEAN FATIGUE STRESS RANGE FOR LOCAL FATIGUE DETAILS IN FIGURE 3.1 (CONSTANT CYCLE - 0.50 RELIABILITY)	15
3.2 FATIGUE BEHAVIOR OF VARIOUS STEELS	19
5.1 CRACKED FATIGUE DETAILS AND DATA AVAILABILITY	39
5.2 SUMMARY OF DATA FOR 12 DETAIL FAMILIES	40
6.1 CHARACTERISTICS OF SHIPS IN DRY CARGO VESSEL PROGRAM	47
6.2 CHARACTERISTICS OF VESSELS IN LARGE TANKER AND BULK CARRIER PROGRAM	48
6.3 CHARACTERISTICS OF <u>SEA-LAND McLEAN</u> (TYPICAL OF VESSELS IN SL-7 PROGRAM).	49
6.4 PROPERTIES OF PROBABILITY DISTRIBUTIONS INVESTIGATED	55
6.5 SHIP LOADING HISTORIES COMPARED WITH WEIBULL DISTRIBUTIONS	58
7.1 SUMMARY OF UNCERTAINTIES IN FATIGUE PARAMETERS	66
7.2 CORRELATION OF APPROXIMATION WITH WEIBULL DISTRIBUTION	72
7.3 RELIABILITY FACTORS - R_F	76
7.4 EXPRESSIONS FOR $E(S^m)$ AND ξ FOR PROBABILITY DISTRIBUTIONS IN TERMS OF S_0 OR $S_{10^{-8}}$ STRESS RANGE	84
7.5 TABLE OF RANDOM LOAD FACTORS FOR WEIBULL DISTRIBUTED LOADING	86
7.6 DESIGN PROCEDURE	87
7.7 SUMMARY OF RELIABILITY FACTORS, R_F , FOR LOCAL FATIGUE DETAILS	88
7.8 FATIGUE DESIGN STRESS RANGES FOR BEAM BRACKET 1A1	94
B.1 MEAN FATIGUE STRENGTH FOR RANGE OF FATIGUE DETAILS IN FIG. B.1	128

LIST OF TABLES (CONTINUED)

Table		Page
D.1	TABLE OF WEIBULL SHAPE PARAMETER VALUES AND CORRESPONDING COEFFICIENTS OF VARIATION	172
F.1	RESULTS OF FATIGUE TESTS ON DETAIL 21	195
F.2	RESULTS OF FATIGUE TESTS ON DETAIL 30A	196
F.3	RESULTS OF FATIGUE TESTS ON DETAILS 51 AND 52	197

LIST OF FIGURES

Figure		Page
2.1	WELDED SPLICES SHOWING LARGE DIFFERENCE IN FATIGUE RESISTANCE	6
2.2	BASIC S-N RELATIONSHIP FOR FATIGUE	8
2.3	FATIGUE DIAGRAM OF CONSTANT-LIFE CURVES	8
2.4	FATIGUE RESISTANCE OF A WELDMENT SUBJECTED TO VARIABLE LOADINGS	10
3.1	STRUCTURAL DETAILS PROVIDED IN AISC FATIGUE PROVISIONS	14
3.2	FATIGUE DIAGRAM FOR VARIOUS DETAILS AT STRESS RATIOS OF -1, 0, and +1/2	17
3.3	DISTRIBUTION OF FATIGUE LIFE AT A GIVEN STRESS LEVEL	21
3.4	VARIABILITY IN FATIGUE RESISTANCE OF STRUCTURAL FATIGUE DETAILS	22
4.1	FORM OF EARLY FATIGUE DESIGN RELATIONSHIPS BASED ON TEST DATA	25
4.2	COMPARISON OF VARIOUS DESIGN STRESSES AT 2,000,000 CYCLES FOR LONGITUDINAL LOAD-CARRYING FILLET WELDED JOINTS	26
5.1	DETAIL CLASSIFICATIONS	31
5.2	EXAMPLE FROM CATALOG OF BEAM BRACKETS DETAILS, FAMILY NO. 1	34
5.3	EXAMPLES OF RELATIONSHIP BETWEEN SHIP STRUCTURE DETAILS AND LOCAL FATIGUE DETAILS	35
6.1	TYPICAL RECORD OF MIDSHIP STRESS VARIATION, <u>M. V. FOTINI L</u> , SHOWING FILTERED WAVE-INDUCED AND DYNAMIC STRESSES	44
6.2	TYPICAL VOYAGE VARIATION OF MIDSHIP VERTICAL BENDING STRESS, <u>R. G. FOLLIS</u>	45
6.3	COMPARISON OF STRESS HISTOGRAM FOR ONE TYPICAL RECORD WITH IDEAL RAYLEIGH CURVE, <u>WOLVERINE STATE</u>	49

LIST OF FIGURES (CONTINUED)

Figure		Page
6.4	LONG-TERM DISTRIBUTION OF STRESSES IN ACTUAL SERVICE	51
6.5	LONG-TERM TRENDS OF STRESS OBTAINED FROM HISTOGRAMS FOR FOUR SHIPS AND COMPUTED FROM RMS VALUES	51
6.6	FATIGUE LOADING OF BOTTOM AND DECK STRUCTURE	52
6.7	HISTOGRAM FROM SL-7 SCRATCH GAGE DATA	53
6.8	SHAPES OF PROBABILITY DENSITY FUNCTIONS	56
6.9	LONG-TERM STRESS DISTRIBUTIONS BY DIFFERENT METHODS	59
6.10	LOADING HISTORIES OF LARGE TANKERS, BULK CARRIERS AND DRY CARGO VESSELS COMPARED WITH WEIBULL	60
6.11	SL-7 SCRATCH GAGE DATA WITH CORRESPONDING WEIBULL DISTRIBUTION	61
7.1	VALUES OF GAMMA FUNCTION	71
7.2	RELATIONSHIP BETWEEN k AND Ω_N AS GIVEN BY EQUATION 7.8	72
7.3	RELATIONSHIP OF FATIGUE LIFE FACTOR AND THE UNCERTAINTY IN FATIGUE LIFE FOR VARIOUS PROBABILITIES OF FAILURE	74
7.4	RELIABILITY FACTOR VS. S-N SLOPE 90% RELIABILITY	77
7.5	RELIABILITY FACTOR VS. S-N SLOPE 95% RELIABILITY	78
7.6	RELIABILITY FACTOR VS. S-N SLOPE 99% RELIABILITY	79
7.7	APPLICATION OF RELIABILITY FACTOR TO MEAN FATIGUE RESISTANCE	80
7.8	RELATIONSHIP BETWEEN MAXIMUM STRESS RANGE OF RANDOM LOADING AND EQUIVALENT CONSTANT-CYCLE STRESS RANGE	83
7.9	VARIATION OF ξ WITH m FOR VARIOUS WEIBULL SHAPES, k	83
7.10	MEAN VALUES OF RELIABILITY FACTOR FOR VARIOUS LEVELS OF RELIABILITY	91
7.11	DESIGN EXAMPLE	93
A.1	BEAM BRACKETS DETAILS, FAMILY NO. 1	100
A.2	TRIPPING BRACKET DETAILS, FAMILY NO. 2	106

LIST OF FIGURES (CONTINUED)

Figure	Page
A.3	NON-TIGHT COLLAR DETAILS, FAMILY NO. 3 109
A.4	TIGHT COLLAR DETAILS, FAMILY NO. 4 111
A.5	GUNWALE CONNECTION DETAILS, FAMILY NO. 5 113
A.6	MISCELLANEOUS CUTOUT DETAILS, FAMILY NO. 7 114
A.7	CLEARANCE CUTOUTS DETAILS, FAMILY NO. 8 116
A.8	DECK CUTOUT DETAILS, FAMILY NO. 9 117
A.9	STANCHION END DETAILS, FAMILY NO. 10 118
A.10	STIFFENER END DETAILS, FAMILY NO. 11 122
A.11	PANEL STIFFENER DETAILS, FAMILY NO. 12 124
B.1	STRUCTURAL FATIGUE - DETAILS 131
B.2	S-N CURVES FOR STRUCTURAL DETAILS 134
D.1	SL-7 SCRATCH GAGE DATA WITH CORRESPONDING WEIBULL DISTRIBUTION 170
D.2	COEFFICIENTS OF VARIATION FOR WEIBULL SHAPE PARAMETER, k 171
F.1	DETAIL 21 AND TESTING FIXTURE 190
F.2	DETAIL 30A AND TESTING FIXTURE 191
F.3	DETAIL 51 AND DETAIL 52 192
F.4	WELDING OF DETAIL 21, SPECIMEN 193
F.5	S-N CURVE FOR TESTS OF DETAIL NO. 21 194
F.6	FRACTURE OF DETAIL 21-5 193
F.7	FRACTURE OF DETAIL 21-6 198
F.8	DETAIL 21 TEST SETUP 198
F.9	S-N CURVE FOR TESTS OF DETAIL NO. 30A 199
F.10	FAILURE LOCATIONS IN 30A SPECIMENS 200
F.11	FRACTURE OF DETAIL 30A-2 201

LIST OF FIGURES (CONTINUED)

Figure		Page
F.12	DETAIL 30A TESTING SETUP	201
F.13	DETAIL 51 AND 52, TESTING IN PROGRESS	202
F.14	DETAIL 51 AND 52-1, STATIC TEST	202
F.15	S-N CURVE FOR TESTS OF DETAILS 51 AND 52	203
F.16	FATIGUE CRACK IN DETAIL 51	204
F.17	STRAIN GAGE LOCATIONS, SPECIMENS 51-6 AND 52-6	205
F.18	STRAIN GAGE DATA FOR GAGE NO. 2 ON SPECIMEN 51-6	205
F.19	STRESSES AT STRAIN GAGE LOCATIONS	206
F.20	DIAL GAGE DATA FOR SPECIMEN 51-6	207

NOMENCLATURE

- a = Shifted exponential distribution, lower limit value (see Table 6.4).
 C = An empirical constant (the intercept of the S-N curve at $S=1$).
 D = Cumulative damage ratio.
 $E(S^m)$ = m^{th} moment of S or expected value of S^m

$$= \int_{-\infty}^{\infty} s^m f_S(s) ds.$$
 F_{\min} = Minimum stress in a stress cycle.
 F_{\max} = Maximum stress in a stress cycle.
 F_R = Fatigue stress range at stress ratio, R .
 F_{r0} = Fatigue stress range for a stress ratio of zero.
 $f_S(s)$ = Probability density function of S .
 $F_S(s)$ = Cumulative distribution function of S

$$= P(S \leq s) \text{ for all } s$$

$$= \int_{-\infty}^s f_S(x) dx.$$
 $h(n)$ = The hazard function, the risk of failure on n^{th} load.
 K = Slope of a constant-life straight line on a constant-life fatigue diagram (see Fig. 4.1), or the negative slope of an S-N curve.
 k = The Weibull scale or shape parameter.
 $L(n)$ = Reliability function through a given number of loading cycles.
 m = Exponent of SN relationship.
 $\frac{1}{m}$ = The negative slope of an S-N curve. (Equal to K)
 \bar{n} = Mean fatigue life.
 $P_f(n)$ = Probability of failure at a given life.
 $P(X)$ = Probability of event X .
 q = Beta distribution shape parameter (see Table 6.4).

- $Q_S(s)$ = Exceedance function of S
 = $P(S \geq s)$ for all s
 = $1 - F_S(s)$.
- r = Beta distribution shape parameter (see Table 6.4).
- R = Stress ratio or ratio of $\frac{F_{min}}{F_{max}}$.
- R_F = Reliability factor = $(\frac{1}{\gamma_L})^{1/m}$
- S = Random variable: stress range.
- s = Stress parameter (tension, compression, bending).
- S_c = Applied constant amplitude stress range.
- S_{char} = Characteristic stress range for a particular loading distribution.
- S_D = Constant-cycle design stress range for a useful life n and a specified reliability $L(n)$.
- s_0 = Beta distribution upper limit value (see Table 6.4).
- S_{RMS} = Root mean square value of S (see Table 6.4).
- $S_{10^{-8}}$ = The value of S at which the probability of exceedance is 10^{-8} .
- w = The characteristic life, or Weibull distribution parameter.
- α = Shifted exponential distribution parameter
 (see Table 7.4) ($\alpha = \frac{a}{S_{10^{-8}}}$).
- Γ = The gamma function.
- γ_L = Fatigue life factor, or scatter factor.
- Δ_f = Possible error in fatigue model.
- δ_f = Coefficient of variation in fatigue life.
- δ_n = Coefficient of variation in fatigue life.
- δ_S = Coefficient of variation of S.
- ϵ = Minimum Life.
- ζ = Lognormal distribution parameter (see Table 6.4).
- λ = Lognormal distribution parameter (see Table 6.4).

- λ_e = Mean value of exponential and shifted exponential distributions (see Table 6.4).
- μ_S = Mean value of S (see Table 6.4).
- ξ = Random load factor.
- σ_n = The standard deviation in fatigue life.
- σ_S = Standard deviation of S (see Table 6.4).
- Ω_C = Uncertainty in the mean intercept of the S-N regression line.
- Ω_n = Total uncertainty in fatigue life.
- Ω_S = Total uncertainty in mean stress range.

FATIGUE CHARACTERIZATION OF FABRICATED SHIP DETAILS FOR DESIGN

1. INTRODUCTION

1.1 Fatigue in Welded Ship Design

Fatigue cracking in ships has for many years been responsible for much costly ship repair work. In fact, as noted by Vedeler (Ref. 1.1)*, shipbuilders in Norway and Sweden considered the problem of fatigue in ships to be of more practical importance for ordinary ships than the question of brittle fracture. Such cracking has been found in the forepeak region, bottom amidships, at the bulwark at both ends of the bridge, at hatch corners, and in hulls at crossings of frames, longitudinals and girders (1.1, 1.2, 1.3, 1.4 and 1.5). Since cracks can be possible points of initiation for catastrophic failures, it is essential that fatigue be given detailed consideration in the design of a ship structure. The designs should be based on design criteria that take into account the latest information on loadings, reliability criteria and fatigue behavior (1.6).

Most current fatigue design criteria for welded structures are based on constant-cycle laboratory fatigue data that have been obtained over the last fifty years or so. However, the loadings used in these laboratory studies differ greatly from the "real" loadings to which the structures are subjected. For more effective fatigue design, more realistic loadings should be used.

Recently, considerable attention has been given to the accumulation of stress history spectra for such ships as dry cargo, large tanker and bulk carriers. Since these more realistic loading data are becoming available for ships, it is now possible to develop fatigue design criteria for ship structures based on these "real" loadings. In addition, the reliability concepts that have been developed in recent years (1.5) can be used in the design criteria to provide for more effective and better justified designs.

1.2 Objective and Scope of Investigation

The objectives of the program are to (a) establish procedures for selecting and evaluating fabricated ship details that are subjected to cyclic loading and (b) establish recommendations and procedures for fatigue design of fabricated ship details.

The program achieves these objectives by assembling fatigue resistance information for structural details, assembling or developing histograms or

*References are listed at the end of each chapter.

loading functions representing "real" ship histories, and using probabilistic concepts to develop structural reliability bases for fatigue design in ships. The results are design criteria and procedures which make possible the design of ship structure details where fatigue cracking can be minimized.

The ship details included in the investigation are representative of current ship design and shipyard practice, and others can be added as needed. References 1.3 and 1.4 list more than 634 ship structural details currently found in ship construction. These details form the basis for this study. Although fatigue tests have not been conducted on all the details, the fatigue behavior of most can be related directly or indirectly to geometries that have been tested.

The identification of the states of stress to which ship details are subjected and the development of representative density functions (mathematical models) to represent "real" ship loading histories are important in developing fatigue design criteria. With such information and using fatigue data from the literature, the desired fatigue design criteria for fabricated ship details can be developed.

To accomplish the above objectives, the study has included the following:

- I: A literature survey. A survey covering (a) the fatigue behavior of welded details, (b) ship structural details, (c) ship loading histories, (d) reliability criteria for fatigue and (e) fatigue design criteria.
- II: An evaluation of current fatigue criteria. An evaluation of current fatigue design criteria and the various factors affecting them.
- III: A classification of fabricated ship details and a summary of their fatigue behavior. An evaluation of welded ship details to establish a fatigue classification system for them.
- IV: The identification of welded ship details for which fatigue data are known, those for which only limited data are available and those for which data are lacking.
- V: Development of fatigue design criteria for ship details: these criteria provide for the level of reliability, the uncertainty in the variables that affect the fatigue behavior and the loading history.
- VI: Laboratory fatigue tests on details for which fatigue data are lacking.

The results of these various studies are presented in the following sections and appendices. The initial sections provide a summary discussion of the principal factors affecting fatigue, the basic fatigue relationships, the fatigue resistance of structural details and a review of current fatigue design criteria. The development of a catalog of ship structural details is presented in Section 5, and the mathematical models representing ship loading histories are presented in Section 6. The principal result of the investigation, the development of fatigue design criteria for ship structural details,

is presented in Section 7, along with examples of the manner in which such criteria can be applied in design. Detailed fatigue data and the results of the laboratory studies are presented in the Appendices.

1.3 References

- 1.1 Vedeler, G. "To What Extent Do Brittle Fracture and Fatigue Interest Shipbuilders Today," Houdremont Lecture 1962, Sveiseteknikk, 1962, No. 3.
- 1.2 Glasfeld, R., Jordan, D., Ken, M., Jr. and Zoller, D. "Review of Ship Structure Details," SSC-266, 1977.
- 1.3 Jordan, C. R. and Cochran, C. S. "In-Service Performance of Structural Details," SSC-272, 1978.
- 1.4 Jordan, C. R. and Knight, L. T. "Further Survey of In-Service Performance of Structural Details," SSC-294, 1980.
- 1.5 Kjellander, S. L. "Hull Damages on Large Swedish-Built Ships," Styrelsen för teknisk utveckling, Report No. 70-1272/u 981, Stockholm, Sweden, December 1972.
- 1.6 ASCE. "Safety and Reliability of Metal Structures," Proceedings, ASCE Specialty Conference, November 1972.

2. STRUCTURAL FATIGUE

2.1 Laboratory Studies

During the last 50 years, thousands of laboratory fatigue studies have been conducted on weldments and numerous papers, conferences or seminar proceedings, and books have provided detailed fatigue data for such weldments (2.1 - 2.9).

One of the principal objectives of this research has been to assemble basic fatigue test data from the literature for the development of fatigue design criteria for ship structures. However, because of the many variables and the large degree of scatter in such data, empirical relationships have been developed for use in design rather than the actual data.

In recent years crack growth studies have led to a more complete understanding of the mechanics of fatigue in welded structures and to the development of design criteria based on such theories. However, more must be done and more complete theories developed before adequate relationships can be developed for effective and complete fatigue design based on fracture mechanics.

Laboratory investigations have demonstrated that numerous factors affect the fatigue behavior of welds and weldments, factors that can be separated into three general categories:

- (1) The geometry of the member or detail: this includes both the general configuration and the local geometry of the member.
- (2) The stresses or loading conditions to which the member or detail is subjected: these include constant amplitude cyclic loads, residual stresses, random loading, frequency of loading, etc.
- (3) The materials from which the members are fabricated: for structural purpose the steels generally have yield strengths ranging from 30 to 100 ksi (207 to 689 M Pa).

2.2 Principal Fatigue Factors

Geometry. Welding is a very effective process and versatile tool that can be used to produce continuity in the joints and members of a welded structure. However, because of the way in which such members are joined, discontinuities in geometry result and produce stress concentrations that cause increased local stresses when loads are applied. These stress concentrations can result from the general configuration of the members, the local configuration of the weld details, angular distortions or misalignment

introduced in design or fabrication, and discontinuities that may occur within the welds (such as porosity, slag inclusions, lack of fusion, lack of penetration, and/or cracks).

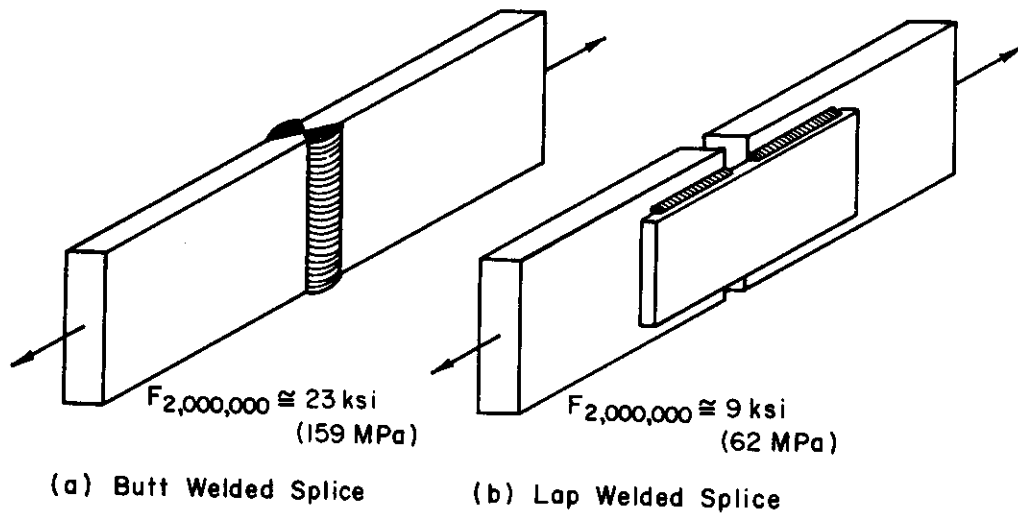
An example of the effect of the general configuration of two members is shown in Fig. 2.1. Here the fatigue resistances of the members shown differ by a factor of more than two-and-a-half. Similarly, the addition of a partial length cover or doubler plate to a rolled I-beam can be expected to reduce the flexural fatigue resistance of the beam by a factor of about three-and-a-half. These are extreme examples, but clearly demonstrate the important role played by the configuration and welded details of the members.

The importance of the local geometry of weldments can be demonstrated by examining in more detail the fatigue resistance at 2,000,000 cycles of a butt welded splice of the type shown in Fig. 2.1a. The introduction of the butt weld reduces the fatigue resistance of the basic plate to about 56 percent of the plate's basic fatigue resistance. The specific magnitude of this reduction depends upon the local configuration or geometry of the weld, the type of steel and a variety of other factors (2.10). Nevertheless, it is clear that the weld and its local geometry have a marked effect on the fatigue behavior of the member.

The fatigue effect of weld geometry has been studied in several investigations in terms of various geometric weld parameters (2.10 - 2.13). These parameters: the radius at the toe of a weld, the angle the reinforcement makes with the surface of a member, the height of the weld reinforcement and the width of the weld reinforcement, are the factors that determine the local stresses at the top of a weld and control the fatigue resistance of the member; however, the effect of each of these factors can vary considerably. The effects of these parameters vary also with the magnitude and type of loading to which the member is subjected: at longer lives (on the order of 1,000,000 to 2,000,000 cycles) the effect of the external geometry of the weld may not be as significant as at the shorter lives (on the order of 10,000 to 50,000 cycles) (2.14).

The third type of geometric parameter that may affect the behavior of a welded joint is the internal weld geometry (internal discontinuities). Internal weld discontinuities may have a greater effect at long lives than at short lives (2.14). This is just the opposite of what has been observed in the case of the external weld geometry.

Small amounts of porosity generally appear to have a relatively minor effect on the fatigue resistance of a sound weld (2.15); however, large clusters can produce a significant reduction in fatigue strength. Two of the more severe internal discontinuities in transverse butt welded joints are a lack of fusion or a lack of penetration (2.16). Such defects can reduce the fatigue strength of a joint with internal discontinuities to but a fraction of the fatigue strength of a sound joint. Clearly, internal weld defects can have a significant effect upon the fatigue resistance of a weld. Since the weld quality is a function of the skill and reliability of the welder, he too plays an important role in establishing the quality and resulting fatigue resistance of a weld.



$F_{2,000,000} \cong 23 \text{ ksi}$
(159 MPa)

$F_{2,000,000} \cong 9 \text{ ksi}$
(62 MPa)

$F_{2,000,000}$ = Fatigue Stress Range For Failure
At Two Million Cycles

Fig. 2.1 Welded Splices Showing Large Difference in Fatigue Resistance.

Stresses. Numerous tests have been made to evaluate the effects of stress cycles on the fatigue of welds and welded members. However, to define all of the effects of the stress parameters is extremely difficult because of the many interrelated variables that affect a weldment's fatigue behavior. Nevertheless, there are a number of general observations that can be made concerning the effects of the stresses and stress cycles.

Because of the limited capabilities of much of the testing equipment used to conduct fatigue tests, most studies have been conducted under simple constant amplitude cyclic conditions. Nevertheless, by conducting tests at various stress ratios and stress levels, various types of fatigue diagrams can be developed to portray or define a general picture of fatigue behavior. The basic diagram is the familiar S-N curve that relates the life of a member to the maximum stress or range of stress to which a given type of test member is subjected. On a log-log basis, such data can generally be represented by a straight line (for what is considered long-life fatigue--lives between about 50,000 and 2,000,000 cycles). (See Fig. 2.2.)

A second type of fatigue diagram often used to portray fatigue behavior is shown in Fig. 2.3. The principal axes in this diagram are the minimum and maximum stress, the axes at forty-five degrees are the range of stress and the mean stress, and the radial lines indicate lines of constant stress ratio (ratio of minimum to maximum stress). The curves in the figure are used to indicate the constant-life (n_1 , n_2 or n_3) fatigue behavior of a given type of member. Thus, this multi-axis diagram can be used to indicate the relationships between life and the various stress parameters noted above. Furthermore, the constant-life curves in such diagrams, because they are nearly linear over much of their range, are often approximated by straight lines and used for the development of relatively simple design relationships.

For members that contain severe geometrical stress concentrations, the fatigue diagram constant-life curves, particularly for long lives, tend to be low and almost parallel to the mean stress axis, thereby indicating that the fatigue resistance is primarily a function of the alternating stress or stress range. However, for some members and details (generally those with higher fatigue strengths), and for shorter lives, there will be an effect of mean stress on the fatigue behavior: the stress range will increase somewhat as the mean stress is decreased, particularly for a reversal of stress. The compressive stresses do not do as much fatigue damage as the tensile stresses and thus reversals are not as damaging as pulsating tensile stresses. Nevertheless, from the laboratory test results it is apparent that the stress range is the overwhelmingly dominant factor controlling the fatigue life of welds and weldments.

In many studies the fatigue data for all stress ratios have been combined in terms of stress range alone. It must be remembered, however, that when this is done, the degree of scatter in the data will be greater than that observed for a single stress ratio (the ratio of minimum to maximum stress) and the extent of bias in the data will depend upon the number of tests conducted at each stress ratio as well as the magnitudes of the stress ratios. Nevertheless, the use of a constant stress range for the development of design criteria, as will be discussed later, makes possible the establishment of greatly simplified design relationships and design procedures.

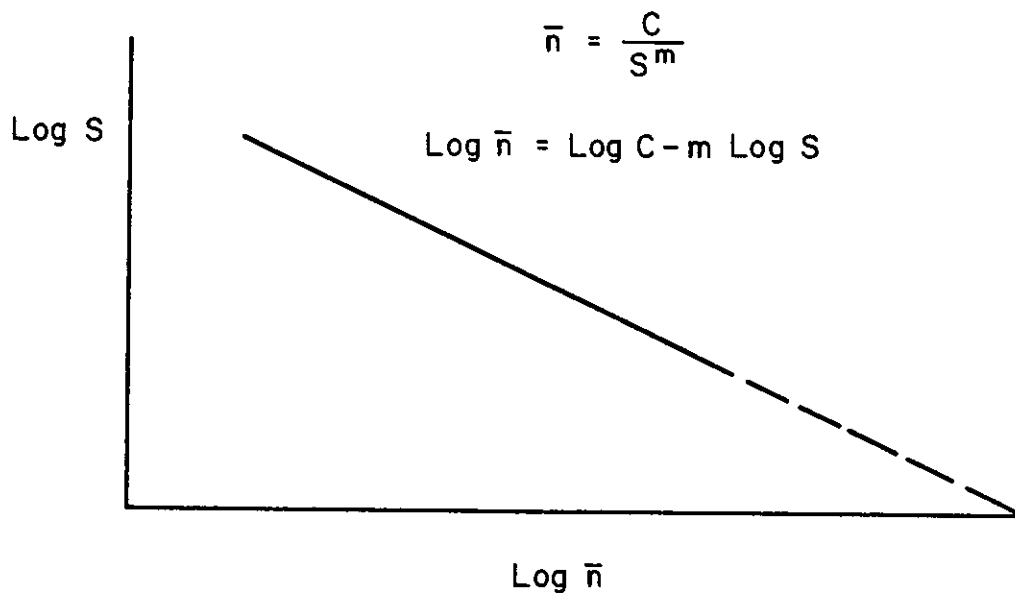


Fig. 2.2 Basic S-N Relationship for Fatigue.

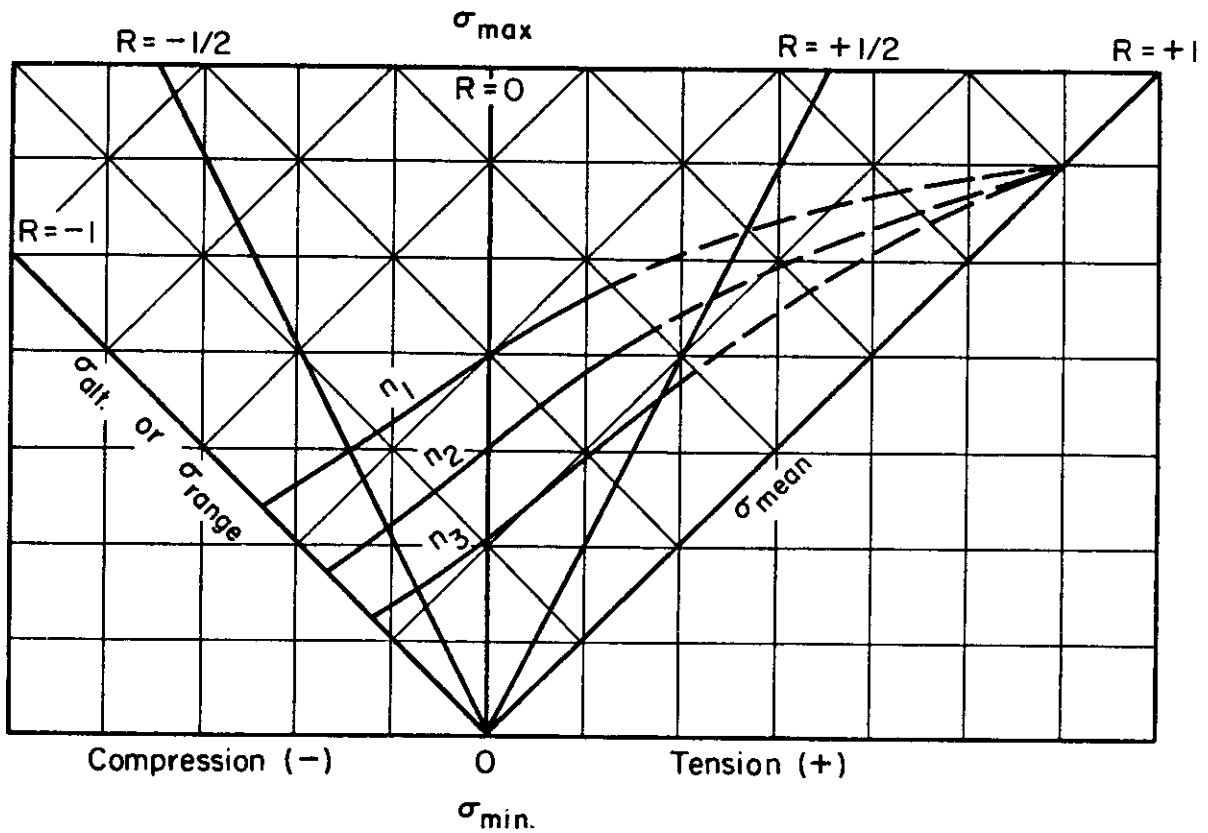


Fig. 2.3 Fatigue Diagram of Constant-Life Curves.

Residual stresses should also be considered. Some studies have shown that residual stresses produced in welding or subsequent to welding may significantly alter the life of a member. Other studies have shown little or no effect. For example, in one recent investigation, the residual stresses associated with periodic overloads were found to provide a significant increase in the fatigue life of a weldment (2.17). In another study (2.18), the importance of the magnitude and type of residual stress is examined and suggests that the effects depend upon the relationship between the residual and applied stresses. Under relatively high applied tensile stresses (short lives) the effects of tensile residual stresses can be quickly relaxed and the effects of the residual stresses become relatively small, whereas at long lives and lower applied stresses the effects become much more significant (2.19).

Another important aspect of the loading or stress cycle question concerns the effects of variable or random loadings. In recent years, as a result of the availability of more versatile testing equipment, increased consideration has been given to the effects of variable or random loadings. The large and important effect of variations in loading on the fatigue behavior of one type of weldment can be seen in Fig. 2.4. When a systematic overload or a systematic variation in the loadings is provided, the resulting changes in the residual stresses caused by the loading may produce beneficial effects (increased life) on the behavior (2.17). However, when the variation in amplitude of applied load is provided in a random manner, the effects of resulting residual stresses appear to be greatly diminished or nonexistent.

The above discussion briefly summarizes the effects of some of the principal stress parameters involved in fatigue. Other stress factors that may affect the fatigue behavior, but to a lesser extent, include frequency of loading, the sequence in which variable loadings are applied, the possibility of extended rest periods between applications of loading, the applications of stresses of such a magnitude that creep may occur, etc.

Material. Fatigue tests of plain steel members, as well as tests of structural welds and weldments, have been conducted on structural steels having tensile strengths ranging from approximately 60 ksi to 120 ksi (414 to 827 M Pa). Based on the results of many such tests, structural fatigue design provisions for these materials and members have been developed on the basis of stress range for the various types of structural steel. In general the same fatigue design criteria are used for all of the steels, regardless of their strength. This is done because repeated loadings and stress concentrations tend to equalize the fatigue strength of members of the various steels. Neglecting the effect of type of steel greatly simplifies the design criteria, but again tends to produce an increase in the degree of scatter in the stress range data. For a given type of member the stress range scatter from all steels is always greater than that for one structural steel.

2.3 Fatigue S-N Relationships

The fatigue behavior of various types of members and details in structural steels has generally been evaluated in constant-cycle fatigue tests and the results presented in terms of the nominal applied stresses and the number

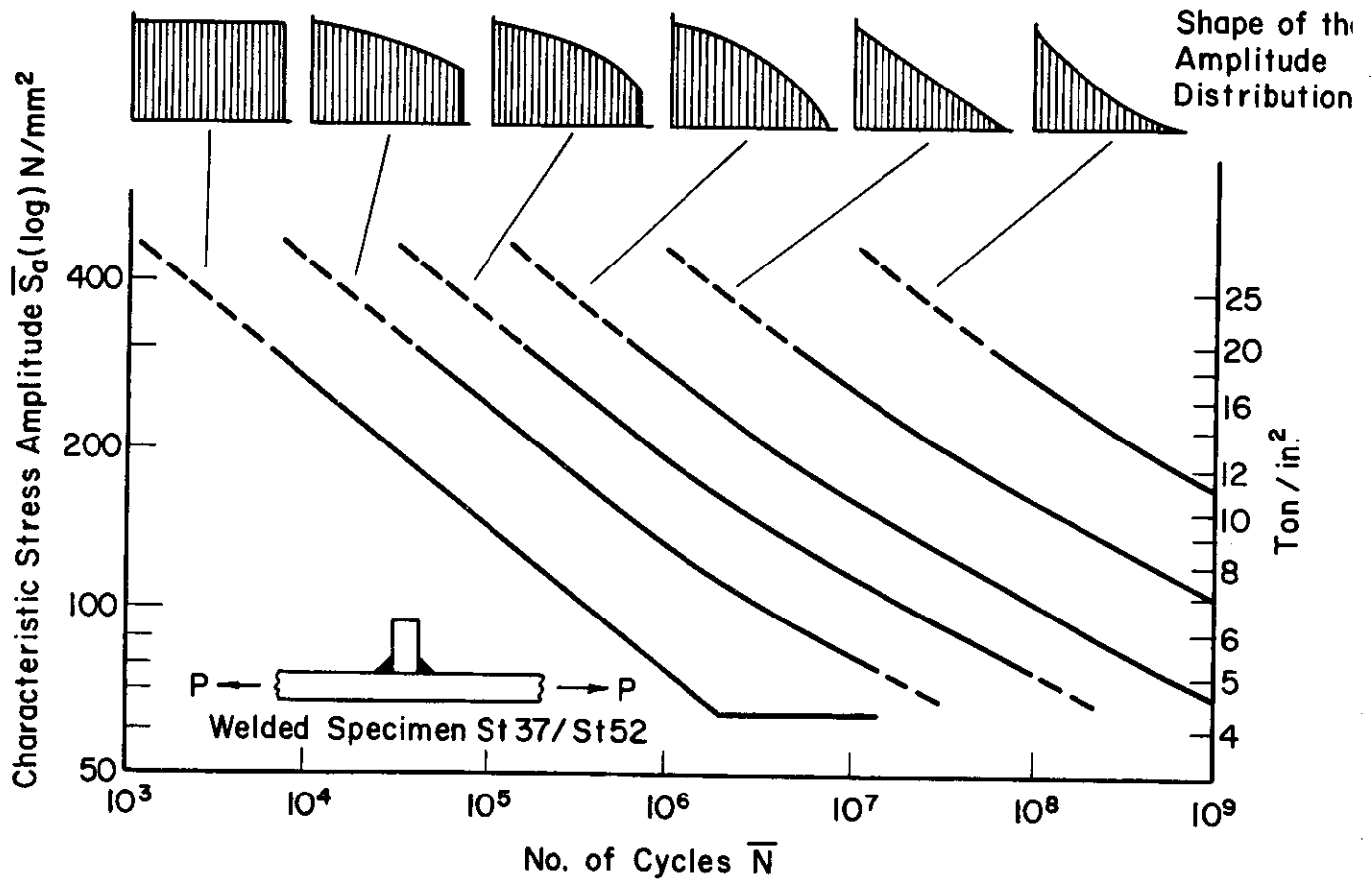


Fig. 2.4 Fatigue Resistance of a Weldment Subjected to Variable Loadings (2.6).

of cycles of loading that produce failure. The resulting S-N diagrams are generally presented as straight lines on a log-log basis as shown in Fig. 2.2, and can be represented by,

$$\bar{n} = \frac{C}{S^m} \quad (2.1)$$

or $\log \bar{n} = \log C - m \log S \quad (2.2)$

where, \bar{n} = mean fatigue life

C = an empirical constant (the intercept of the S-N curve at $S = 1$)

S = stress parameter (tension, compression, bending)

$\frac{1}{m}$ = the negative slope of the S-N curve

Thus, the fatigue strength can be computed over the range of lives covered by the sloping straight line, S-N curve for any selected number of cycles, if the slope of the line and one point on the line are known. However, only one type of stress cycle and one detail are represented on an individual S-N diagram. In general, a least-squares analysis of $\log n$ given S is used to establish the S-N curve.

If the data are analyzed in terms of the maximum stress in a stress cycle, S-N curves for a variety of stress cycles would be required to provide constant life diagrams of the type shown in Fig. 2.3. However, if the effects of mean stress are neglected (data are presented in terms of stress range alone), the constant-life curves of Fig. 2.3 are parallel to the mean-stress axis and a single stress range versus life curve can be used for all stress ratios (stress ratio is the ratio of minimum stress to the maximum stress in a stress cycle). Even with this simplification for design, it is still desirable to have constant-life relationships for each detail. With such relationships, fatigue design criteria and design relationships can readily be developed for structures that are subjected to cyclic loadings.

2.4 References

- 2.1 Munse, W. H. Fatigue of Welded Steel Structures, Welding Research Council, New York, 1964. (L. Grover, editor).
- 2.2 Gurney, T. R. Fatigue of Welded Structures, Cambridge University Press, England, 1968.
- 2.3 BWRA. "Symposium on the Fatigue of Welded Structures, March 29-April 1, 1960," British Welding Journal, March-September, 1960.
- 2.4 Munse, W. H., Stallmeyer, J. E. and Drew, F. P. "Structural Fatigue of Steel Railroad Bridges," Proceedings of AREA Seminar, 1968.
- 2.5 ASCE. "Symposium on Structural Fatigue," Journal of the Structural Division, American Society of Civil Engineers, Vol. 44, No. ST12, December 1968, pp. 2663-2797.

- 2.6 The Welding Institute. "Proceedings of the Conference on Fatigue of Welded Structures," July 6-9, 1970, The Welding Institute, Cambridge, England, 1971.
- 2.7 Pollard, B. and Cover, R. J. "Fatigue of Steel Weldments," Welding Journal, American Welding Society, Vol. 51, No. 11, November 1972, pp. 544s-554s.
- 2.8 Sanders, W. W., Derecho, A. T. and Munse, W. H. "Effect of External Geometry on Fatigue Behavior of Welded Joints," Welding Journal, American Welding Society, Vol. 44, No. 2, February 1965, pp. 49s-55s.
- 2.9 Fisher, J. W., Albrecht, P. A., Yen, B. T., Klingerman, D. J. and McNamee, B. M. "Fatigue Strength of Steel Beams with Welded Stiffeners and Attachments," NCHRP Report 147, Transportation Research Board, 1974.
- 2.10 Sanders, W. W., Derecho, A. T. and Munse, W. H. Welding Journal, American Welding Society, Vol. 44, No. 2, February 1965, pp. 49s-55s.
- 2.11 Lawrence, F. V. and Mainali, P. C. "Fatigue Crack Propagation Life Predictions for Butt and Fillet Welds," FCP Report No. 11, College of Engineering, University of Illinois, Urbana-Champaign, March 1974.
- 2.12 Williams, H. E., Ottsen, H., Lawrence, F. V. and Munse, W. H. "The Effects of Weld Geometry on the Fatigue Behavior of Welded Connections," SRS No. 366, Department of Civil Engineering, University of Illinois, Urbana-Champaign, August 1970.
- 2.13 Derecho, A. T. and Munse, W. H. "Stress Concentration at External Notches in Members Subjected to Axial Loadings," Engineering Experiment Station Bulletin 494, University of Illinois, Urbana-Champaign, January 5, 1968.
- 2.14 Munse, W. H. "Fatigue of Weldments--Tests, Design and Service," American Society for Testing and Materials, Special Technical Publication 648, 1978.
- 2.15 Ekstrom, D. H. and Munse, W. H. "The Effect of Internal Weld Defects on the Fatigue Behavior of Welded Connections," SRS No. 395, Department of Civil Engineering, University of Illinois, Urbana-Champaign, February 1973.
- 2.16 Bowman, M. D. and Munse, W. H. "The Effect of Discontinuities on the Fatigue Behavior of Transverse Butt Welds in Steel," University of Illinois, SRS No. 491, April 1981.
- 2.17 Abtahi, A., Albrecht, P. and Irwin, G. R. "Fatigue of Periodically Overloaded Stiffener Detail," Journal of the Structural Division, Proceedings of the ASCE, Vol. 102, No. ST11, November 1976, pp. 2103-2119.
- 2.18 Mattos, R. J. and Lawrence, F. V. "Estimation of the Fatigue Crack Initiation Life in Welds Using Low Cycle Fatigue Concepts," FCP Report No. 19, College of Engineering, University of Illinois Urbana-Champaign, October 1975.
- 2.19 Burk, J. D. and Lawrence, F. V. "The Effect of Residual Stresses in Weld Fatigue Life," FCP Report No. 29, College of Engineering, University of Illinois, Urbana-Champaign, January 1978.

3. FATIGUE BEHAVIOR OF WELDED DETAILS

The fatigue behavior of various types of welds and weldments has been discussed in detail in books by Munse (3.1) and Gurney (3.2), and the actual data presented in numerous technical papers and reports. Much of the detailed test information has been summarized and placed in a Fatigue Data Bank (3.3) currently in use at the University of Illinois. It is this data bank has been used in this investigation to provide the basic fatigue strengths of welds, welded details and welded members.

As indicated in Section 2, the fatigue behavior of a structural detail is a function of a variety of factors. Some of these factors have relatively little effect and can be neglected in design, while others have a significant effect and should be included in the design process. The geometry of a member or detail is of major importance and has a significant effect on its resistance. Thus, the classification of members serves to separate them on the basis of their geometry and fatigue resistance and makes possible the establishment of the mean fatigue resistance of each of the different types of members.

3.1 Mean Fatigue Resistance - Fatigue Details

The laboratory studies used to establish the fatigue resistance of many types of structural members and details have been conducted over a period of more than 50 years. Although conducted many years ago, the early fatigue test results appear to be in excellent agreement with the results of more recent tests using the latest welding techniques and, consequently, all of the data are suitable for fatigue evaluations.

In a recent investigation conducted at the University of Illinois for the Association of American Railroads and the Department of Transportation*, the University of Illinois' Fatigue Data Bank was used to provide values of the mean fatigue strength for many different types of structural details. Sketches of many of the details included in this AAR study and in an AISC design specification (3.4) are shown in Fig. 3.1 and are identified by individual fatigue detail numbers. An earlier summary of the mean fatigue stress range for these details is given in Table 3.1.

In the AAR investigation, mean S-N curves, based on stress range, were established using a least-squares, best fit, straight line evaluation of the data. These relationships will provide the basic fatigue resistance in the design procedure to be developed for ship structure details. Of great value in this approach is the fact that, in the future, as new or adjusted data and/or details become available, these mean stress range values can be readily updated and

*Determination of Basic Material Properties for use in Freight Car Fatigue Analysis," (Contract U.S. AAR-SBC 2.5/DOT FR64228).

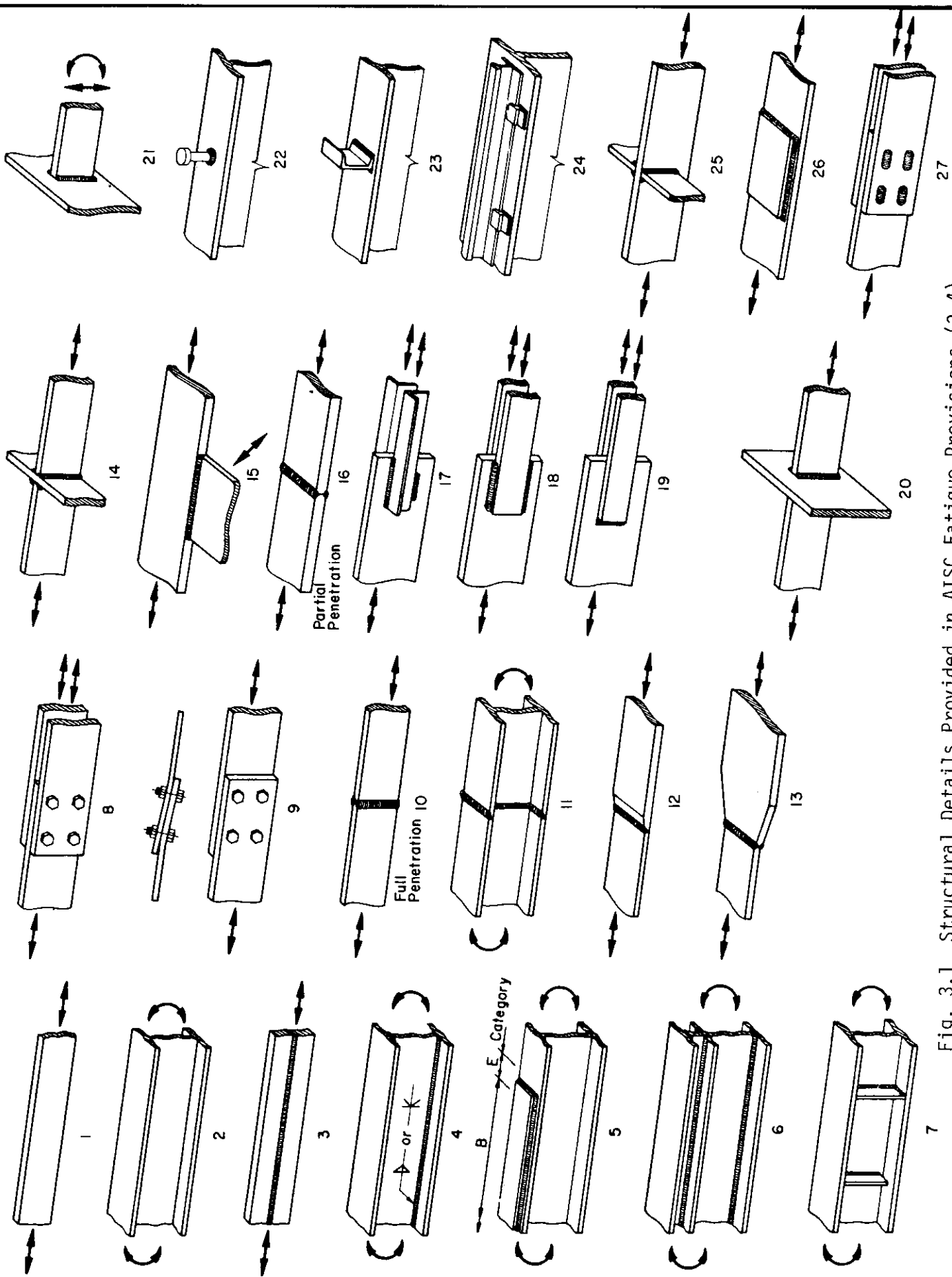


Fig. 3.1 Structural Details Provided in AISC Fatigue Provisions (3.4).

TABLE 3.1

Mean Fatigue Stress Range for Local Fatigue Details in Figure 3.1 (3.5)
(Constant Cycle - 0.50 Reliability)

(Based on Equation 2.2 - No Fatigue Limit Specified)

Detail No.* See Fig. 3.1	Stress Range, ksi, for n Cycles			
	n = 10 ⁵	n = 10 ⁶	n = 10 ⁷	n = 10 ⁸
1	48.8	38.6	30.5	24.0
2	50.0	35.0	24.6	17.2
3	43.0	28.3	18.7	12.3
4	58.5	25.3	11.0	4.75
5	24.2	11.7	5.7	2.73
6	58.5	25.3	11.0	4.75
7	40.0	20.7	10.7	5.56
8	56.1	41.5	30.7	22.7
9	31.8	23.3	17.1	12.6
9(S)	42.8	31.4	23.0	16.9
10	46.0	23.3	11.8	5.99
11	42.2	23.2	12.7	7.00
12	42.4	19.1	8.64	3.90
13	43.1	25.9	15.6	9.37
14	37.0	18.9	9.68	4.95
15	26.0	13.4	6.91	3.57
16	36.9	19.9	10.7	5.77
17	27.4	14.0	7.15	3.66
18	20.0	7.93	3.14	1.25
19	28.7	19.6	13.3	9.09
19(S)	28.7	19.6	13.3	9.09
20	40.3	19.0	8.93	4.20
20(S)	19.5	11.76	7.10	4.28
21	42.2	29.9	21.2	15.0
22	45.2	19.4	8.29	3.55
23	35.7	17.6	8.64	4.25
24	35.7	17.6	8.74	4.25
25	48.4	19.5	7.82	3.14
26	27.4	14.8	8.01	4.33
27	22.3	13.58	8.28	5.05
27(S)	22.6	13.63	8.16	4.88

* (S) indicates shear stress on fasteners or welds.

new values readily introduced, thereby providing a design based on the best available data.

One of the factors that should be introduced at an early date is the effect of corrosion from the sea or shipboard atmosphere. The data used to date to provide the basic fatigue resistances are for tests conducted in the research laboratory atmosphere.

3.2 Effect of Mean Stress

An examination of the results of the fatigue tests of various types of welded details and joints under stress cycles ranging from reversals (mean stress equal to zero) to pulsating tension (high values of mean stress) has given an indication of the effect of mean stress that can be expected in fatigue (see Fig. 3.2). Although there is considerable variation in the slopes of the curves, it is evident that, with few exceptions, the range of stress for failure increases slightly when there is a reversal of stress and decreases somewhat when the minimum stress is greater than zero (a positive stress ratio).

Under a stress cycle of complete reversal ($R = -1$) (as shown in Fig. 3.2), the average stress range for failure is approximately 25 percent greater than it is for a cycle of zero-to-tension ($R = 0$) (there are only two marked exceptions in the diagram). For a stress cycle of half-tension to tension ($R = +\frac{1}{2}$), the average stress range for failure is generally 15 to 20 percent greater than it is for a cycle of zero-to-tension ($R = 0$). Based on these average results of over 3,000 tests, an empirical adjustment of the following form could be employed.

$$\text{Stress ratio adjustment factor} = (1 - 0.25R) \quad (3.1)$$

Using Eqn. (3.1), the stress range for failure at a given stress ratio and in terms of the zero-to-tension stress range can then be written as,

$$F_R = F_{r0}(1 - 0.25R) \quad (3.2)$$

where, F_R = fatigue stress range at a stress ratio, R .

F_{r0} = fatigue stress range for a stress ratio of zero (zero-to-tension stress cycle).

R = stress ratio, ratio of minimum to maximum stress in a stress cycle.

For any given stress ratio and constant-cycle loading, based on Fig. 3.2, Eqn. (3.2) can be expected to provide an estimated value of fatigue strength for any stress ratio if only the value for $R = 0$ is known. However, since both the mean stress and the stress ratio may vary considerably during the life of a structure such as a ship, the use of a constant range of stress (equivalent to an average stress ratio adjustment factor equal to one) will probably be more realistic and certainly easier to apply in design.

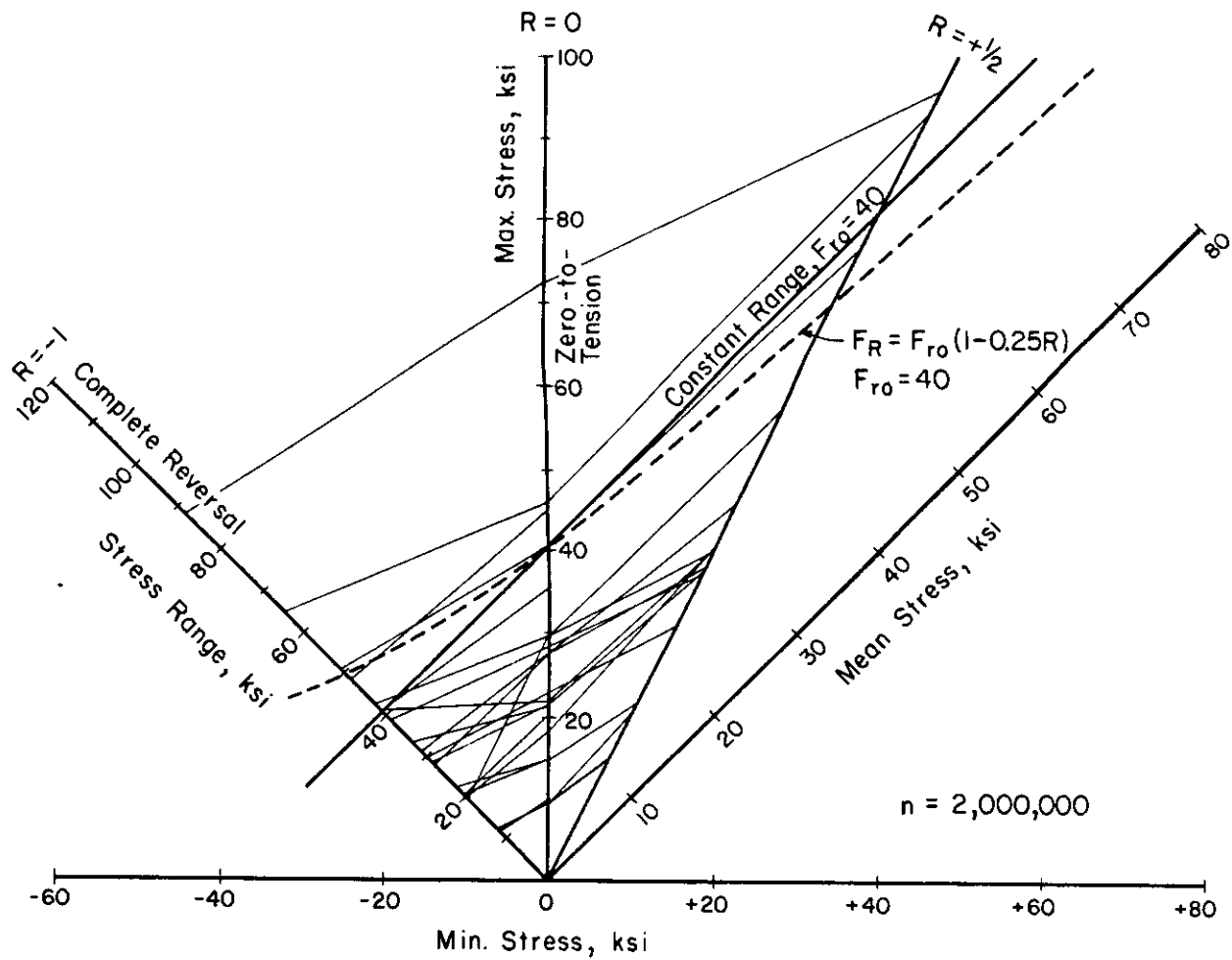


Fig. 3.2 Fatigue Diagram for Various Details at Stress Ratios of -1, 0 and $+\frac{1}{2}$.

3.3 Effects of Residual Stresses

As noted earlier, the effects of residual weld stresses in fatigue are complex and difficult to take into account in any simple design procedure. Gurney and Maddox (3.6), based on an analysis of the fatigue behavior obtained in 15 tests (two limited series of tests at stress ratios of $R = 0$ and $R = +\frac{1}{2}$), concluded that at 2×10^6 cycles and for large structures, the fatigue strength of fillet welded joints and transverse butt welded joints should be adjusted by a factor of 0.815 to correct for residual stress effects that would exist in such structures. This correction is made by rotating the S-N curves to provide the adjustment. At short lives (higher stresses) there would be little or no adjustment. However, nothing is suggested concerning the effects to be expected under fully reversed loading, under flexural loadings, under random loadings, for quenched and tempered steels versus mild structural steels, or for other types of joints or members. The evaluation is very limited and consequently should be used only for the specific conditions tested.

In a study by Burk and Lawrence (3.7), the residual stress effect is related to a mean stress effect. Furthermore, they observe that the residual stresses can be relaxed by the application of levels of mean stress that produce local yielding. They also note that the material properties (tensile yield strength) influence the effect of residual stresses on weld fatigue life.

Because of the complexity of the residual weld stress effects in fatigue and since the effects may be small or nonexistent, many fatigue design criteria now neglect the effect in the same manner and on the same basis as is used in neglecting the effects of mean stresses (see Sec. 3.2). Furthermore, since the effects of residual stresses are already included in the fatigue studies of some weldments, a design philosophy which neglects residual stresses appears to be well justified.

3.4 Effect of Material

Numerous fatigue tests have been conducted on plates and on weldments fabricated of structural steels having yield strength ranging from 30 to 100 ksi (207 to 689 M Pa); this makes possible an examination of the effect of the type of steel on the fatigue resistance of the steels and of weldments in these steels. In an evaluation based on the stress ranges for failure at 10^5 and 2×10^6 cycles, the steels have been grouped into three categories: mild steel (M) of approximately 36 ksi (248 M Pa) yield strength, high strength low alloy steel (H) of approximately 50 ksi (345 M Pa) yield strength, and quenched and tempered steels (Q) of approximately 100 ksi (689 M Pa) yield strength.

Based on the results of 441 fatigue tests of plain plates of the steels noted, the mean fatigue strength at 2,000,000 cycles is within 5.2 ksi (35.9 M Pa) of the mean fatigue strength for each of the steels considered separately (see Table 3.2a). At 100,000 cycles the corresponding value is 23.2 ksi (160 M Pa). By combining the three types of steels, since there were nearly twice as many tests of the quenched and tempered steels as there were of either of the other steels, the average values are biased towards the results from

TABLE 3.2

Fatigue Behavior of Various Steels

(a) Mean Fatigue Strength of Plain As-Rolled Plates Under Axial Loading (Based on Stress Range).

Type of Steel	No. of Tests	n = 100,000 cycles		n = 2,000,000 cycles	
		F _{100,000} ksi (M Pa)	% of combined value	F _{2,000,000} ksi (M Pa)	% of combined value
Mild Steel (M)	101	46.2 (319)	67	36.2 (250)	88
H.S.L.A. (H)	128	56.3 (388)	81	46.4 (320)	113
Q & T (Q)	212	80.6 (556)	116	45.3 (312)	110
Combined	441	69.4 (478)	100	41.2 (284)	100

(b) Mean Fatigue Strength of Transverse Butt Welded Joints Under Axial Loading (Based on Stress Range).

Type of Steel	No. of Tests	n = 100,000 cycles		n = 2,000,000 cycles	
		F _{100,000} ksi (M Pa)	% of combined value	F _{2,000,000} ksi (M Pa)	% of combined value
Mild Steel (M)	857	34.1 (235)	94	23.0 (159)	86
H.S.L.A. (H)	387	43.2 (298)	119	34.2 (235)	128
Q & T (Q)	400	48.9 (337)	134	27.3 (188)	102
Combined *	726	36.4 (251)	100	26.7 (184)	100

* The combined values are only for single-V full penetration welds. Computer capacity limited the number of tests to 1,000. The values for M, H, and Q steels are for all types of full penetration welds.

the higher strength steels. At 100,000 cycles, the mean fatigue resistance for the mild steel (46.2 ksi) is far below (about two-thirds) that of the three steels combined (69.4 ksi): at 2,000,000 cycles the difference is much smaller. For this particular type of member and test (plain plate under axial loading) it may be best to separate the steels in establishing the basic fatigue data. However, seldom is the fatigue design of a member or structure based on plain plate behavior. When structural details are introduced, as they are in most structures, the differences generally become smaller. An indication of this can be seen in Table 3.2(b) where the mean fatigue strengths are presented for 726 tests of single-V full penetration transverse butt welded joints. When details that produce stress concentrations greater than that in the transverse butt welded joints are introduced, the differences between the steels become even smaller.

In view of the small magnitude of the differences generally obtained in fatigue strengths of most welded members and details fabricated from the M-H-Q range of structural steels, it is considered desirable to improve design simplicity by disregarding, in most instances, the material factor in fatigue design.

3.5 Evaluation of Variability in Fatigue Life

Another factor that will be taken into account in the fatigue design criteria is the variability in the fatigue data. Members tested at a given stress level will be found to fail at various lives, the distribution of which is generally considered to follow a log-normal or Weibull distribution (see Fig. 3.3). The measure of this variability is represented by a coefficient of variation.

$$\text{C.O.V.} = \frac{\sigma_n}{\bar{n}} = \delta_n \quad (3.3)$$

where, δ_n = coefficient of variation in life.

σ_n = the standard deviation in fatigue life.

\bar{n} = mean fatigue life.

Values of the coefficients of variation have been assembled from the Fatigue Data Bank at the University of Illinois for the fatigue details for which there are fatigue data. A summary of these values is plotted in Fig. 3.4. These values will be used in Section 7 to establish reliability for fatigue design.

3.6 References

- 3.1 Munse, W. H. "Fatigue of Welded Steel Structures," Welding Research Council, New York. 1964.
- 3.2 Gurney, T. R. "Fatigue of Welded Structures," Cambridge University Press, England, 1968.

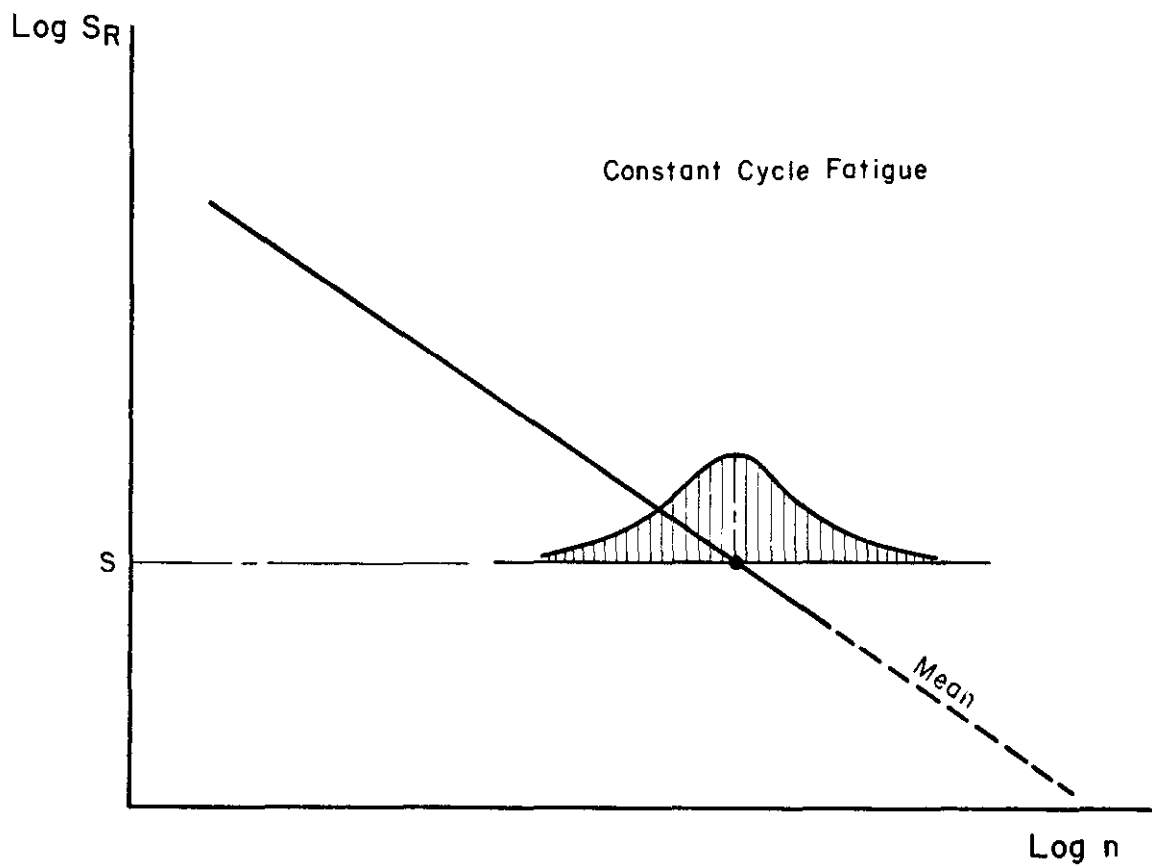


Fig. 3.3 Distribution of Fatigue Life at a Given Stress Level.

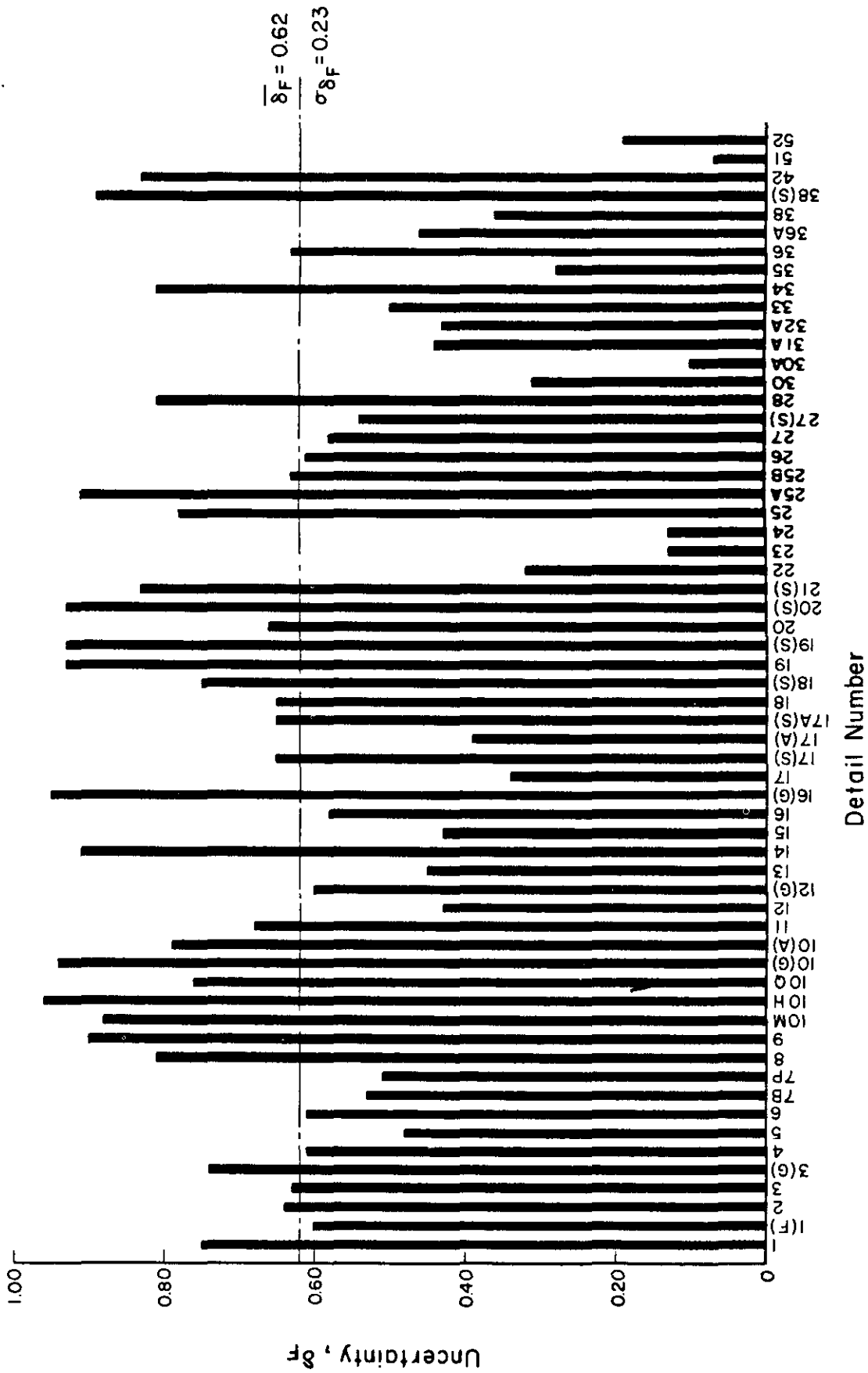


Fig. 3.4 Variability in Fatigue Resistance of Structural Fatigue Details.

- 3.3 Radziminski, J. B., Srinivasan, R., Moore, D., Thrasher, C. and Munse, W. H. "Fatigue Data Bank and Data Analysis Investigation," SRS No. 405, Department of Civil Engineering, University of Illinois, Urbana-Champaign, June 1973.
- 3.4 AISC. "Specification for the Design, Fabrication and Erection of Structural Steel for Buildings," American Institute of Steel Construction, 1969.
- 3.5 Munse, W. H. "Predicting the Fatigue Behavior of Weldments for Random Loads," for presentation at Offshore Technology Conference, May 10, 1978, Paper 3300.
- 3.6 Gurney, T. R. and Maddox, S. J. "A Re-Analysis of Fatigue Data for Welded Joints in Steel" British Welding Institute, Report No. E/44/72, 1972.
- 3.7 Burk, J. D. and Lawrence, F. V. "The Effect of Residual Stresses on Weld Fatigue Life," FCP Report No. 29, College of Engineering, University of Illinois, Urbana-Champaign, January 1978.

4. FATIGUE DESIGN

4.1 Current Fatigue Design Criteria

Laboratory fatigue test results and constant-life fatigue diagrams of the type in Fig. 4.1 provided the basic information on which many of the early fatigue design relationships were developed. The 1947 edition of the American Welding Society's Bridge Specifications (4.1) introduced straight line relationships to approximate the test curves and added a factor of safety that provided maximum allowable design stresses in the form of Eqn. 4.1 for a variety of design details.

$$F_{\max} = \frac{F_{ro}}{1 - KR} \quad (4.1)$$

where, F_{\max} = maximum allowable repeated stress.

F_{ro} = the fatigue resistance under a zero-to-tension loading reduced by the desired factor of safety (this is also the range of stress).

R = the ratio of minimum to maximum stress.

K = slope of the straight line, constant-life fatigue relationship.

Eqn. 4.1 was used for a number of years but, in many instances proved to be rather difficult to apply. A constant range of stress criteria that relates the fatigue behavior to the live-load stress range is much simpler to use. Because of this ease of application, and the fact that this simplification generally provides a good approximation, a stress range design criteria has now been introduced into most of the current structural fatigue design specifications (4.2, 4.3, 4.4, 4.5). The use of a constant stress range for design corresponds to a value of $K = 1.0$ in Eqn. 4.1. However, as noted previously, the use of a constant stress range neglects some of the stress and material factors that may affect fatigue.

There has been considerable difference of opinion around the world as to the best or appropriate design criteria to be used for fatigue. Figure 4.2 (4.6) shows the marked difference in fatigue design criteria used by several different countries for a single type of welded joint at a life of 2,000,000 cycles. Markedly different basic assumptions and levels of reliability have been used in developing the various design criteria.

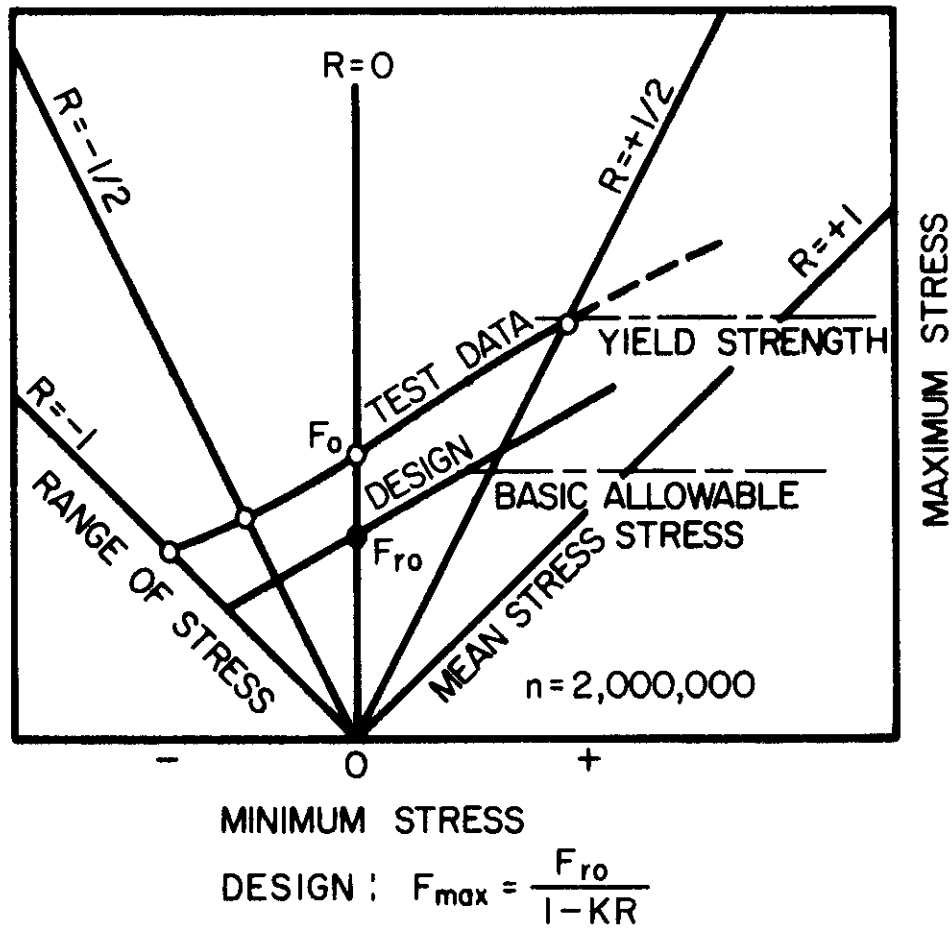


Fig. 4.1 Form of Early Fatigue Design Relationships Based on Test Data.

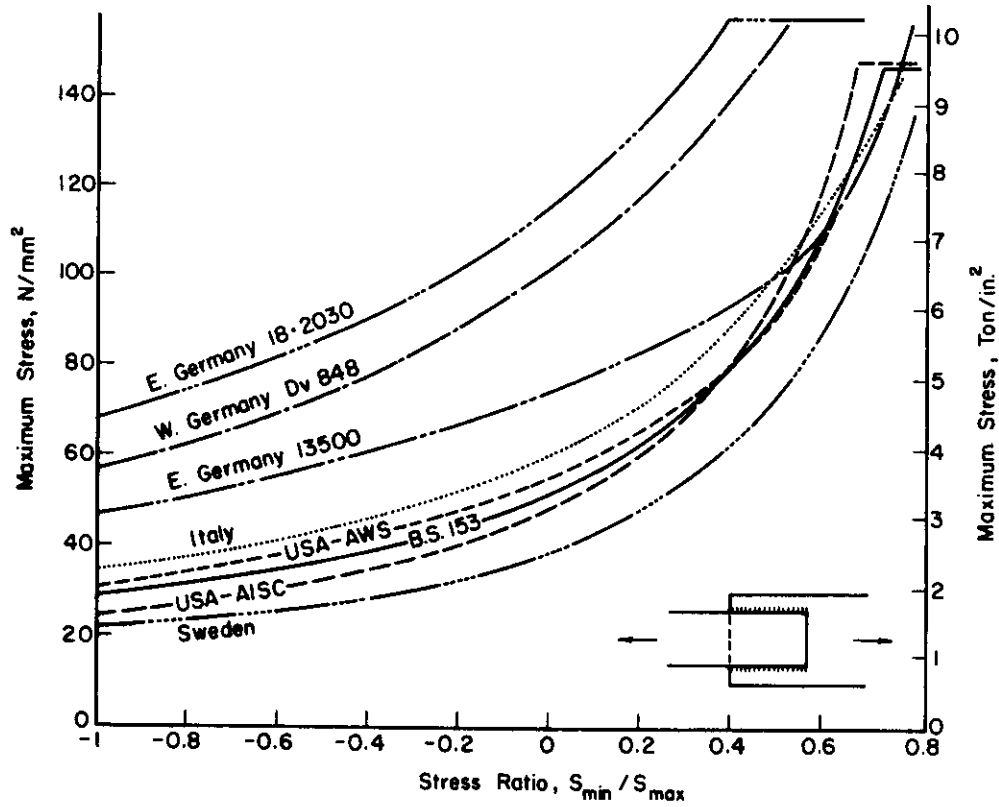


Fig. 4.2 Comparison of Various Design Stresses at 2,000,000 Cycles for Longitudinal Load-Carrying Fillet Welded Joints (4.6).

Although fatigue design provisions are already included in many specifications, studies (4.7, 4.8, 4.9, 4.10, 4.11 and 4.12) have been under way in recent years to develop more realistic design criteria. The developments in some of these new studies are based on a philosophy of separating the problem into two functions, a resistance function and a loading function, and in introducing consideration of a level of structural reliability rather than a factor of safety. The degree of variability in the fatigue behavior of many welded details (one of the factors required for a reliability analysis) has been obtained from the laboratory data (see Fig. 3.4). However, to this must be added the effects of other variables: errors in analysis, variation in fabrication, the effects of corrosion, and the effects of any other variables that may be involved.

The variability in loading must also be taken into account. For some structures, loading information in the form of histograms is available; however, a great need exists for more realistic information concerning loadings, predictions of loadings, and of the uncertainty in these predictions. With improved fatigue information and better loading predictions greater economy and safety through design will be possible.

The structural fatigue reliability design philosophy suggested by Ang and Munse (4.7) makes possible the fatigue design of structures that are subjected to random loading conditions and for a selected level of reliability. Welded members and details for which constant-cycle fatigue data are available can readily be covered by such a design philosophy. The variability in the fatigue data (coefficient of variation) as well as estimates of the effects of errors in analysis, the uncertainty in the slope of the fatigue regression relationships, and possible errors in the use of a linear damage rule can also be introduced. For the complete criteria, the selection of a loading function must also be made. To do this, realistic data in the form of histograms are essential. Then, the appropriate probability density functions that best represent the expected loading histories can be selected. Various distribution functions can be used for this purpose and will be discussed in detail in Section 6.

Based on an examination of the various fatigue design criteria noted above, simple reliability design criteria have been developed to provide for the fatigue design of ship structure details. Ship details have been examined extensively, a catalog of these details assembled, and the various locations that may be susceptible to fatigue have been categorized (see Section 5). As a second step in the process, ship-loading-history data have been examined, appropriate probability density functions selected to represent such loadings, and fatigue design reliability criteria developed (Section 7). Combining these developments with the available fatigue data for welded members and details then makes possible the development of the desired simple ship structure fatigue design criteria (Section 7).

4.2 References

- 4.1 AWS. "Standard Specifications for Welded Highway and Railway Bridges," American Welding Society, D2.0-47, 1947.
- 4.2 AWS. "Structural Welding Code," American Welding Society, D1.1-80, 1980.

- 4.3 AISC. "Specification for the Design, Fabrication and Erection of Structural Steel for Buildings," American Institute of Steel Construction, November 1, 1978.
- 4.4 AASHTO. "Standard Specifications for Highway Bridges," American Association of State Highway and Transportation Officials, 1977.
- 4.5 AREA. "Steel Structures-Specifications for Steel Railway Bridges," American Railway Engineering Association, 1978.
- 4.6 The Welding Institute. "Proceedings of the Conference on Fatigue of Welded Structures," July 6-9, 1970, The Welding Institute, Cambridge, England, 1971.
- 4.7 Ang, A. H.-S. and Munse, W. H. "Practical Reliability Basis for Structural Fatigue," ASCE National Structural Engineering Conference, Preprint 2492, April 14-18, 1975.
- 4.8 Moses, Fred. "New Procedure for Fatigue Design of Highway Bridge Girders," Transportation Research Record, No. 507, Washington, DC, 1974, pp. 58-67.
- 4.9 Schilling, C. G., Klippstein, K. H. and Reilly, R. J. "Simulated Traffic Fatigue Loading of Steel Bridges," Proceedings, ASCE Specialty Conference on Metal Bridges, St. Louis, MO, November 12-13, 1974, pp. 379-410.
- 4.10 Wirsching, P. M. "Fatigue Reliability of Welded Joints in Offshore Structures," 1979 Offshore Technology Conference, OTC 3380, also published in the International Journal of Fatigue, April 1980.
- 4.11 Nolte, K. G. and Hansford, J. E. "Closed-Form Expressions for Determining the Fatigue Damage of Structures Due to Ocean Waves," Offshore Technology Conference, Paper 2607, May 3-6, 1976.
- 4.12 Munse, W. H. "Predicting the Fatigue Behavior of Weldments for Random Loads," for presentation at Offshore Technology Conference, May 10, 1978, Paper 3300.

5. SHIP STRUCTURE - DETAILS AND ASSEMBLIES

5.1 Classification of Ship Details

In any fatigue evaluation of ship structures, the importance of the structural details cannot be overemphasized. Unfortunately, ship structural details have often been developed with little or no fatigue analysis included in the detail selection and design process and, consequently, fatigue has become a serious problem. Although there are some basic selection factors used in terms of size and configurations, only limited fatigue design information has been available to the designer or detailer to aid in his selection. The details have often been chosen because they have been used previously or are easy to assemble. The result has been a large variety of structural details with greatly varying fatigue strengths.

Recent studies of ships (5.1 and 5.2) have been conducted to provide data on the performance of structural details. The immediate result of these studies should be to identify poor details, to reduce the number of variations in details, and to decrease fabrication and construction costs; however, the development of suitable fatigue design criteria should, in addition, make improvements in safety and design, and further reductions in cost possible.

The general review of ship structural details by Glasfeld et al. (5.3) and the General Dynamics report on Standard Structural Arrangements (5.4) provide an excellent summary of the variability in and design of structural details and should help to reduce the number of variations in these details now in use. Surveys of actual in-service performance of many of these structural details are provided by Jordan and Cochran (5.1, 5.2). In these surveys, the details have been categorized into twelve families and cover 634 structural configurations. Eighty-six ships, involving seven types, were surveyed for service failures. Approximately 600,000 details were observed and 6,856 of these exhibited failures. These, and other efforts directed at the evaluation of ship structural details have helped greatly to define the critical locations in the details. However, as noted in the Committee III.1 report of the Proceedings of the 7th International Ship Structures Congress (5.5), fatigue still remains a serious problem in large ships. About 70% of the total damage in ships over 200 m in length may be classified as fatigue damage. However, in small ships less than 200 m in length, damage due to fatigue cracking seems to be much lower, approximately 20%.

This study uses the recent studies of structural details to help identify those locations that may be fatigue critical and to establish design criteria for such details. To identify the possible critical locations, a catalog of ship structure details and assemblies has been established,

based on the 634 configurations identified by Jordan and Cochran (5.1, 5.2).

5.2 Catalog of Welded Ship Structure Details and Assemblies

The ship structure details identified for use in this study are found in SSC reports 272 and 294 (5.1, 5.2). These reports also give detailed information with respect to crack locations, detail descriptions, and other general failure information. The catalog consists of 12 families of details (see Fig. 5.1), each of which is divided into subfamilies on the basis of their function, and then into individual details in the subfamilies. The complete catalog of details is presented in Appendix A. In this catalog a detail that is identified as 2B13, for example, is a detail from family 2, subfamily B, and is number 13 in the subfamily. The twelve family classifications are presented as Fig. 5.1 and shows a typical configuration, the family name, and the general function of the family.

A catalog example of the Beam Bracket Details of family No. 1 and subfamilies A and B are presented in Fig. 5.2. The locations on each of the ship structure details and assemblies at which fatigue should be considered are identified with a solid or open circle and a number or numbers. These locations, in turn, will be related to the design process presented in Section 7.

5.3 Local Fatigue Details

Numerous locations in the twelve families of ship details have been found to contain cracks (5.1 and 5.2), many of which can probably be assumed to be fatigue cracks. To provide a basis on which fatigue design criteria might be developed for the ship details, these critical locations and other possible critical locations have been identified in terms of a "local fatigue detail," such as those shown in Fig. 3.1, for which fatigue strengths are in general available.

The "local fatigue details" identified in the families of ship details, or for which fatigue data are available, are assembled in Appendix B, along with a tabular summary of their fatigue strengths. The diagrams in this Appendix illustrate the general features of the details and the type of loading to which the detail is subjected. The identification of these "local fatigue details," in the Appendix A catalog of ship details and assemblies is provided by the numbers at the solid or open circles on the ship details. These numbers correspond to the details in Appendix B, and identify details of comparable geometry.

An indication of the relationship between the catalog of welded ship structure details and the local fatigue details is given in Fig. 5.3. In beam bracket 1C10 it can be seen that four critical locations are identified in the angles and the corner gusset; two of these locations are comparable to local fatigue detail No. 21, and the other two are comparable to local fatigue detail No. 30. With a prediction of the loading history (history of the nominal stress in the direction indicated by the arrows) to which the beam bracket will be subjected during its lifetime and values of the fatigue resistance of fatigue details No. 21 and 30, the adequacy of the

FIG. 5.1 DETAIL CLASSIFICATIONS (5.1)

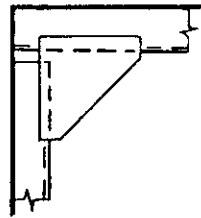
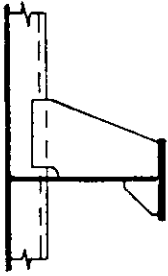
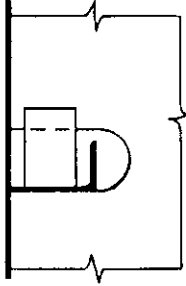
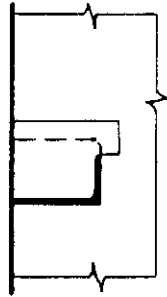
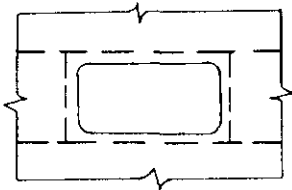
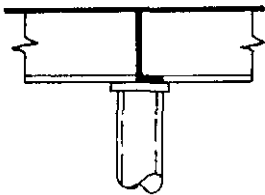
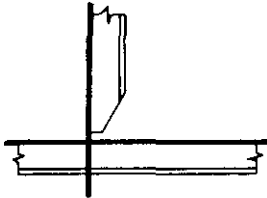
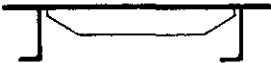
Type No.	Name	Functional Provision	Typical Configuration
1	Beam Bracket	Increase strength of framing and stiffening members at their supports.	
2	Tripping Brackets	Laterally support framing and stiffening members.	
3	Non-Tight Collars	Provide a connection from webs of framing and stiffening members to the plating of supports that have cutouts at the members.	
4	Tight Collar	Same as 3 above except also cover the cutouts to prevent passage of fluid or objects through the cutout.	

Fig. 5.1 Detail Classification (Con't.)

Type No.	Name	Functional Provision	Typical Configuration
5	Gunwale Connection	Join the strength deck stringer plate to the shear strake.	
6	Knife Edge Crossing	(Permits complimentary stiffening systems on opposite sides of plate)*	
7	Miscellaneous Cutouts	Provide a wide variety of holes for access, drainage, ease of fabrication, cableways, pipes, stress relief, etc.	
8	Clearance Cutouts	Provide a hole in an intersecting member to allow another member to go through.	

*Author's addition to figure from reference 5.1.

Fig. 5.1 Detail Classification (Con't.)

Type No.	Name	Functional Provision	Typical Configuration
9	Structural Deck Cuts	Allow passage through decks for access, tank cleaning, piping, cables, etc.	
10	Stanchion Ends	Transfer loads between stanchions and deck supporting members.	
11	Stiffener Ends	Connect an unbracketed non-continuing stiffener to a supporting member.	
12	Panel Stiffeners	Stiffen plating and webs of girders. These are non-load carrying members.	

CONTINUOUS

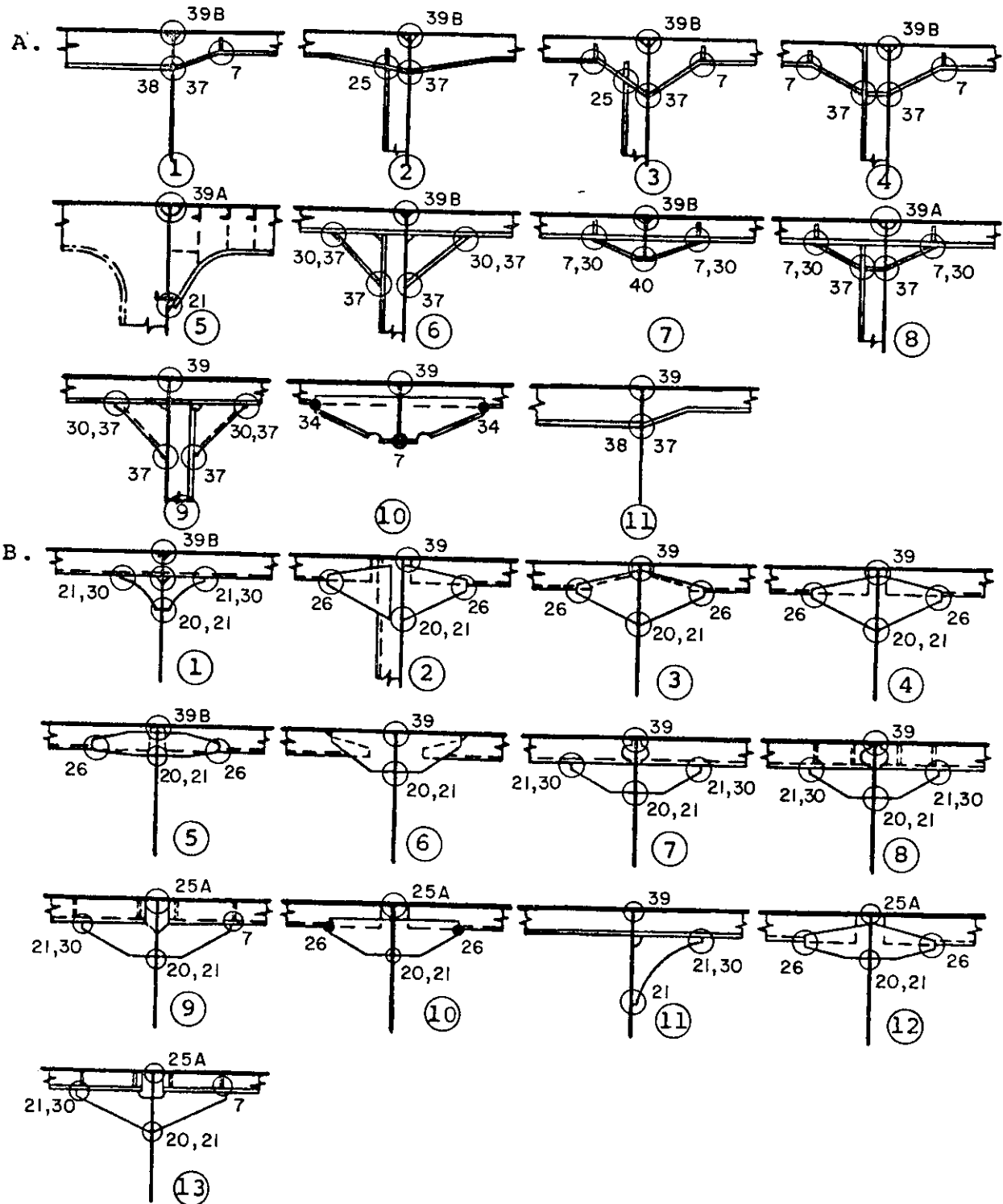
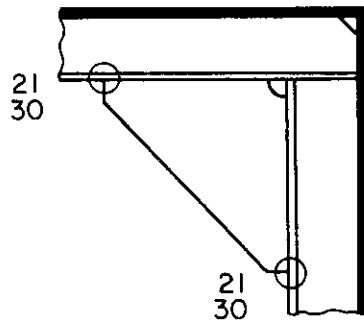
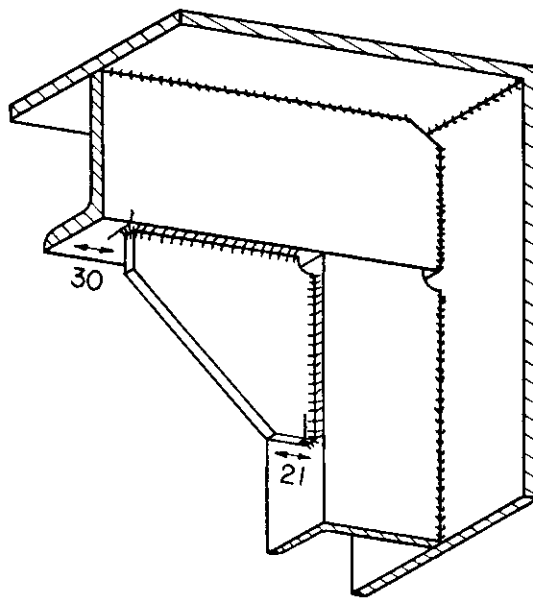


Fig. 5.2 Example from Catalog of Beam Brackets Details, Family No. 1.

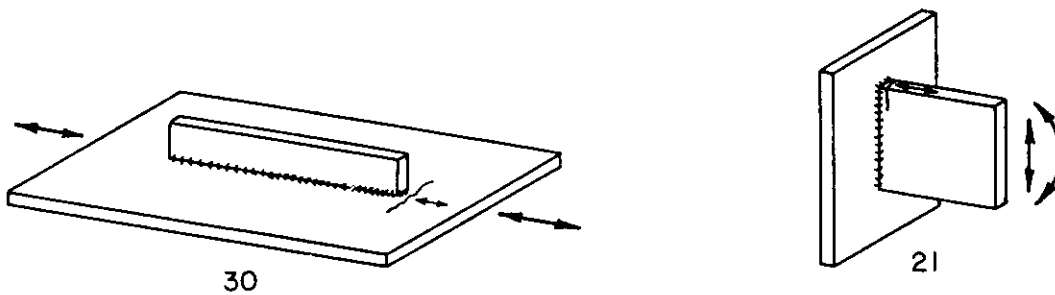


Beam Bracket
IC10

(a) Ship Structure Detail - (From Appendix A)

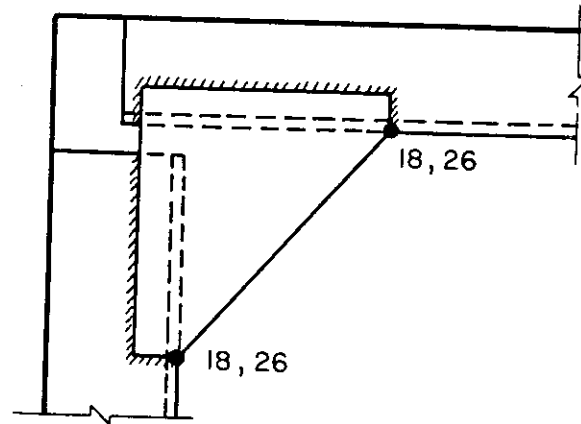


(b) Possible Fatigue Critical Locations In Beam Bracket IC10

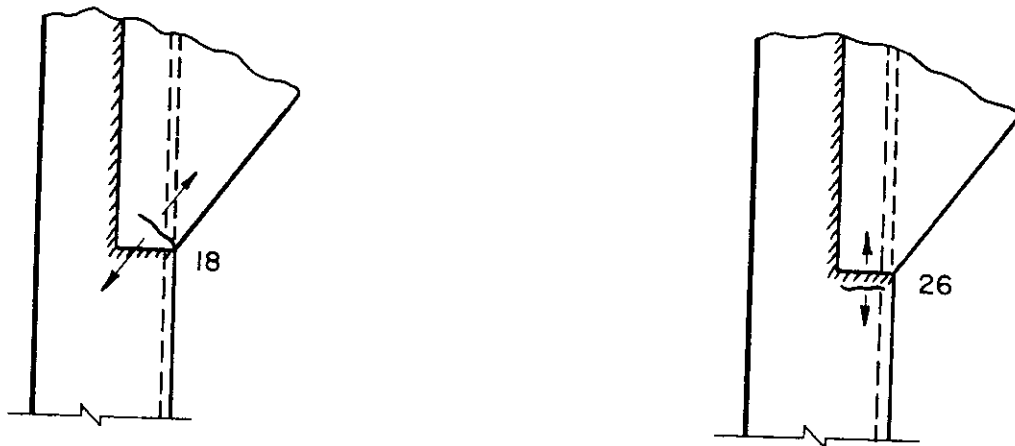


(c) Local Fatigue Details Number 21 and 30. (From Appendix B)

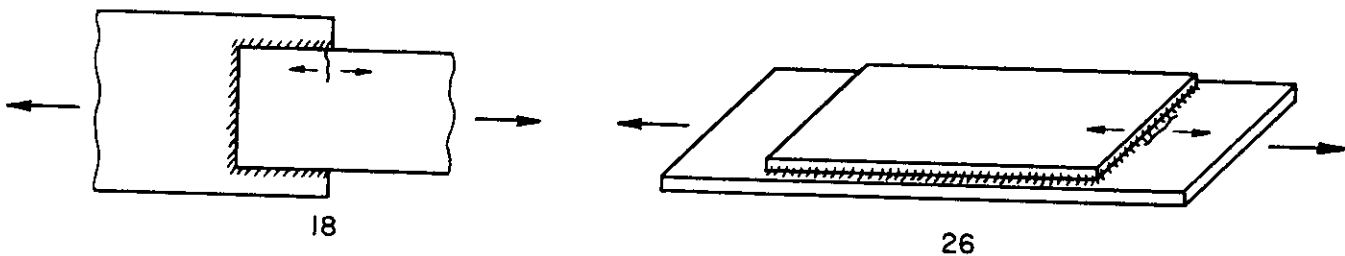
Fig. 5.3 Examples of Relationship Between Ship Structure Details and Local Fatigue Details.



(g) Beam Bracket IC4

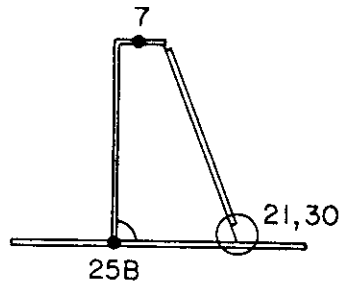


(h) Possible Fatigue Critical Locations In Beam Bracket IC4

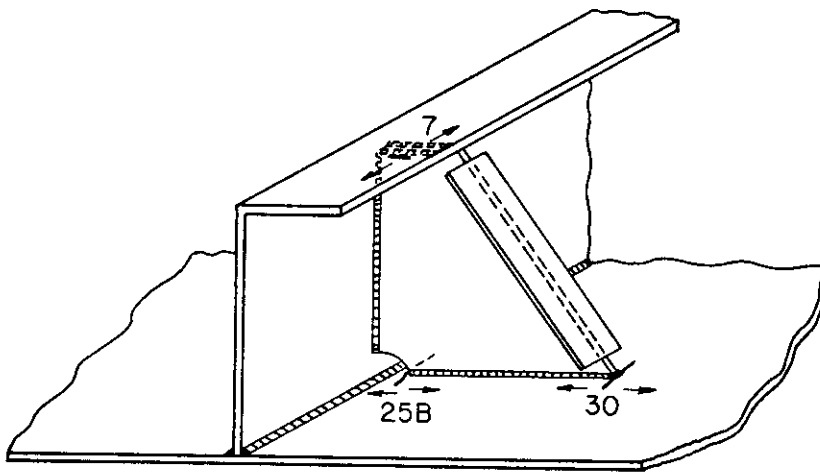


(i) Local Fatigue Details Number 18 and 26

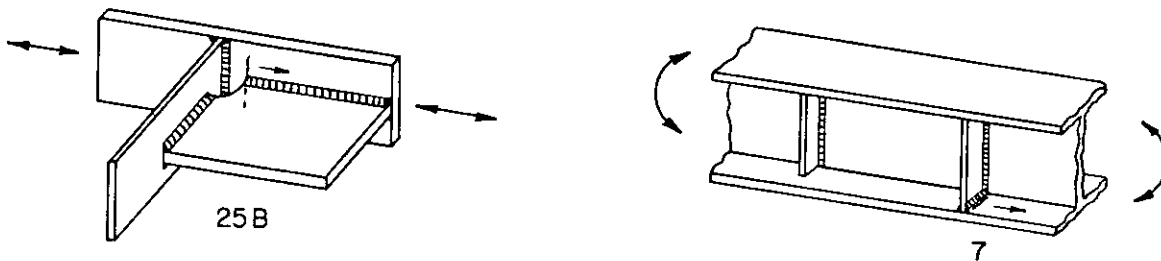
Fig. 5.3 (Cont'd) Examples of Relationship Between Ship Structure Details and Local Fatigue Details.



(d) Tripping Bracket 2C6



(e) Possible Fatigue Critical Location In Tripping Bracket 2C6



(f) Local Fatigue Details Number 7 and 25B

Fig. 5.3 (Cont'd.) Examples of Relationship Between Ship Structure Details and Local Fatigue Details.

bracket in fatigue can then be evaluated. This is basically the process used to provide a fatigue design (verification of adequacy) of ship structure details. It is important to note that the direction of stressing must be the same in the ship structure detail and the local fatigue detail for which data are provided.

It is apparent that, because of the great duplication of local fatigue details in the ship structure details, the problem of fatigue design for ship structure details will be greatly simplified. The catalog of ship structure details in Appendix A and the pre-identification of the local fatigue details should also make possible the development of relative ratings for many of the ship details in a given family and eventually simplify the designer's initial selection process for such details.

5.4 Fatigue Cracking in Ship Details

Fatigue cracks have been observed in the various types of ships and at various locations throughout the ships. In a report entitled "Hull Damages on Large Swedish Built Ships," 85 ships were studied for damage; damage caused by collision was excluded (5.6). Three basic types of damage were identified and have been classified as cracks, deformations, and corrosion. Of the 3161 areas of damage reported, 2227, or 70.45%, were cracks. Of these 2227 cracks, 1135, or 50.97%, were located in bracketed connections; 1907, or 85%, of the cracks were found in the cargo space, with a majority in the lower part of the ship. Oil tankers contained a disproportionate number of the damaged areas, many more than the other three ship types studied. The results of the Swedish survey show a good correlation with the results of the survey reported in SSC Report No. 272 (5.1); however, the SSC report included damage resulting from collision as well as buckling and cracking. Of the 3307 damaged locations reported in SSC 272, 1297, or 39.22%, were found in beam bracket connections and 358, or an additional 10.83%, were found in tripping brackets. In general, cracks tended to develop near the exterior of the ship, the exterior being the side shell, the bottom plating and the main deck.

Unfortunately, many of the fatigue cracks discussed in various reports are not well illustrated. Often, only the general location of a crack is indicated without regard to direction or position. However, a variety of diagrams showing crack locations are reproduced in Appendix C. These should be of assistance in identifying some of the critical fatigue locations in ship structure details. The cracks have been identified further in terms of the families of ship details. They also identify possible critical locations in the ship detail and are the types of cracks that proper fatigue design will help to minimize.

The two SSC reports on the in-service performance of structural ship details (5.1 and 5.2) have clearly helped to define possible fatigue critical locations in ships and to show the seriousness of the cracking problems. In addition, the identification of crack locations has helped to identify the types of "local fatigue details" for which fatigue resistances are required. These details are summarized in Table 5.1, along with an indication of the local fatigue details for which fatigue data or estimates of fatigue resistance are available. Not all details have been studied, and so additional

TABLE 5.1

Cracked Fatigue Details and Data Availability

<u>Detail No.</u>	<u>Total No. of Detail Classifications at Cracks*</u>	<u>Fatigue Data Available (or estimates of fatigue strength)</u>
7	272	Yes
9	7	Yes
14	7	Yes
17	2	Yes
17S	2	Yes
19	42	Yes
19S	40	Yes
20	318	Yes
21	1300	Yes
21S	54	Yes
26	155	Yes
28	208	Yes
28F	222	Yes
29	9	No
29R	3	No
29F	7	No
30	142	Yes
30A	672	Yes
32B	2	Yes
33	36	Yes
33S	20	Yes
34	23	No
34S	17	No
36	600	Yes
37	462	No
38	8	Yes
40	2	Yes
41	11	No
42	7	Yes
43	75	No
44	14	No
47	29	No
48R	25	No
50	2	No
51	687	Yes
52	105	Yes
53	8	No

* Multiple detail classifications (two or at most three) are often indicated for a single crack because the specific crack location can not be identified.

TABLE 5.2

Summary of Data for 12 Detail Families

Family No.	Detail Family Name	Totals Observed		
		Total No. Details	Total No. Failures	% Failures
1	Beam Bracket	68586	2252	3.28
2	Tripping Bracket	34012	1587	4.67
3	Non-Tight Collar	20974	33	0.16
4	Tight Collar	20654	46	0.22
5	Gunwale Connection	172	5	2.91
6	Knife Edges	0	0	-
7	Miscellaneous Cutouts	296689	853	0.29
8	Clearance Cutouts	57307	843	1.47
9	Deck Cutouts	7534	29	0.38
10	Stanchion Ends	7090	122	1.72
11	Stiffener Ends	40729	298	0.73
12	Panel Stiffeners	53837	788	1.46
TOTALS		607584	6856	1.13

investigations and/or fatigue analyses are needed to provide the required basic fatigue design data. (Results of tests conducted on details 21, 30A, 51 and 52 are reported in Appendix F.) The fatigue strengths determined from these tests are presented in Table B.1 of Appendix B, along with the fatigue strengths for the many other details.

An indication of the extent of failures in the 86 ships reported in references 5.1 and 5.2 is presented in Table 5.2. The percentage of the twelve family details showing failures does not appear to be large. However, the total number of failures reported is 6856 and is a significant number, a number that can be reduced greatly by the introduction of appropriate fatigue design requirements. It is toward this end that Sections 6 and 7 have been developed.

5.5 References

- 5.1 Jordan, C. R. and Cochran, C. S. "In-Service Performance of Structural Details," SSC-272, 1978.
- 5.2 Jordan, C. R. and Cochran, C. S. "Further Survey of In-Service Performance of Structural Details," SSC-294, 1980.
- 5.3 Glasfeld, R., Jordan, D., Ken, M., Jr. and Zoller, D. "Review of Ship Structure Details," SSC-266, 1977.
- 5.4 General Dynamics Corporation, Quincy Shipbuilding Division. "A Report of Research Conducted Under Marad Task S-11 of the Ship Producibility Research Program to Determine the Value of Standard Structural Arrangements."
- 5.5 Committee III.1 Report, Proceedings of the Seventh International Ship Structures Congress, Paris, August 1979.
- 5.6 Kjellander, S. L. "Hull Damages on Large Swedish-Built Ships," Styrelsen för teknisk utveckling, Report No. 70-1272/U 981, Stockholm, Sweden, December 1972.

6. SHIP LOADING HISTORIES

6.1 Ship Loads

The types of loadings which are of primary concern in fatigue are those which are cyclic in nature and applied numerous times. Hence, loads such as those experienced in launching the ship, in ship collisions and in ship groundings are not considered here; they would be of concern in the basic design of the ship. The four main categories of cyclic loads to be considered are tabulated below along with the estimated cycles of load reversals in a typical ship's lifetime (6.1):

<u>Loading Category</u>	<u>Cycles</u>
(1) Low frequency, wave-induced (quasi-static)	$10^7 - 10^8$
(2) High frequency (dynamic)	10^6
(3) Still water	340
(4) Thermal	7,000

There may also be certain portions of a ship that are periodically subjected to other specific loadings not noted above, but which can be expected to cause fatigue damage. These too should be included in the loading history for those details when they are evaluated. A brief discussion of the characteristics of each loading category follows. For a more detailed discussion the reader is referred to the literature (6.1 through 6.18).

6.1.1 Low Frequency Wave-Induced Loading (Quasi-Static)

Low frequency wave-induced loads are considered to be those caused by waves. These loads vary irregularly with an average period of 5 to 10 seconds, depending on the type of ship (6.1).

Some of the factors known to affect the wave loading are as follows (6.2, 6.3):

- (1) Ship SWBM, draft and trim.
- (2) Ship speed.
- (3) Ship heading.
- (4) Sea conditions.

In a study of dry cargo vessels, Lewis (6.4, 6.6) suggests that ship loading condition and ship speed have little effect on wave bending moments, and are not as significant as sea conditions. Hence, the sea conditions

encountered during the life of a ship are probably of basic importance in its wave-induced loading history.

6.1.2 High Frequency Loading (Dynamic)

The record of ship response in Fig. 6.1 shows high frequency dynamic stresses that are superimposed on the low frequency wave-induced stress variations. Such high frequency loadings are important in terms of the manner in which they add to the wave-induced stresses to establish the maximum stress ranges (see Fig. 6.1(a)), but are of little significance in terms of the high frequency small stress fluctuations shown in Fig. 6.1 (c).

High frequency loadings can generally be subdivided into two categories based on the nature of the excitation: transient and steady-state (6.1). A transient dynamic loading is generally attributed to loadings such as slamming and whipping. Nibbering (6.5) defines a slam as "any load causing vertical two node vibration of a ship," and is usually caused by bottom impact or bow flare immersion. Slamming usually refers to the initial effect of a wave-ship impact, while whipping refers to the hull vibration subsequent to the slam (6.6).

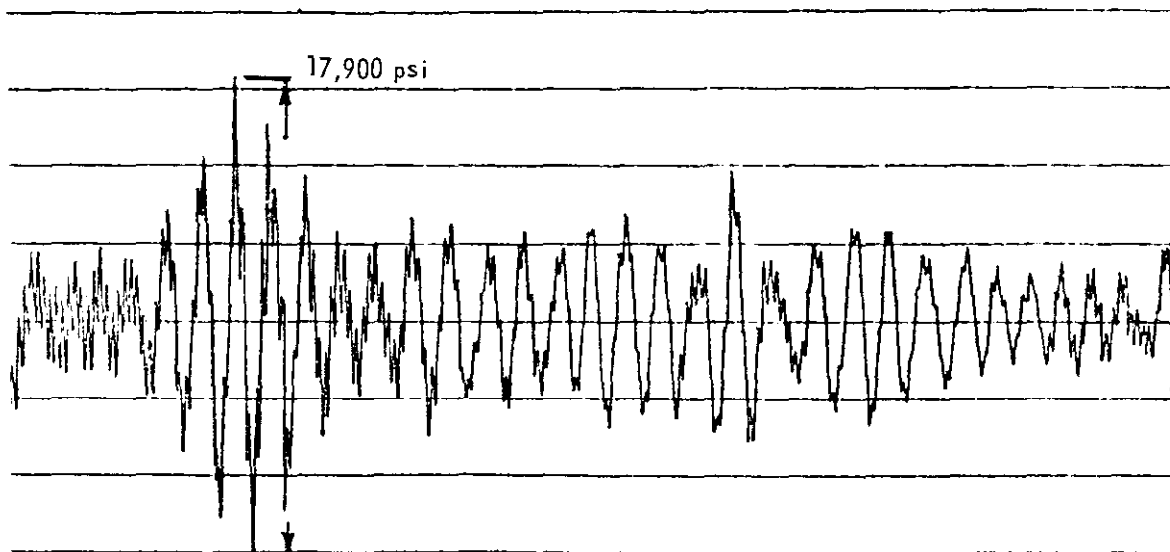
Since severe slamming can often be avoided or minimized by a reduction in speed and/or a change in course, the amount and severity of slamming experienced by a ship is, to some extent, controlled by the shipmaster (6.5, 6.6). In this respect, slamming loads differ from the low frequency wave loading in that they are relatively independent of sea conditions. This is due to the fact that ships are normally forced to reduce speed in the rough seas which are generally responsible for the slamming (6.1).

Steady-state dynamic loadings can be either self-excited by the ship's machinery or propellers, or externally excited by the waves (6.7). Wave-excited steady-state response is usually referred to as springing.

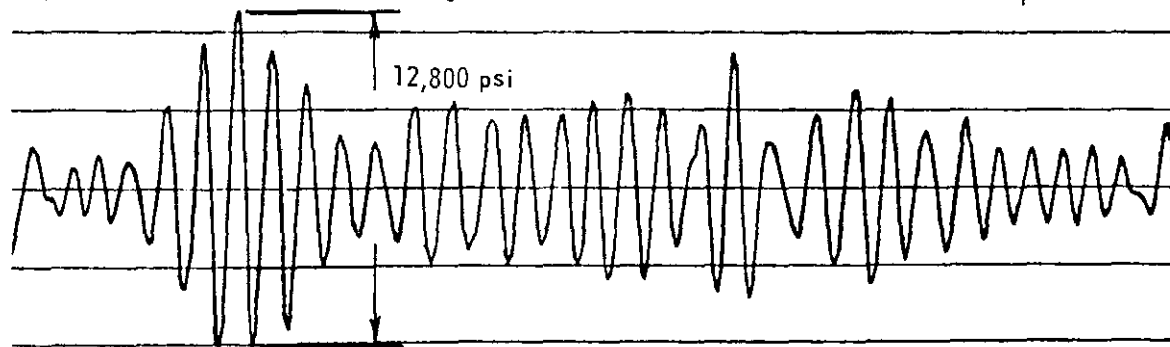
6.1.3 Still Water Loading

Still water loads due to ship weight and buoyancy represent the fluctuating mean values about which the wave loads vary. These mean loads vary gradually during a voyage (Fig. 6.2) as fuel is consumed and as ballast is added or shifted. There may also be large variations in still water loading from voyage to voyage, depending on the loading condition and the distribution of the cargo (6.1).

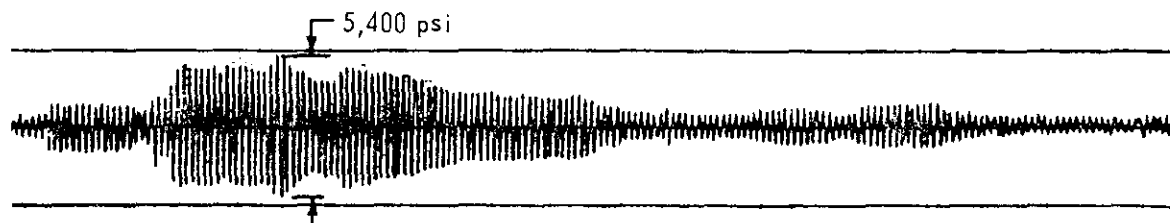
High speed ships may also experience variations in bending moments as a result of the ship's own wave. A significant sagging moment can be created by the bow and stern waves. This loading, induced by the ship's own wave train, can be considered as a component of the still water bending moment (6.6).



a) Total Stress Variations Including Both Wave-Induced and First-Mode Stress Components



b) Wave-Induced Stress Variations (Frequency Approx. 0.1 Hz)



c) First-Mode (Springing) Stress Variations (Frequency Approx. 0.70 Hz)

Fig. 6.1 Typical Record of Midship Stress Variation, M. V. Fotini L, Showing Filtered Wave-Induced and Dynamic Stresses (6.1).

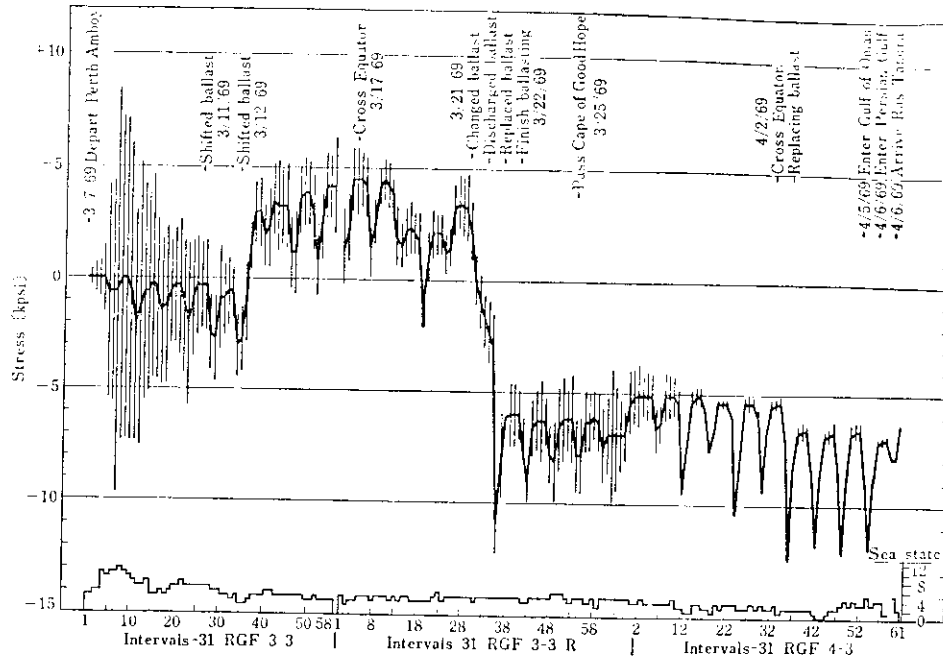


Fig. 6.2 Typical Voyage Variation of Midship Vertical Bending Stress, R. G. Follis (6.20).

6.1.4 Thermal Loading

Thermal stresses are induced in ship structures by the presence of an irregular thermal gradient and can be considered as a type of loading. The thermal gradient in a ship depends on the weather, sea-air temperature differential and exposure to the sun. Consequently, the thermal-load variation generally follows the diurnal changes in air temperature (6.1). This type of effect is evident in the stress history shown in Fig. 6.2.

Thermal stresses may also exist in localized areas of the ship due to heated or cooled (refrigerated) cargoes (6.6).

6.2 Measurement of Ship Response

In recent years, considerable research has been conducted to study or determine ship response, primarily in the midship region and under service conditions. The research has involved full-scale ship stress collection programs, model tests and theoretical analyses. The full-scale studies provide a means for verifying results obtained in model testing and theoretical analyses. One of the aims of the research has been to develop reliable theoretical calculation procedures so that costly model testing and full-scale data collection programs can be eliminated (6.8).

This study uses actual stress histories as measured in three full-scale ship instrumentation programs: the Dry Cargo Vessel Research Program, the Large Tanker and Bulk Carrier Research Program and SL-7 Research Program. A primary purpose of these programs was to obtain midship bending stress data and to study long-term statistical trends (6.4, 6.9, 6.10).

The characteristics of the nine vessels involved in these full-scale programs are given Tables 6.1, 6.2 and 6.3.

6.3 Ship Loading Stress Histories

6.3.1 Low Frequency Wave-Induced Load Histories

Much of the research in the Dry Cargo, Large Tanker and Bulk Carrier programs has involved wave-induced loading. In these programs the dynamic stress components are generally filtered out of the stress record leaving only those stresses due to wave-induced bending as shown in Fig. 6.1(b). Both the short-term and long-term trends of the wave-induced stresses can be studied in such records.

The short-term load history consists of the distribution of stress variations (usually peak-to-peak values) over a short period of time, on the order of one hour, during which ship speed, ship heading and sea state are assumed to be constant (6.14, 6.15). It has been observed that short-term load histories may be closely approximated by Rayleigh distributions (6.16, 6.14, 6.2, 6.15). An example of a short-term stress histogram along with the corresponding Rayleigh distribution is given in Fig. 6.3.

TABLE 6.1

Characteristics of Ships in Dry Cargo Vessel Program (6.11)

	<u>WOLVERINE STATE</u>	<u>MORMACSCAN</u>	<u>CALIFORNIA BEAR</u>
Type:	C-4-S-B5 Machinery-Aft Dry Cargo Vessel	1624 Machinery Amidships Dry Cargo Vessel	C4-S-1A Standard Mariner Dry Cargo Vessel
Builder:	Sun Shipbuilding and Drydock Company, Chester, PA	Sun Shipbuilding and Drydock Company, Chester, PA	Bethlehem Pacific Coast Steel Co. Shipbuilding Division San Francisco, CA
Date:	September 1945	October 1960	February 1954
Hull Number:	359	622	5463
Length Overall:	520' - 0"	483' - 3"	563' - 7 3/4"
Length Between Perp.:	496' - 0"	458' - 0"	528' - 6"
Beam, Molded:	71' - 6"	68' - 0"	76' - 0"
Depth, Molded:	54' - 0"	41' - 6"	44' - 6"
Load Draft, Molded, Design:	30' - 0"	28' - 6"	27' - 0"
Load Draft, Keel:	32' - 9 7/8"	31' - 5"	29' - 10 1/16"
Gross Tonnage:	10,747 L. T.	9,315 L. T.	9,216 L. T.
Net Tonnage:	6,657 L. T.	5,609 L. T.	5,366 L. T.
Midship Section Modulus:	45,631 in. ² ft. (to top of upper deck)	30,464 in. ² ft. (to top of upper deck)	43,900 in. ² ft. (to top of upper deck)
Light Ship Weight:	6,746 L. T.	5,882 L. T.	7,675 L. T.
Dead Weight at Load Draft:	15,348 L. T.	12,483 L. T.	13,418 L. T.
Propeller, Normal Operating RPM:	80	93	85
Shaft Horsepower, Normal:	9,000	11,000	17,500
Shaft Horsepower, Maximum:	9,900	12,000	19,250

TABLE 6.2

Characteristics of Vessels in Large Tanker and Bulk Carrier Program (6.12)

Ship:	<u>Idemitsu Maru</u>	<u>Fotini L</u>	<u>R. G. Follis</u>	<u>Eso Malaysia</u>	<u>Universe Ireland</u>
Owner:	Idemitsu	Seres	Chevron	Eso	NBC
Type:	Tanker	Bulk Carrier	Tanker	Tanker	Tanker
Approximate dwt, tons:	206,106	74,203	66,500	190,800	326,585
Overall Length, ft.:	1,122	820	784.12	1,062.15	1,135.17
L_{BP} , ft.:	1,069.25	800	754.6	1,000	1,076
Breadth, ft.:	163.25	106	104.46	154.76	174.87
Depth, ft.:	76.08	60.04	57.58	77.76	105
Design Draft (keel), ft-in.:	58-0½	44-6½	44-4¾	60-5½	81-5
Builder:	Ishikawajima Harima	Hakodate	Hitachi	Kieler Howaldtswerke	Ishikawajima Harima
Block Coefficient (L_{WL}):	0.83	0.84	0.82	0.83	0.86
Section modulus, top, in. ² -ft.:	417,224	158,556	170,900	404,000	566,794

TABLE 6.3

Characteristics of Sea-Land McLean
 (Typical of Vessels in SL-7 Program) (6.13)

Name:	SEA-LAND McLEAN
Builder:	Rotterdam Dry Dock (HULL 330)
Class:	SL-7 Containership
Length, overall:	946' 1½"
Length, between perpendiculars:	880' 6"
Beam, molded:	105' 6"
Depth to main deck, forward:	64' 0"
Depth to main deck, aft:	68' 6"
Draft, design:	30' 0"
Draft, scantling:	34' 0"
Dead weight - long tons:	27,315
Displacement (34' 0" draft)- long tons:	50,315
Machinery:	Two separate cross-compound steam turbines driving two propeller shafts.
Shaft horsepower-maximum continuous, both shafts:	120,000
Propeller RPM:	135
Speed, maximum, knots:	33
Center of gravity - full load:	399.32' forward of aft perpendicular 42.65' above base line.

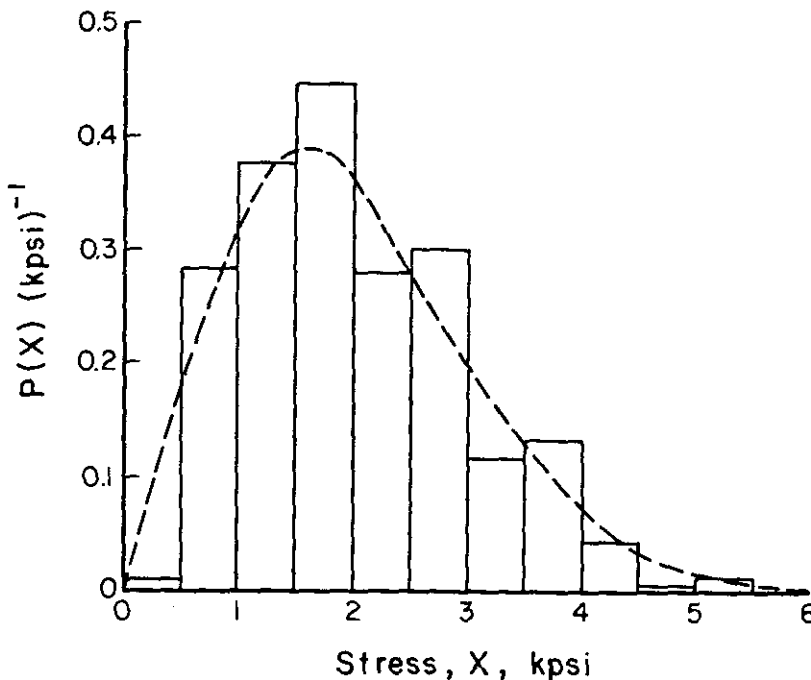


Fig. 6.3 Comparison of Stress Histogram for One Typical Record with Ideal Rayleigh Curve, Wolverine State (6.17).

The long-term load history, which is of paramount concern in fatigue analysis, consists of the distribution of stress variations over a longer period of time in which a variety of ship speeds, ship headings and sea states are experienced (6.14). Since there is a limited amount of full-scale "long-term" ship loading data available, and then only for a limited length of time, it is necessary to extrapolate over an extended period of time to obtain the lifetime wave-induced load spectrum (6.14, 6.4, 6.15, 6.2). While these extrapolations have been developed to predict extreme stress values for the design of the hull girders, they also provide random stress distributions that can be used for fatigue considerations.

These extrapolated long-term stress histories are commonly plotted on semi-log cumulative distribution diagrams. Diagrams of this type for Large Tankers and Dry Cargo Vessels are shown in Figs. 6.4 and 6.5, respectively.

6.3.2 Complete Stress Histories

The construction of a complete ship loading history requires consideration of stresses due to still water, thermal and dynamic effects in addition to low frequency wave-induced stresses discussed in the previous section.

As noted earlier, the still water and thermal stresses are very low frequency, and their effect is primarily to shift the mean stress. These stresses will have relatively little effect on the lifetime load history (see Section 3.7 - Effect of Mean Stress).

The dynamic loads are high frequency and do contribute to fatigue damage. Hence, the problem reduces to synthesizing the dynamic and wave-induced loads into a complete load history. Although some progress has been made in this area (6.1, 6.18), the problem has not yet been completely resolved.

Nibbering (6.5) developed an approximation of a complete stress history by "correcting" the wave-induced cumulative distribution diagram for dynamic (slamming) effects as well as for other effects, such as corrosion. Figure 6.6 shows the corrections he applied to the wave-induced stress curve for the Canada.

Some full-scale ship studies, notably the SL-7 scratch gage program, include both the wave-induced and dynamic stresses on the same record. In these cases the complete load history can be assembled directly from the recorded data. Figure 6.7 is a histogram of stress data from eight SL-7 ships during a five-year period (6.10).

6.4 Selection of Probability Distributions to Describe Ship Loading Histories

The fatigue design criteria developed here requires that the complete loading history at the location of interest be presented in probabilistic terms, i.e., be represented by a probability distribution function. Consequently, it was necessary to find a distribution or distributions which

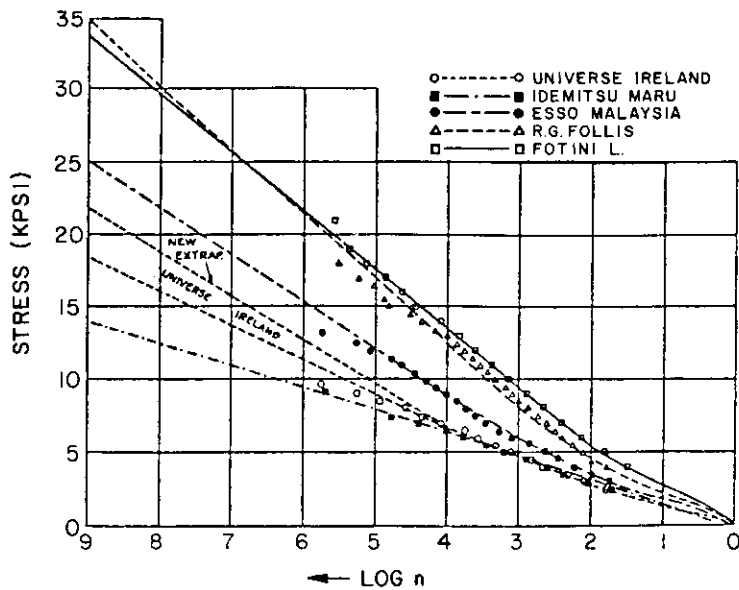


Fig. 6.4 Long-Term Distribution of Stresses in Actual Service (Fig. 8 of 6.6).

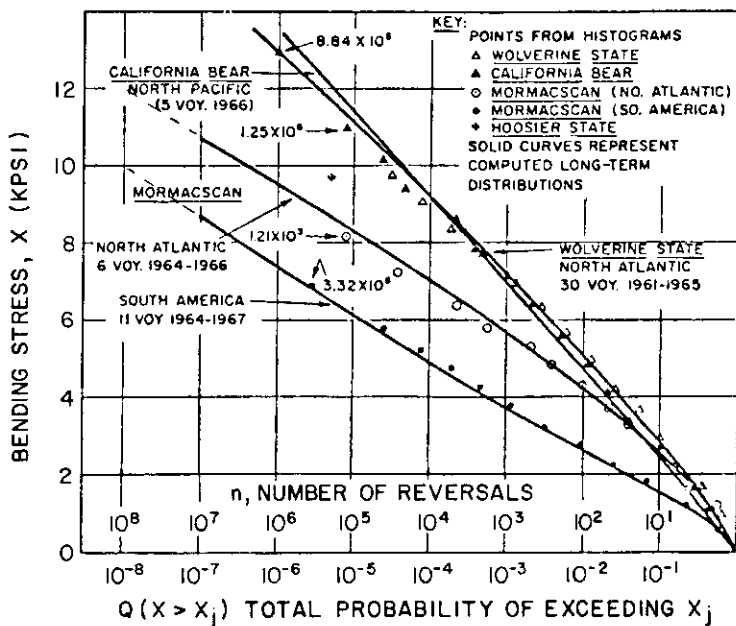


Fig. 6.5 Long-Term Trends of Stress Obtained from Histograms for Four Ships and Computed from rms Values (6.2).

DOUBLE AMPLITUDE
OF STRESS (σ)
KG/mm²

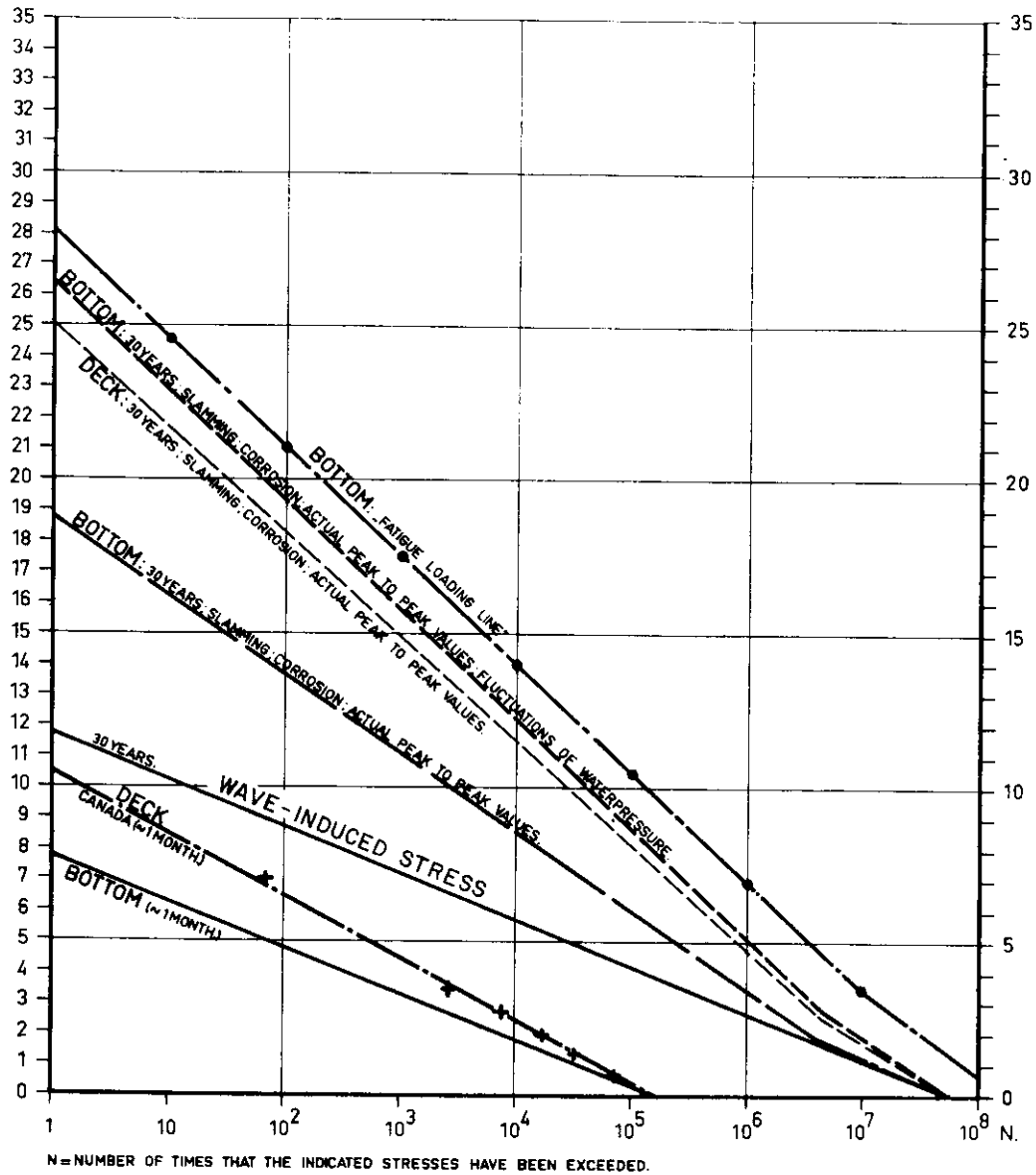


Fig. 6.6 Fatigue Loading of Bottom and Deck Structure (6.5).

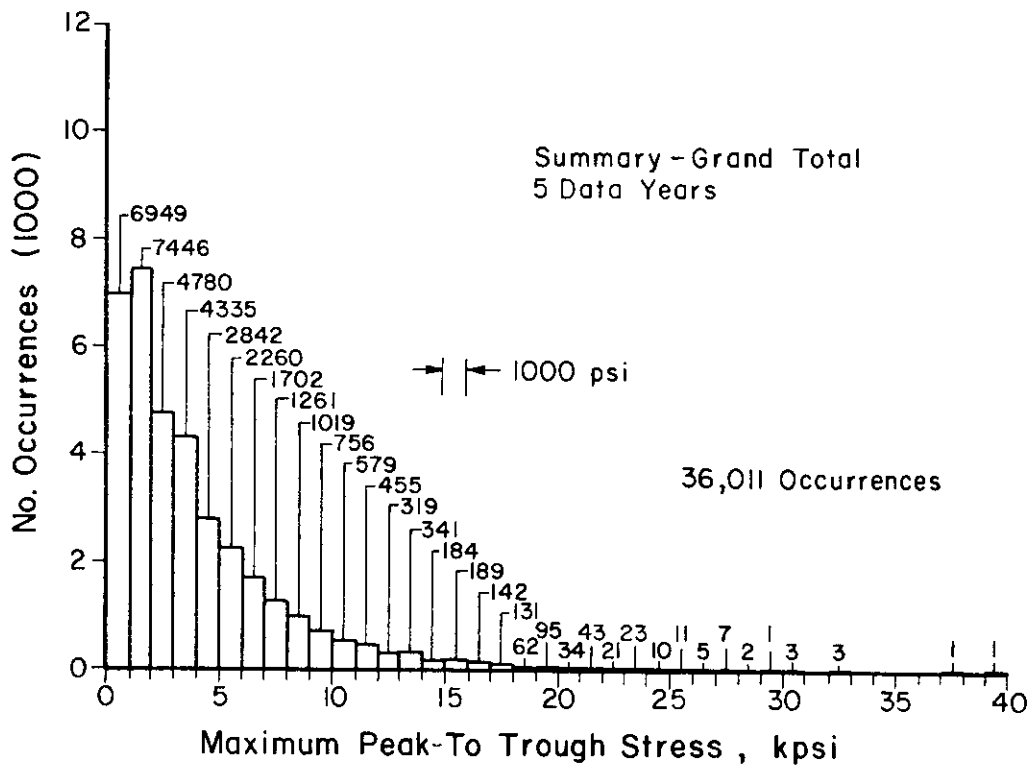


Fig. 6.7 Histogram from SL-7 Scratch Gage Data (6.10).
(One occurrence is approximately 1920 cycles.)

provide the best fit to the long-term ship loading histories found in the literature. Emphasis was placed on finding a distribution general enough to approximate the loading histories of various types of ships subjected to a variety of loading conditions.

It should be noted that it is not the intent of the authors to specify the use of a specific loading history for all ships and details, but rather to provide an indication of those distribution functions that appear to be usable for ship structures fatigue design criteria.

6.4.1 Probability Distributions

Six probability distribution functions were investigated. These consisted of the Beta, Lognormal, Weibull, Exponential, Rayleigh and a Shifted Exponential distribution function. Some of the basic properties of these distributions are given in Table 6.4, and the general shapes are shown in Fig. 6.8.

The beta distribution is a versatile function, with finite lower and upper bounds, that may be skewed in one direction or the other, depending on the relative values of the shape parameters q and r (see Fig. 6.8(a)). This distribution has been used in fatigue analyses by Ang and Munse (6.19) to model the random loadings in highway bridges subjected to heavy truck loadings. However, the beta distribution, with its upper bound limitation, does not appear to be compatible with the statistical extrapolation methods commonly used in wave spectral analysis. Hence, the beta distribution is probably not appropriate for ship structures.

The lognormal distribution is a lower bounded non-negative probability distribution with a "tail" that trails off to the right (Fig. 6.8(b)). Jasper (6.16) proposed the use of the lognormal distribution to represent the long-term trends of wave-induced stresses in ships.

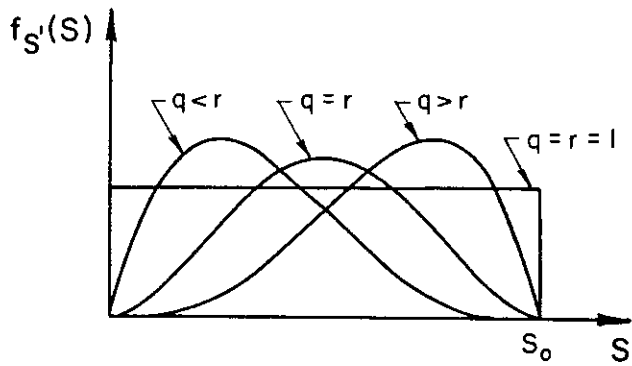
The two-parameter Weibull distribution, like the lognormal, is a lower bounded non-negative distribution with a tail to the right (Fig. 6.8(c)). However, the Weibull distribution can take on many different shapes depending on the shape parameter, k . The exponential and Rayleigh distributions (Figs. 6.8(d) and 6.8(e)) are special cases of the Weibull distribution, where $k=1$ and $k=2$, respectively. Nordenström (6.15) found that long-term distributions of waves and wave-induced structural response can be closely approximated by Weibull distributions with shape parameters close to unity, i.e., approximately exponential distributions.

The shifted exponential distribution is simply an exponential distribution which starts at a non-zero value (Fig. 6.8(f)). This distribution, which can be considered as a special case of the exponential distribution, fits many of the ship histories closely. However, the introduction of the non-zero lower bound implies that the lowest possible stress variation is a non-zero value which is not physically true and tends to complicate the analysis.

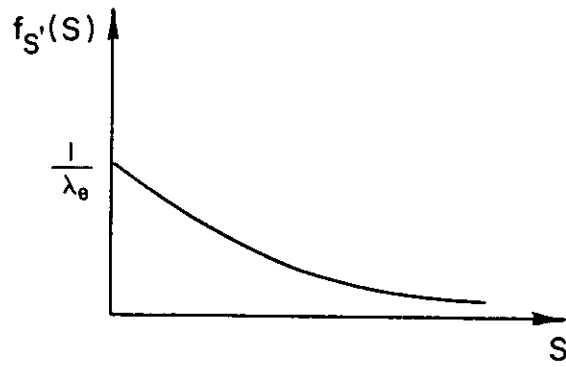
TABLE 6.4

Properties of Probability Distributions Investigated

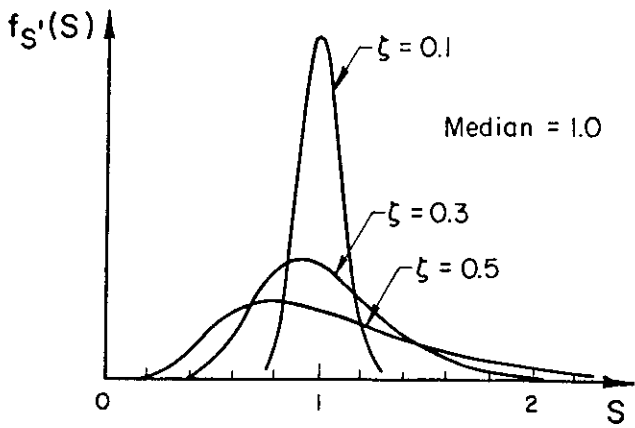
Distribution	Probability Density Function	Characteristic Parameters	Mean Stress, μ_S	Standard Deviation, σ_S
Beta	$f_S^B(s) = \frac{\Gamma(q+r)}{\Gamma(q)\Gamma(r)} \frac{s^{q-1}(s_0-s)^{r-1}}{s_0^{q+r-1}}$ $0 \leq s \leq s_0$	q, r, s_0	$\frac{qs_0}{q+r}$	$\frac{s_0}{(q+r)} \sqrt{\frac{qr}{q+r+1}}$
Lognormal	$f_S^L(s) = \frac{1}{\sqrt{2\pi} \zeta s} \exp\left[-\frac{1}{2} \left(\frac{\ln s - \lambda}{\zeta}\right)^2\right]$ $s \geq 0$	λ, ζ	$\exp\left(\lambda + \frac{1}{2}\zeta^2\right)$	$\sqrt{e^{\zeta^2} - 1} \exp\left(\lambda + \frac{1}{2}\zeta^2\right)$
Weibull	$f_S^W(s) = \frac{k}{w} \left(\frac{s}{w}\right)^{k-1} \exp\left[-\left(\frac{s}{w}\right)^k\right]$ $s \geq 0$	k, w	$w\Gamma\left(1 + \frac{1}{k}\right)$	$w\left[\Gamma\left(1 + \frac{2}{k}\right) - \Gamma^2\left(1 + \frac{1}{k}\right)\right]^{\frac{1}{2}}$
Exponential	$f_S^E(s) = \frac{1}{\lambda_e} \exp\left[-\left(\frac{s}{\lambda_e}\right)\right]$ $s \geq 0$	λ_e	λ_e	λ_e
Rayleigh	$f_S^R(s) = \frac{2}{S_{RMS}} \left(\frac{s}{S_{RMS}}\right) \exp\left[-\left(\frac{s}{S_{RMS}}\right)^2\right]$ $s \geq 0$	S_{RMS}	$\frac{\sqrt{\pi}}{2} S_{RMS}$	$\sqrt{1 - \frac{\pi}{4}} S_{RMS}$
Shifted Exponential	$f_S^{SE}(s) = \frac{1}{\lambda_e} \exp\left[-\left(\frac{s-a}{\lambda_e}\right)\right]$ $s \geq a$	λ_e, a	$\lambda_e + a$	λ_e



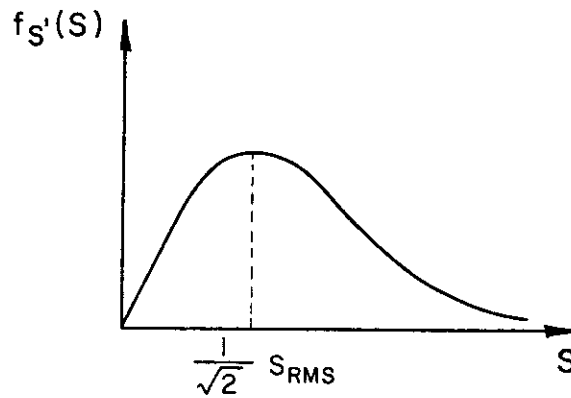
(a) Beta Distributions



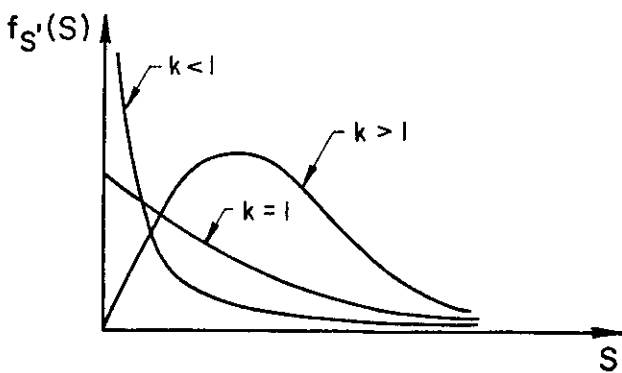
(d) Exponential Distribution



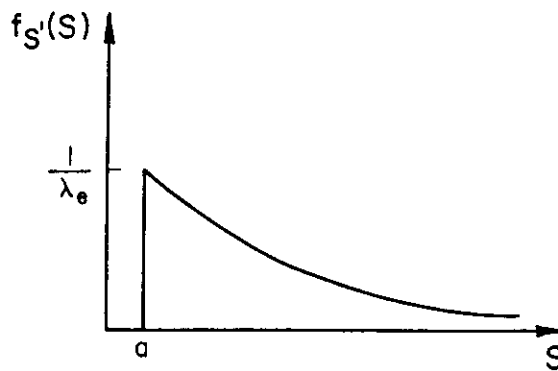
(b) Lognormal Distributions
(Fig. 3.8, Ref. 6.21)



(e) Rayleigh Distribution



(c) Weibull Distributions



(f) Shifted Exponential Distribution

Fig. 6.8 Shapes of Probability Density Functions (see Table 6.4 for Probability Density Functions).

6.4.2 Comparison of Probability Distributions with Long-Term

Loading Histories

A study of alternative long-term probability distributions was made by Lewis (6.20) utilizing the extensive data base existing for the Wolverine State. The long-term distribution indicated by the actual stress data was compared with long-term extrapolations based on various probability distributions. The results shown in Fig. 6.9 clearly indicate that the Weibull and normal distributions give excellent agreement with the actual data. Nördenstrom, in reference 6.15, indicates a preference for the use of the Weibull distribution rather than the normal or lognormal distributions to describe long-term wave-induced load histories.

As a result of these studies it was decided to compare also the long-term wave-induced load histories of ships in the Large Tanker and Dry Cargo vessel programs with Weibull distributions. The results are plotted in Fig. 6.10. In this presentation the maximum loading, a bending stress range function of 1.0, is expected to be reached once in 10^8 cycles of loading. It appears that all the loading histories can be approximated by Weibull distributions with the shape factor, k , in the range of 0.7 to 1.3 (Table 6.5).

One obvious trend noted in this study is that the large ships (tankers and bulk carriers) tend to have loading shape parameters less than or equal to 1.0 while the smaller ships (dry cargo) tend to have loading shape parameters greater than or equal to 1.0.

The stress value at a probability of exceedance of 10^{-8} , ($s_{10^{-8}}$), was found to vary considerably among the ships in each category. For example, the Idemitsu Maru and Esso Malaysia have very similar distribution characteristics (see Table 6.5), but their respective $s_{10^{-8}}$ values are 12.3 ksi and 21.8 ksi. These differences are apparently due to the different sea conditions encountered by each ship and possibly to differences in design.

The above analysis supports the use of the Weibull distribution to describe long-term wave-induced loading. However, as noted in Section 6.3.2, complete loading histories including dynamic effects should be used in the fatigue analysis. It is difficult, at this time, to establish whether the Weibull distribution accurately describes the complete load history of a ship because a satisfactory method for synthesizing all of the appropriate loading spectra has not yet been developed (6.18). Still, there does appear to be some evidence that the Weibull distribution would be appropriate for the complete loading history.

From an inspection of Fig. 6.6 it can be seen that Nibbering's fatigue loading curves for the Canada, with corrections for slamming (and other) effects, can be approximated by a Weibull distribution with $k = 1.0$. A further test of the applicability of the Weibull distribution to a complete load history was made utilizing the SL-7 scratch gage data which includes both wave-induced and first- (or higher) mode vibratory stresses (6.10). The appropriate Weibull distribution is determined for the SL-7 histogram of Fig. 6.7 in Appendix D and is compared with the histogram in Fig. 6.11. This figure shows excellent agreement between the histogram and the Weibull distribution.

TABLE 6.5

SHIP LOADING HISTORIES COMPARED WITH WEIBULL DISTRIBUTIONS

Type of Ship	Name of Ship	Notes	Weibull Load Shape, k	Stress at Probability of Exceedance = 10^{-8} , S_{10^8} (ksi)
Dry Cargo	<u>Wolverine State</u>	1,5	1.2	16.5
	<u>California State</u>	1,5	1.0	18.0
	<u>Mormacscan</u>	1,5,7	1.3	12.0
	<u>Mormacscan</u>	1,5,8	1.0	10.0
Large Tankers	<u>Idemitsu Maru</u>	2,5	1.0	12.3
	<u>R. G. Follis</u>	2,5	0.8	30.0
	<u>Esso Malaysia</u>	2,5	0.8	21.8
	<u>Universe Ireland</u>	2,3,5	0.7	18.7
Bulk Carrier	<u>Fotini L.</u>	2,5	0.9	29.5
SL-7 Container-ships	See Note 9	4,6,9	1.2	34.1

Notes:

- 1) Data from ref. 6.2.
- 2) Data from ref. 6.12.
- 3) Data from ref. 6.6.
- 4) Data from ref. 6.10.
- 5) Load history is for wave-induced loading with dynamic effects filtered.
- 6) Load history is for wave-induced loading with dynamic effect included.
- 7) Load history based on North Atlantic voyages.
- 8) Load history based on South American voyages.
- 9) Load history based on data collected from eight SL-7 container-ships (see Appendix D).

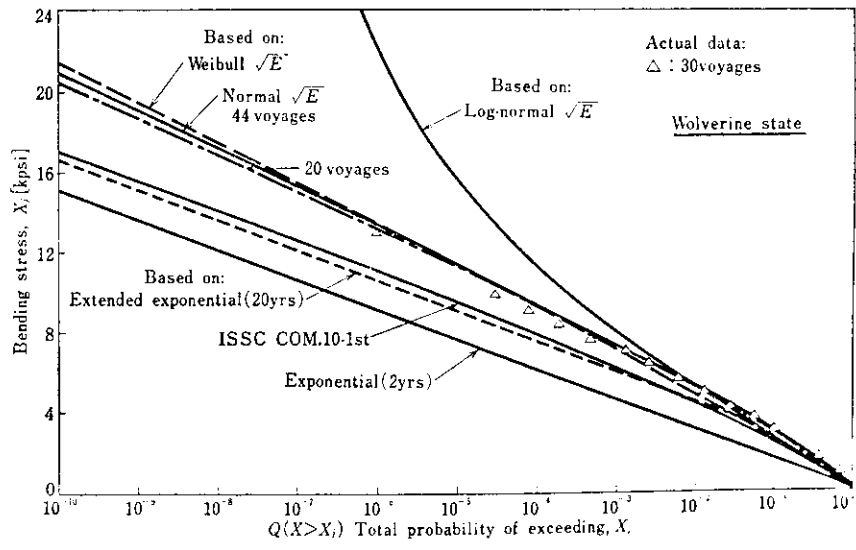


Fig. 6.9 Long-Term Stress Distributions by Different Methods (6.20).

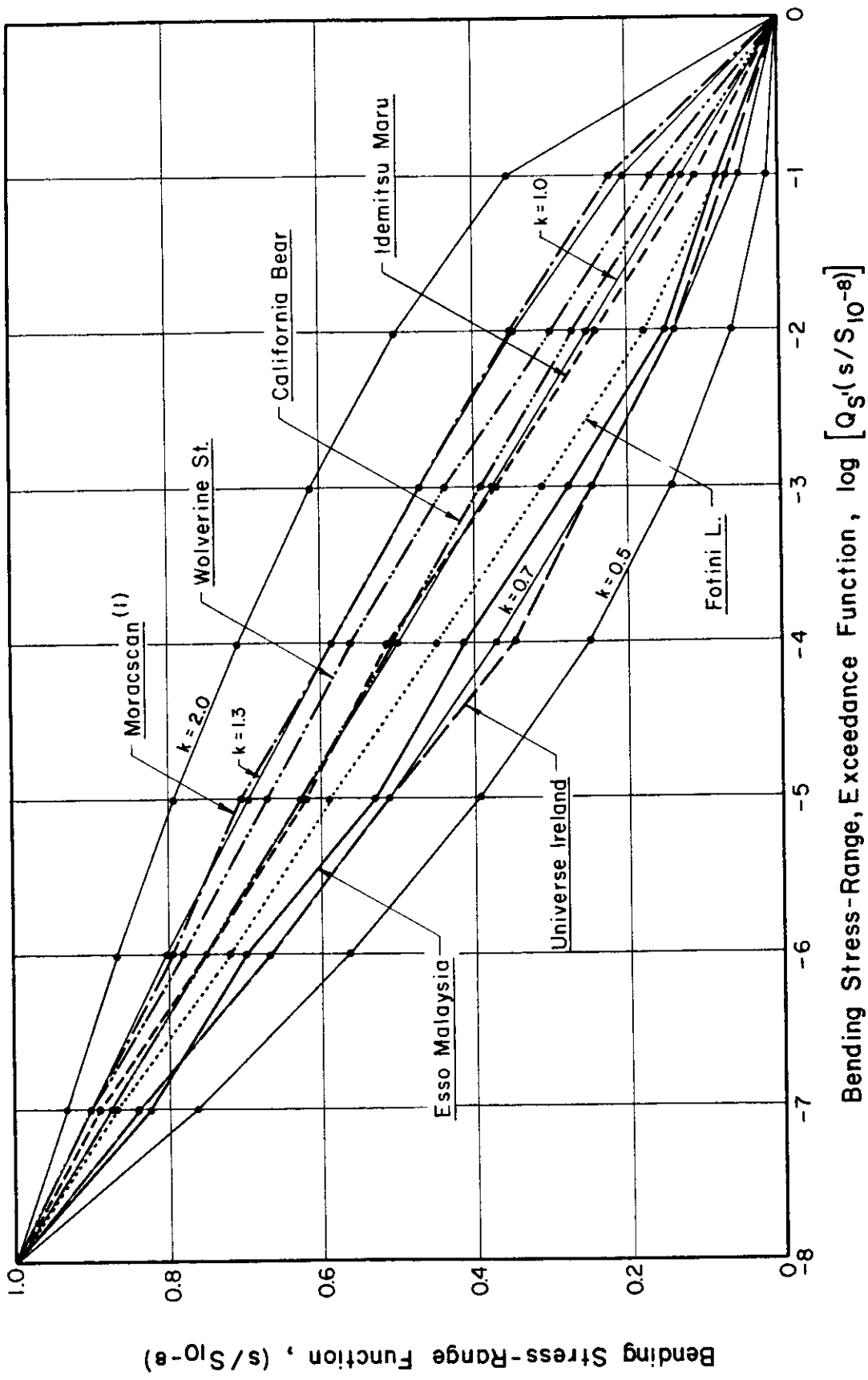


Fig. 6.10 Loading Histories of Large Tankers, Bulk Carriers and Dry Cargo Vessels Compared with Weibull.

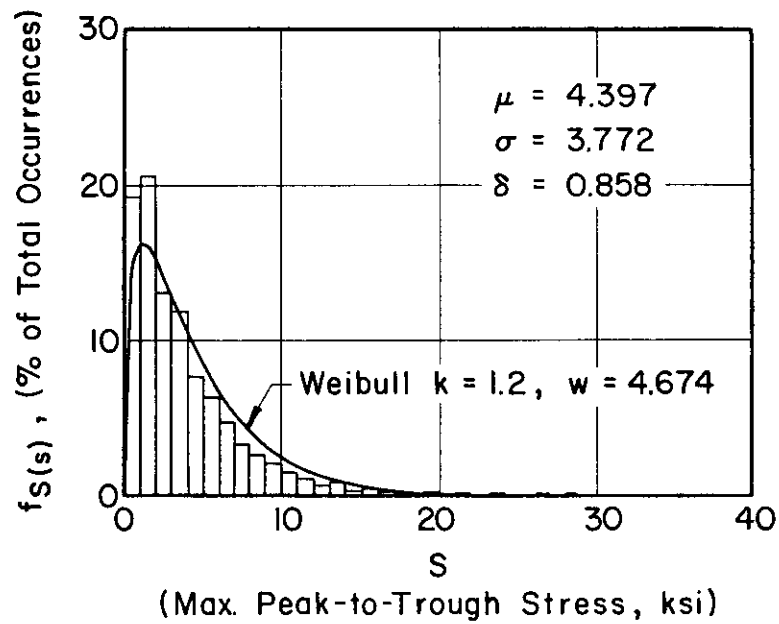


Fig. 6.11 SL-7 Scratch Gage Data with Corresponding Weibull Distribution (6.10).

6.5 References

- 6.1 Lewis, E. V., Van Hoof, R., Hoffman, D., Zubaly, R. B. and Maclean, W. M. "Load Criteria for Ship Structural Design," SSC Report No. 240, 1973.
- 6.2 Hoffman, D. and Lewis, E. V. "Analysis and Interpretation of Full-Scale Data on Midship Bending Stresses of Dry Cargo Ships," SSC-196, June 1969.
- 6.3 Lewis, Edward V. and Zubaly, Robert B. "Predicting Hull Bending Moments for Design," Proceedings, Extreme Loads Response Symposium, SSC and SNAME., October 19-21, 1981.
- 6.4 Lewis, E. V. "Predicting Long-Term Distributions of Wave-Induced Bending Moment on Ship Hulls," SNAME Spring Meeting, March 1967.
- 6.5 Nibbering, J. J. W. "Fatigue of Ship Structures," ("Vermoeiing Van Scheepsconstructies") Netherlands Research Centre T.N.O. for Shipbuilding and Navigation, Report No. 55S, September 1963.
- 6.6 Lewis, E. V. and Zubaly, R. B. "Dynamic Loadings Due to Waves and Ship Motions," SNAME, 1975.
- 6.7 "Structural Test of the Philip Schuyler," US Maritime Commission Report, (unpublished).
- 6.8 Siekierka, W. J., Johnson, R. A. and CDR Loosmore, C. S., USCG. "SL-7 Instrumentation Program Background and Research Plan," SSC Report No. 257, 1976.
- 6.9 Fritch, D. J., Bailey, F. C. and Wheaton, J. W. "Results From Full-Scale Measurements on Midship Bending Stresses on Two Dry-Cargo Ships-Report #2." SSC-181, March 1967.
- 6.10 Fain, R. A. and Booth, E. T. "Results of the First Five 'Data Years' of Extreme Stress Scratch Gauge Data Collected Aboard Sea Land's SL-7's," SSC-286, March 1979
- 6.11 Walters, I. J. and Bailey, F. C. "Results from Full-Scale Measurements of Midship Bending Stresses on Three Dry Cargo Ships," SSC-209, 1970.
- 6.12 Little, R. S., Lewis, E. V. and Bailey, F. C. "A Statistical Study of Wave Induced Bending Moments on Large Oceangoing Tankers and Bulk Carriers," Trans. SNAME, 1971.
- 6.13 Fain, R. A. "Design and Installation of a Ship Response Instrumentation System Aboard the SL-7 Class Containership Sea-Land McLean," SSC-238, 1973.
- 6.14 Fritch, D. J., Bailey, F. C. and Wise, N. S. "Preliminary Analysis of Bending Moment Data from Ships at Sea," SSC-153, December 27, 1963.
- 6.15 Nordenström, N. "A Method to Predict Long-Term Distributions of Waves and Wave-Induced Motions and Loads on Ships and Other Floating Structures," Det Norske Veritas, Publ. No. 81, April 1973.
- 6.16 Jasper, N. H. "Statistical Distribution Patterns of Ocean Waves and of Wave Induced Ship Stresses and Motion with Engineering Applications," The Catholic University of America Press, Washington, D. C., 1956.

- 6.17 Fritch, D. J., Bailey, F. C. and Wise, N. S. "Results from Full-Scale Measurements of Midship Bending Stresses on Two C-4-5-B5 Dry-Cargo Ships Operating in North Atlantic Service," SSC-164, September 1964.
- 6.18 Dalzell, J. F., Maniar, N. M. and Hsu, M. W. "Examination of Service and Stress Data of Three Ships for Development of Hull Girder Load Criteria," SSC-287, April 1979.
- 6.19 Ang, A. H.-S. and Munse, W. H. "Practical Reliability Basis for Structural Fatigue," ASCE National Structural Engineering Conference, April 14-18, 1975. (Preprint No. 2494).
- 6.20 Lewis, Edward V. "The Reliability Approach to Ship Structural Design," Tokyo, 1975.
- 6.21 Ang, A. H.-S. and Tang, W. H. "Probability Concepts in Engineering Planning and Design," Volume I-Basic Principles, Wiley, 1975.

7. DEVELOPMENT OF SHIP STRUCTURE FATIGUE DESIGN CRITERIA

As noted earlier, the principal objective of this investigation is the development of a ship structure fatigue design criteria. Although a variety of factors have been considered in developing the design criteria, only the three most important factors (those considered to have the greatest effect on the fatigue behavior) have been included. These are (a) the mean fatigue resistance of the local fatigue details, (b) a "Reliability Factor" (factor of safety) that is a function of the slope of the S-N curve, level of reliability, and a coefficient of variation (see Section 7.3) and (c) a "Random Load Factor" that is a function of the expected loading history and slope of the S-N curve (see Section 7.4).

7.1 S-N Relationships

The mean fatigue resistance of the local fatigue details, the basic information used for design, is presented in Table B.1 (Appendix B). The values in the table are based on laboratory test data and presented in terms of stress range; the secondary effects of mean stress (including residual stresses, stress shift due to temperature changes, etc.), and in most cases the type of steel (mild, high strength low alloy, or quenched and tempered) have been neglected, except to the extent they are included in the "Reliability Factor."

Because of the relatively small differences in fatigue strength for details of various steels (see Section 3.4), and the magnitude of scatter generally obtained in fatigue data, it is considered appropriate to neglect any material factor in fatigue design of most details. Similarly, because of the complexities caused by a consideration of mean stress and the relatively small magnitude of the mean stress effect (see Fig. 3.2), it is recommended that this factor also be neglected in design; low or compressive mean stresses will make the design process a little conservative and high mean stresses a little less conservative. Thermal effects, residual stresses, shifting of ballast, distribution and magnitude of cargo, consumption of fuel, etc., all affect the mean stress, sometimes increasing it and in other instances decreasing it. Consequently, there will be a tendency for the mean stress effects to balance one another and thus justify neglecting the mean stress effects in design. This shifting of mean stress for the R. G. Follis (7.1) is evident in the bending stress history shown in Fig. 6.2.

Clearly, the use in design of the mean fatigue stress range is desirable and makes possible the development of a simple fatigue design criteria for ship structures.

7.2 Uncertainty - Coefficient of Variation

As shown by Ang (7.2), the reliability model for fatigue design is a function of the "total" uncertainty in fatigue life. In establishing this total uncertainty, it is essential to take into account all sources of uncertainty: the scatter in the fatigue data, the uncertainty in the fatigue model, the uncertainty in the fatigue damage model (Miner's linear damage rule), the uncertainty in the stress-range distribution and error in stress analysis, the effects of the quality of fabrication and workmanship, and the uncertainty produced by any other design and fabrication factors.

The measure of total uncertainty in fatigue life (7.3), Ω_n , is given as a function of the variability (coefficient of variation) in fatigue data life, δ_f , any prediction error, Δ_f , and the uncertainty in the individual stresses and stress effects. The value of Ω_n may be determined from Equation 7.1 using a first-order analysis (7.4).

$$\Omega_n^2 \cong \Omega_f^2 + m^2 \Omega_S^2 + \Omega_C^2 \quad (7.1)$$

where,

Ω_n = the total uncertainty in fatigue life.

Ω_f = the uncertainty in the fatigue data life.

$= \sqrt{\delta_f^2 + \Delta_f^2}$; in which δ_f is the coefficient of variation in the fatigue life data about the S-N regression line; and Δ_f is the error in the fatigue model (the S-N equation, including such effects as mean stress), and the imperfections in the use of the linear damage rule (Miner) and the Weibull distribution approximations.

Ω_C = the uncertainty in the mean intercept of the S-N regression line and includes in particular the effects of workmanship and fabrication.

Ω_S = measure of total uncertainty in mean stress range, including the effects of impact and error of stress analysis and stress determination.

The values of δ_f , as obtained from the available fatigue data, are tabulated in Table 7.1 for the fatigue details included in this study. Since the mean fatigue stress range is used herein (combining materials of all strengths and stress cycles of various mean stress levels), the tabulated uncertainty in life includes the effect of both material strength and mean stress. The scatter in the fatigue data does not include the effect of corrosion. This is a factor that should be included as soon as adequate data are available. The error in the fatigue model, Δ_f , including the uncertainty

TABLE 7.1

Summary of Uncertainties in Fatigue Parameters

Detail No. (See Fig. B.1)	m	$\log_{10} C$	δ_f	Δ_f	Ω_c	Ω_s	Ω_n
1(all steels)	5.729	15.55	0.75	0.15	0.40	0.10	1.04
1M	12.229	25.36	0.71	0.15	0.40	0.10	1.48
1H	15.449	32.04	0.91	0.15	0.40	0.10	1.84
1Q	5.199	14.91	0.68	0.15	0.40	0.10	0.96
1(F)	4.805	13.78	0.60	0.15	0.40	0.10	0.88
2	6.048	15.82	0.64	0.15	0.40	0.10	0.98
3	5.946	14.80	0.63	0.15	0.40	0.10	0.96
3(G)	6.370	15.52	0.74	0.15	0.40	0.10	1.07
4	5.663	14.22	0.61	0.15	0.40	0.10	0.93
5	3.278	9.65	0.48	0.15	0.40	0.10	0.72
6	5.663	14.22	0.61	0.15	0.40	0.10	0.93
7 B	3.771	11.23	0.53	0.15	0.40	0.10	0.78
7 P	4.172	11.46	0.51	0.15	0.40	0.10	0.78
8	6.549	16.44	0.81	0.15	0.40	0.10	1.13
9	9.643	19.59	0.90	0.15	0.40	0.10	1.39
10M	7.589	16.63	0.88	0.15	0.40	0.10	1.24
10H	12.795	25.92	0.96	0.15	0.40	0.10	1.66
10Q	5.124	13.65	0.76	0.15	0.40	0.10	1.01
10(G)	7.130	16.93	0.94	0.15	0.40	0.10	1.25
10 A	5.468	14.14	0.79	0.15	0.40	0.10	1.05
10A(G) [†]	--	--	--	0.15	0.40	0.10	--
11	5.765	13.77	0.68	0.15	0.40	0.10	0.99
12	4.398	11.69	0.43	0.15	0.40	0.10	0.75
12(G)	5.663	14.12	0.60	0.15	0.40	0.10	0.93
13	4.229	12.12	0.45	0.15	0.40	0.10	0.75
14	7.439	16.96	0.91	0.15	0.40	0.10	1.25
14A [†]	--	--	--	0.15	0.40	0.10	--
15	4.200	10.83	0.43	0.15	0.40	0.10	0.74
16	4.631	12.02	0.58	0.15	0.40	0.10	0.85
16(G)	6.960	15.55	0.95	0.15	0.40	0.10	1.25
17	3.736	10.39	0.34	0.15	0.40	0.10	0.66
17(S)	7.782	16.28	0.65	0.15	0.40	0.10	1.10
17 A	3.465	10.14	0.39	0.15	0.40	0.10	0.67

Table 7.1 (cont.)

Detail No. (See Fig. B.1)	m	$\log_{10} C$	δ_f	Δ_f	Ω_c	Ω_s	Ω_n
17A(S)	7.782	16.28	0.65	0.15	0.40	0.10	1.10
18	4.027	10.26	0.65	0.15	0.40	0.10	0.88
18(S)	9.233	18.02	0.75	0.15	0.40	0.10	1.26
19	7.472	15.19	0.93	0.15	0.40	0.10	1.27
19(S)	7.520	15.83	0.93	0.15	0.40	0.10	1.27
20	4.619	11.57	0.66	0.15	0.40	0.10	0.92
20(S)	6.759	14.73	0.93	0.15	0.40	0.10	1.22
21(1/4" weld)*	14.245	26.72	--	0.15	0.40	0.10	--
21(3/8" weld)*	15.494	25.49	--	0.15	0.40	0.10	--
21(S)	7.358	16.98	0.83	0.15	0.40	0.10	1.19
22	3.147	10.04	0.32	0.15	0.40	0.10	0.62
23	3.187	9.94	0.13	0.15	0.40	0.10	0.55
24	3.187	9.94	0.13	0.15	0.40	0.10	0.55
25	7.090	15.79	0.78	0.15	0.40	0.10	1.14
25A	8.518	19.47	0.91	0.15	0.40	0.10	1.32
25B	6.966	15.15	0.63	0.15	0.40	0.10	1.03
26	3.348	10.13	0.61	0.15	0.40	0.10	0.82
27	3.146	9.40	0.58	0.15	0.40	0.10	0.78
27(S)	5.277	12.06	0.54	0.15	0.40	0.10	0.87
28	7.746	17.41	0.81	0.15	0.40	0.10	1.20
28(F) ⁺⁺	--	--	--	0.15	0.40	0.10	--
30	3.159	9.87	0.31	0.15	0.40	0.10	0.62
30A	3.368	10.58	0.10	0.15	0.40	0.10	0.55
31**	4.348	10.67	--	0.15	0.40	0.10	--
31A	3.453	10.13	0.44	0.15	0.40	0.10	0.71
32A	4.200	10.83	0.43	0.15	0.40	0.10	0.74
32B**	3.533	9.71	--	0.15	0.40	0.10	--
33	3.660	9.86	0.50	0.15	0.40	0.10	0.75
33(S)	10.368	19.59	0.81	0.15	0.40	0.10	1.38
35	3.808	10.75	0.28	0.15	0.40	0.10	0.64
36	6.966	15.15	0.63	0.15	0.40	0.10	1.03
36A	5.163	12.88	0.46	0.15	0.40	0.10	0.81
38	3.462	10.17	0.36	0.15	0.40	0.10	0.66
38(S)	10.225	17.39	0.88	0.15	0.40	0.10	1.42

Table 7.1 (cont.)

Detail No. (See Fig. B.1)	m	$\log_{10} C$	Δ_f	Δ_f	Ω_c	Ω_s	Ω_n
40**	3.533	9.71	--	0.15	0.40	0.10	--
42	7.358	16.98	0.83	0.15	0.40	0.10	1.19
46**	4.348	10.67	--	0.15	0.40	0.10	--
51(V)	3.818	10.93	0.07	0.15	0.40	0.10	0.58
52(V)	4.042	11.24	0.19	0.15	0.40	0.10	0.62
Mean Value	--	--	0.62	--	--	--	0.96
Std. Dev.	--	--	0.23	--	--	--	0.26

- * Only three test points available. Not enough data to calculate δ_f .
- ** These are the estimated values.
- + Data scatter makes evaluation questionable.
- †† Range in lives is small--extrapolation questionable.

Notes:

B = bending stress, P = principal stress, M = mild steel, H = high strength low alloy steel, Q = quenched and tempered steel, (S) = shear stress on fasteners or welds, (F) = flame cut surfaces, (G) = surfaces have been ground flush, (V) = average shear stress based on net area of web.

in the Miner damage rule, is estimated to be about 15% ($\Delta_f = 0.15$). The coefficient of variation in the value of $\log c$ for the various details has been examined and found to average about 37%; a value of $\Omega_c = 0.40$ has been assumed (7.4). This value, as noted in the above definitions, includes the effects of the quality of fabrication and workmanship. Based on a recent study of weld discontinuities (7.5), it is believed that the mean data used provide for typical welded fabrication. However, if the weld quality is unusually poor, a further adjustment should be made in the allowable design stress.

Finally, the uncertainty in the calculated maximum nominal stress range, including the errors in stress analysis, must be selected or established. It is believed that any such error will generally not be severe; in fact, designers will often tend to err on the safe side. Nevertheless, it is suggested that a value of $\Omega_s = 0.10$ be used.

Based on the above values, the uncertainty in fatigue life was obtained from Eqn. 7.1. The mean value for the sixty values of δ_f , the coefficient of variation in the fatigue life data, is 0.62 with a standard deviation of 0.23. The mean value for Ω_n , the total uncertainty in fatigue life, is 0.96 with a standard deviation of 0.26.

7.3 Reliability Factor (Factor of Safety)

The basic relationships for the fatigue reliability design criteria developed here have been presented by Ang (7.2) in his development of reliability analysis for design. In this analysis it is recognized that the fatigue life of a structural detail is a random variable, and it is assumed that the distribution of life can be represented by the Weibull distribution (7.6). This distribution is often used in fatigue for a variety of reasons (7.8).

If $L(n)$ is the probability of survival through a given number of loading cycles, then

$$L(n) = L(n-1) [1-h(n)] \quad (7.2)$$

where $h(n)$ is the hazard function (7.7).

Assuming the Weibull Distribution for fatigue life (7.8), the hazard function is then given by (7.7),

$$h(n) = \frac{k}{w - \epsilon} \left(\frac{n - \epsilon}{w - \epsilon} \right)^{k-1}; k \geq 1.0 \quad (7.3)$$

where, ϵ = the minimum life
 w = the characteristic life
 k = the Weibull scale parameter

Ang (7.7) shows that the parameters w , k and ϵ can be related to \bar{n} and σ_n , the mean fatigue life and its standard deviation, as follows:

$$\bar{n} - \epsilon = (w - \epsilon) \Gamma\left(1 + \frac{1}{k}\right) \quad (7.4)$$

$$\sigma_n = (w - \epsilon) \left[\Gamma\left(1 + \frac{2}{k}\right) - \Gamma^2\left(1 + \frac{1}{k}\right) \right]^{\frac{1}{2}} \quad (7.5)$$

where Γ = the gamma function (see Fig. 7.1)

If the minimum life ϵ is assumed to be equal to zero or very small, the ratio of the standard deviation to the mean life is:

$$\frac{\sigma_n}{\bar{n} - \epsilon} = \frac{\left[\Gamma\left(1 + \frac{2}{k}\right) - \Gamma^2\left(1 + \frac{1}{k}\right) \right]^{\frac{1}{2}}}{\Gamma\left(1 + \frac{1}{k}\right)} \quad (7.6)$$

or

$$\frac{\sigma_n}{\bar{n}} \cong \Omega_n \quad (7.7)$$

Ang (7.2) has suggested that the shape parameter k can be approximated by:

$$k \cong \Omega_n^{-1.08} \quad (7.8)$$

This equation is shown in Fig. 7.2 and the correlation with the appropriate values of k is presented in Table 7.2. The use of this approximation greatly simplifies the development of a simple reliability relationship.

Using the Weibull distribution and the hazard function of Eqn. 7.3, the reliability function can be expressed as (7.2):

$$\begin{aligned} L(n) &= \exp \left[- \left(\frac{n - \epsilon}{w - \epsilon} \right)^k \right]; \quad n \geq \epsilon \\ &= 1.0 \quad ; \quad n < \epsilon \end{aligned} \quad (7.9)$$

Introducing Eqns. 7.4 and 7.8, this can be written as:

$$L(n) = \exp \left\{ - \left[\frac{n}{\bar{n}} \Gamma\left(1 + \Omega_n^{1.08}\right) \right]^{\Omega_n^{-1.08}} \right\} \quad (7.10)$$

Then, for a specified probability of survival, $L(n)$,

$$\frac{n - \epsilon}{w - \epsilon} = [-\ln L(n)]^{1/k} \cong [p_f(n)]^{1/k} \quad (7.11)$$

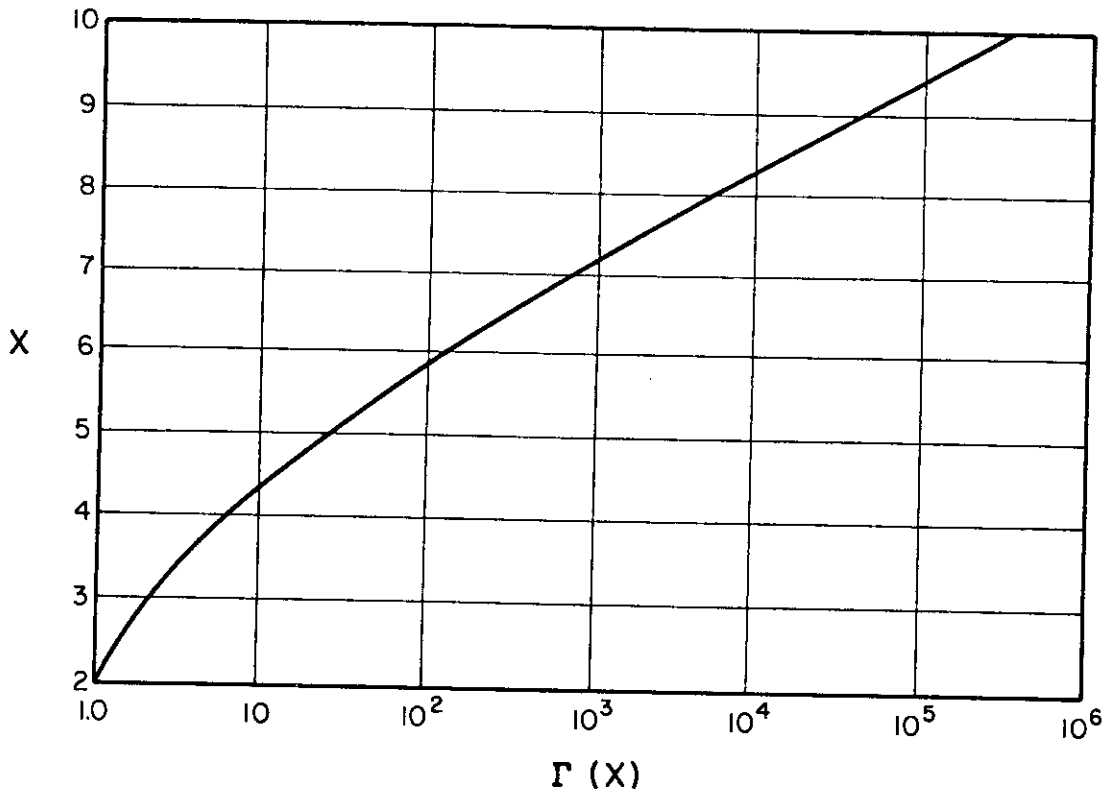


Fig. 7.1 Values of Gamma Function.

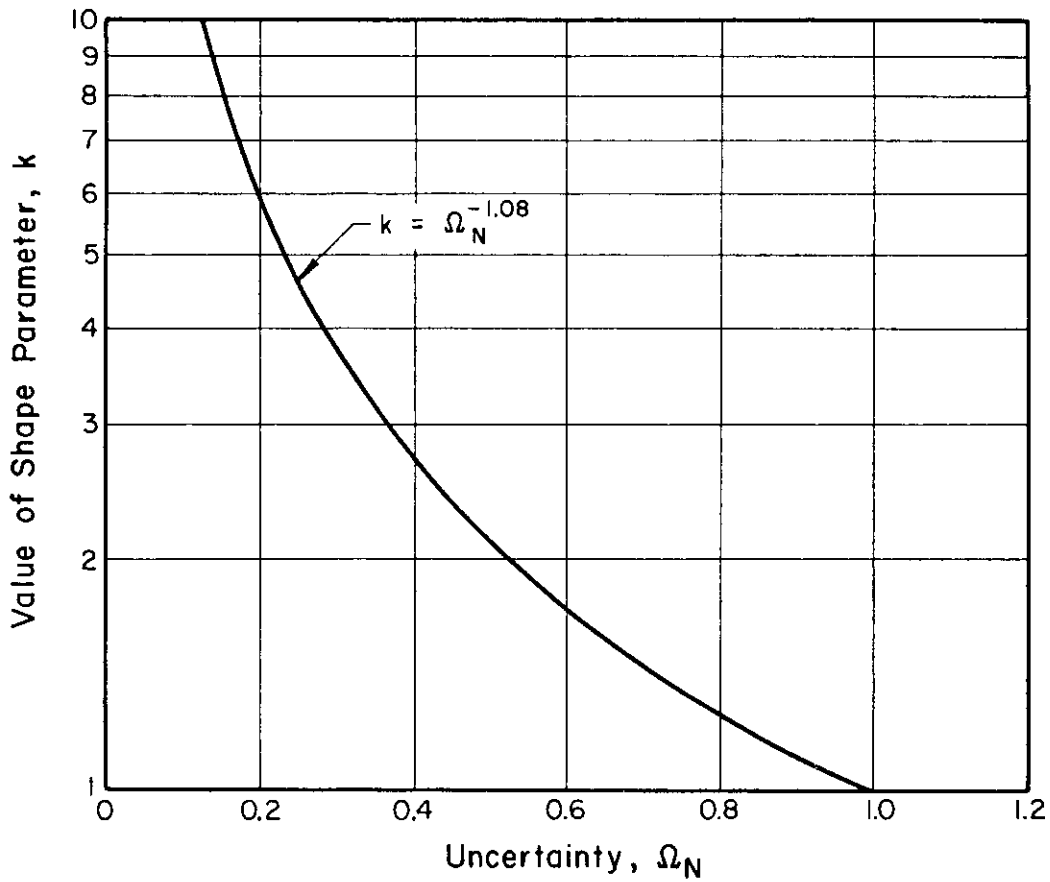


Fig. 7.2 Relationship Between k and Ω_N as Given by Equation 7.8 (7.2).

TABLE 7.2

Correlation of Approximation With Weibull Distribution

$\frac{\sigma_N}{\bar{N}-\epsilon}$	k	$\left(\frac{\sigma_N}{\bar{N}}\right)^{-1.08}$	$\frac{\sigma_N}{\bar{N}-\epsilon}$	k	$\left(\frac{\sigma_N}{\bar{N}}\right)^{-1.08}$
0	α	-			
0.05	24.9	25.4	0.55	1.89	1.91
0.10	12.15	12.02	0.60	1.72	1.74
0.15	7.91	7.76	0.65	1.57	1.59
0.20	5.79	5.69	0.70	1.45	1.47
0.25	4.54	4.47	0.75	1.35	1.36
0.30	3.71	3.67	0.80	1.26	1.27
0.35	3.13	3.11	0.85	1.18	1.19
0.40	2.69	2.69	0.90	1.11	1.12
0.45	2.36	2.37	0.95	1.05	1.05
0.50	2.10	2.11	1.00	1.00	1.00

and for a mean life \bar{n} ,

$$\frac{\bar{n} - \epsilon}{n - \epsilon} \cong \frac{\Gamma(1 + \frac{1}{k})}{[-\ln L(n)]^{1/k}} \cong \frac{\Gamma(1 + \frac{1}{k})}{[p_f(n)]^{1/k}} \quad (7.12)$$

This ratio has been defined by Ang (7.2) as the fatigue life factor, γ_L .

$$\gamma_L = \frac{\Gamma(1 + \Omega_n^{1.08})}{[p_f(n)]^{\Omega_n^{1.08}}} \quad (7.13)$$

and,

$$\bar{n} = n\gamma_L \quad (7.14)$$

where, \bar{n} is the required mean life that would be necessary to insure a useful life n with a reliability of $L(n)$ or probability of failure of $p_f(n)$. The relationships between the fatigue risk factor and the uncertainty in fatigue life for various probabilities of failure are shown in Fig. 7.3. Thus, a 90 percent level of reliability and an uncertainty in life 0.5 would require design for a mean life equal to $2\frac{1}{2}$ times the useful life. Under a constant stress range the required design stress is then given by,

$$S_D = \left(\frac{C}{\bar{n}}\right)^{1/m} \quad (7.15)$$

or,

$$S_D = \left(\frac{C}{n\gamma_L}\right)^{1/m} = \left(\frac{C}{n}\right)^{1/m} \left(\frac{1}{\gamma_L}\right)^{1/m} \quad (7.16)$$

Designating the last term of Eqn. 7.16 as the reliability factor, R_F ,

$$R_F = \left(\frac{1}{\gamma_L}\right)^{1/m} = \left\{ \frac{[p_f(n)]^{\Omega_n^{1.08}}}{\Gamma(1 + \Omega_n^{1.08})} \right\}^{1/m} \quad (7.17)$$

then, the allowable design stress would be,

$$S_D = \left(\frac{C}{n}\right)^{1/m} \cdot R_F \quad (7.18)$$

$$S_D = S \cdot R_F \quad (7.19)$$

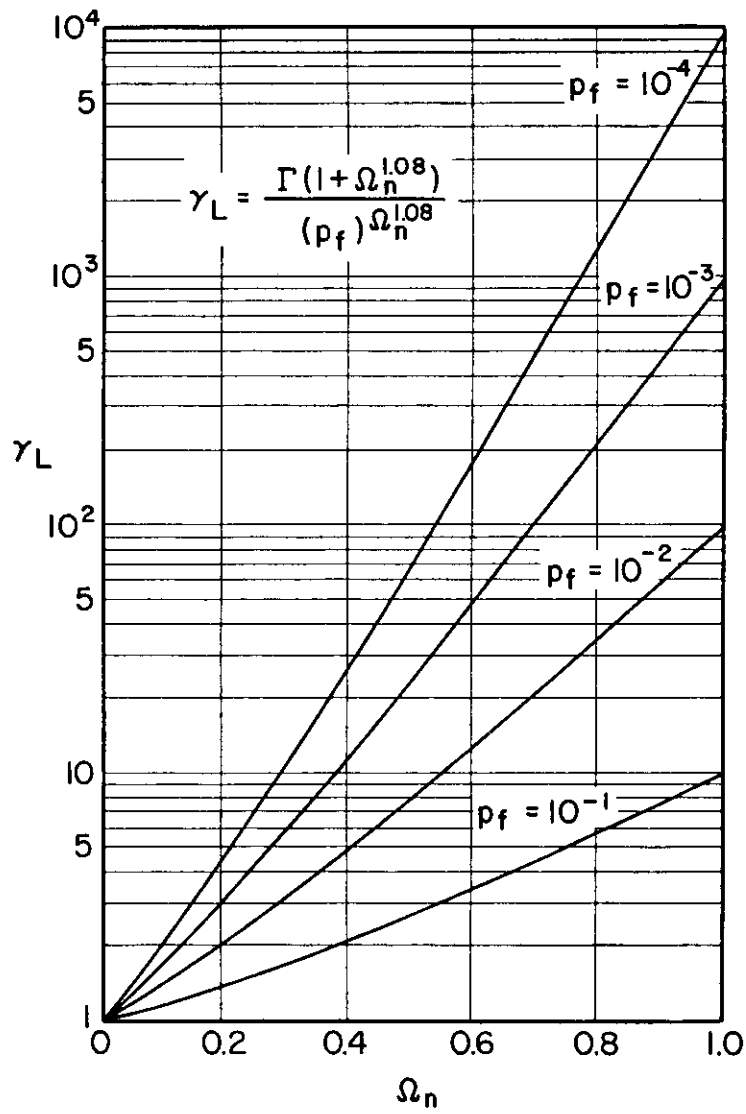


Fig. 7.3 Relationship of Fatigue Life Factor and the Uncertainty in Fatigue Life for Various Probabilities of Failure (7.6).

where, $\frac{1}{m}$ corresponds to the slope of the S-N curve for the member in question, C, the m intercept of the S-N curve, and S, the stress range corresponding to the desired useful life, n. A summary of computed values of reliability factors for three levels of reliability (0.90, 0.95 and 0.99), five coefficients of uncertainty (0.40, 0.60, 0.80, 1.0 and 1.2), and for various S-N curve slopes ($m = 2$ to 13) are given in Table 7.3 and Figs. 7.4, 7.5 and 7.6. An indication of the manner in which the reliability factor provides for the desired useful life is provided diagrammatically in Fig. 7.7 for constant-cycle fatigue behavior.

For a number of years a factor of safety of approximately 1.4 was used for fatigue design of bridges. This corresponds to a reliability factor of $1/1.4$ or 0.71. Based on the data in Table 7.3, a reliability factor of approximately 0.7 corresponds to a ninety-five percent level of reliability for an uncertainty of 0.60 and an S-N curve slope of approximately 0.22. Such values of uncertainty and slope were representative for the fatigue data that was available at the time and give a general indication of the approximate reliability provided in some of the earlier fatigue design procedures.

7.4 Variable Loading - Random Load Factor

In considering fatigue in terms of a constant amplitude stress-range, the mean fatigue life is given by the well known S-N relationship (see Section 2.3),

$$\bar{n} = \frac{C}{s_c^m} \quad (7.20)$$

However, as discussed in Section 2, such a relationship cannot be applied directly to ship structures that are subjected to a variable or random loading. Other relationships must be developed to modify Equation 7.20.

A relationship between a variable amplitude stress range and the mean fatigue life, comparable to Eqn. 7.20, has been presented by Ang (7.2, 7.9) utilizing the S-N relationship and the Palmgren-Miner linear damage rule (7.10).

The Miner damage rule may be stated as follows (7.9),

(i) The damage contributed by one cycle of stress range s_i is equal to $\frac{1}{\bar{n}(s_i)}$, where $\bar{n}(s_i)$ is the mean fatigue life under a constant amplitude,

stress range s_i .

(ii) By superposition, the total damage D caused by stress ranges s_1, s_2, \dots, s_k applied n_1, n_2, \dots, n_k cycles, respectively, is

TABLE 7.3

Reliability Factors - R_F

m	K	Reliability, L(n)														
		0.90					0.95					0.99				
		$\Omega_n =$ 0.40	$\Omega_n =$ 0.60	$\Omega_n =$ 0.80	$\Omega_n =$ 1.0	$\Omega_n =$ 1.2	$\Omega_n =$ 0.40	$\Omega_n =$ 0.60	$\Omega_n =$ 0.80	$\Omega_n =$ 1.0	$\Omega_n =$ 1.2	$\Omega_n =$ 0.40	$\Omega_n =$ 0.60	$\Omega_n =$ 0.80	$\Omega_n =$ 1.0	$\Omega_n =$ 1.2
2.0	.500	.691	.546	.420	.316	.233	.608	.447	.320	.224	.153	.451	.276	.170	.100	.057
2.5	.400	.744	.616	.500	.398	.312	.671	.525	.402	.302	.223	.528	.357	.242	.158	.102
3.0	.333	.782	.668	.561	.464	.379	.717	.585	.468	.368	.286	.588	.424	.307	.215	.149
3.5	.290	.810	.708	.609	.518	.435	.752	.631	.521	.425	.342	.634	.479	.363	.268	.195
4.0	.250	.831	.739	.648	.562	.483	.780	.669	.566	.473	.391	.671	.525	.412	.316	.240
4.5	.220	.849	.764	.680	.599	.524	.801	.699	.603	.514	.434	.702	.564	.455	.359	.281
5.0	.200	.863	.785	.707	.631	.559	.819	.725	.634	.549	.472	.727	.597	.492	.398	.319
5.5	.180	.874	.802	.730	.658	.589	.834	.746	.661	.580	.505	.748	.626	.525	.433	.354
6.0	.170	.884	.817	.749	.681	.616	.847	.765	.684	.607	.535	.767	.651	.554	.464	.386
6.5	.150	.893	.830	.766	.702	.639	.858	.781	.704	.630	.561	.782	.673	.580	.492	.415
7.0	.140	.900	.841	.781	.720	.660	.867	.795	.722	.652	.585	.796	.692	.603	.518	.442
7.5	.130	.906	.841	.794	.736	.678	.876	.807	.738	.671	.606	.808	.703	.623	.541	.467
8.0	.130	.912	.860	.805	.750	.695	.883	.818	.752	.688	.625	.819	.725	.642	.562	.490
8.5	.120	.917	.867	.815	.763	.710	.889	.827	.765	.703	.643	.829	.738	.659	.582	.511
9.0	.111	.921	.874	.825	.774	.724	.895	.836	.776	.717	.659	.838	.751	.675	.599	.530
9.5	.105	.925	.881	.833	.785	.736	.901	.844	.787	.730	.674	.846	.763	.689	.616	.548
10.0	.100	.929	.886	.841	.794	.747	.905	.851	.796	.741	.687	.853	.773	.702	.631	.565
10.5	.095	.932	.891	.848	.803	.758	.910	.858	.805	.752	.699	.859	.783	.714	.645	.580
11.0	.091	.935	.896	.854	.811	.768	.913	.864	.813	.762	.711	.865	.791	.724	.658	.595
11.5	.087	.938	.900	.860	.819	.776	.917	.869	.820	.771	.721	.870	.799	.735	.670	.608
12.0	.083	.941	.904	.866	.825	.785	.921	.875	.828	.779	.731	.876	.807	.745	.681	.621
12.5	.080	.943	.908	.870	.832	.792	.923	.879	.833	.787	.741	.880	.814	.753	.692	.633
13.0	.077	.945	.911	.875	.838	.799	.926	.883	.839	.794	.749	.884	.820	.761	.702	.644

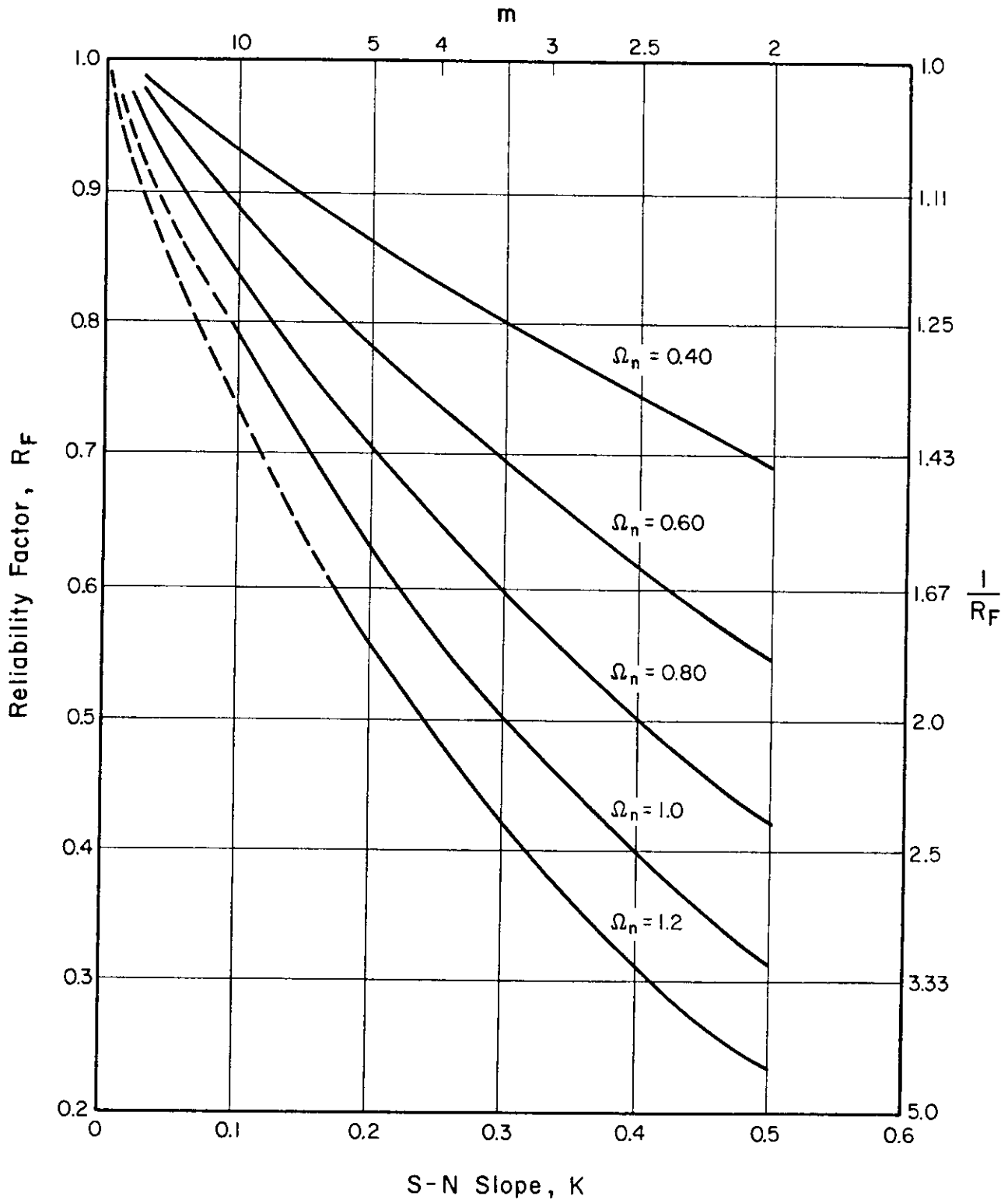


Fig. 7.4 Reliability Factor vs. S-N Slope 90% Reliability.

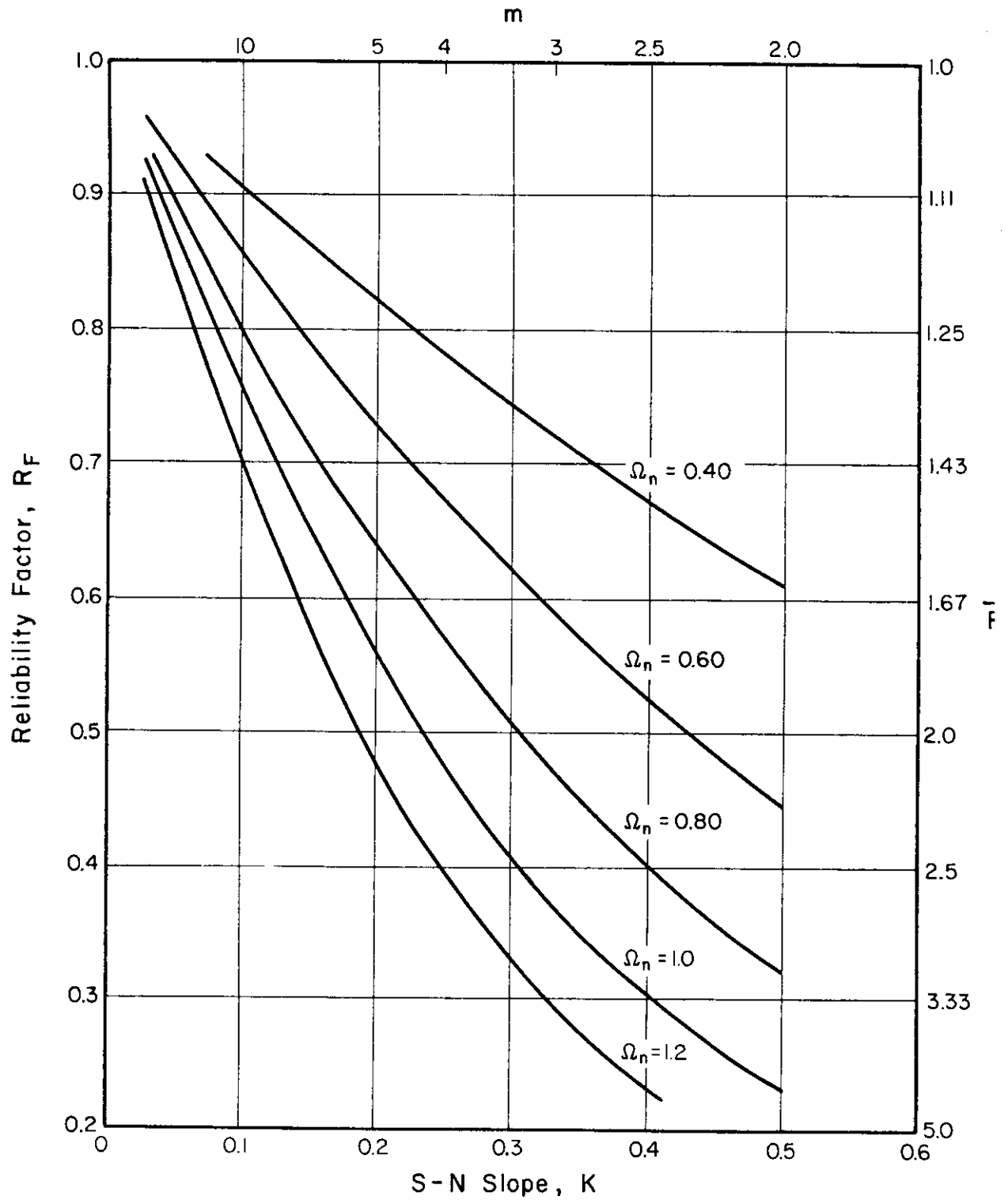


Fig. 7.5 Reliability Factor vs. S-N Slope 95% Reliability.

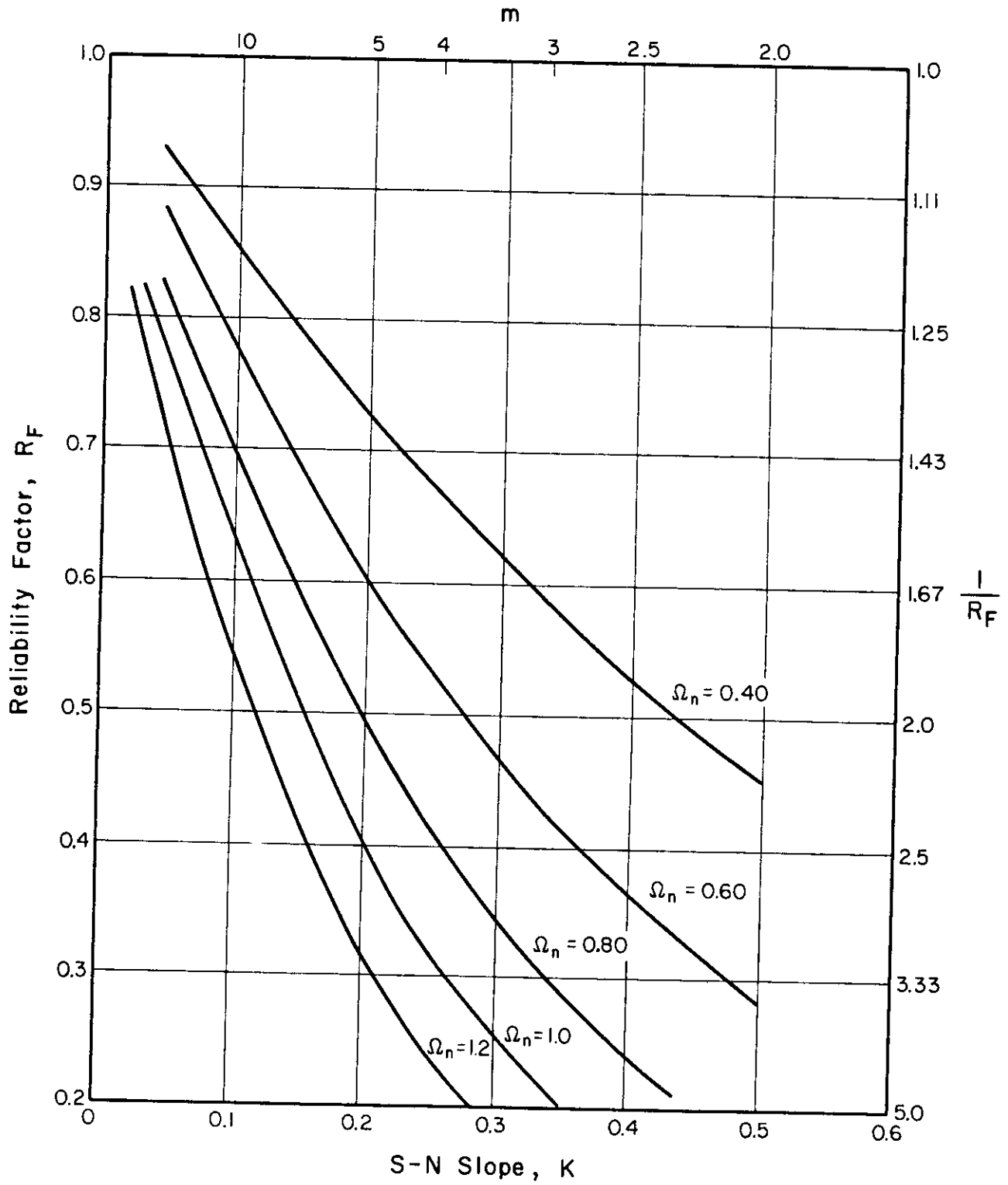
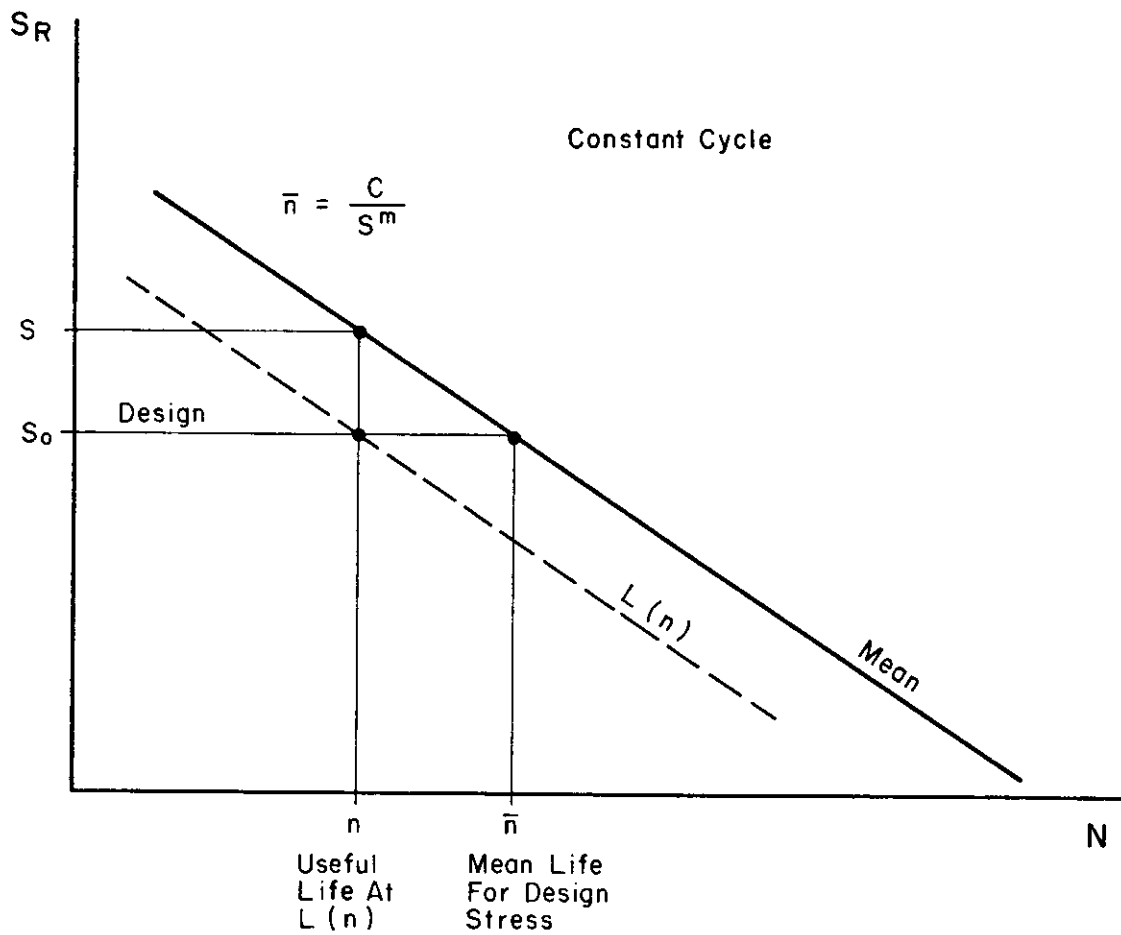


Fig. 7.6 Reliability Factor vs. S-N Slope 99% Reliability.



$$\bar{n} = n \cdot \gamma_L$$

$$S_0 = S \times R_F = S \times \left(\frac{1}{\gamma_L}\right)^{1/m} \quad \text{--- (7.19)}$$

Fig. 7.7 Application of Reliability Factor to Mean Fatigue Resistance.

$$D = \sum_{i=1}^k \frac{n_i}{\bar{n}(s_i)} \quad (7.21)$$

(iii) Fatigue failure occurs when the linear cumulative damage ratio D is equal to unity, i.e., $D = 1.0$.

A variable amplitude stress range can be considered as a random variable S with a probability density function $f_S(s)$. Then, for n cycles of the variable stress range, the number of cycles at stress range $S = s$ is $nf_S(s) ds$. Based on Eqn. 7.21, the expected cumulative damage is,

$$E(D) = \int_0^{\infty} \frac{nf_S(s) ds}{\bar{n}(s)} \quad (7.22)$$

where $\bar{n}(s) =$ mean fatigue life under constant amplitude stress range s .

$f_S(s) =$ a probability density function representing the random cyclic stress range.

Introducing the basic relationship of Eqn. 7.20 and equating the damage to 1.0, the damage relationship may be written,

$$E(D) = \frac{\bar{n}}{C} \int_0^{\infty} s^m f_S(s) ds = 1.0 \quad (7.23)$$

Rearranging terms yields,

$$\bar{n} = \frac{C}{\int_0^{\infty} s^m f_S(s) ds} = \frac{C}{E(S^m)} \quad (7.24)$$

where,

$E(S^m) =$ m^{th} moment of S , the randomly varying stress range (or the expected value of S^m) (7.11)

Eqn. 7.24 represents the relationship between an applied variable amplitude stress range and the mean fatigue life. Note that Eqn. 7.20 is the same as Eqn. 7.24 except that the s^m term is replaced by its expected value $E(S^m)$.

Very little fatigue testing has been done under variable loading conditions. In order to utilize the vast amount of constant amplitude fatigue data (i.e., S - N curve data) available, it is necessary to develop a relationship between the constant-cycle and variable-cycle cases. For a given detail, a random stress range S can be related to a constant-cycle stress range s_c with the same mean fatigue life by combining Eqns. 7.20 and 7.24 to give the following,

$$E(S^m) = s_c^m$$

$$\text{or} \quad [E(S^m)]^{1/m} = s_c \quad (7.25)$$

Eqn. 7.25 applies to any distribution of applied stress range S . A convenient design relationship can then be developed from Eqn. 7.25 by introducing a random load factor, ξ , such that,

$$[E(S^m)]^{1/m} = \frac{s_0}{\xi} = s_c \quad (7.26)$$

$$\text{or} \quad s_0 = \xi s_c \quad (7.27)$$

where,

s_0 = the maximum stress range in a random loading that can be represented by a Beta Distribution. (For the other distributions presented herein the value is the maximum stress range expected only once in 10^8 cycles of loading, $S_{10^{-8}}$.)

ξ = "random load factor"

By combining the above equations, the following general relationships are obtained,

$$E(S^m) = \int_0^\infty s^m f_S(s) ds = \left(\frac{s_0}{\xi}\right)^m = (s_c)^m \quad (7.28)$$

$$\xi = \frac{s_0}{\left[\int_0^\infty s^m f_S(s) ds\right]^{1/m}} = \frac{s_0}{[E(S^m)]^{1/m}} \quad (7.29)$$

$$\text{and} \quad s_c = \frac{s_0}{\xi} = \left[\int_0^\infty s^m f_S(s) ds\right]^{1/m} \quad (7.30)$$

Thus, the constant-cycle stress range representing the variable load distribution can be represented as a function of the constant amplitude stress range having the same mean fatigue life \bar{n} (see Fig. 7.8).

The expressions for $E(S^m)$ and ξ for the distributions examined herein (Section 6) are given in Table 7.4. The derivations of these formulae are given in Appendix E. For the Weibull distribution function, the random load factor in terms of $S_{10^{-8}}$ is a function of the inverse slope m of the S-N curve for the detail to which the loading is to be applied and the Weibull shape parameter k :

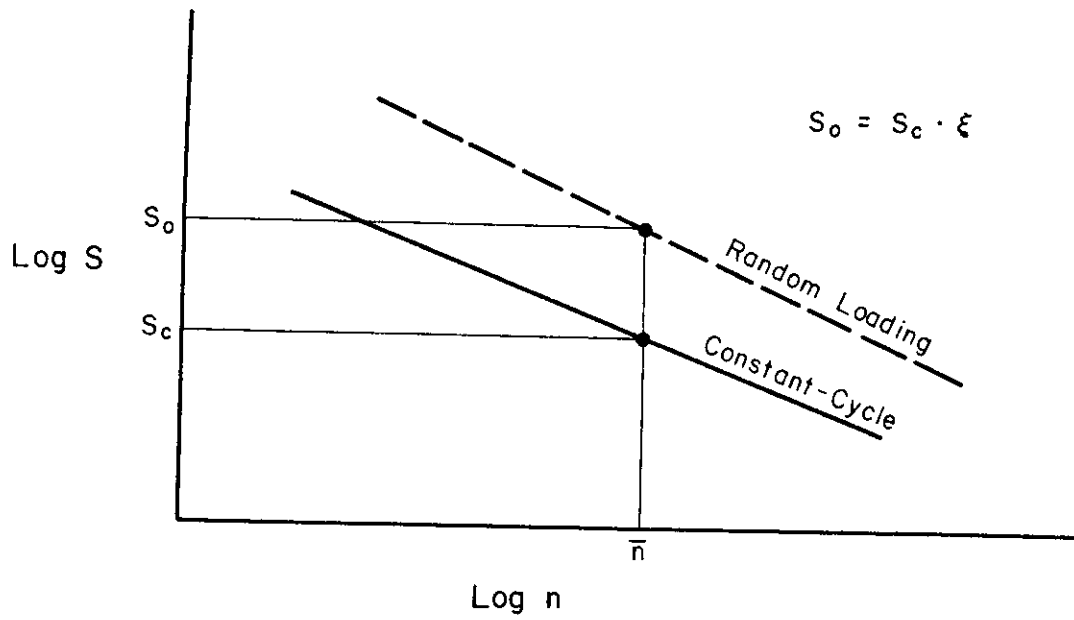


Fig. 7.8 Relationship Between Maximum Stress Range of Random Loading and Equivalent Constant-Cycle Stress Range.

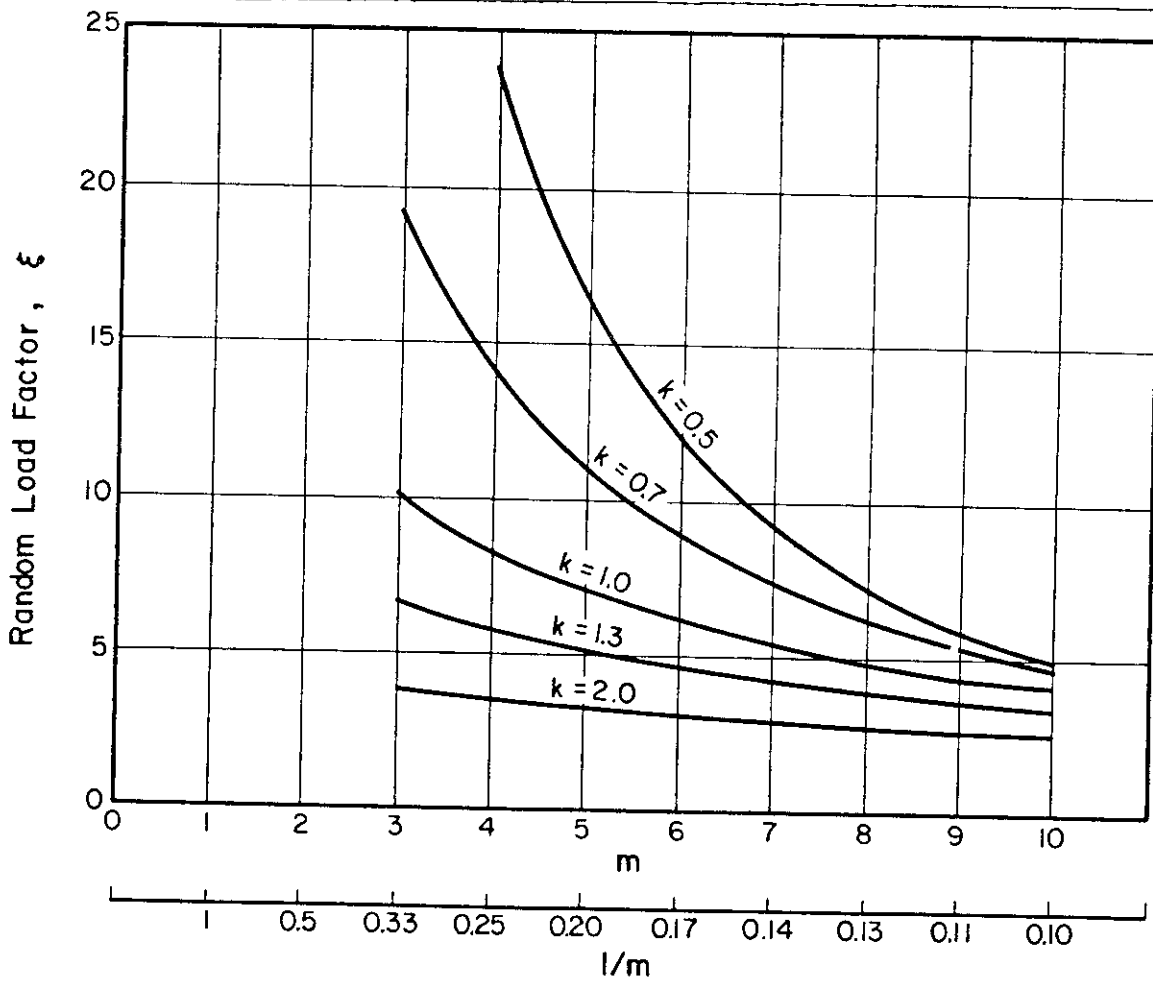


Fig. 7.9 Variation of ξ with m for Various Weibull Shapes, k .

TABLE 7.4

Expressions for $E(S^m)$ and ξ for Probability Distributions in Terms of S_0 or $S_{10^{-8}}$ Stress Range.
(See Appendix E for Derivations)

Distribution	$E(S^m)$ (Characteristic Parameters)	$E(S^m)$ (In Terms of Stress Range)	Maximum Stress Range*	Random Load Factor, ξ
Beta	$S_0^m \frac{\Gamma(m+q)\Gamma(q+r)}{\Gamma(q)\Gamma(m+q+r)}$	$S_0^m \frac{\Gamma(m+q)\Gamma(q+r)}{\Gamma(q)\Gamma(m+q+r)}$	S_0	$\left[\frac{\Gamma(q)\Gamma(m+q+r)}{\Gamma(m+q)\Gamma(q+r)} \right]^{1/m}$
Lognormal	$\mu_s^m [1 + \delta_s^2]^{-\frac{1}{2}m(m-1)}$ where $\delta_s = \frac{\sigma_s}{\mu_s}$	$S_{10^{-8}}^m (1 + \delta_s^2)^{m^2/2} \exp[-5.6m \sqrt{\ln(1 + \delta_s^2)}]$	$S_{10^{-8}}$	$(1 + \delta_s^2)^{-m/2} [\exp(5.60 \sqrt{\ln(1 + \delta_s^2)})]^{-1/m}$
Weibull	$w^m \Gamma(1 + \frac{m}{k})$	$S_{10^{-8}}^m (18.42)^{-m/k} \Gamma(1 + \frac{m}{k})$	$S_{10^{-8}}$	$(18.42)^{1/k} [\Gamma(1 + \frac{m}{k})]^{-1/m}$
Exponential	$\lambda^m \Gamma(1 + m)$	$S_{10^{-8}}^m (18.42)^{-m} \Gamma(1 + m)$	$S_{10^{-8}}$	$18.42 [\Gamma(1 + m)]^{-1/m}$
Rayleigh	$S_{RMS}^m \Gamma(1 + \frac{m}{2})$	$S_{10^{-8}}^m (18.42)^{-m/2} \Gamma(1 + \frac{m}{2})$	$S_{10^{-8}}$	$\sqrt{18.42} [\Gamma(1 + \frac{m}{2})]^{-1/m}$
Shifted Exponential	$\sum_{n=0}^m \frac{m!}{(m-n)!} \lambda^n a^{m-n}$	$S_{10^{-8}}^m \left[\sum_{n=0}^m \frac{m!}{(m-n)!} (18.42)^{-n} (1-\alpha)^n \alpha^{m-n} \right]$ where $\alpha = a/S_{10^{-8}}$	$S_{10^{-8}}$	$\left[\sum_{n=0}^m \frac{m!}{(m-n)!} (18.42)^{-n} (1-\alpha)^n \alpha^{m-n} \right]^{-1/m}$

*The Beta distribution is a "limited" distribution with S_0 being the maximum stress range of the distribution for any specified life. For all other distributions shown, $S_{10^{-8}}$ is the maximum stress range that is expected only once in 10^8 cycles of loading.

$$\xi = (18.42)^{1/k} \left[\Gamma \left(1 + \frac{m}{k} \right) \right]^{-1/m} \quad (7.31)$$

A summary of the random load factors for various values of m and k is presented in Table 7.5 and in Fig. 7.9. These data will be used in the design criteria developed in the next section. The appropriate values provide a measure of the increase in constant-cycle stress range that a given detail will be able to withstand once during a 20-yr. life (10^8 cycles of loading).

7.5 Design Procedure - Examples

With the relationships presented above, a simple fatigue verification or design procedure that takes into account the principal fatigue parameters can now be provided. Table 7.6 shows the six steps of the procedure to be followed to verify the adequacy of a given ship structure detail in fatigue.

In step 1 the expected loading history for the ship detail must be established (the shape factor for the Weibull distribution selected). Some guidance can be obtained from Table 6.5 if more complete data are not available.

In the second step the ship details at which the fatigue resistance should be checked must be identified. The critical locations in the ship assemblies, shown in Appendix A - Figs. A.1 through A.12, can be used as a guide to identify the critical details in terms of the numerous local fatigue details shown in Appendix B - Fig. B.1.

The third step is to obtain, for the local detail, the fatigue strength and slope of the S-N curve (this comes from Table B.1 of Appendix B or must be estimated).

The fourth step is to obtain the random load factor from Table 7.5 or Eqn. 7.31, and the fifth step is to obtain the appropriate reliability factor from Table 7.7 or Eqn. 7.17. (Since the values for each level of reliability are relatively constant, a further simplification can be provided by using a mean value for the reliability factor. As shown in Table 7.7, mean values of 0.67, 0.60 and 0.46 can be used for reliabilities of 0.90, 0.95 and 0.99, respectively. These data, along with their standard deviations are presented in Fig. 7.10. The data can be represented by a straight line and also provide a means whereby reliability factors for other levels of reliability can be obtained.)

The maximum allowable fatigue stress range, $(S_D)^*$, is then obtained from the following equation.

$$(S_D) = S_N \cdot \xi \cdot R_F \quad (7.32)$$

* The maximum allowable stress range at the point in question is the maximum peak-to-trough stress range expected once under the most severe sea state and during the entire life of the structure.

TABLE 7.5

Table of Random Load Factors for Weibull
Distributed Loading.

m	Random Load Factors for Various Weibull Shape Factors, k.															
	0.5	0.6	0.7	0.8	0.9	1.0 ⁽¹⁾	1.1	1.2	1.3	1.4	1.5	1.6	1.7	1.8	1.9	2.0 ⁽²⁾
2.0	69.26	42.22	28.63	20.93	16.17	13.02	10.83	9.24	8.05	7.12	6.39	5.80	5.32	4.92	4.58	4.29
2.5	49.99	32.55	23.12	17.49	13.86	11.39	9.63	8.33	7.33	6.55	5.92	5.41	4.99	4.64	4.34	4.08
3.0	37.86	26.05	19.23	14.96	12.12	10.14	8.69	7.60	6.75	6.08	5.54	5.09	4.72	4.40	4.13	3.90
3.5	29.70	21.42	16.35	13.04	10.77	9.14	7.93	7.00	6.27	5.69	5.21	4.81	4.48	4.20	3.96	3.75
4.0	23.94	18.00	14.15	11.53	9.68	8.32	7.30	6.50	5.86	5.35	4.93	4.58	4.28	4.02	3.80	3.61
4.5	19.73	15.39	12.41	10.31	8.79	7.64	6.76	6.07	5.52	5.06	4.68	4.37	4.10	3.86	3.66	3.49
5.0	16.54	13.34	11.01	9.31	8.04	7.07	6.31	5.71	5.21	4.81	4.47	4.18	3.94	3.72	3.54	3.38
5.5	14.08	11.70	9.87	8.48	7.41	6.58	5.92	5.39	4.95	4.58	4.28	4.02	3.79	3.60	3.43	3.28
6.0	12.13	10.36	8.91	7.77	6.87	6.15	5.58	5.10	4.71	4.38	4.11	3.87	3.66	3.48	3.32	3.18
6.5	10.56	9.26	8.11	7.16	6.40	5.78	5.27	4.85	4.50	4.21	3.95	3.73	3.54	3.38	3.23	3.10
7.0	9.28	8.33	7.42	6.64	5.99	5.45	5.00	4.63	4.31	4.04	3.81	3.61	3.44	3.28	3.14	3.02
7.5	8.22	7.55	6.83	6.18	5.62	5.16	4.76	4.43	4.14	3.90	3.68	3.50	3.34	3.19	3.07	2.95
8.0	7.34	6.87	6.31	5.78	5.30	4.89	4.54	4.24	3.98	3.76	3.57	3.40	3.24	3.11	2.99	2.88
8.5	6.59	6.29	5.86	5.42	5.01	4.66	4.35	4.08	3.84	3.64	3.46	3.30	3.16	3.04	2.92	2.82
9.0	5.95	5.79	5.46	5.10	4.75	4.44	4.17	3.92	3.71	3.52	3.36	3.21	3.08	2.96	2.86	2.76
9.5	5.40	5.35	5.11	4.81	4.52	4.25	4.00	3.78	3.59	3.42	3.26	3.13	3.01	2.90	2.80	2.71
10.0	4.92	4.95	4.79	4.55	4.30	4.07	3.85	3.65	3.48	3.32	3.18	3.05	2.94	2.84	2.74	2.66

Note: Values are based on a life of 10^8 cycles. For any other life N the values in this table would be multiplied by:

$$\frac{(\ln N)^{1/k}}{(18.42)^{1/k}}$$

(1) Values for exponential distribution.

(2) Values for Rayleigh distribution.

TABLE 7.6

Design Procedure

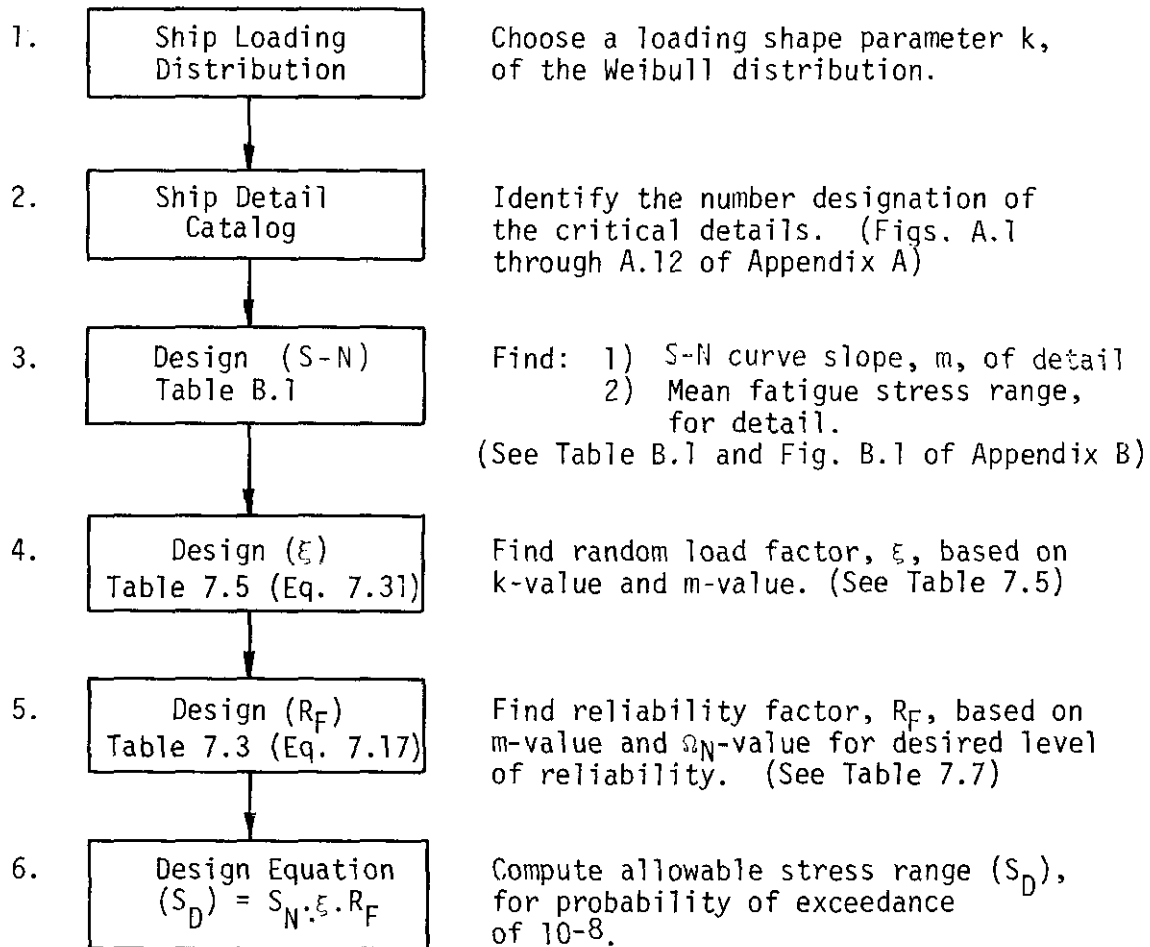


TABLE 7.7

Summary of Reliability Factors, R_F , for Local Fatigue Details
(Based on Table 7.1 and Equation 7.17)

Detail No.	m	Ω_n	Reliability, L(n)		
			0.90	0.95	0.99
1 (all steels)	5.729	1.04	0.655	0.578	0.431
1M	12.229	1.48	0.732	0.671(M)	0.549(M)
1H	15.449	1.84	0.719	0.660	0.540
1Q	5.199	0.96	0.657	0.578	0.430
1F	4.805	0.88	0.666	0.587	0.438
2	6.048	0.98	0.690	0.617	0.475
3	5.946	0.96	0.692	0.619	0.478
3(G)	6.370	1.07	0.674	0.600	0.457
4	5.663	0.93	0.690	0.616	0.474
5	3.278	0.72	0.629	0.542	0.384
6	5.663	0.93	0.690	0.616	0.474
7(B)	3.771	0.78	0.640	0.557	0.402
7(P)	4.172	0.78	0.668	0.589	0.438
8	6.549	1.13	0.663	0.587	0.444
9	9.643	1.39	0.694	0.626	0.494
10M	7.589	1.24	0.670	0.597	0.457
10H	12.795	1.66	0.707	0.644	0.518
10Q	5.124	1.01	0.634	0.553	0.403
10(G)	7.130	1.25	0.650	0.575	0.431
10A	5.468	1.05	0.639	0.559	0.410
10A(G)	--	--	--	--	--
11	5.765	0.99	0.674	0.599	0.454
12	4.398	0.75	0.695	0.619	0.474
12G	5.663	0.93	0.690	0.616	0.474
13	4.229	0.75	0.685	0.608	0.460
14	7.439	1.25	0.662	0.588	0.447
14A	--	--	--	--	--
15	4.200	0.74	0.688	0.610	0.463
16	4.631	0.85	0.667	0.589	0.440

TABLE 7.7 (cont.)

Detail No.	m	Ω_n	Reliability, L(n)		
			0.90	0.95	0.99
16(G)	6.960	1.25	0.643	0.567	0.422
17	3.736	0.66	0.694	0.617	0.468
17(S)	7.782	1.10	0.725	0.657	0.523
17A	3.465	0.67	0.670	0.588	0.435
17A(S)	7.782	1.10	0.725	0.657	0.523
18	4.027	0.88	0.615	0.530	0.374
18(S)	9.233	1.26	0.715	0.649	0.519
19	7.472	1.27	0.658	0.583	0.441
19(S)	7.520	1.27	0.659	0.585	0.444
20	4.619	0.92	0.639	0.557	0.405
20(S)	6.759	1.22	0.644	0.567	0.422
21 (1/4")	14.245	--	--	--	--
21 (3/8")	15.494	--	--	--	--
21(S)	7.358	1.19	0.676	0.604	0.464
22	3.147	0.62	0.670	0.587	0.432
23	3.187	0.55	0.600	0.535	0.411
24	3.187	0.55	0.600	0.535	0.411
25	7.090	1.14	0.681	0.608	0.468
25A	8.518	1.32	0.679	0.609	0.472
25B	6.966	1.03	0.709	0.640	0.504
26	3.348	0.82	<u>0.586(m)</u>	0.496	0.336
27	3.146	0.78	<u>0.586(m)</u>	<u>0.495(m)</u>	<u>0.335(m)</u>
27(S)	5.277	0.87	0.694	0.620	0.477
28	7.746	1.20	0.687	0.616	0.478
28(F)	--	--	--	--	--
30	3.159	0.62	0.671	0.589	0.434
30A	3.368	0.55	0.724	0.650	0.506
31	4.348	--	--	--	--
31A	3.453	0.71	0.649	0.565	0.409
32A	4.200	0.74	0.688	0.610	0.463
32B	3.533	--	--	--	--
33	3.660	0.75	0.646	0.562	0.407

TABLE 7.7 (cont.)

Detail No.	m	Ω_n	Reliability, L(n)		
			0.90	0.95	0.99
33(S)	10.368	1.38	0.714	0.650	0.522
35	3.808	0.64	0.709	0.633	0.488
36	6.966	1.03	0.709	0.640	0.504
36A	5.163	0.81	0.711	0.639	0.498
38	3.462	0.66	0.675	0.594	0.441
38(S)	10.225	1.42	0.702	0.635	0.505
42	3.533	--	--	--	--
42	7.358	1.19	0.676	0.604	0.464
46	4.348	--	--	--	--
51(V)	3.818	0.58	0.738(M)	0.667	0.528
52(V)	4.042	0.62	0.732	0.661	0.521
Mean Value	--	--	0.674	0.598	0.455
Standard Deviation	--	--	0.0345	0.0384	0.0437

Note:

M = Maximum value

m = Minimum value

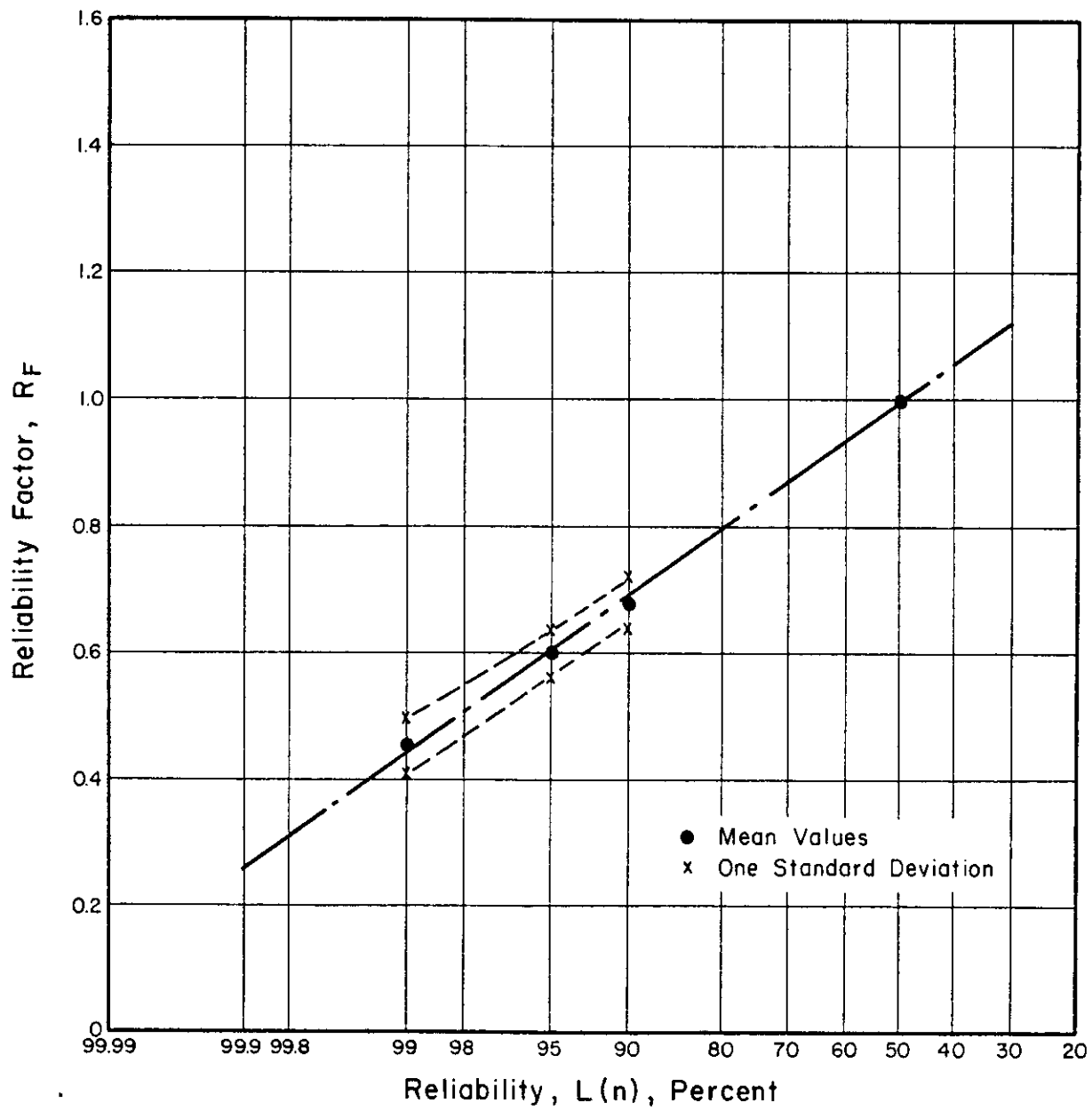


Fig. 7.10 Mean Values of Reliability Factor for Various Levels of Reliability.

This relationship, using Tables B.1, 7.5 and 7.7, is based on a desired life of 10^8 cycles. For any other life the values of random load factors, as noted in Table 7.5, would need to be modified.

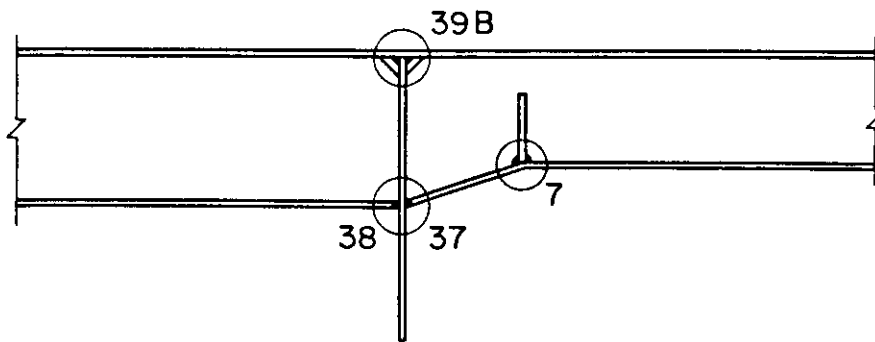
A design example for a beam bracket with four structural details is presented in Fig. 7.11. In this instance, the Weibull shape factor for the loading history, k , was taken as 1.0, and the desired level of reliability was assumed to be equal to 90 percent. The resulting maximum allowable bending fatigue stress range at the deck-bulkhead intersection (detail 39B) is found to be 32.9 ksi. (The mean value of the reliability factor (from Table 7.7) was used in this case.) This maximum stress range provides only for fatigue; in addition, the maximum stress must not exceed the nominal permissible stress permitted once by the basic design rules (7.13). For detail number 7, at the toe of the stiffener weld in the web and flange, the maximum allowable bending fatigue stress range is 40.1 ksi for a 20-year life.

Similar calculations can be made for the other details (No. 37 and 38) and for other levels of reliability. A summary of such calculations is presented in Table 7.8 and shows the effect of a variation in desired level of reliability on maximum fatigue stress range.

7.6 References

- 7.1 Lewis, Edward V. "The Reliability Approach to Ship Structural Design," Tokyo, 1975.
- 7.2 Ang, A. H.-S. "A Comprehensive Basis for Reliability Analysis and Design," Tokyo, 1974.
- 7.3 Ang, Alfredo H.-S. "Structural Risk Analysis and Reliability-Based Design," Journal of the Structural Division, American Society of Civil Engineers, Vol. 99, No. ST9, September 1973, pp. 1891-1910.
- 7.4. Ang, A. H.-S. and Munse, W. H. "Practical Reliability Basis for Structural Fatigue," ASCE National Structural Engineering Conference, April 14-18, 1975. (Preprint No. 2494).
- 7.5 Bowman, M. D. and Munse, W. H., "The Effect of Discontinuities on the Fatigue Behavior of Transverse Butt Welds in Steel," University of Illinois, SRS No. 491, April 1981.
- 7.6 Freudenthal, A. M. "Prediction of Fatigue Failure," J. Appl. Phys. (Dec. 1960) Vol. 31, No. 12, 2196-2198.
- 7.7 Ang, A. H.-S. "Probabilistic Bases of Safety, Performance and Design," prepared for ASCE Specialty Conference on Safety and Reliability of Metal Structures, Pittsburgh, November 1972.
- 7.8 Wirsching, Paul H. and Yao, James T. P. "Statistical Methods in Structural Fatigue," ASCE Proceedings, Vol. 96, No. ST6, June 1970.
- 7.9 Ang, A. H.-S. "Bases for Reliability Approach to Structural Fatigue," 2nd International Conference on Structural Safety and Reliability, Munich, September 1977.
- 7.10 Miner, M. A. "Cumulative Damage in Fatigue," Trans. of ASME, Vol. 67, 1945.

Ship Assembly IAI - Beam Bracket



Detail No. (See Fig. B.1)	$(S)_{108}$ (See Table B.1)	m	
7	7.2	3.77	Reliability - 0.90 Weibull Dist. $k = 1.0$
39B	5.9 Est.	4.0 Est.	
37	5.0 Est.	3.7 Est.	
38	4.2	3.46	

A. Considering Deck Plate - Detail 39B

$(S)_{108} = 5.9 \text{ ksi Est.}$ $m = 4.0 \text{ Est.}$ (Table B.1 or Estimated)
 Reliability Factor = 0.67 (R_F) (Table 7.7 or Eqn. 7.3)
 Random Load Factor = 8.32 (ξ) (Table 7.5 or Eqn. 7.31)
 Max. Allowable Stress Range = $5.9 \times 0.67 \times 8.32 = 32.9 \text{ ksi}$
 (The Maximum Stress Not To Be Greater Than the Nominal Stress Permitted Once During the Ships Lifetime)

B. Considering Stiffener Detail - Detail 7

$(S)_{108} = 7.2 \text{ ksi}$ $m = 3.77$
 $R_F = 0.64$ $\xi = 8.70$
 Max. Allowable Stress Range = $7.2 \times 0.64 \times 8.70 = 40.1 \text{ ksi}$
 (The Maximum Stress Not To Be Greater Than the Nominal Stress Permitted Once During the Ships Lifetime)

Fig. 7.11 Design Example.

TABLE 7.8

Fatigue Design Stress Ranges for Beam Bracket 1A1 (Fig. 7.11)
(Weibull Distribution $k=1.0$)

Detail No. (Fig. B.1)	$(S)10^8$, ksi (Table B.1)	m (Table 7.1)	Reliability*	C.O.V. Ω_n	R_F (Table 7.7)	ξ (Table 7.5)	S_D , ksi
7(B)	7.2	3.77	0.90	0.78	0.640	8.70	40.1
(P)	6.8	4.17	0.90	0.78	0.668	8.09	36.7
37	(5.0)	(3.7)	0.90	--	0.67	8.81	29.5
38	4.2	3.46	0.90	0.66	0.675	9.22	26.1
39B	(5.9)	(4.0)	0.90	--	0.67	8.32	32.9
7(B)	7.2	3.77	0.95	0.78	0.557	8.70	34.9
(P)	6.8	4.17	0.95	0.78	0.589	8.09	32.4
37	(5.0)	(3.7)	0.95	--	0.60	8.81	26.4
38	4.2	3.46	0.95	0.66	0.594	9.22	23.0
39B	(5.9)	4.0	0.95	--	0.60	8.32	29.5
7(B)	7.2	3.77	0.99	0.78	0.402	8.70	25.2
(P)	6.8	4.17	0.99	0.78	0.438	8.09	24.1
37	(5.0)	(3.7)	0.99	--	0.46	8.81	20.3
38	4.2	3.46	0.99	0.66	0.441	9.22	17.1
39B	(5.9)	(4.0)	0.99	--	0.46	8.32	22.6

*Values from Table 7.7 or the mean value where no specific value was available.

76

- 7.11 Ang, A. H.-S. and Tang, W. H. "Probability Concepts in Engineering Planning and Design," Volume I-Basic Principles, Wiley, 1975.
- 7.12 Lewis, E. V. and Zubaly, R. B. "Dynamic Loadings Due to Waves and Ship Motions," SNAME, 1975.
- 7.13 "Rules for Building and Classing Steel Vessels," American Bureau of Shipping, 1979.

8. SUMMARY AND CONCLUSIONS

This report presents a simple design procedure that has been developed to provide for fatigue strength verification in ship design. The criteria provide for:

- (a) A large variety in ship structure details (Appendix A).
- (b) The basic fatigue resistance of numerous welded details (Appendix B).
- (c) A distribution function that can be used to represent the long life loading (10^8 cycles--20 years) for various types of ships (Chapter 6).
- (d) A random loading factor that accounts for the randomness of the entire loading history during the life of the structure (Table 7.5).
- (3) A reliability factor (factor of safety) that accounts for the many uncertainties that exist (Table 7.7 or Fig. 7.10).

The values of maximum allowable fatigue stress range obtained in the design examples appear to provide an excellent calibration of the procedure, based on the past performance of such details in the ships at sea. It is important to note that in the application of these design criteria, it is essential that the direction of stressing be the same for the "local fatigue detail" and of the "ship detail" being considered. Additional studies and evaluations now should be made of those details at which fatigue failures have developed to further evaluate and calibrate the procedure. It should be possible also to use the procedure to develop relative fatigue ratings for the many details used for ship structures.

In addition to a more extensive verification of the adequacy of the basic criteria, needs exist for further information and data to make the criteria more complete. These needs include the following.

- (a) Stress histories for more ships and types of ships for the critical details and locations in these ships. These loading histories must include all loadings to which the details are subjected, including the effects of local loadings. Measures of the uncertainty or variability in these stress histories are also needed.
- (b) Data are required to provide for the development of reduction factors to account for the effects of corrosion from the sea or shipboard atmosphere on the long-time fatigue resistance of the ship details.
- (c) Further laboratory studies should be planned to obtain the fatigue behavior of those details for which the basic fatigue resistance is most critically needed (see Table 5.1).
- (d) The basic fatigue data for the various local fatigue details should be further up-dated to include as much of the latest fatigue data as possible.

9. ACKNOWLEDGMENTS

This report is a summary of the research conducted in the Civil Engineering Department of the University of Illinois at Urbana-Champaign as Project SR-1257 of the Ship Structure Committee program to develop fatigue design criteria for ship details under U.S. Coast Guard contract No. DOT-CG-923889A.

The research was conducted by Kim Nicholl, Thomas W. Wilbur, Martin Tellalian, and Kevin Wilson, Research Assistants in Civil Engineering under the direction of W. H. Munse, Professor of Civil Engineering. Appreciation is extended to Mr. John R. Williams who prepared the weldments, to Mr. Glen Lafenhagen who assisted in the fatigue testing, to Pat Griffis who typed the manuscript for this report, and to the draftsmen and other laboratory personnel who assisted with the analyses, tests, and the preparation of this report.

In addition, the authors would like to express their appreciation to Professors Edward V. Lewis and D. Hoffman who served as consultants on the subject program, and the Project SR-1257 Advisory Committee for their counsel and guidance during the conduct of the various studies.

Finally, it should be noted that the opinions, findings and conclusions expressed herein are those of the authors and not necessarily those of the sponsors.

Appendix A

Catalog of Ship Details and Assemblies

This catalog of ship details and assemblies has been taken directly from references A.1 and A.2. The local fatigue details of Appendix B are identified on the sketches by the numbers at the solid or open circles. The details are identified individually by the family numbers, a sub-family letter, and the circled individual detail or assembly number; i.e., 1A1, 1A2, . . . , 12F5.

Fig. A.1 Beam Brackets Details, Family No. 1.

CONTINUOUS

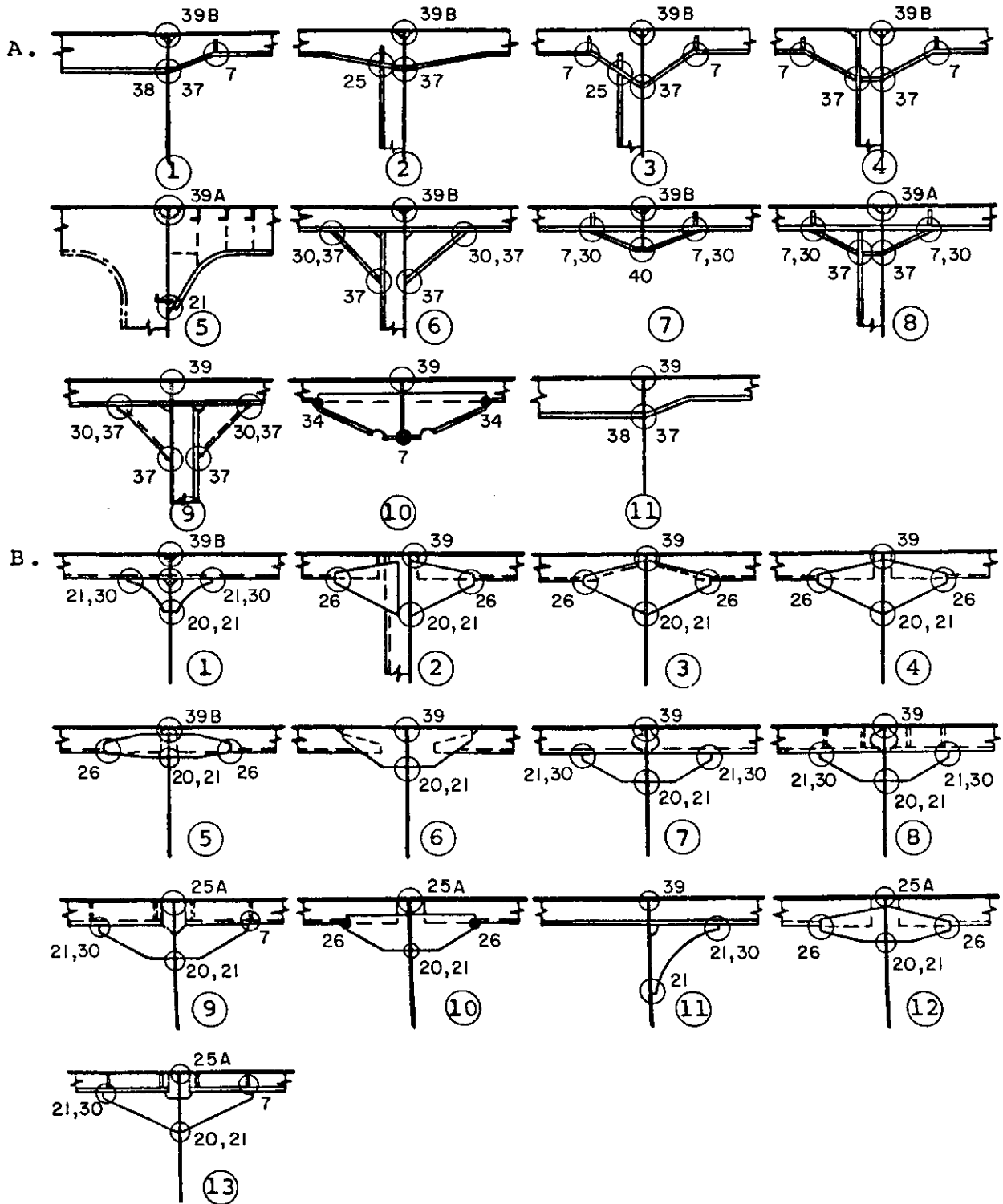
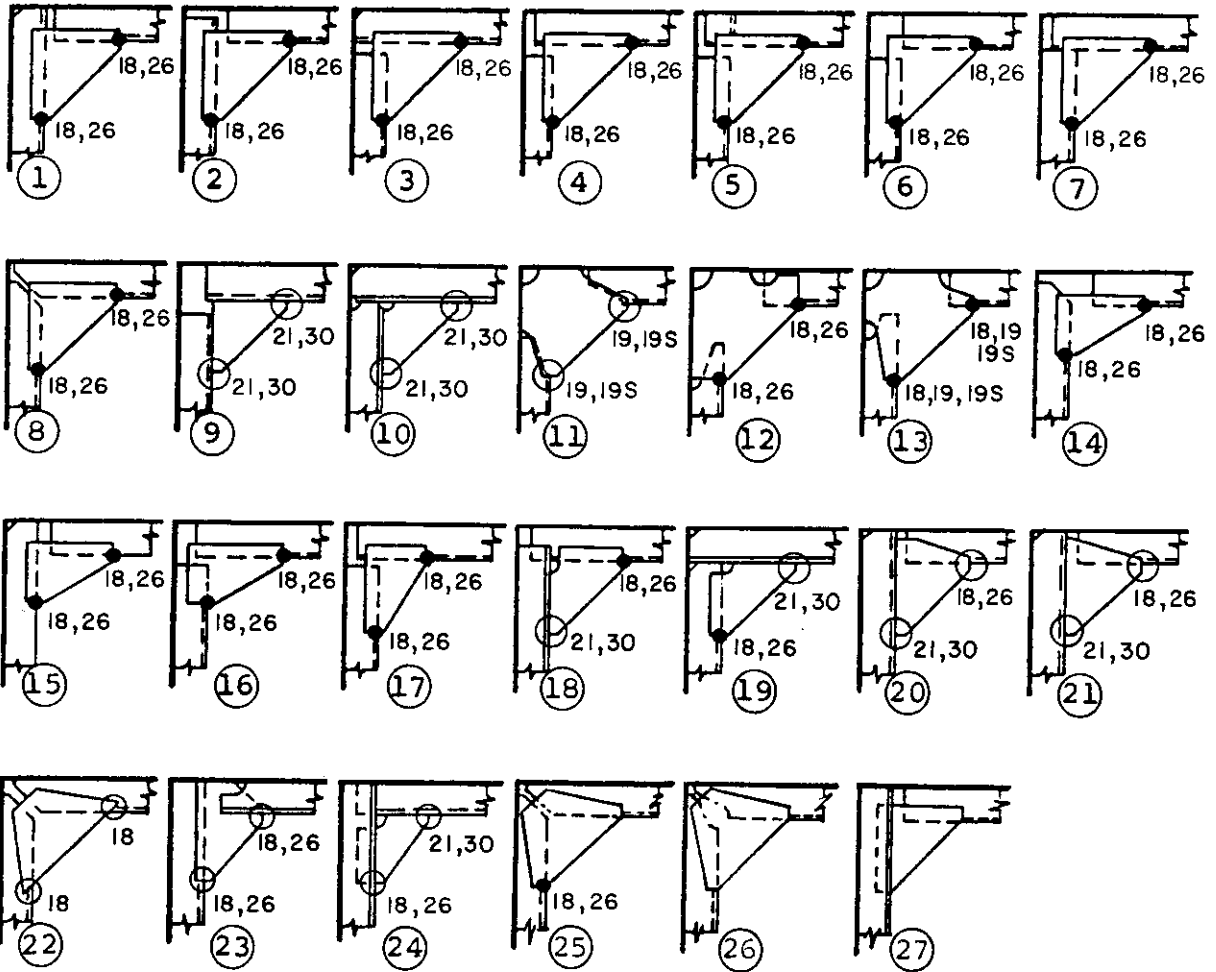


Fig. A.1 Beam Brackets Details, Family No. 1 (Cont.),

CORNER

C.



D.

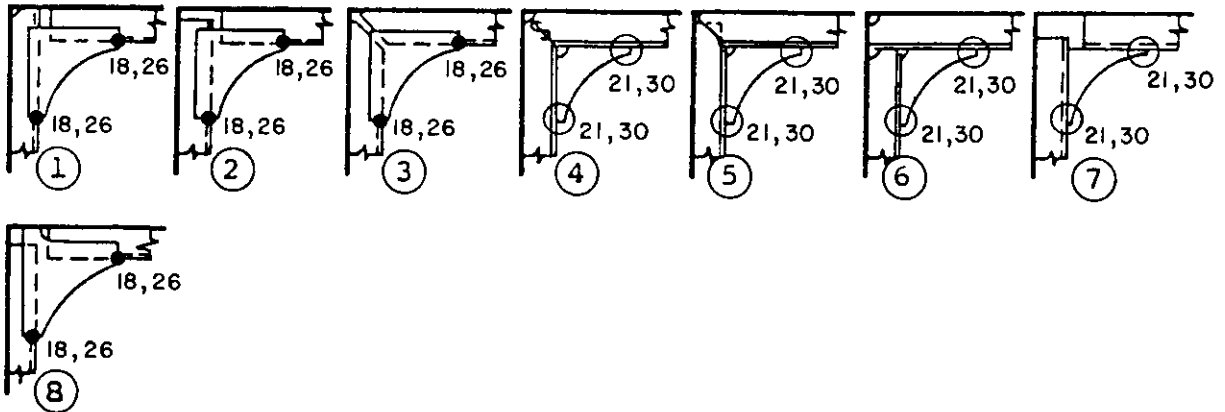


Fig. A.1 Beam Brackets Details, Family No. 1 (Cont.).

CORNER (Cont'd)

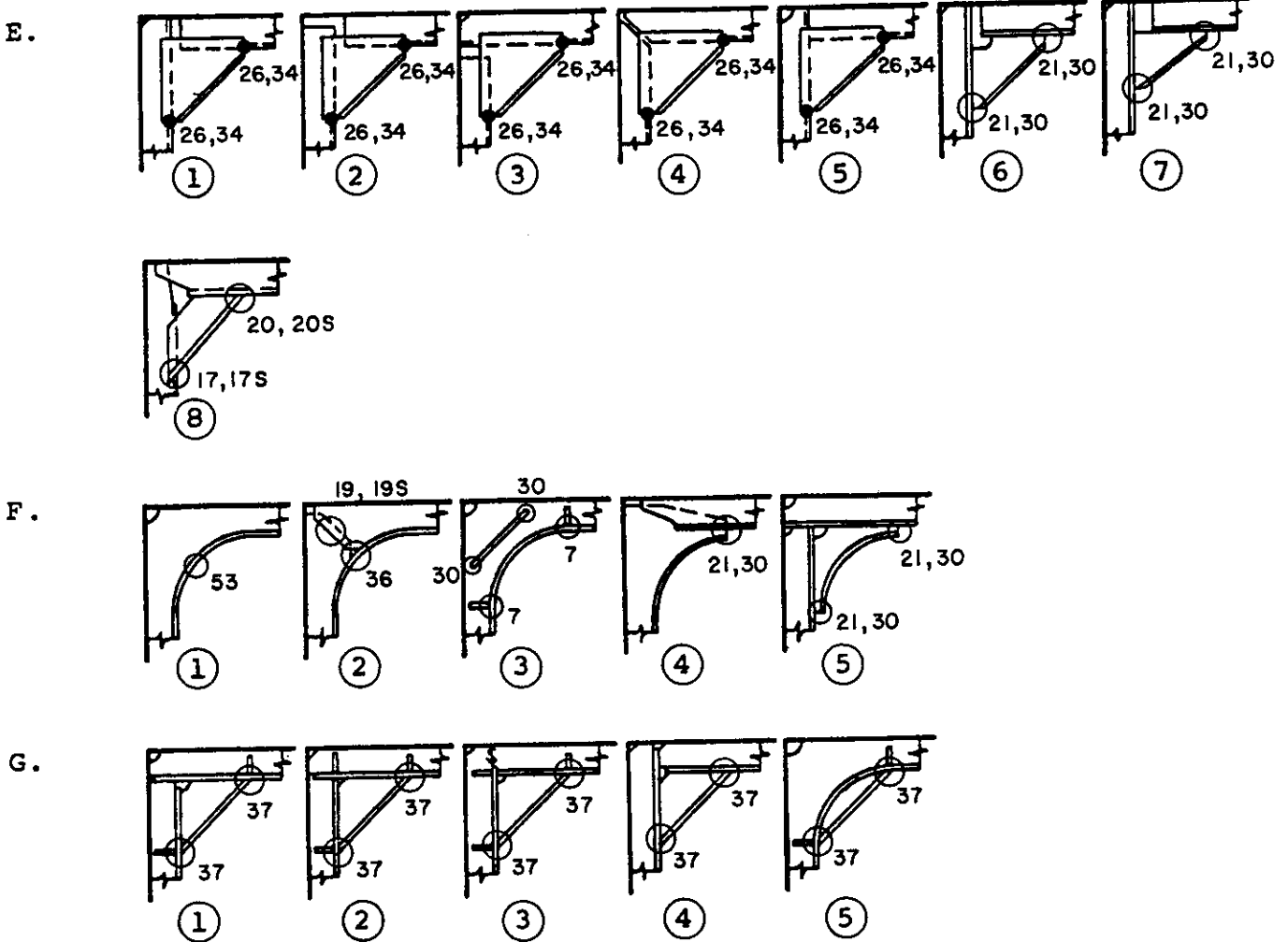
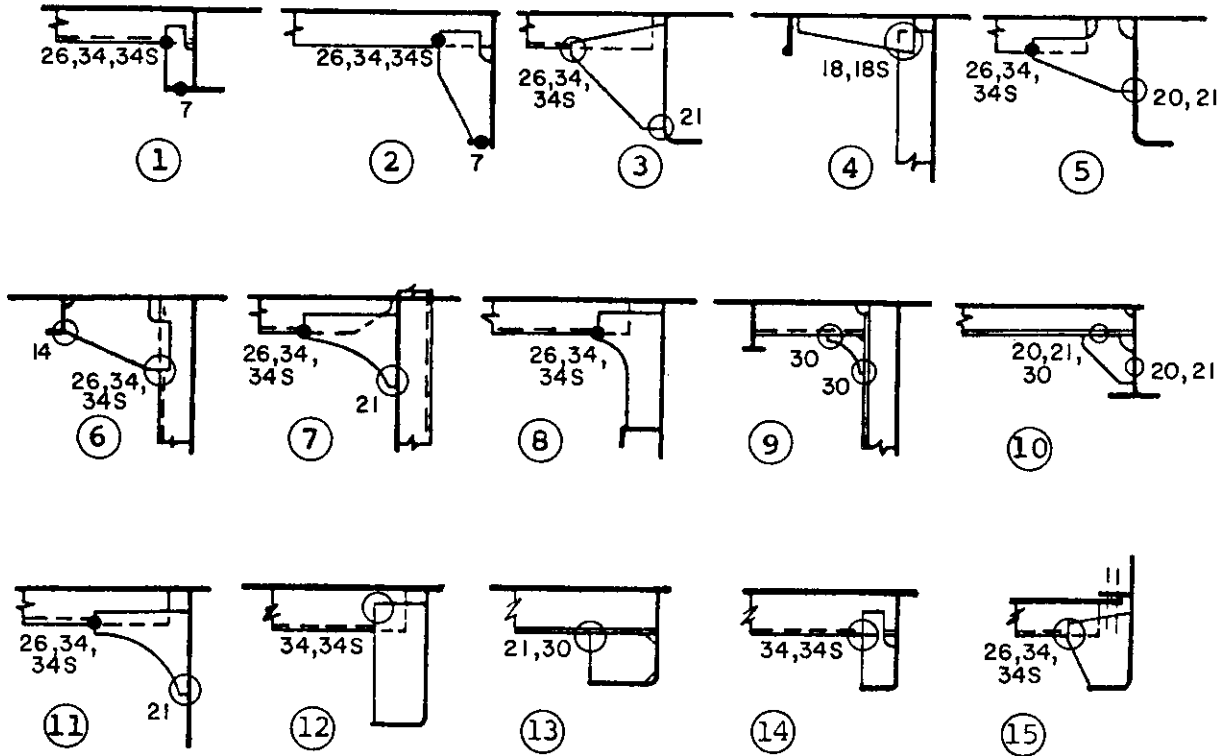


Fig. A.1 Beam Brackets Details, Family No. 1 (Cont.).

END

H.



J.

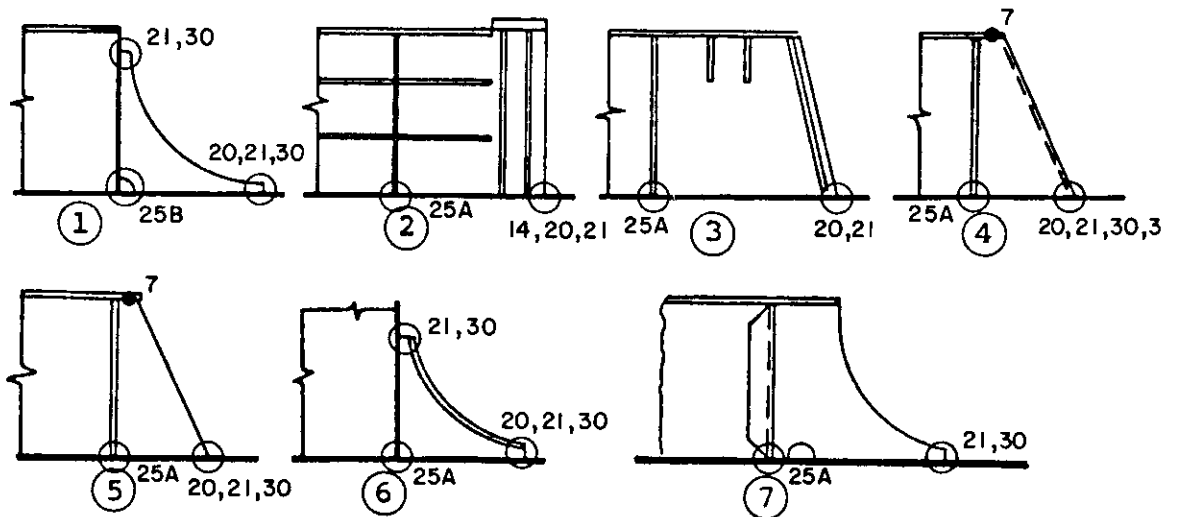


Fig. A.1 Beam Brackets Details, Family No. 1 (Cont.).

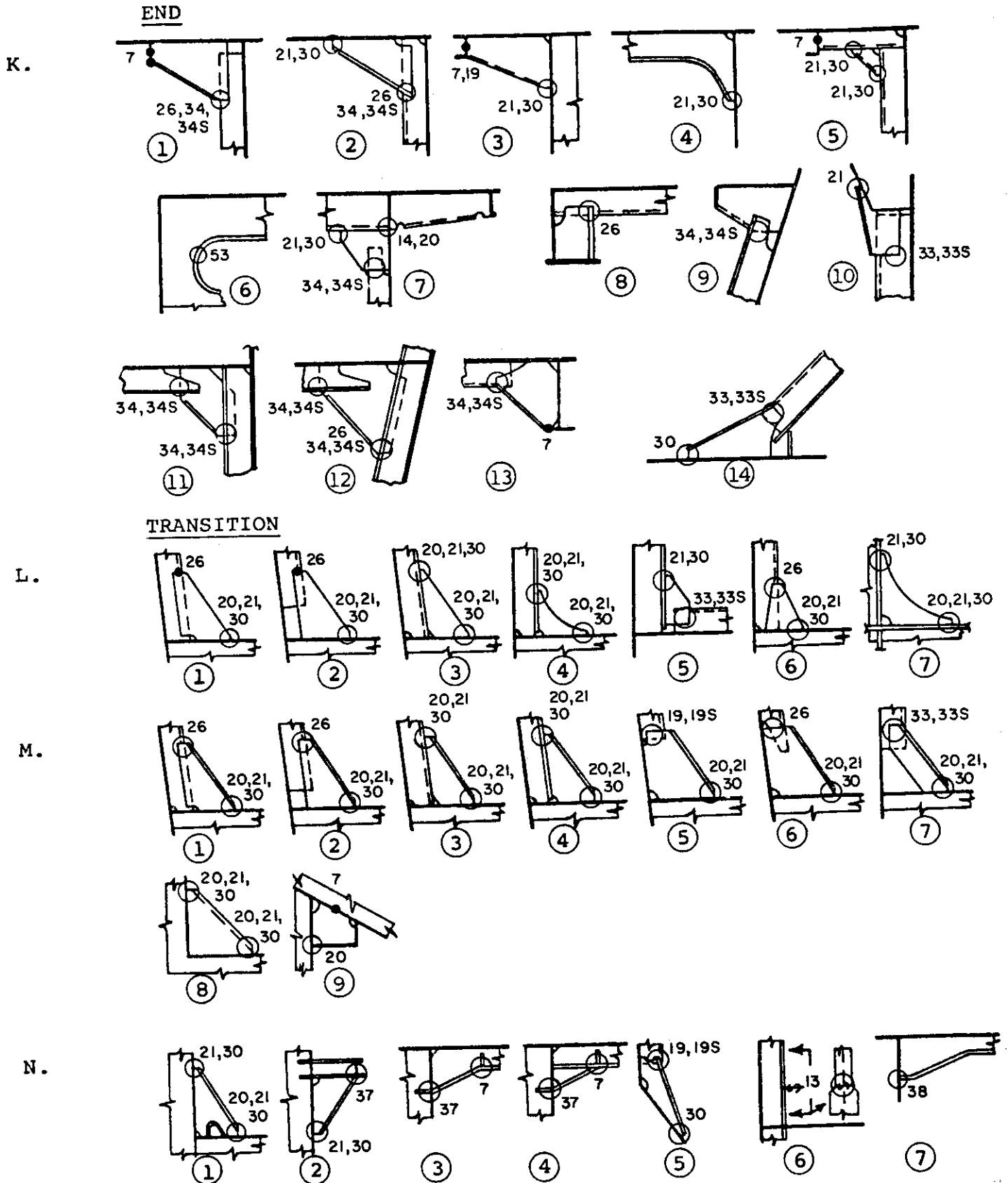


Fig. A.1 Beam Brackets Details, Family No. 1 (Cont.).

TRANSITION (Cont'd)

P.

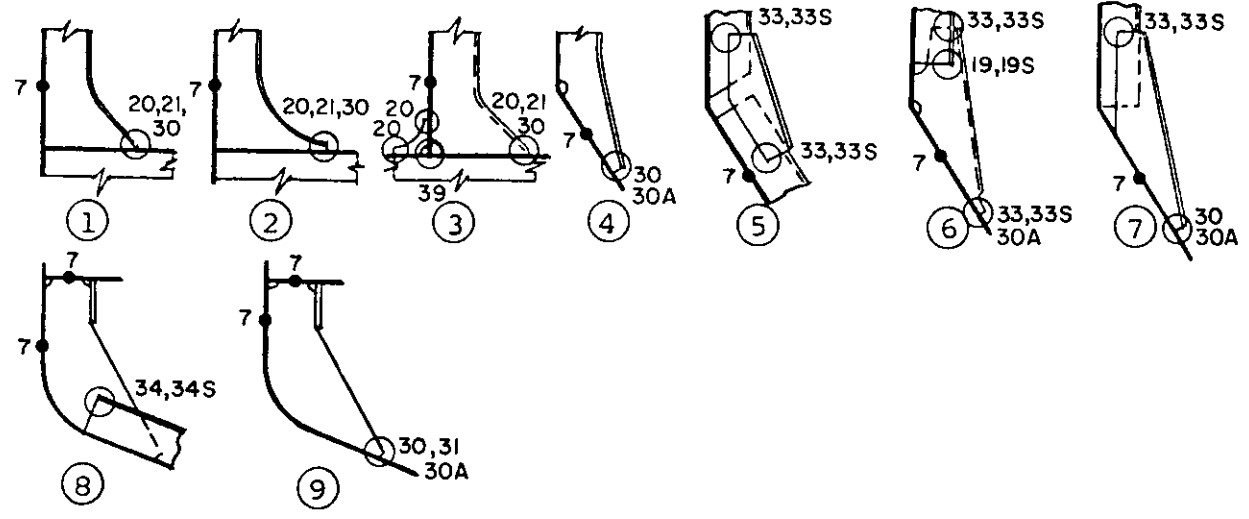


Fig. A.2 Tripping Bracket Details, Family No. 2.

A.

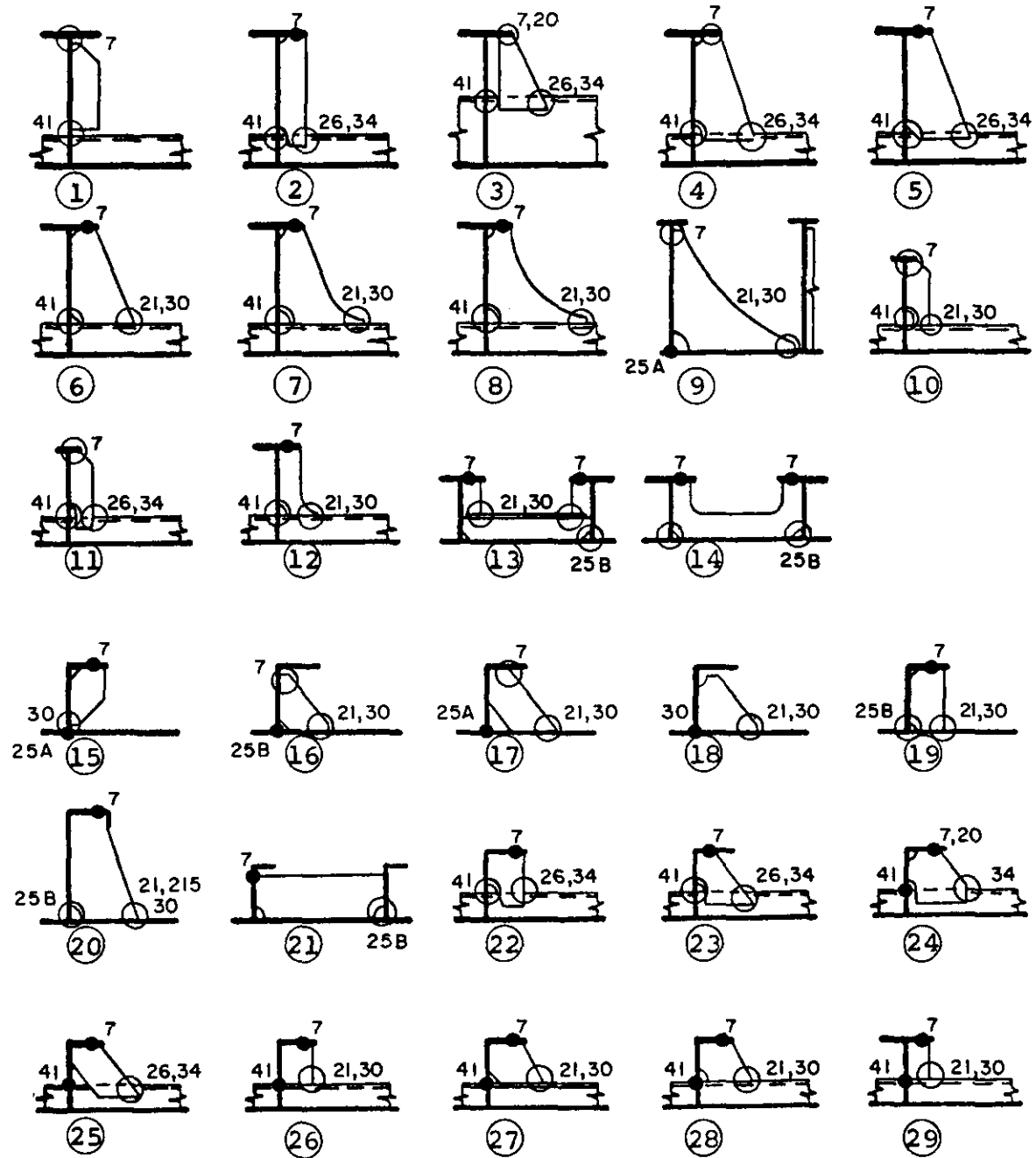
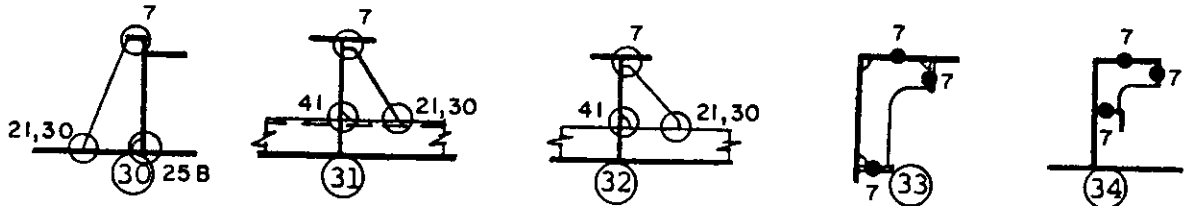


Fig. A.2 Tripping Bracket Details, Family No. 2 (Cont.).



B.

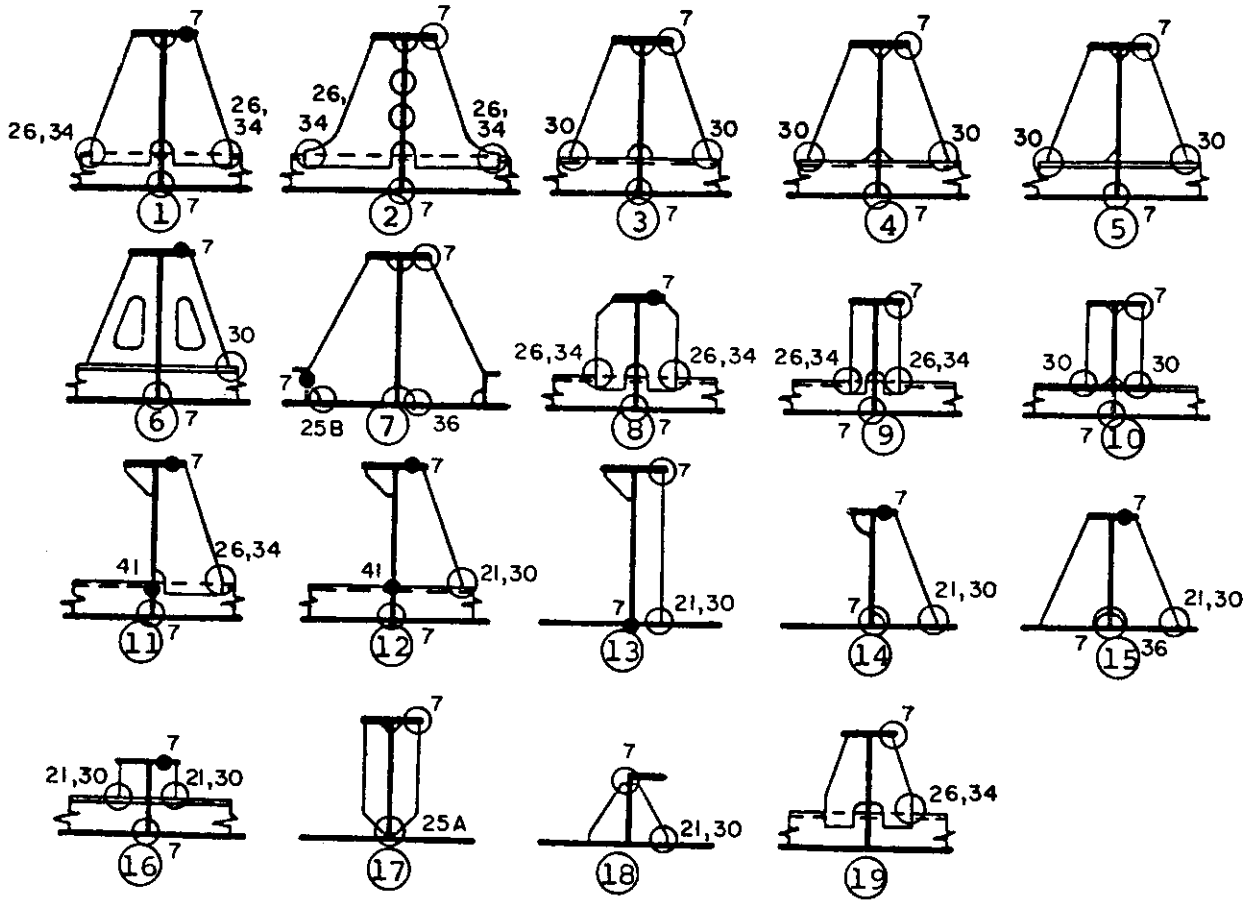


Fig. A.2 Tripping Bracket Details, Family No. 2 (Cont.).

C.

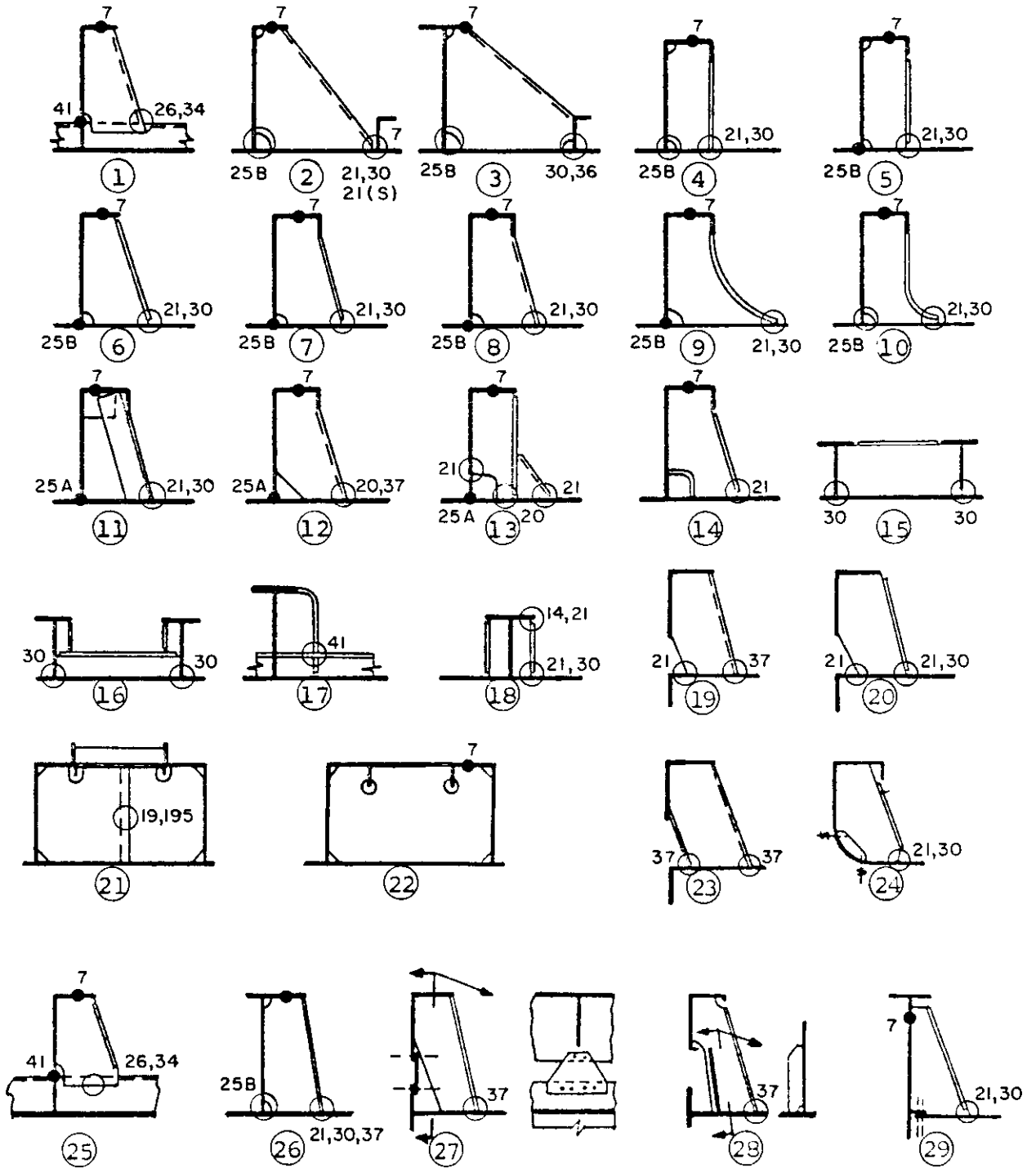
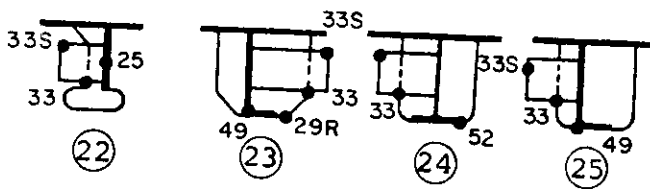
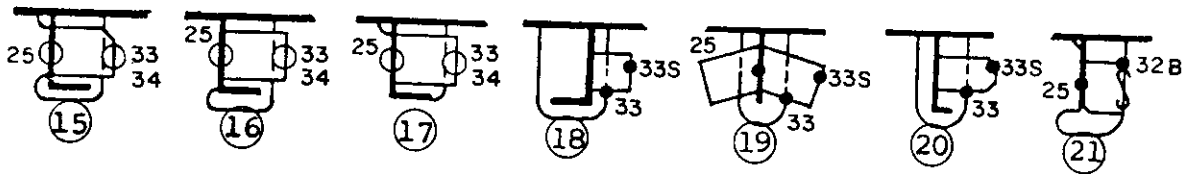
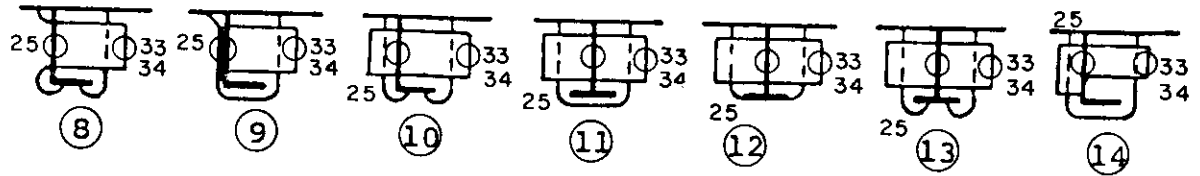
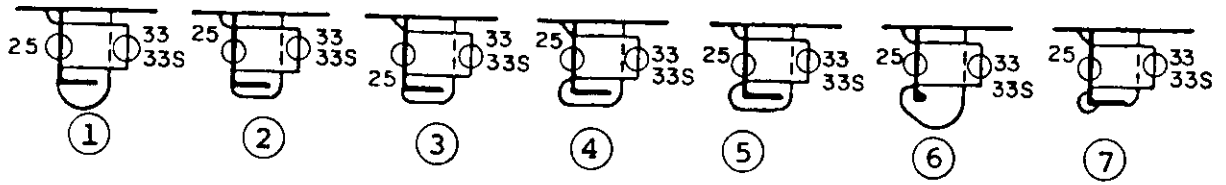


Fig. A.3 Non-Tight Collar Details, Family No. 3.

A.



B.

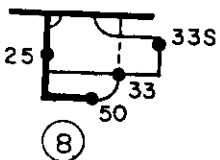
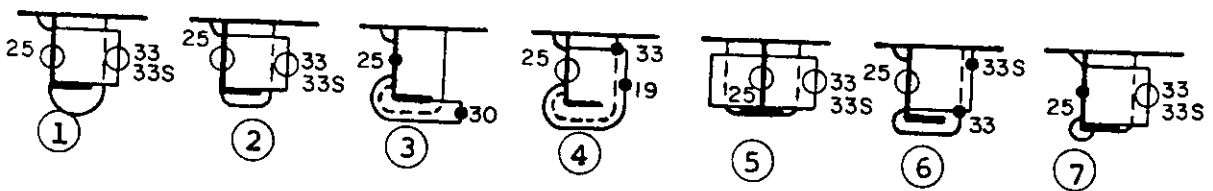


Fig. A.3 Non-Tight Collar Details, Family No. 3 (Cont.).

C.

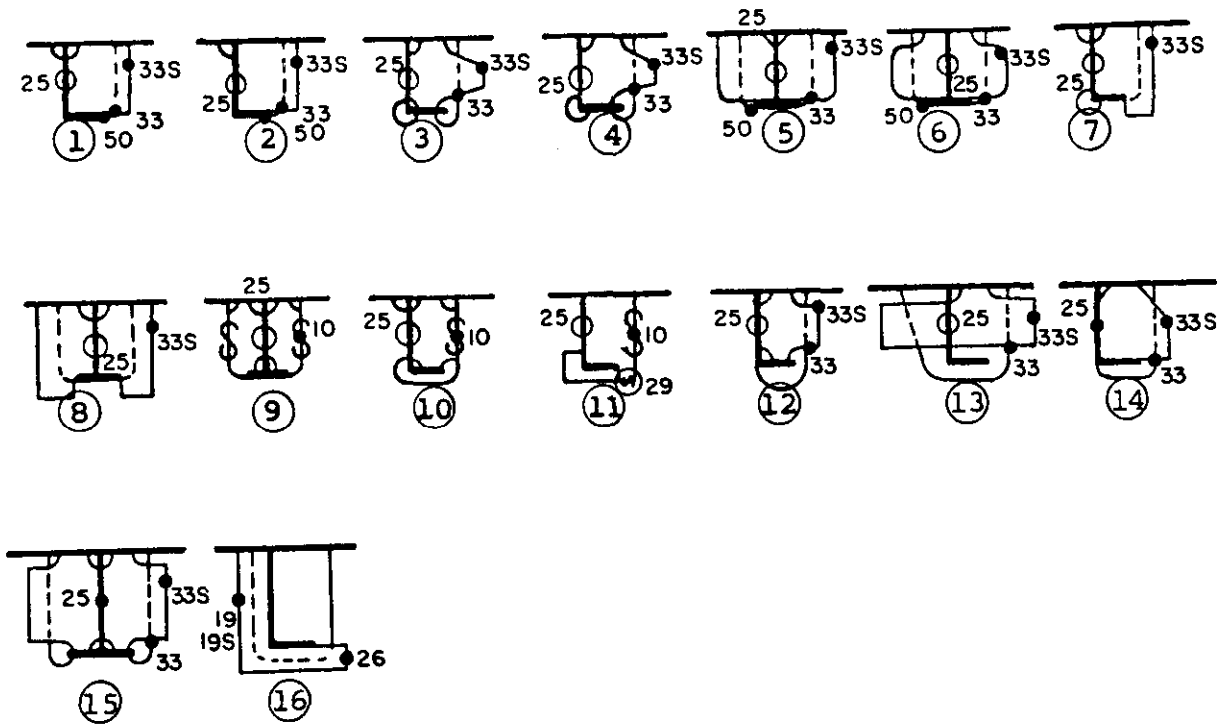
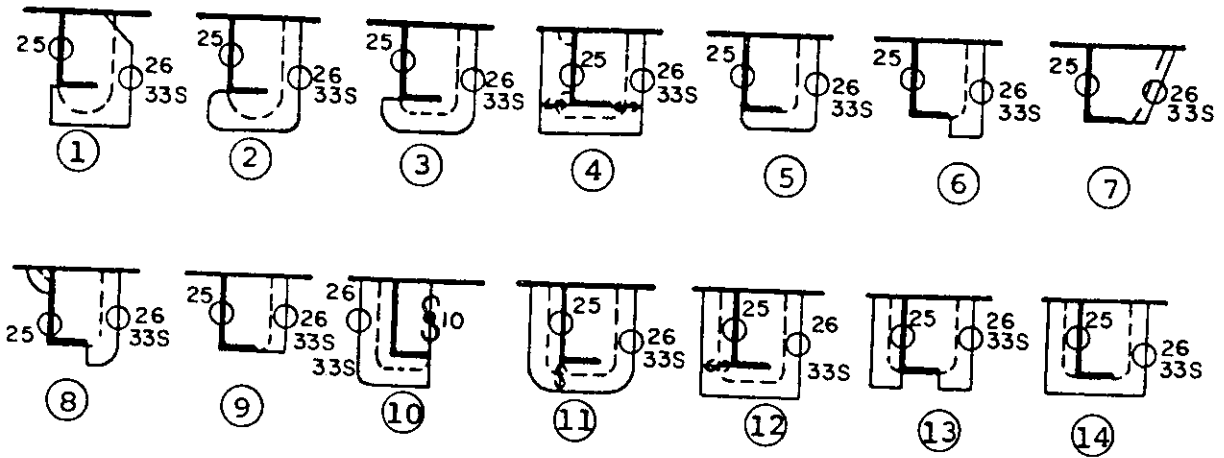
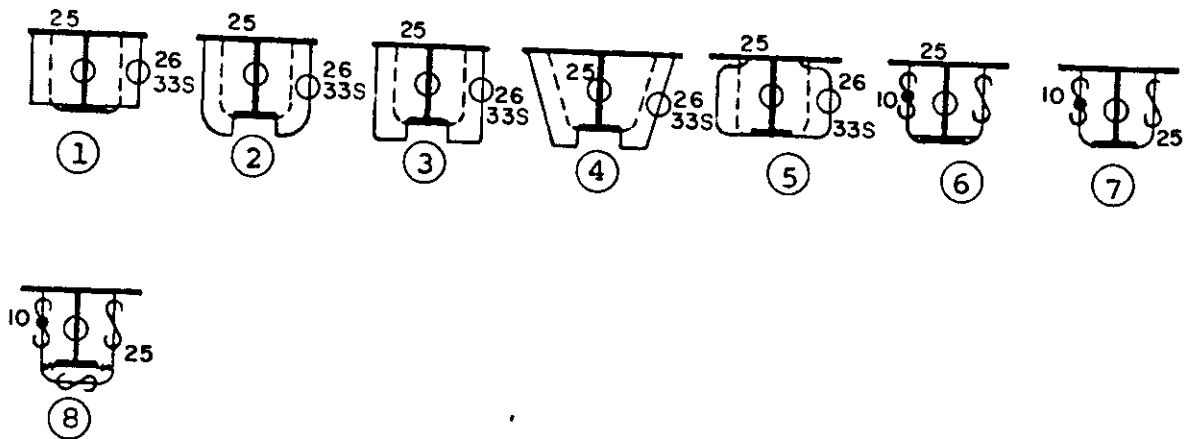


Fig. A.4 Tight Collar Details, Family No. 4.

A.



B.



C.

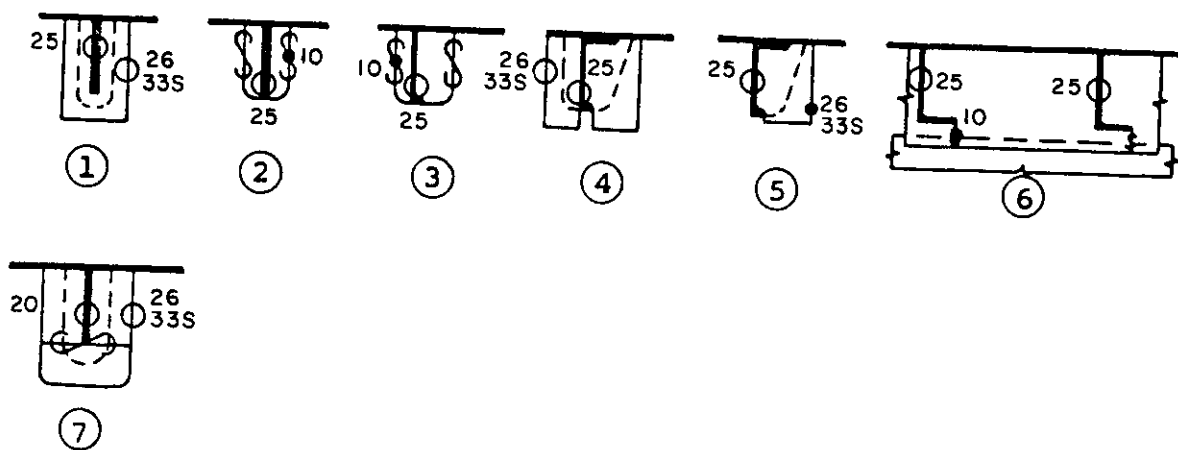


Fig. A.4 Tight Collar Details, Family No. 4 (Cont.).

D.

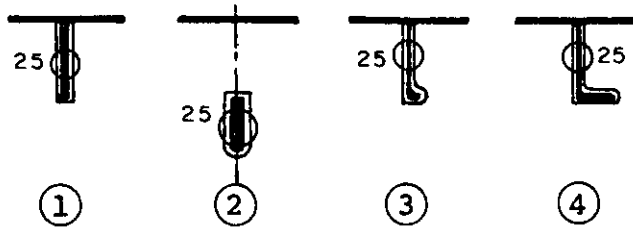


Fig. A.5 Gunwale Connection Details, Family No. 5.

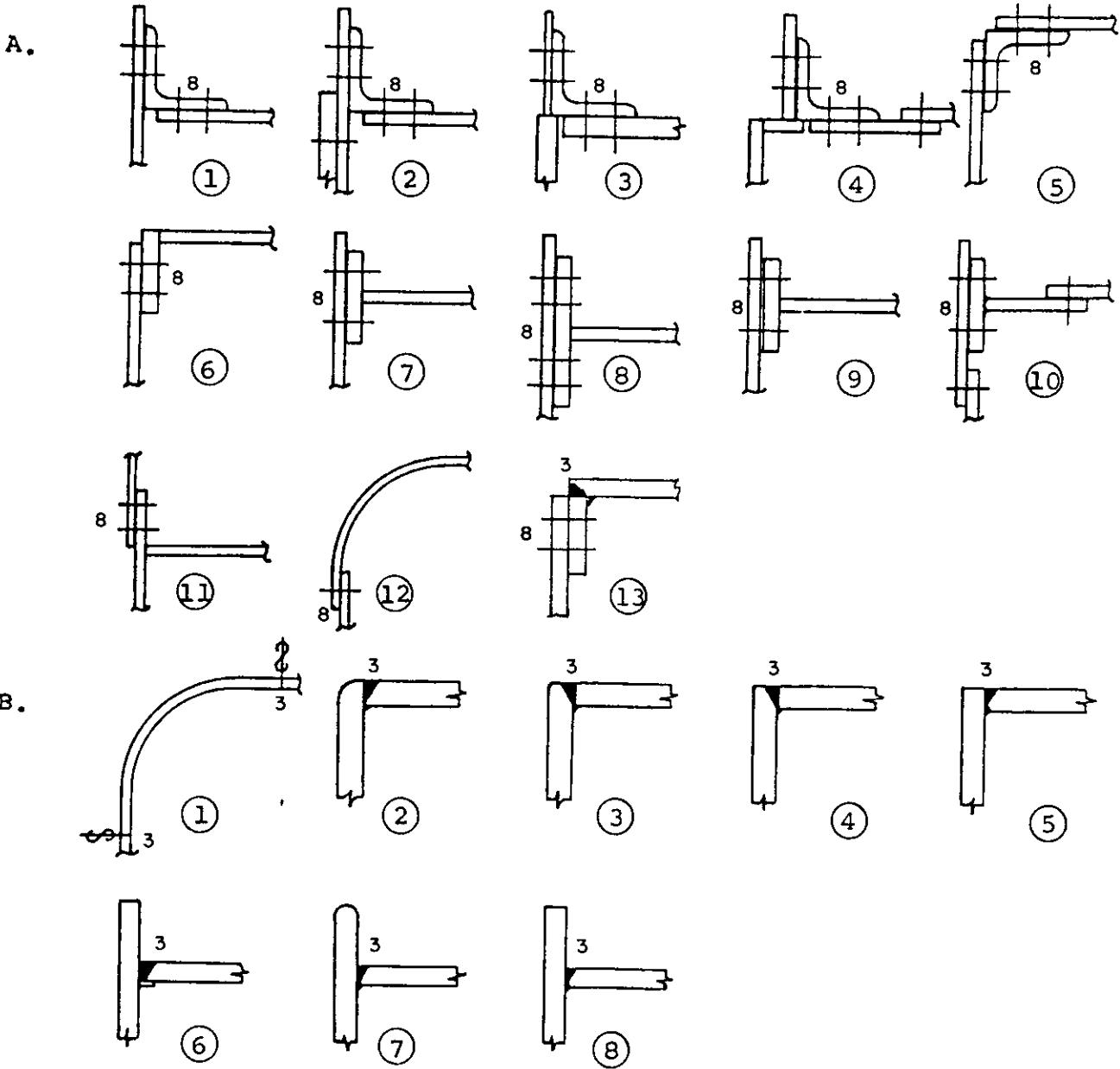


Fig. A.6 Miscellaneous Cutout Details, Family No. 7.

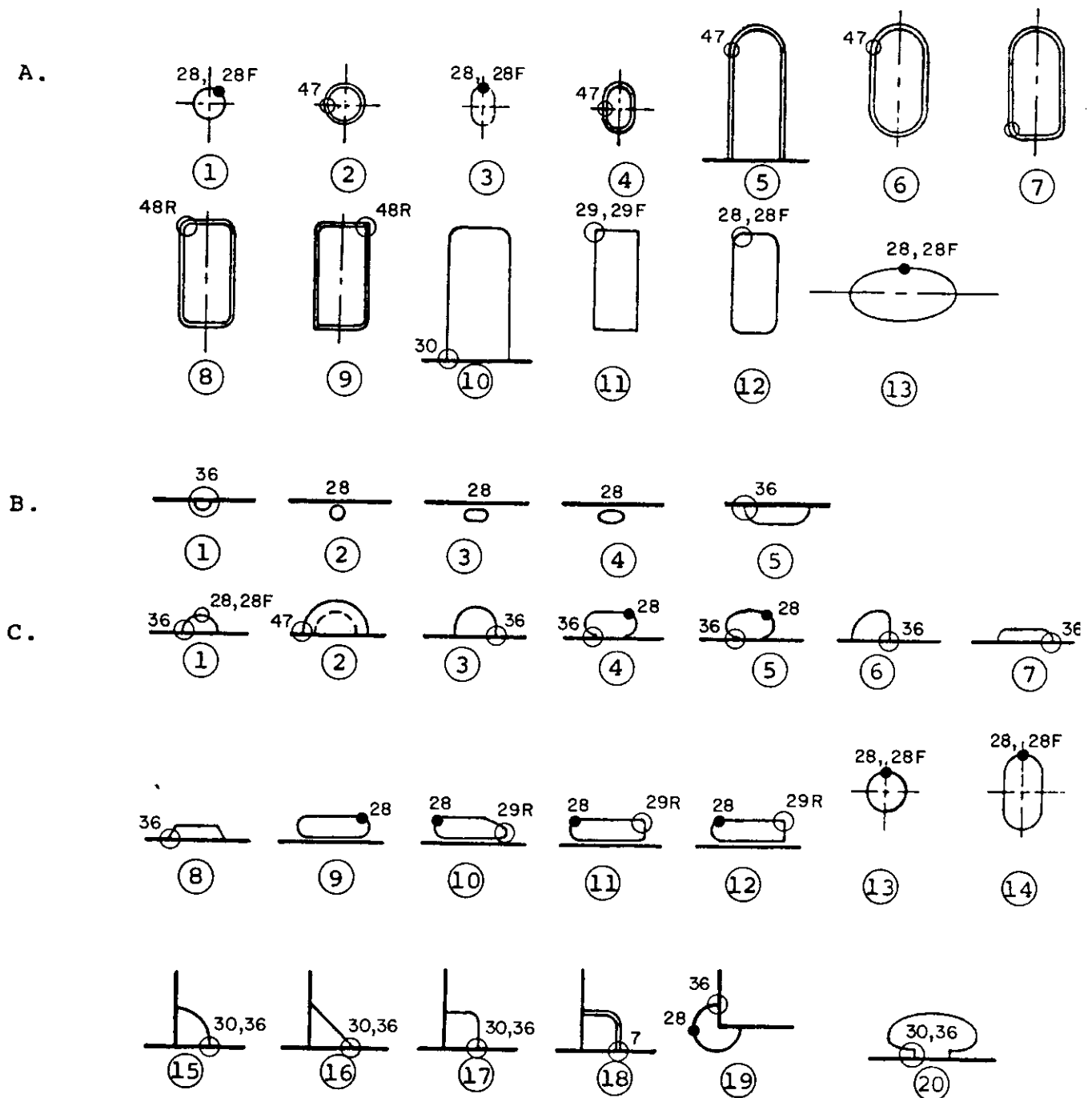


Fig. A.6 Miscellaneous Cutout Details, Family No. 7 (Cont'd).

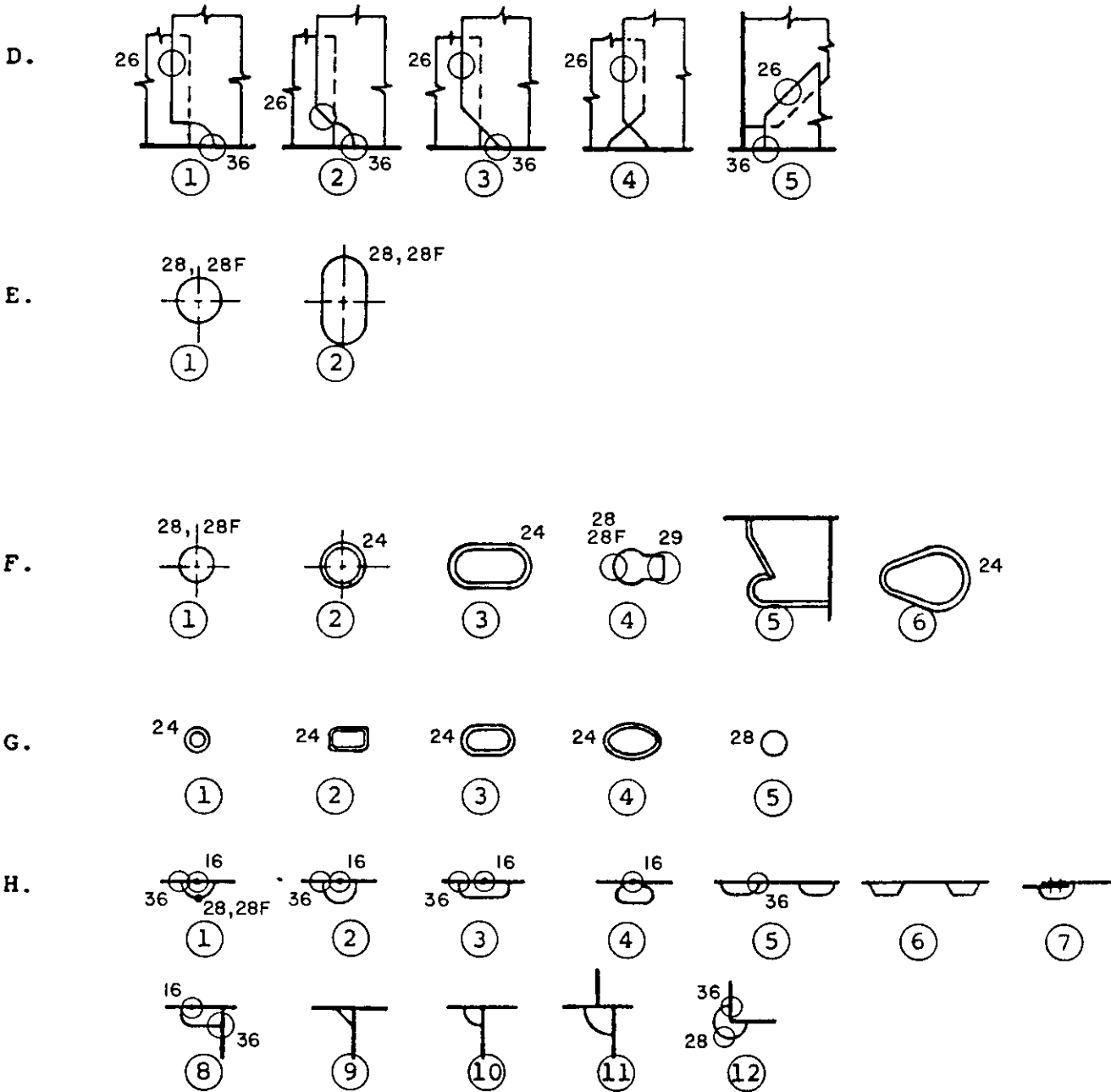


Fig. A.7 Clearance Cutouts Details, Family No. 8.

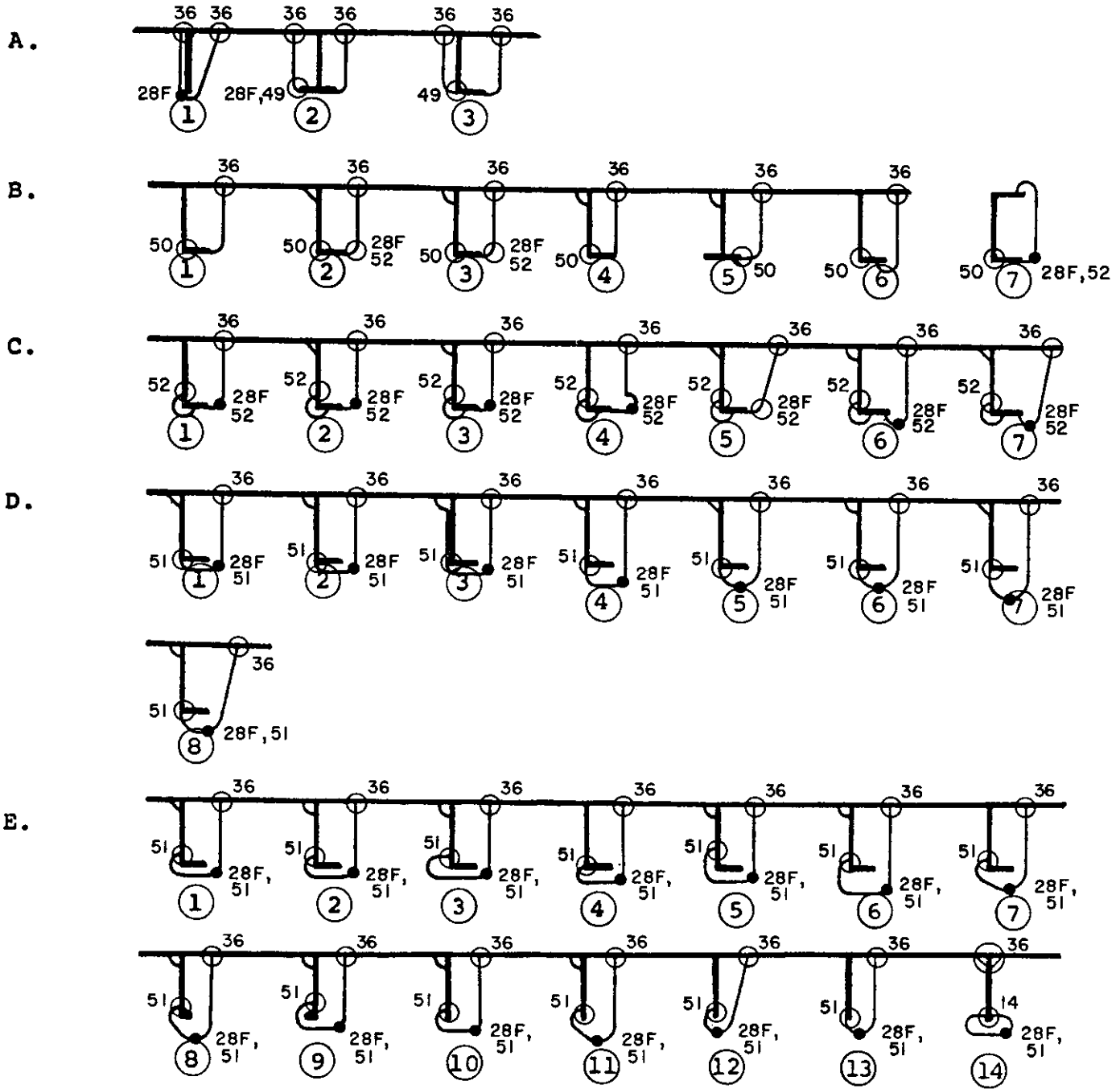


Fig. A.8 Deck Cutout Details, Family No. 9.

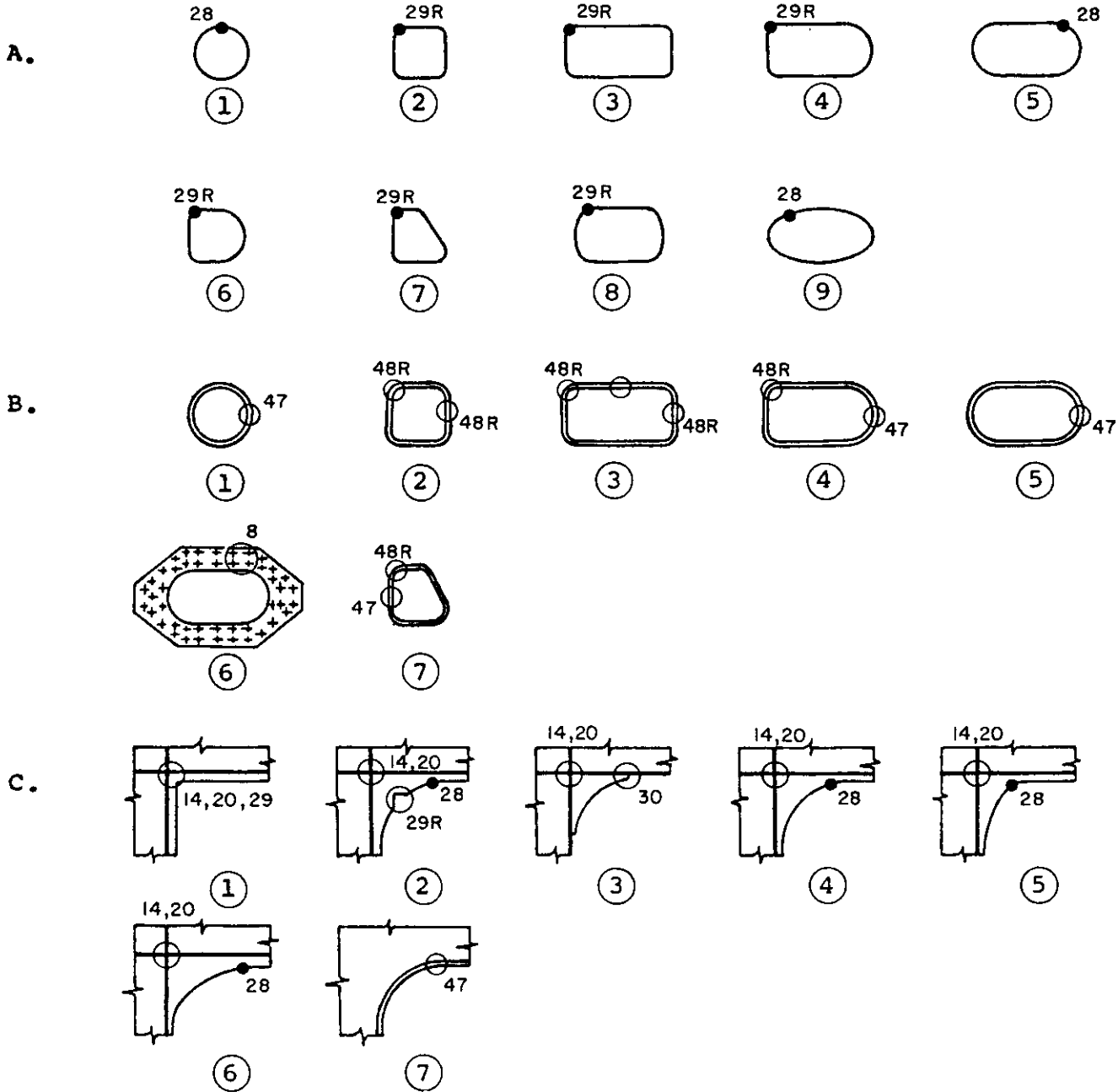


Fig. A.9 Stanchion End Details, Family No. 10.

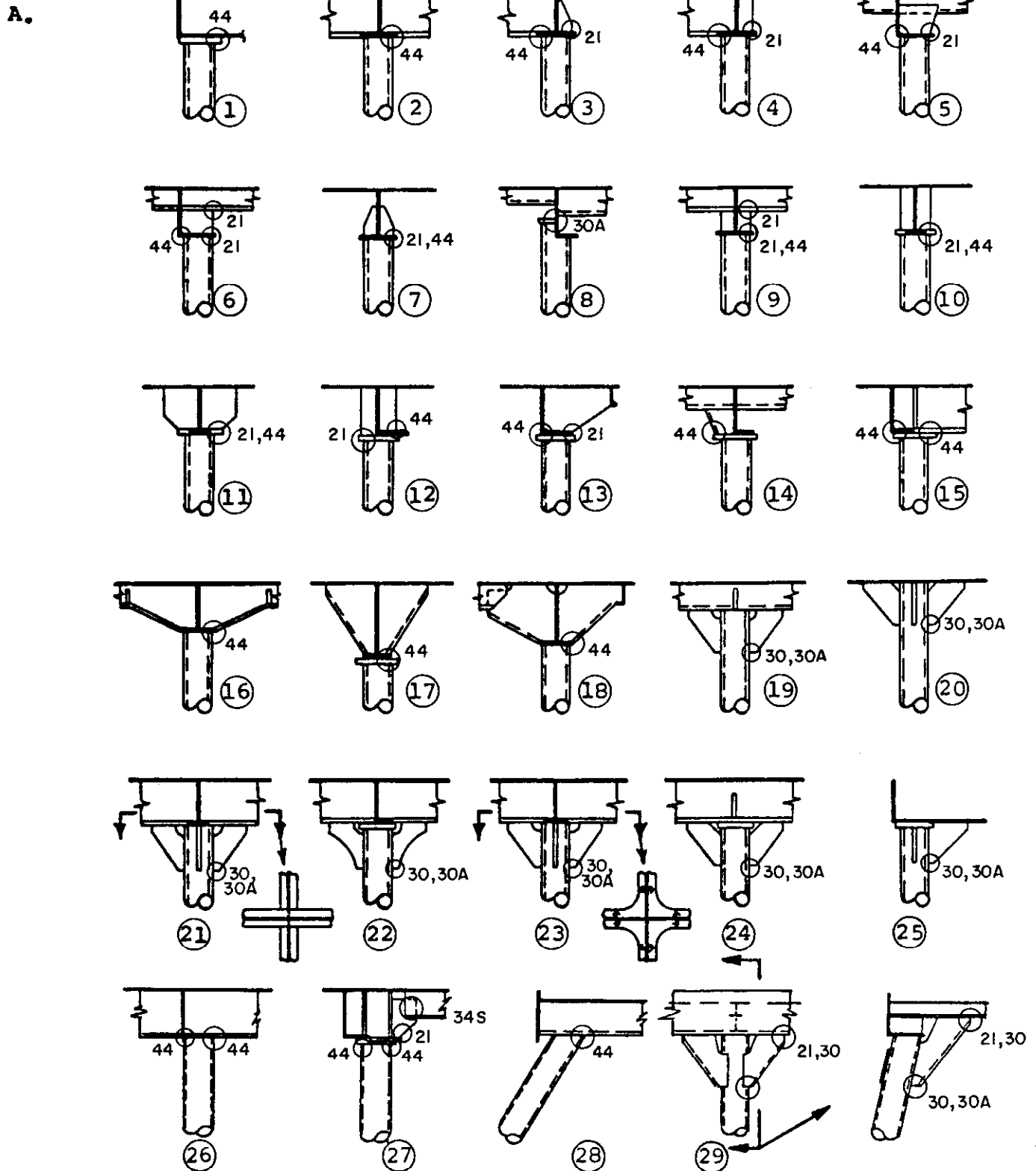


Fig. A. 9 Stanchion End Details, Family No. 10 (Cont'd).

B.

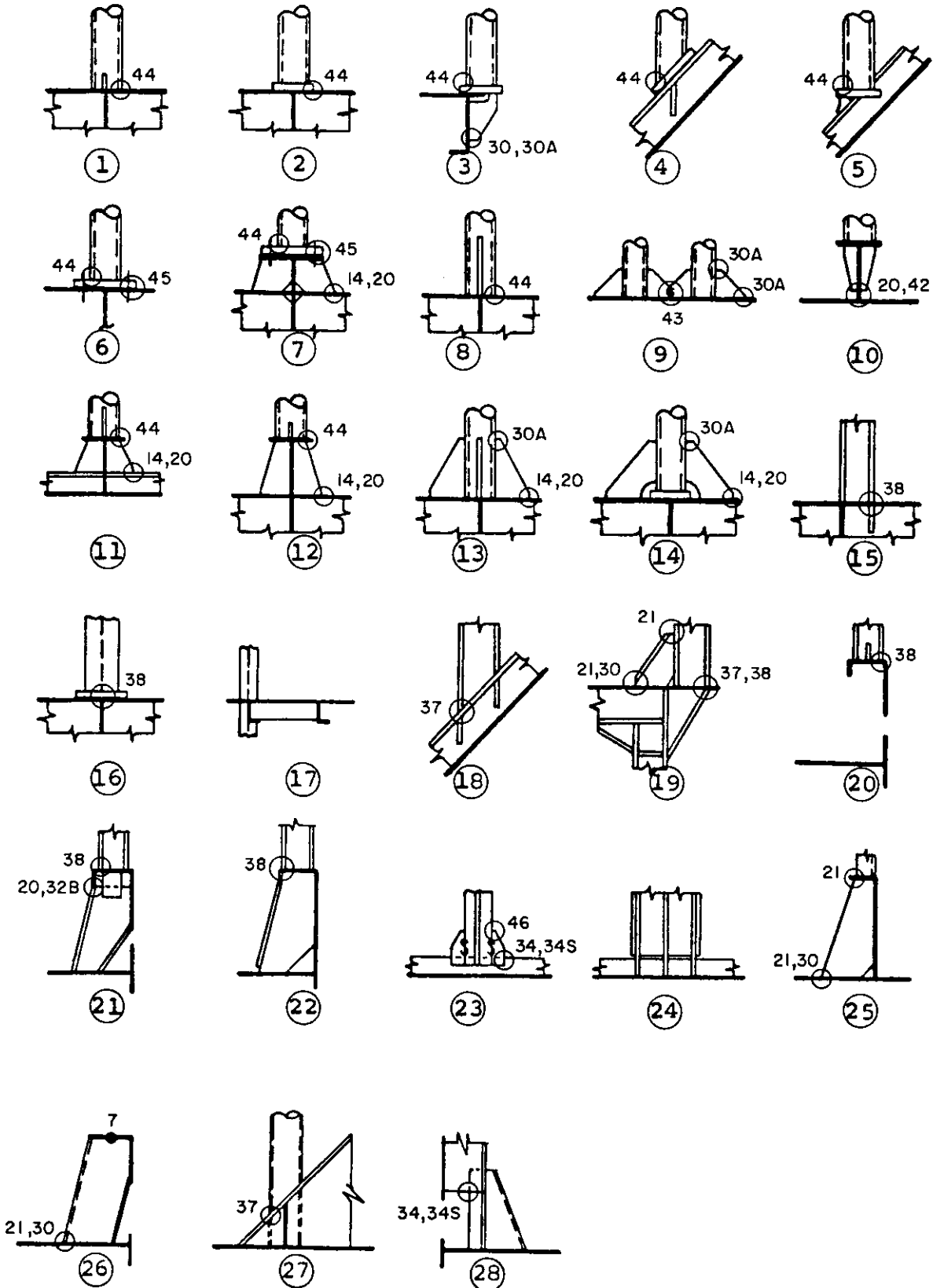


Fig. A. 9 Stanchion End Details, Family No. 10 (Cont'd).

c.

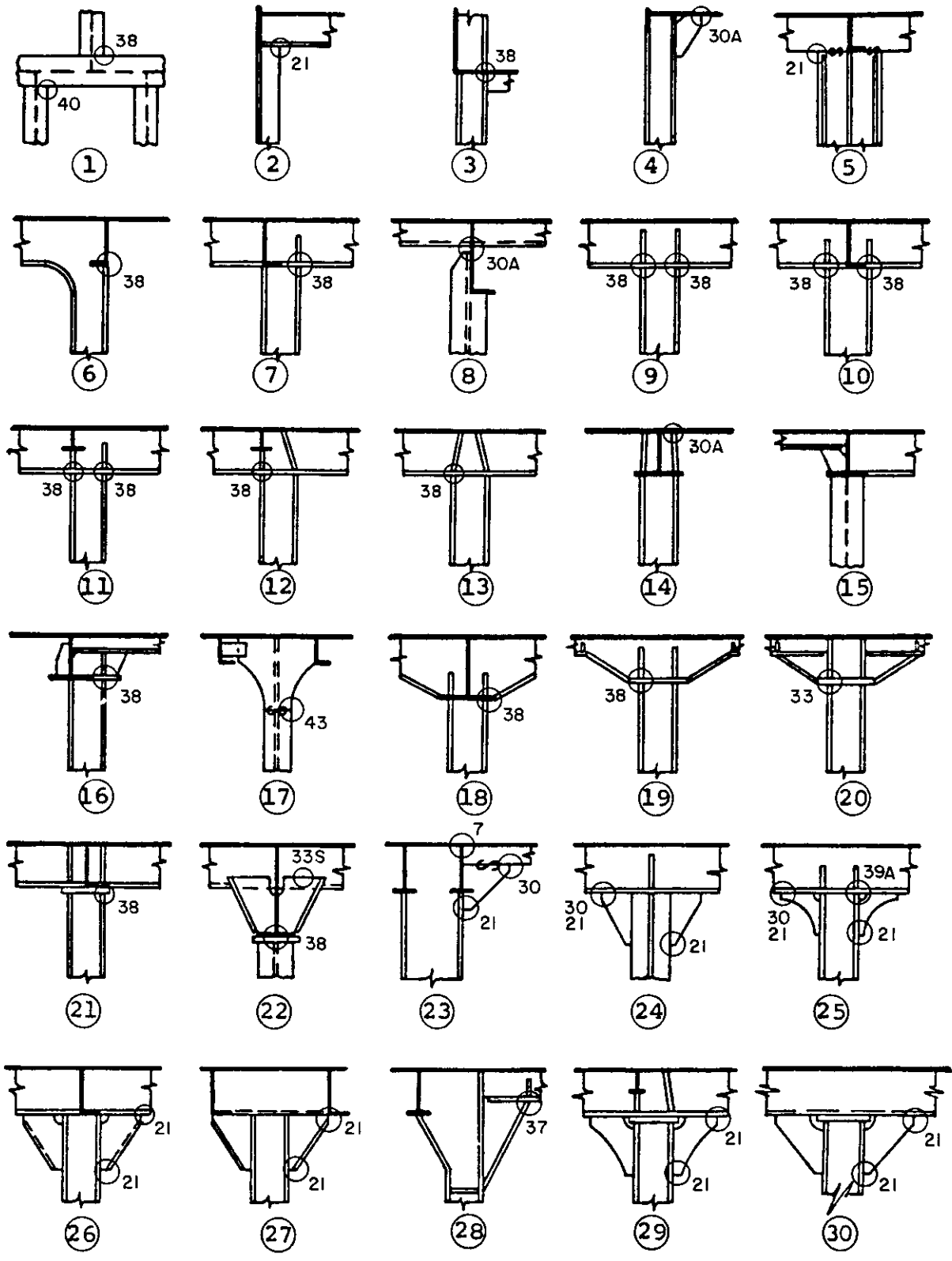


Fig. A. 9 Stanchion End Details, Family No. 10 (Cont'd).

C. Cont'd

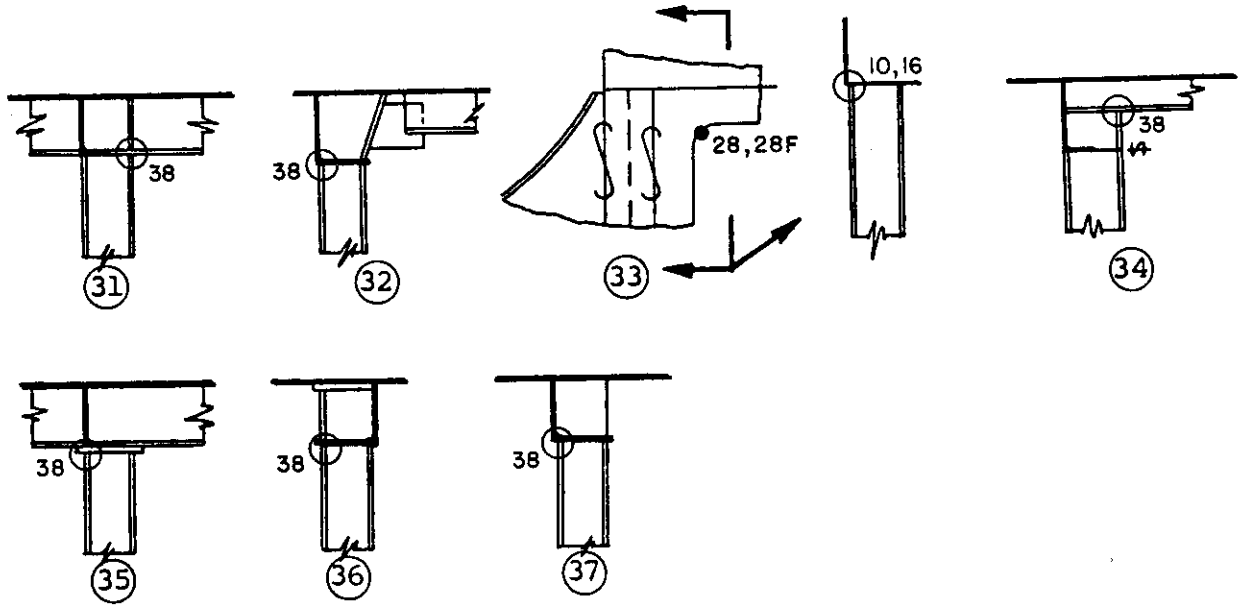


Fig. A.10 Stiffener End Details, Family No. 11.

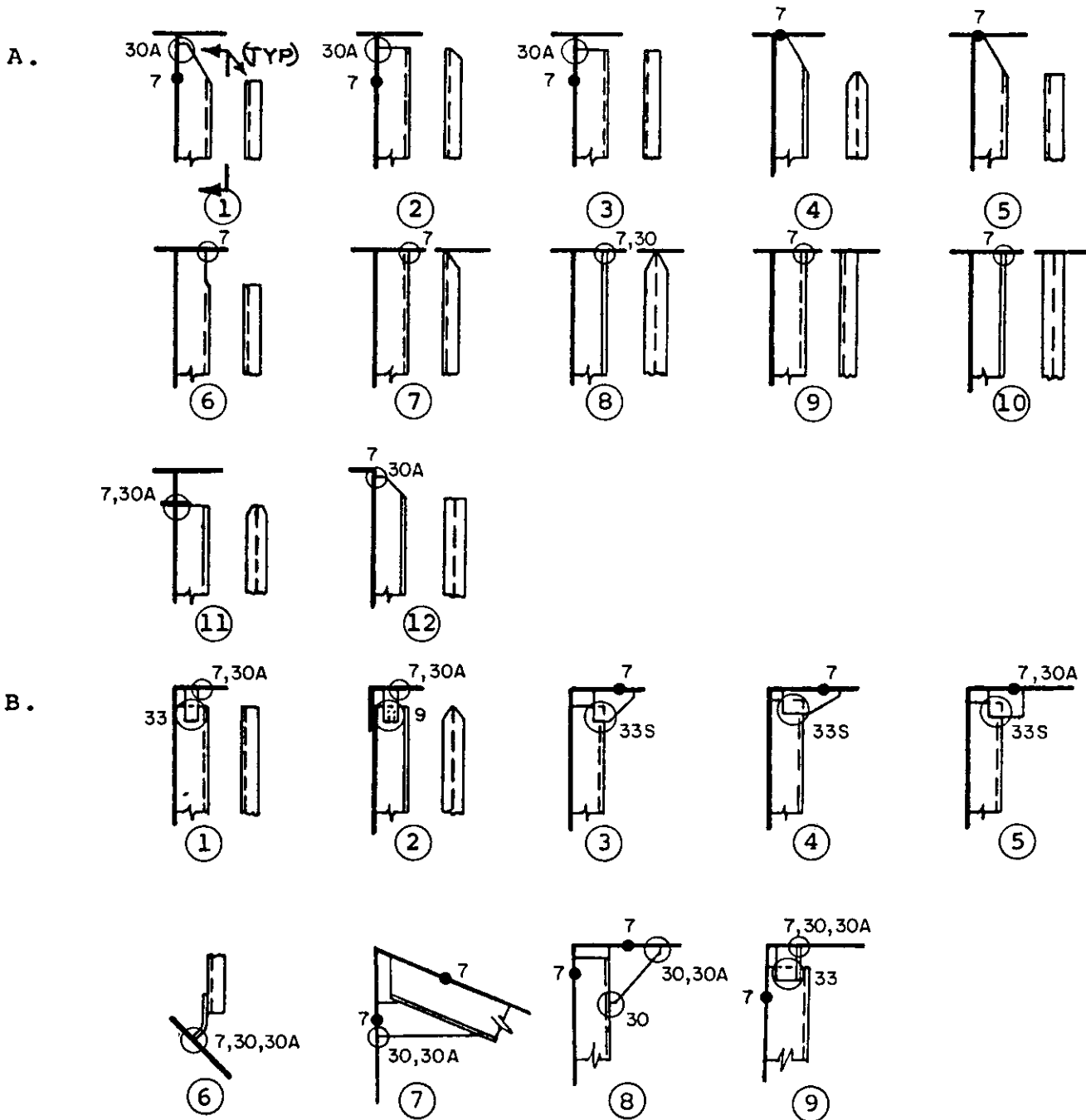


Fig. A.10 Stiffener End Details, Family No. 11 (Cont'd).

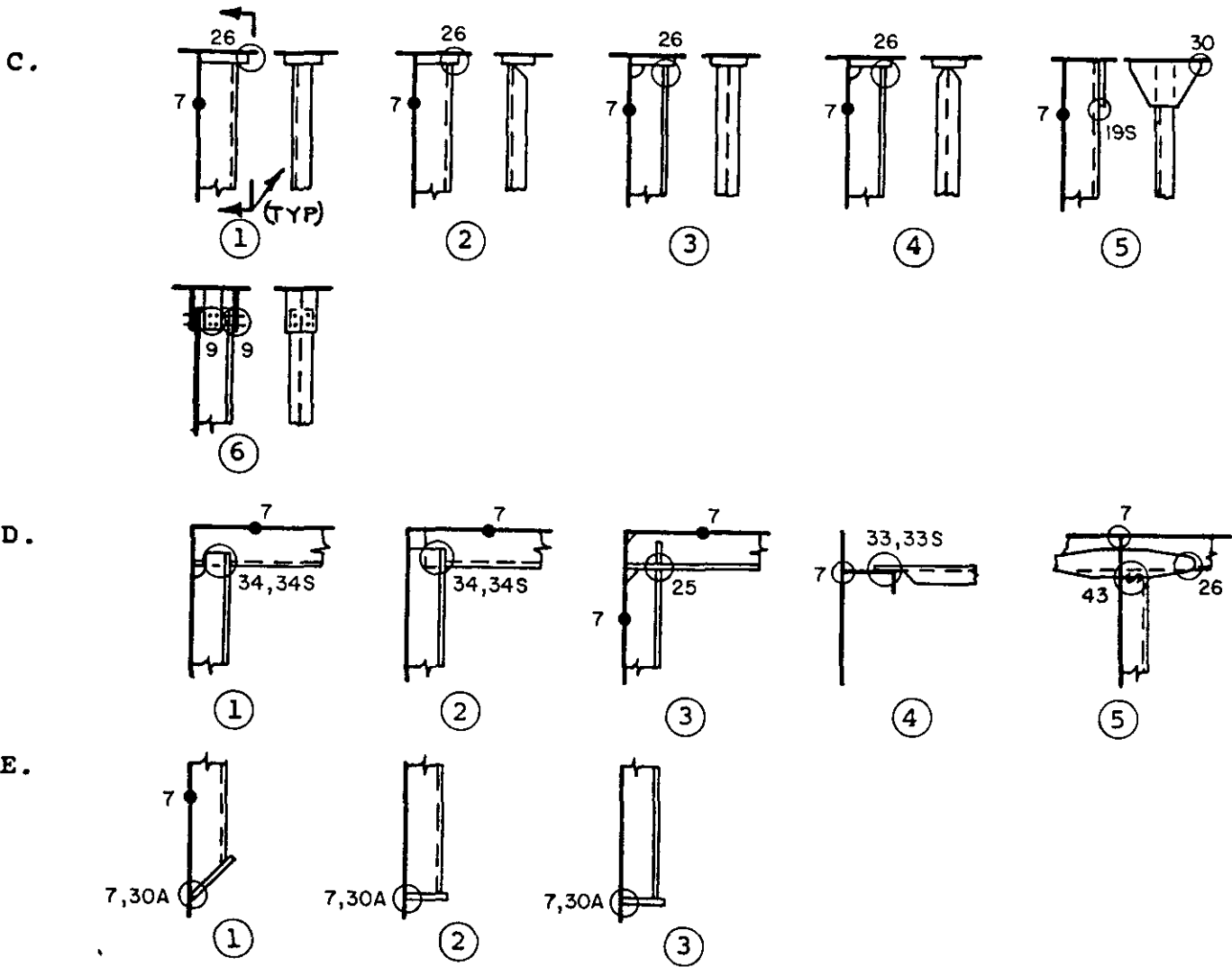


Fig. A.11 Panel Stiffener Details, Family No. 12.

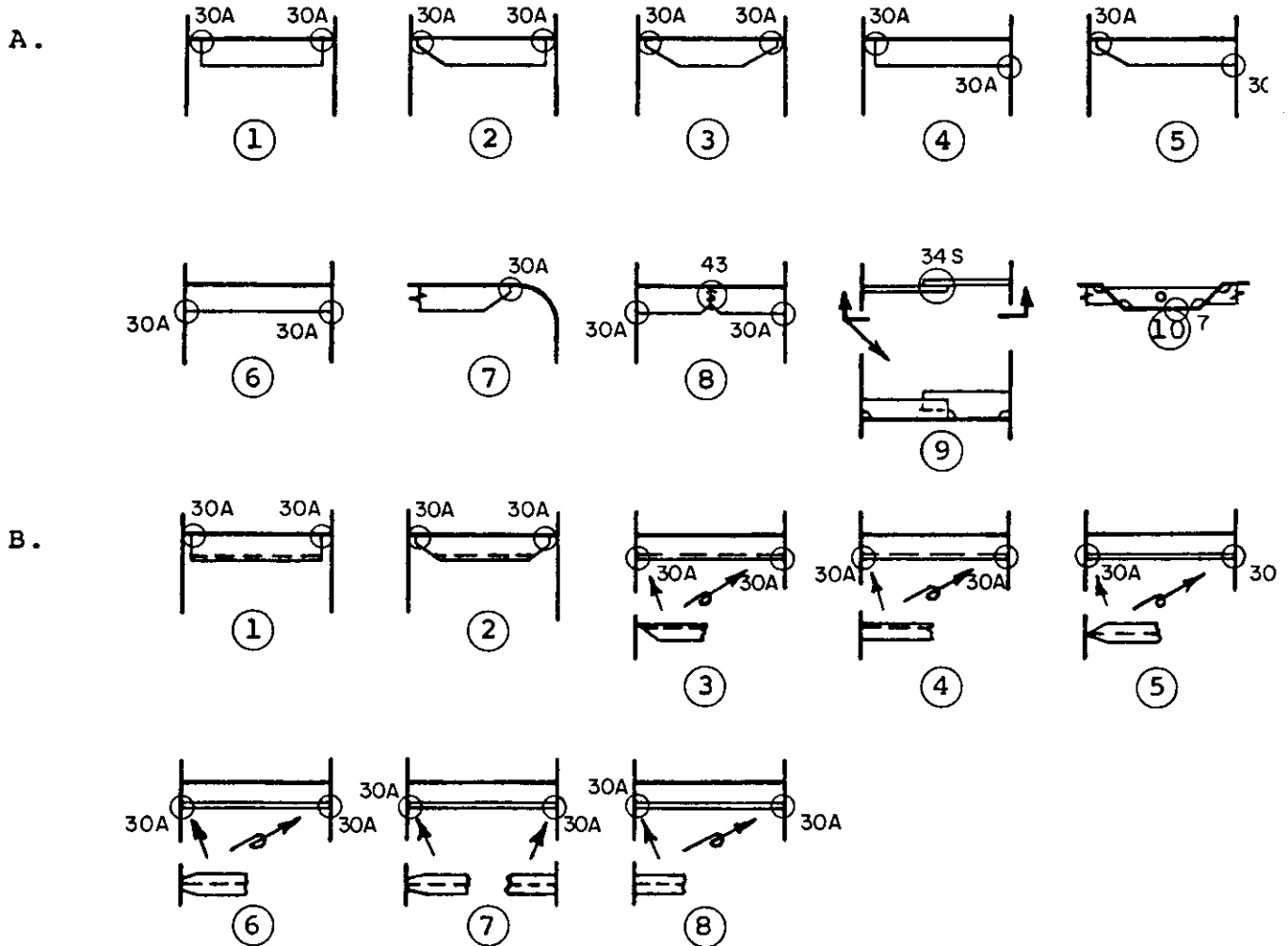
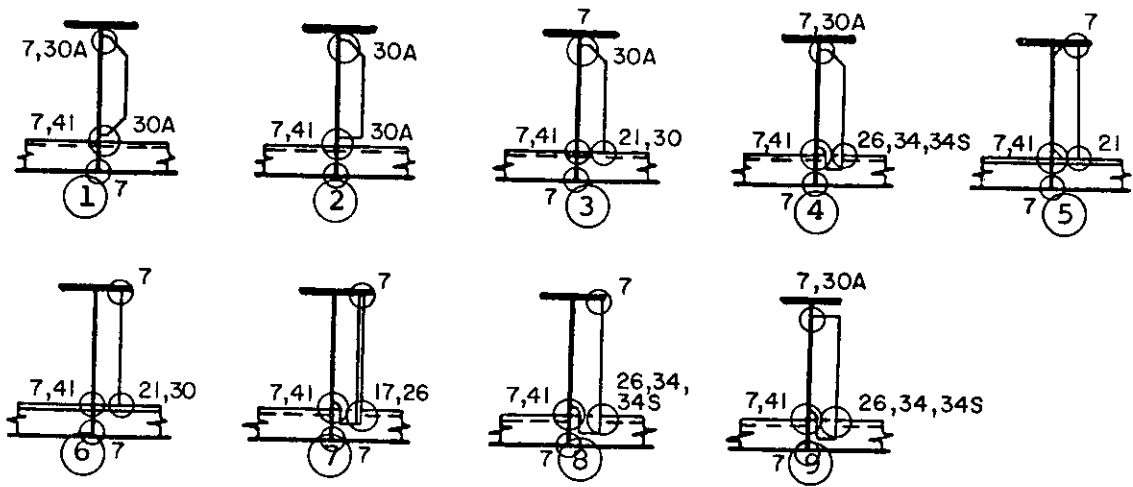
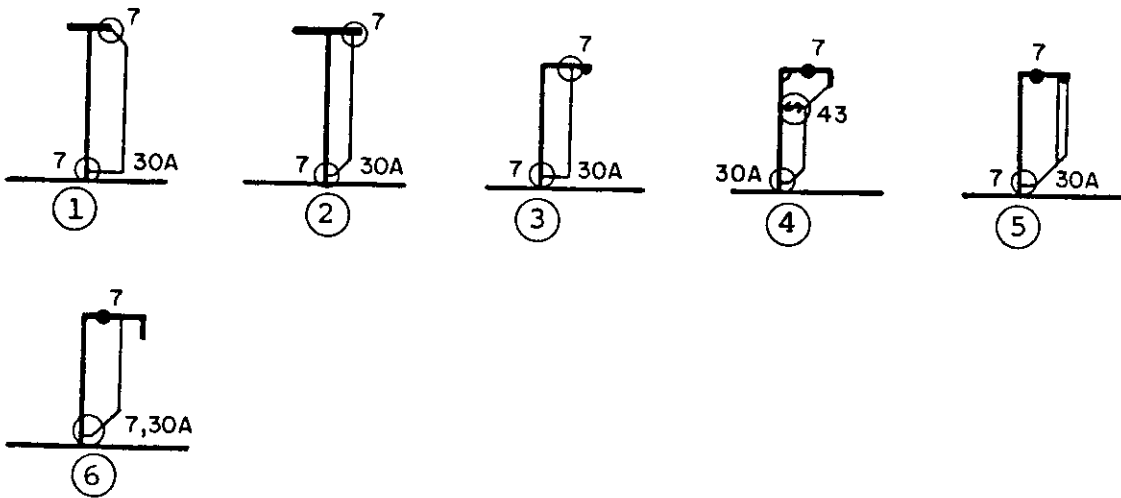


Fig. A.11 Panel Stiffener Details, Family No. 12 (Cont'd).

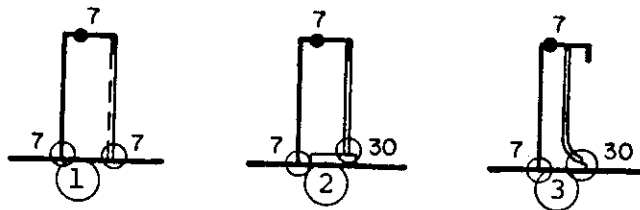
C.



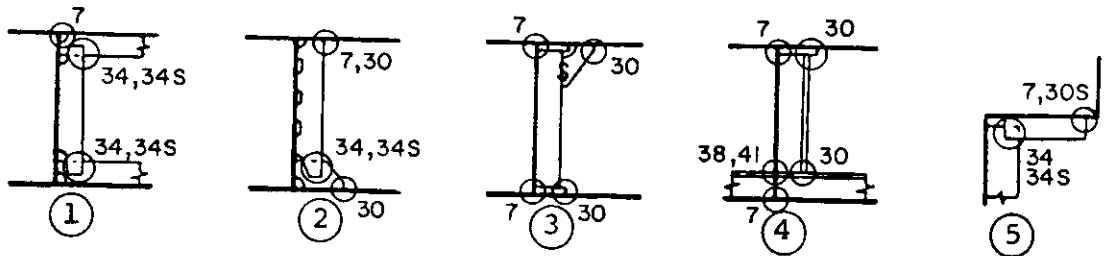
D.



E.



F.



A. References

- A.1 Jordan, C. R. and Cochran, C. S. "In-Service Performance of Structural Details," SSC-272, 1978.
- A.2 Jordan, C. R. and Knight, L. T. "Further Survey of In-Service Performance of Structural Details," SSC-294, 1980.

Appendix B

Fatigue Properties of Local Fatigue Details

A catalog of the local fatigue details, each of which is numbered individually, is presented in Fig. B.1. The mean fatigue resistance of each of these details, as obtained from a least squares regression analysis of available data, is presented in Table B.1, along with the slope of the straight line S-N curve. The S-N curves from which the fatigue data has been obtained are presented in Fig. B.2.

TABLE B.1

Mean Fatigue Strength for Range of Fatigue Details in Fig. B.1
(Constant Cycle - 0.50 Reliability)

Detail No. (See Fig. B.1)	S-N curve slope, m	Stress range, ksi, for n cycles			
		$n=10^5$ (100,000)	$n=10^6$ (1 mill)	$n=10^7$ (10 mill)	$n=10^8$ (100 mill)
1 (All Steels)	5.729	69.4	46.5	31.1	20.8
1M	12.229	46.2	38.3	31.7	26.3
1H	15.449	56.3	48.5	41.8	36.0
1Q	5.199	80.6	51.8	33.2	21.3
1(F)	4.805	67.1	41.5	25.7	15.9
2	6.048	61.5	42.0	28.7	19.6
3	5.946	44.6	30.3	20.5	13.9
3(G)	6.370	44.9	31.3	21.8	15.2
4	5.663	42.5	28.3	18.8	12.5
5	3.278	26.3	13.0	6.4	3.2
6	5.663	42.5	28.3	18.8	12.5
7(B)	3.771	44.8	24.3	13.2	7.2
7(P)	4.172	35.5	20.4	11.8	6.8
8	6.549	55.8	39.2	27.6	19.4
9	9.643	32.6	25.7	20.2	15.92
10M	7.589	34.1	25.2	18.6	13.7
10H	12.795	43.2	36.1	30.1	25.2
10Q	5.124	48.9	31.2	19.9	12.7
10(G)	7.130	47.1	34.1	24.7	17.9
10A	5.468	47.1	30.9	20.3	13.3
10A(G) [†]	--	--	--	--	--
11	5.765	33.2	22.3	14.9	10.0
12	4.398	33.2	19.6	11.6	6.9
12(G)	5.663	40.8	27.2	18.09	12.05
13	4.229	48.3	28.0	16.3	9.44
14	7.439	40.6	29.8	21.8	16.03
14A [†]	--	--	--	--	--
15	4.200	24.4	14.1	8.2	4.7
16*	4.631	32.8	19.9	12.1	7.37
16(G)*	6.960	32.8	23.6	16.9	12.2

TABLE B.1 (cont.)

Detail No. (See Fig. B.1)	S-N curve slope, m	Stress range, ksi, for n cycles			
		$n=10^5$ (100,000)	$n=10^6$ (1 mill)	$n=10^7$ (10 mill)	$n=10^8$ (100 mill)
17	3.736	27.8	15.0	8.1	4.4
17(S)	7.782	28.2	21.0	15.6	11.6
17A	3.465	30.4	15.6	8.0	4.1
17A(S)	7.782	28.2	21.0	15.6	11.6
18	4.027	20.3	11.5	6.5	3.6
18(S)	9.233	25.7	20.0	15.6	12.2
19	7.472	23.1	17.0	12.5	9.2
19(S)	7.520	27.5	20.3	14.9	11
20	4.619	26.5	16.1	9.8	5.9
20(S)	6.759	27.5	19.6	13.9	9.9
21(1/4"weld)	14.245	33.5	28.5	24.2	20.6
21(3/8"weld)	15.494	21	18.1	15.6	13.4
21(S)	7.358	42.4	31.0	22.7	16.6
22	3.147	39.8	19.2	9.2	4.4
23	3.187	35.4	17.2	8.3	4.1
24	3.187	35.4	17.2	8.3	4.1
25	7.090	33.2	24.0	17.4	12.5
25A	8.518	49.9	38.1	29.1	22.5
25B	6.966	28.6	20.6	14.8	10.6
26	3.348	34.0	17.1	8.6	4.3
27	3.146	25.0	12.0	5.8	2.8
27(S)	5.277	21.8	14.1	9.1	5.9
28	7.746	40.1	29.8	22.1	16.4
28(F) ⁺⁺	--	29.3	--	--	--
30	3.159	34.7	16.7	8.1	3.9
30A	3.368	45.6	23.0	11.6	5.8
31	4.348	20.16	11.87	6.99	4.12
31A	3.453	30.6	15.7	8.1	4.1
32A	4.200	24.4	14.1	8.2	4.7
32B	3.533	21.5	11.21	5.84	3.04
33	3.660	21.3	11.4	6.1	3.2
33(S)	10.368	25.5	20.5	16.4	13.1

TABLE B.1 (cont.)

Detail No. (See Fig. B.1)	S-N curve slope, m	Stress range, ksi, for n cycles			
		$n=10^5$ (100,000)	$n=10^6$ (1 mill)	$n=10^7$ (10 mill)	$n=10^8$ (100 mill)
35	3.808	32.4	17.7	9.7	5.3
36	6.966	28.6	20.6	14.8	10.6
36A	5.163	33.6	21.5	13.8	8.8
38	3.462	31.1	16.0	8.2	4.2
38(S)	10.225	16.3	13.0	10.4	8.3
40	3.533	21.5	11.21	5.84	3.04
42	7.358	42.4	31.0	22.7	16.6
46	4.348	20.16	11.87	6.99	4.12
51(V)	3.813	35.9	19.6	10.8	5.87
52(V)	4.042	34.9	19.8	11.2	6.32

+ Data scatter makes evaluation questionable.

++ Range in lives is small - extrapolation questionable.

* Partial penetration groove weld.

Note:

(B) = bending stress, (P) = principal stress, M = mild steel, H = high strength low alloy steel, Q = quenched and tempered steel, (S) = shear stress on fasteners of welds, (F) = flame cut surfaces, (G) = indicates the surfaces have been ground flush, (V) = average shear stress based on net area of web.

The values for details 21, 30A, 51 and 52 were obtained from the tests reported in Appendix F.

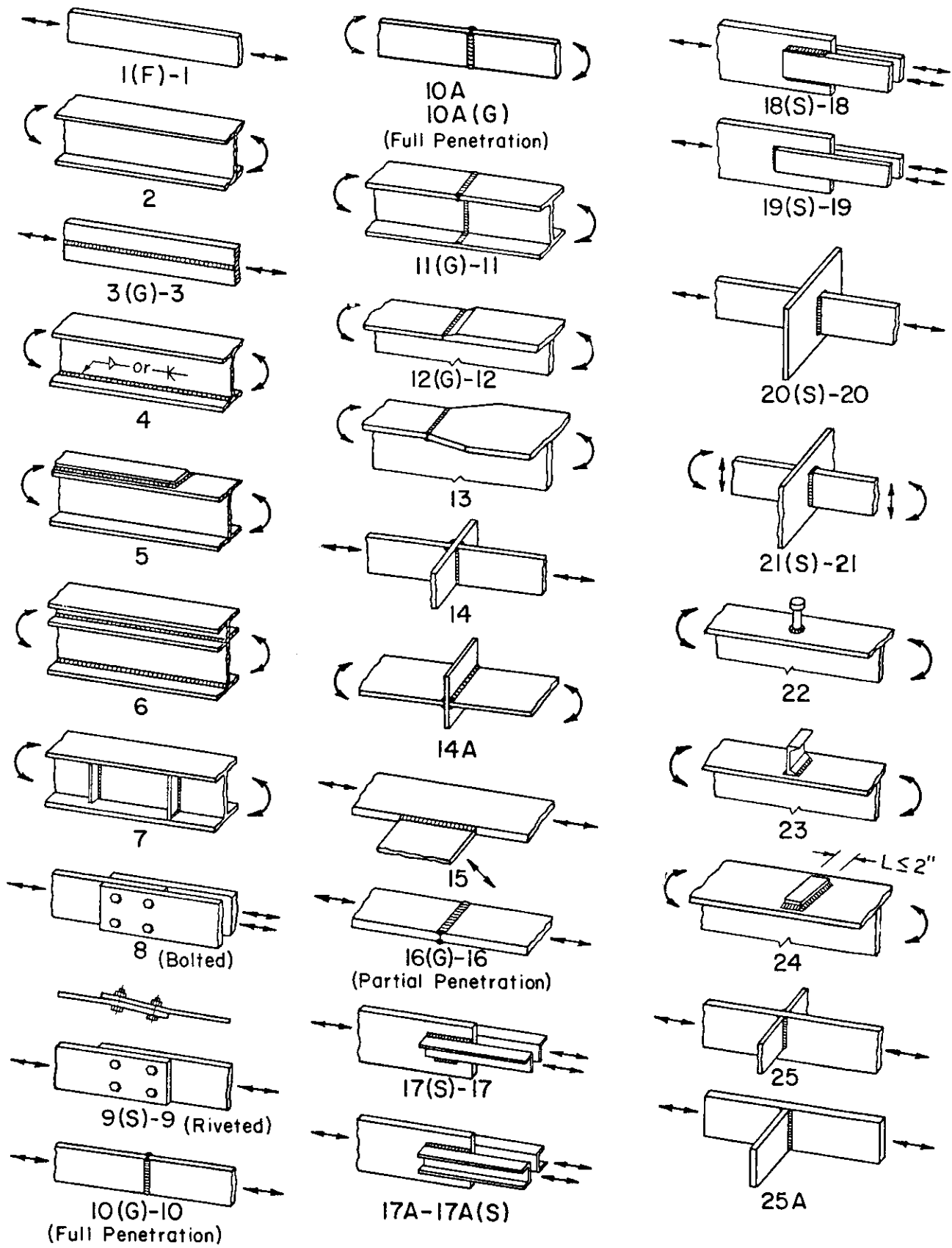


Fig. B.1 Structural Fatigue - Details.

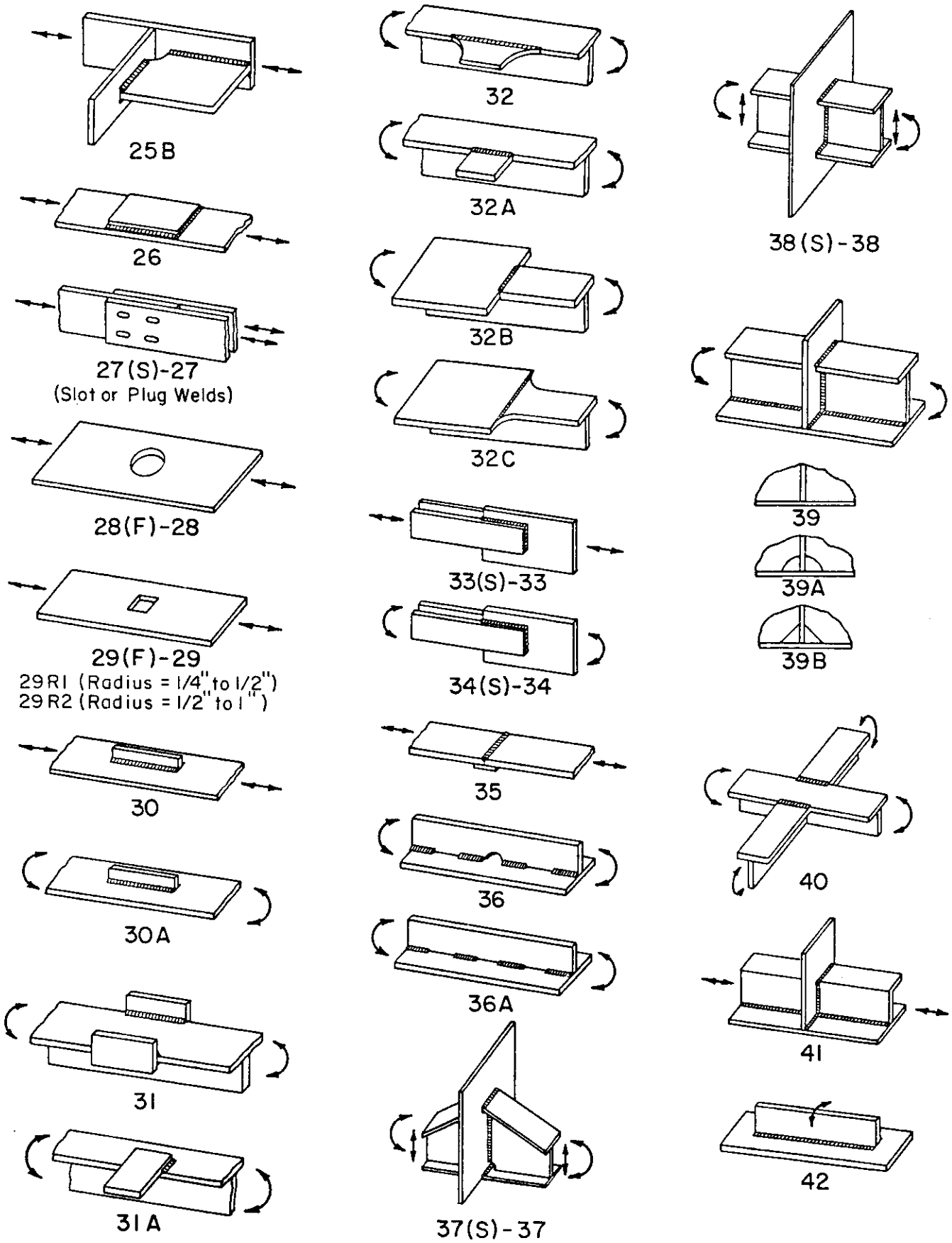


Fig. B.1 Structural Fatigue - Details (Cont.).

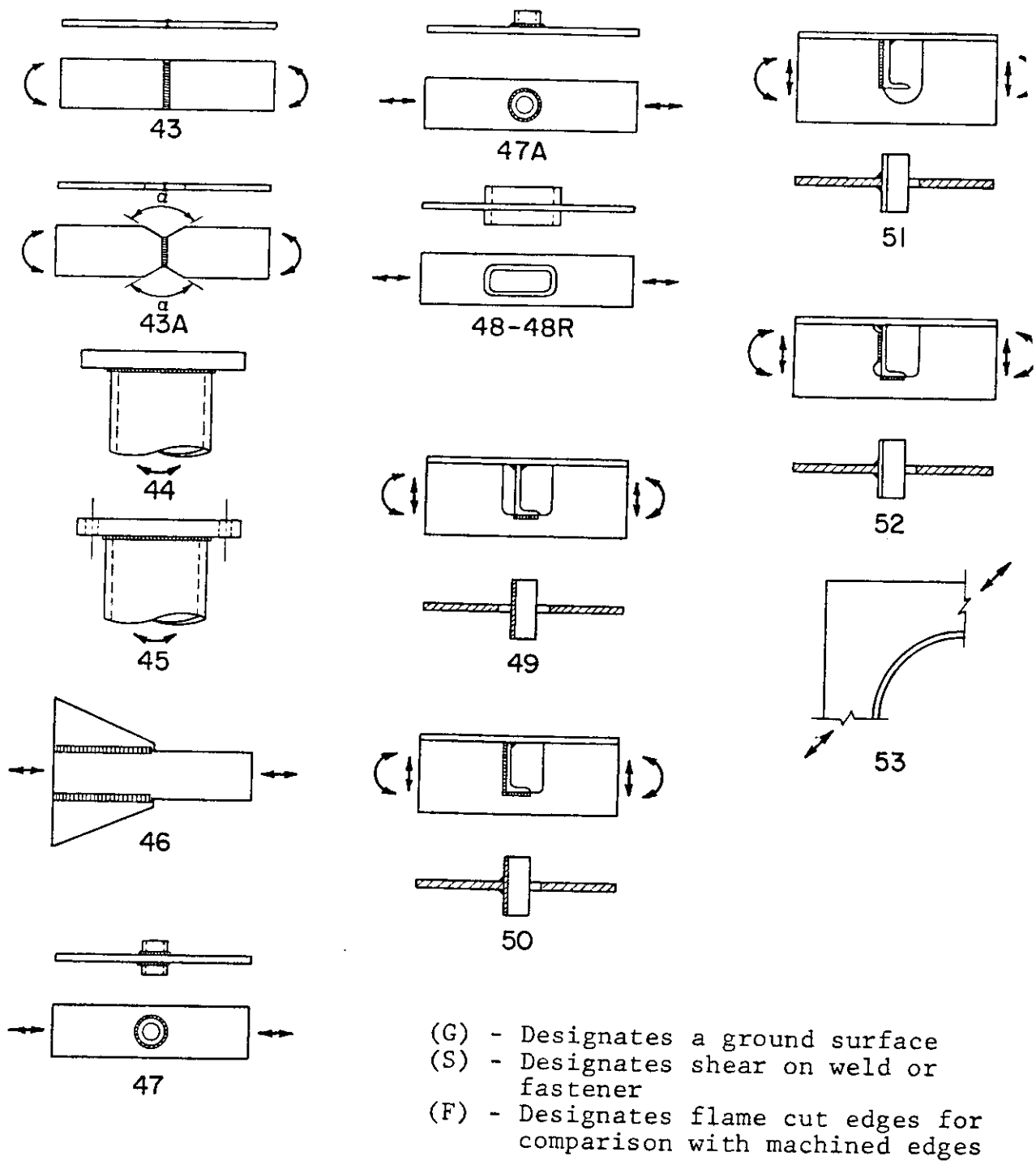
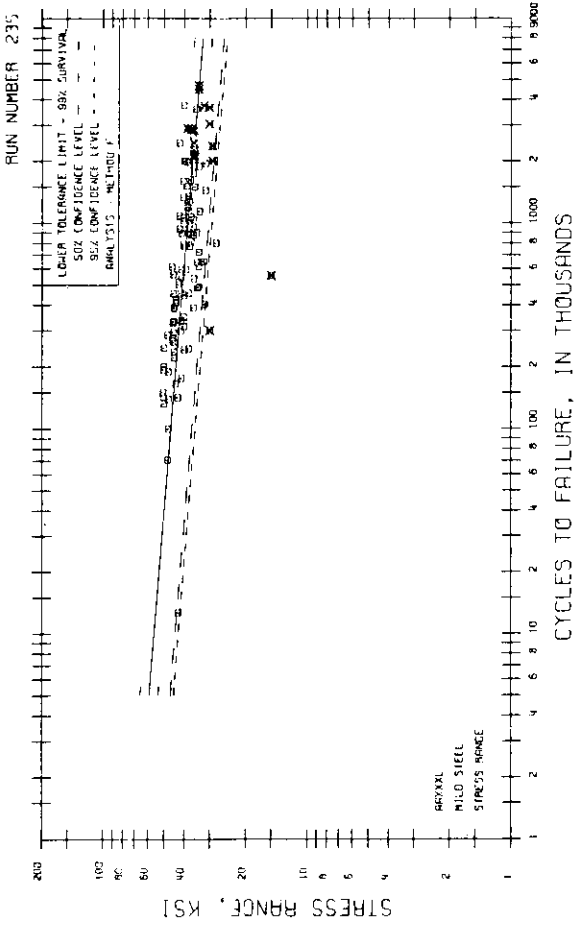
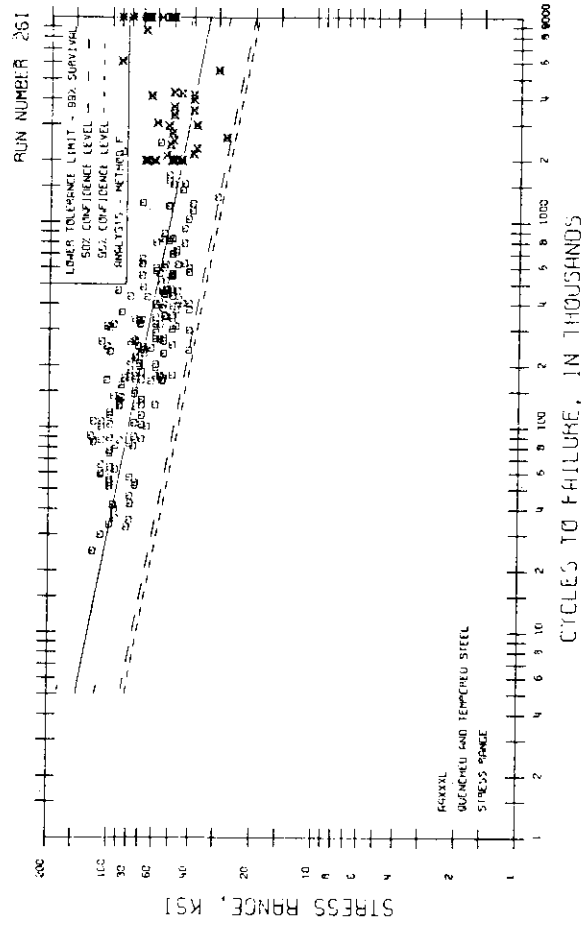


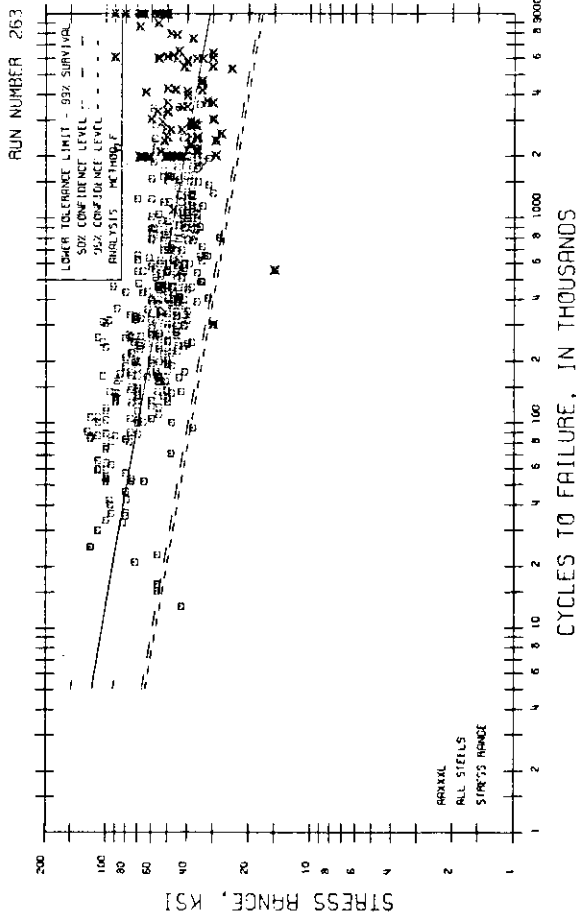
Fig. B.1 Structural Fatigue - Details (Cont.).



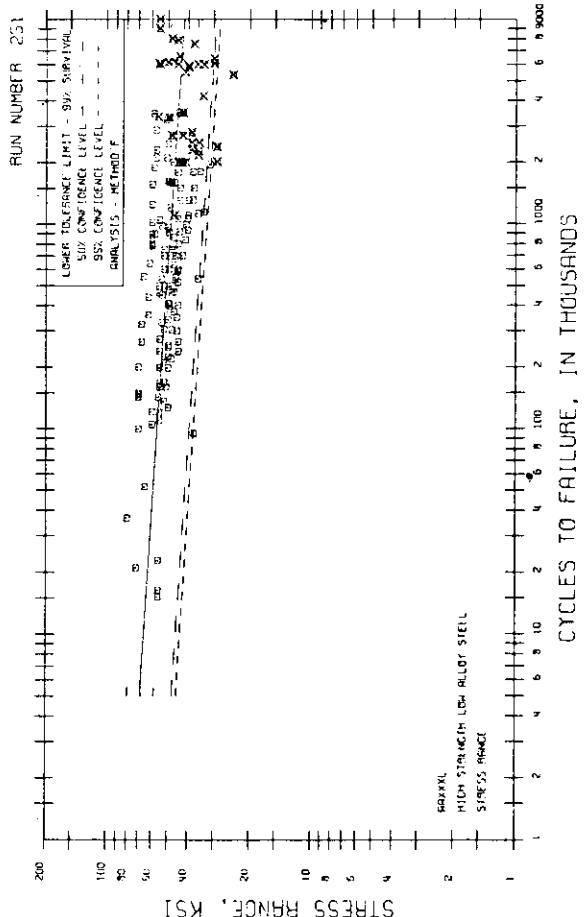
Detail No. 1M



Detail No. 1Q



Detail No. 1H



Detail No. 1H

Fig. B.2 S-N Curves for Structural Details.

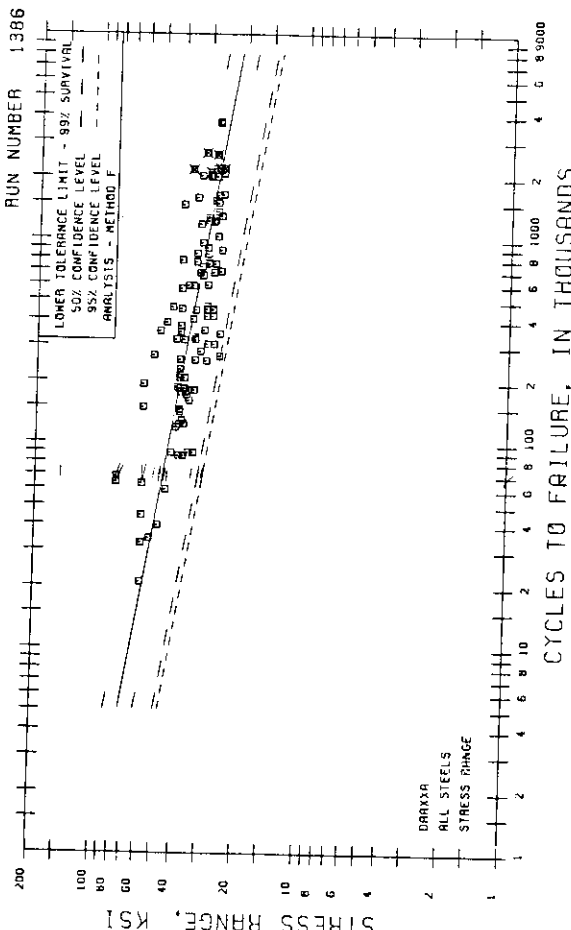
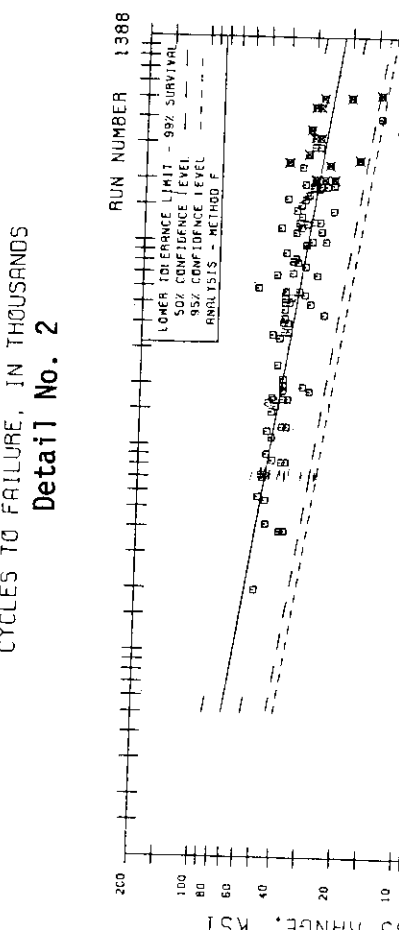
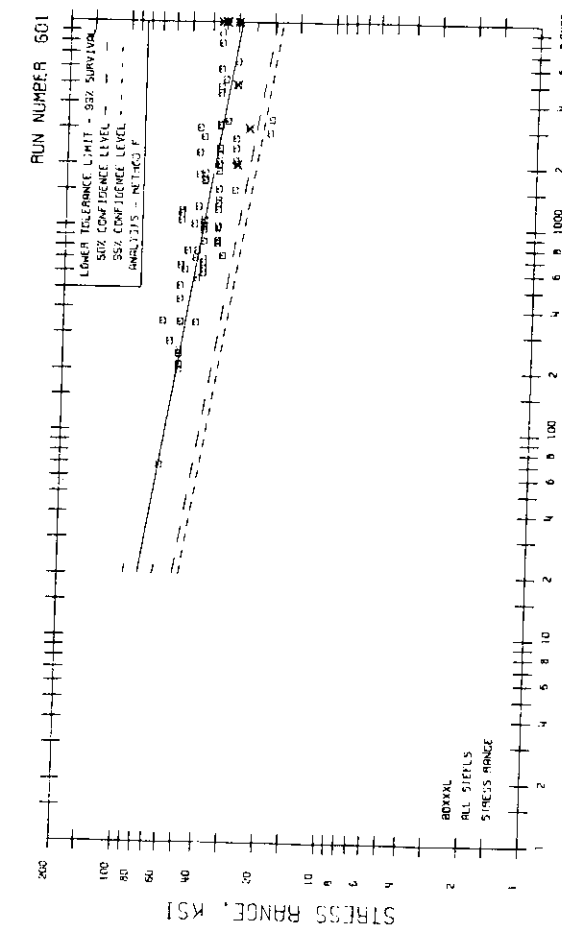
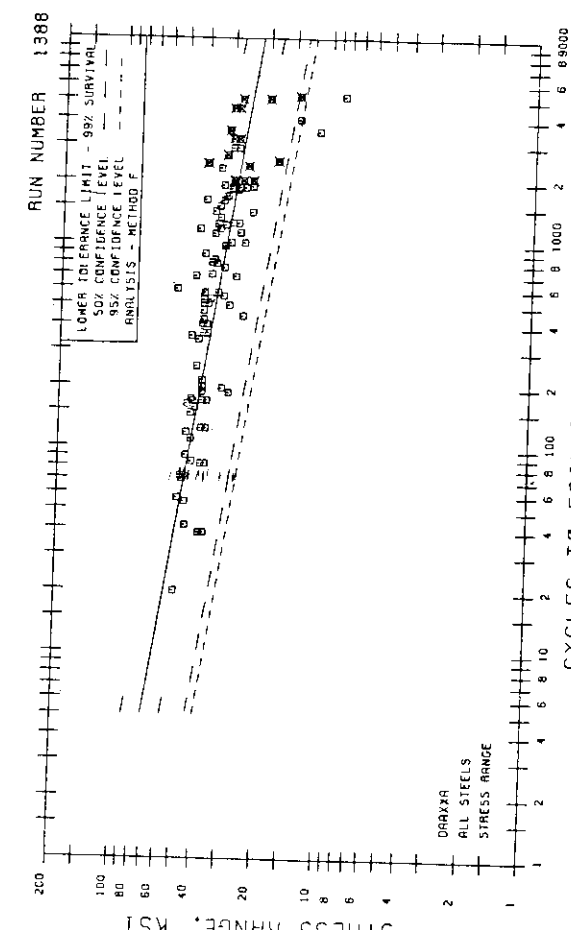
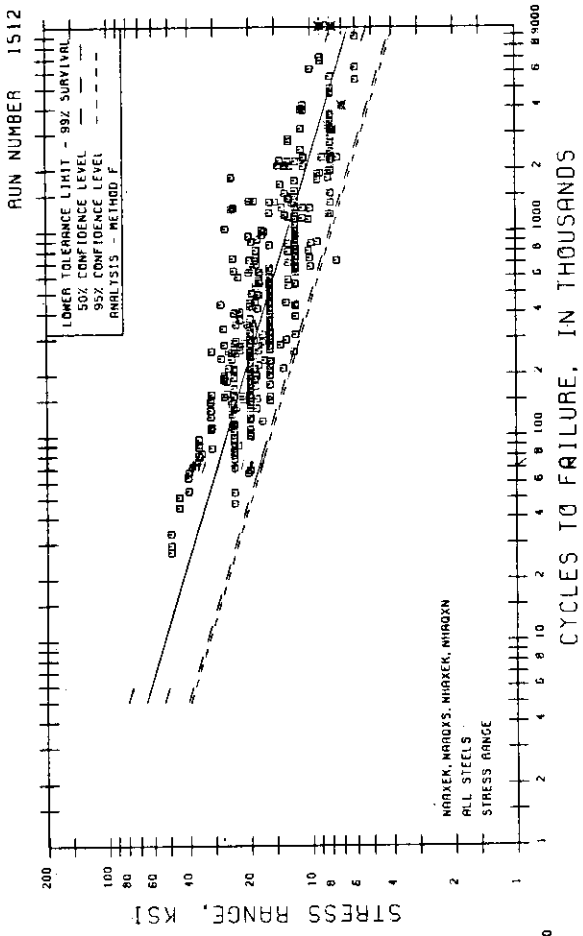


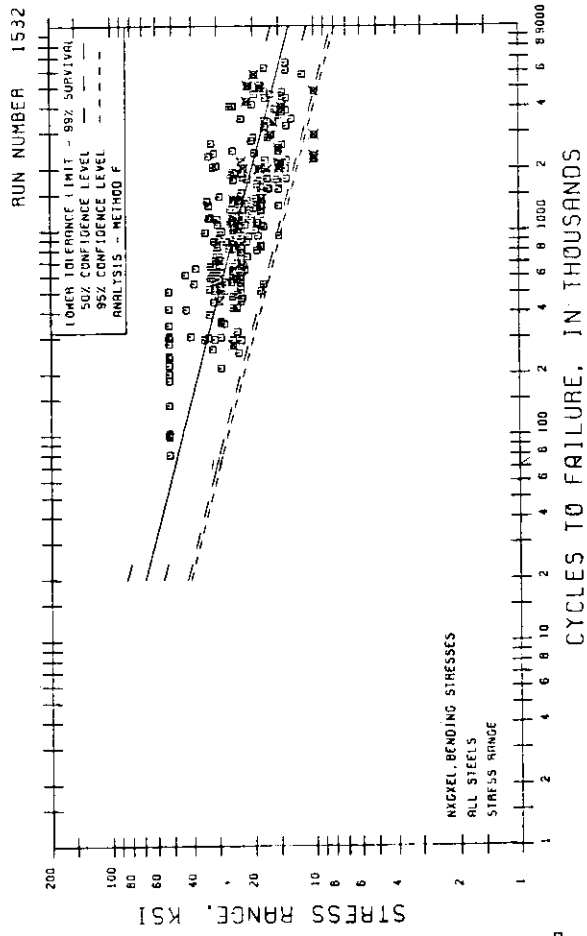
Fig. B.2 S-N Curves for Structural Details (Cont.).

Detail No. 3(G)

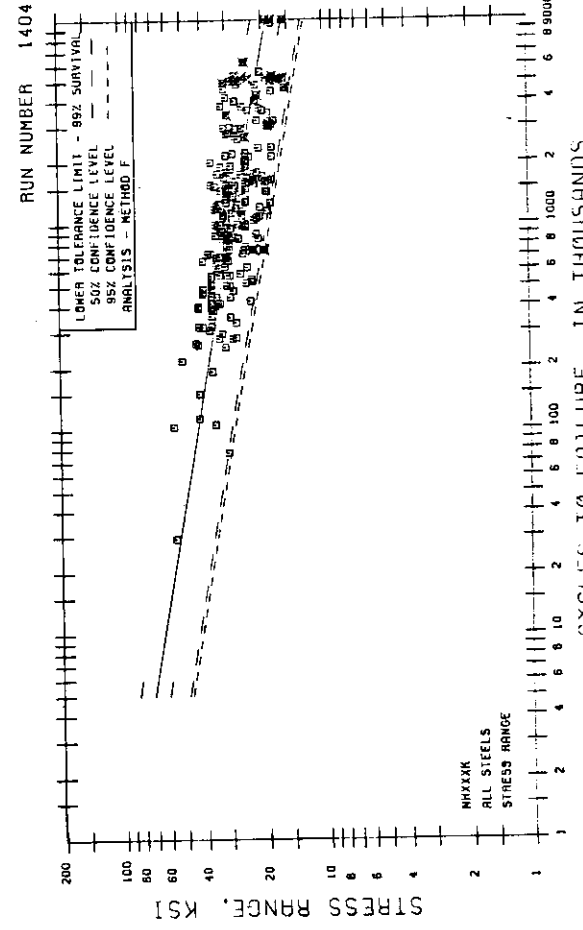




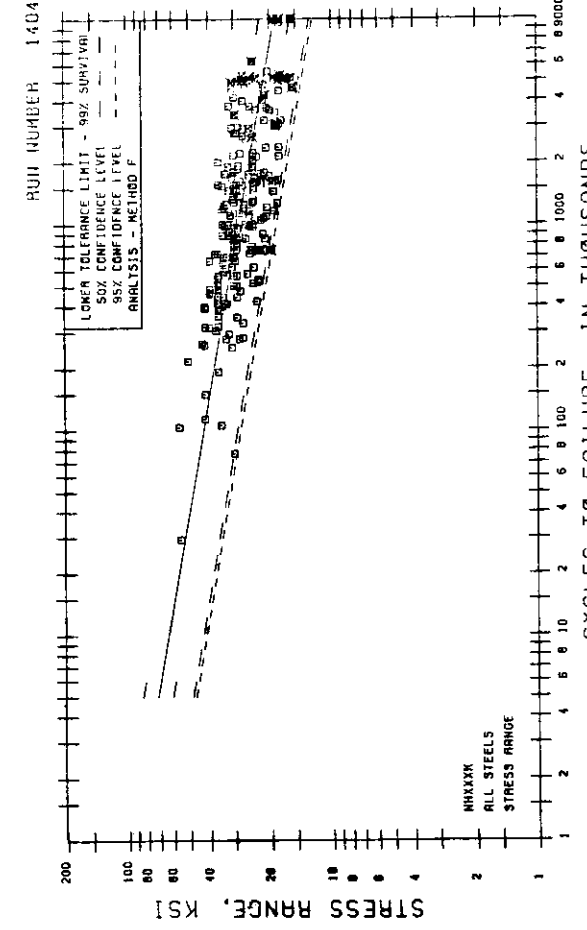
Detail No. 5



Detail No. 7(B)

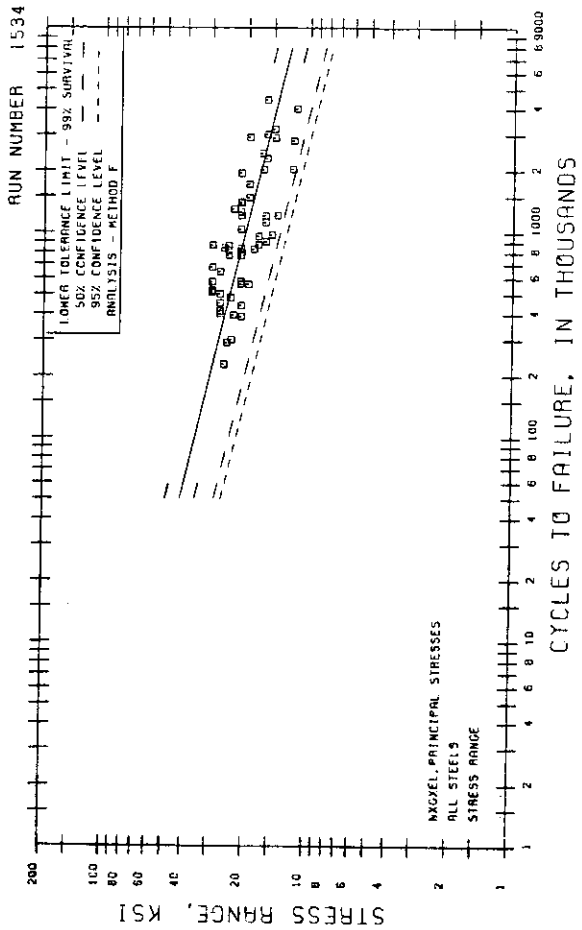


Detail No. 4

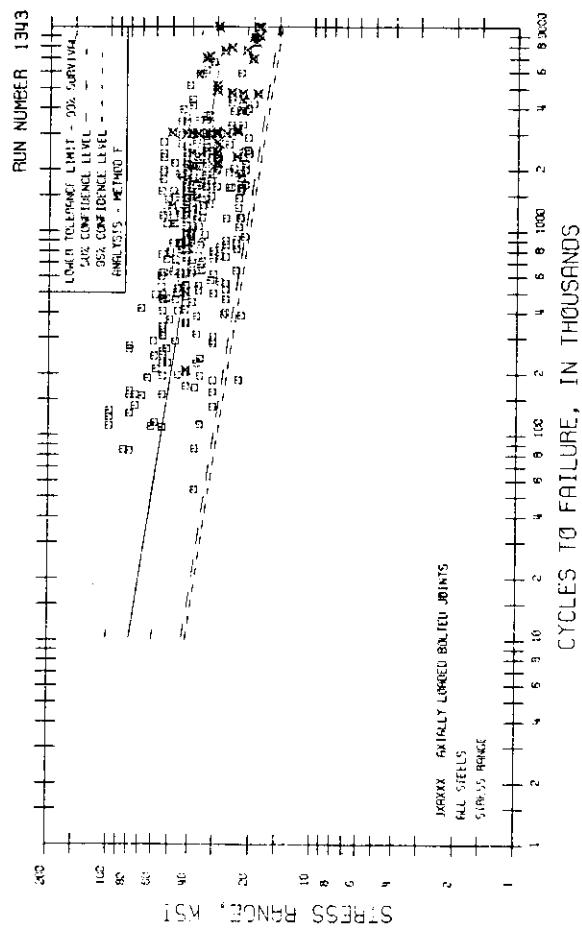


Detail No. 6

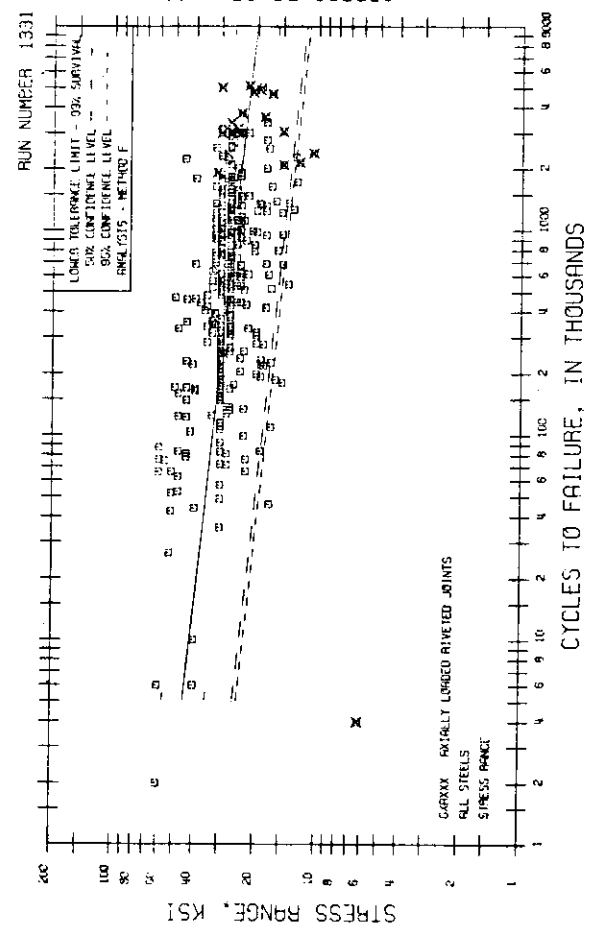
Fig. B.2 S-N Curves for Structural Details (Cont.).



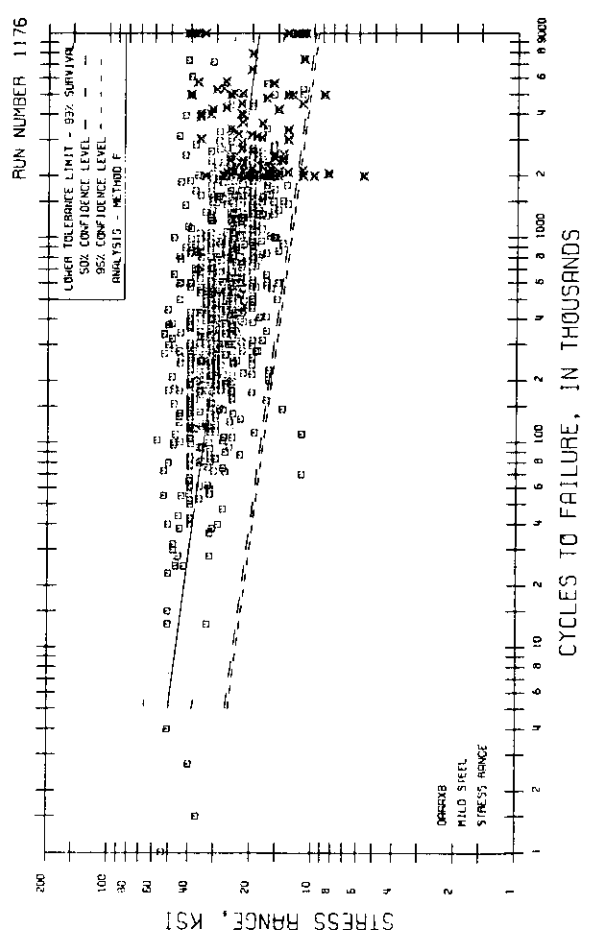
Detail No. 7(P)



Detail No. 8

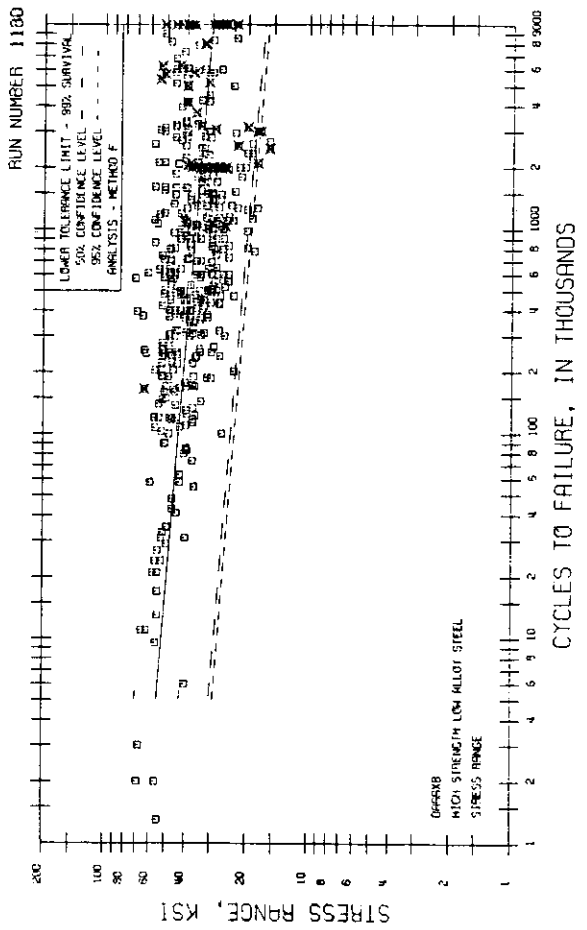


Detail No. 9

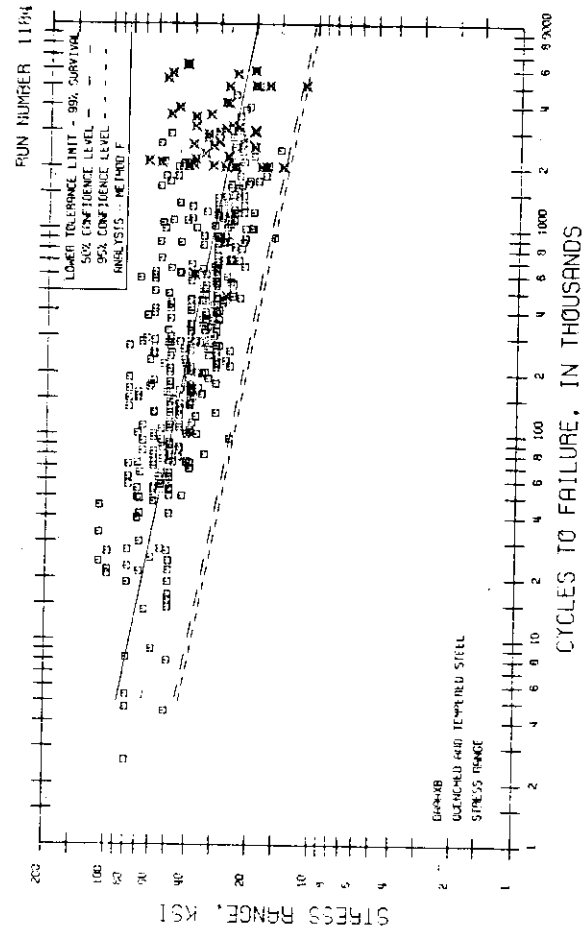


Detail No. 10M

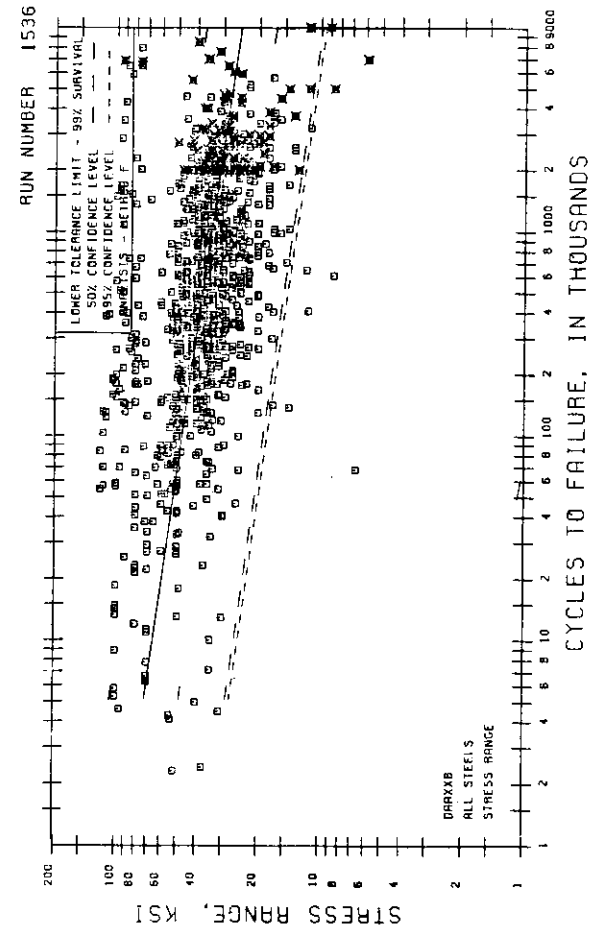
Fig. B.2 S-N Curves for Structural Details (Cont.).



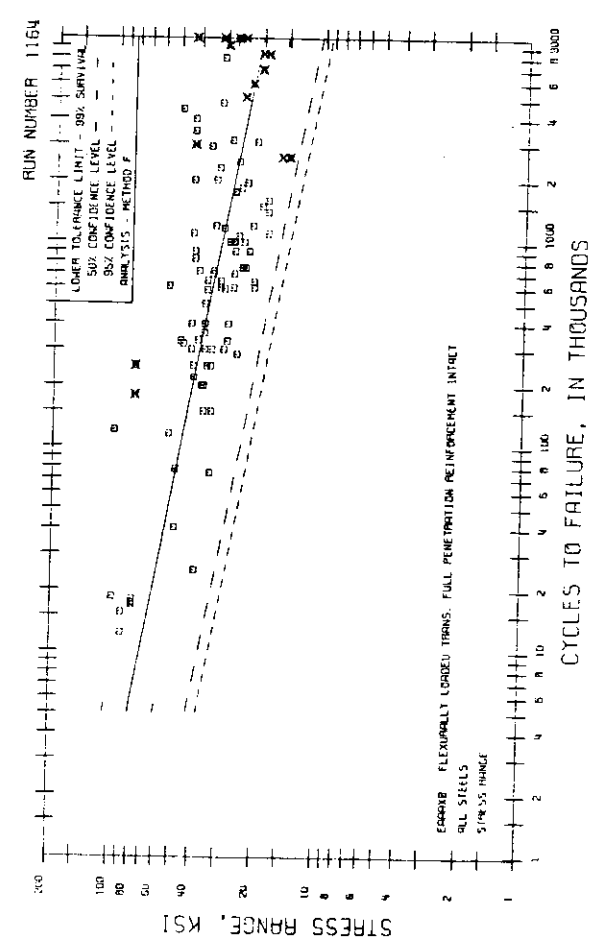
Detail No. 10H



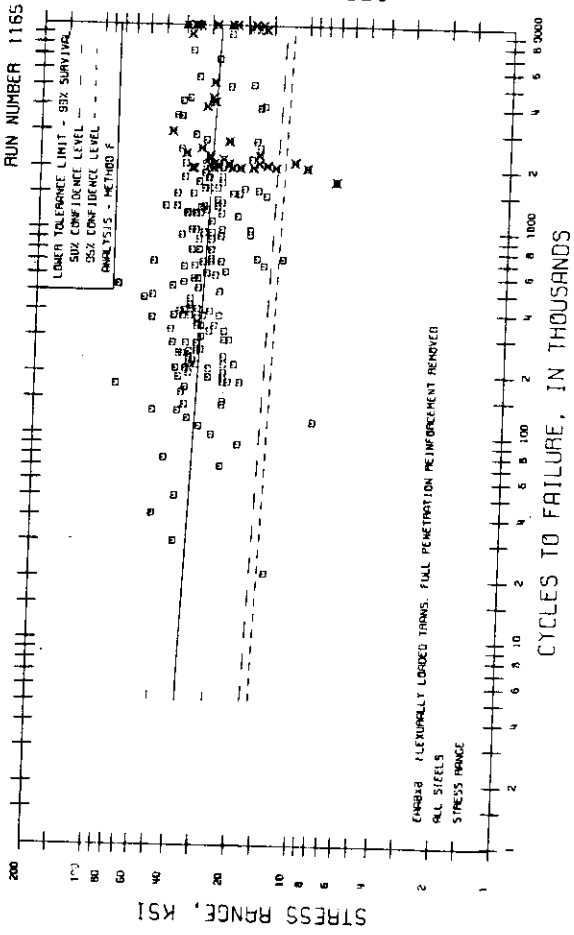
Detail No. 10Q



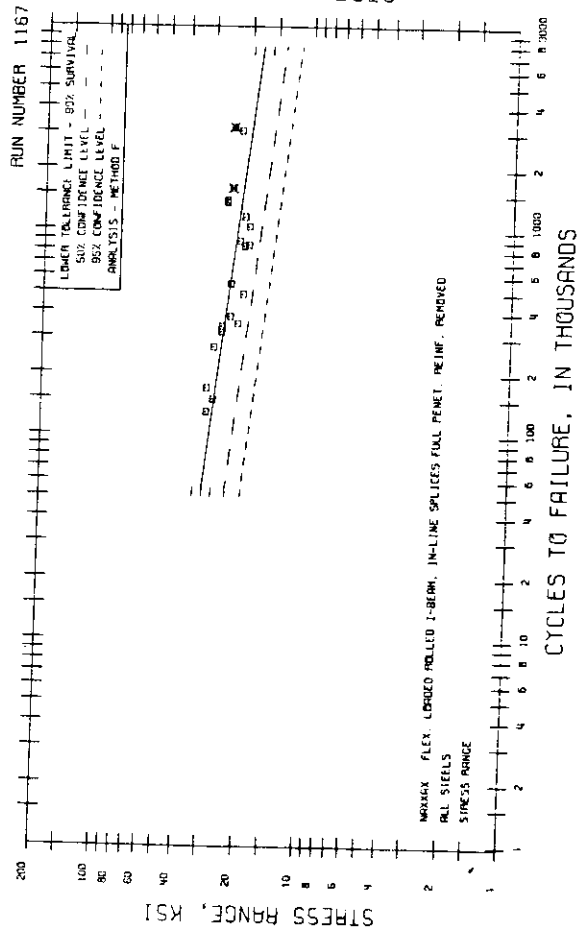
Detail No. 10(G)



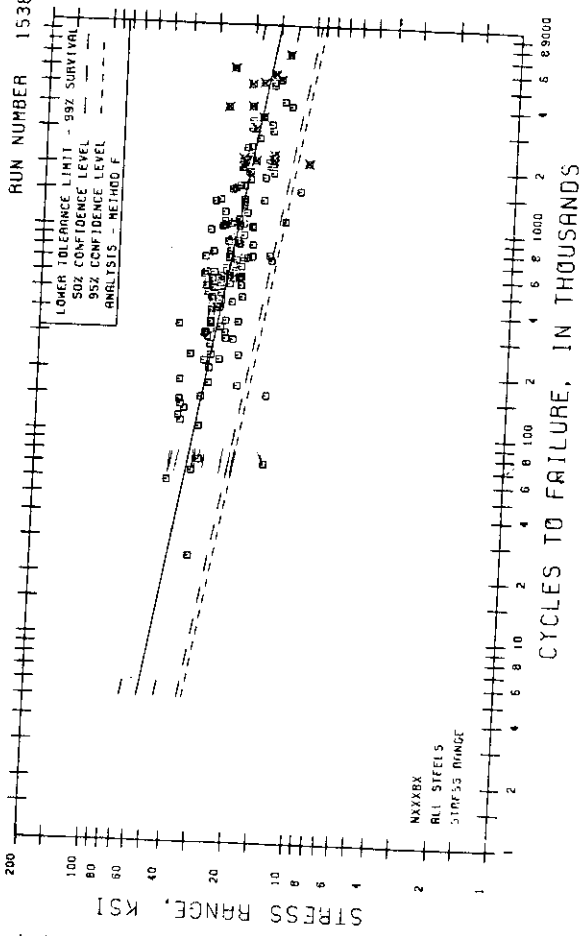
Detail No. 10A



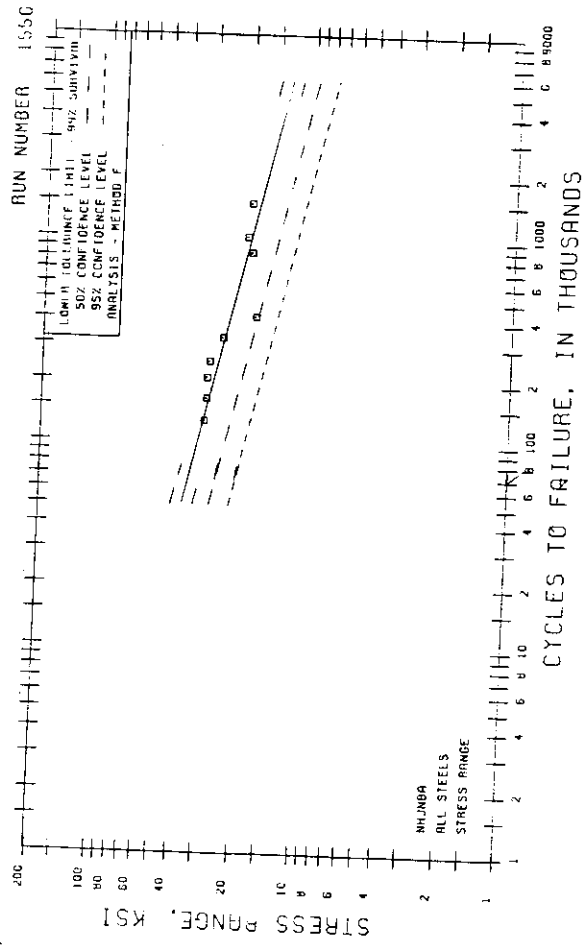
Detail No. 10A(G)



Detail No. 11(G)

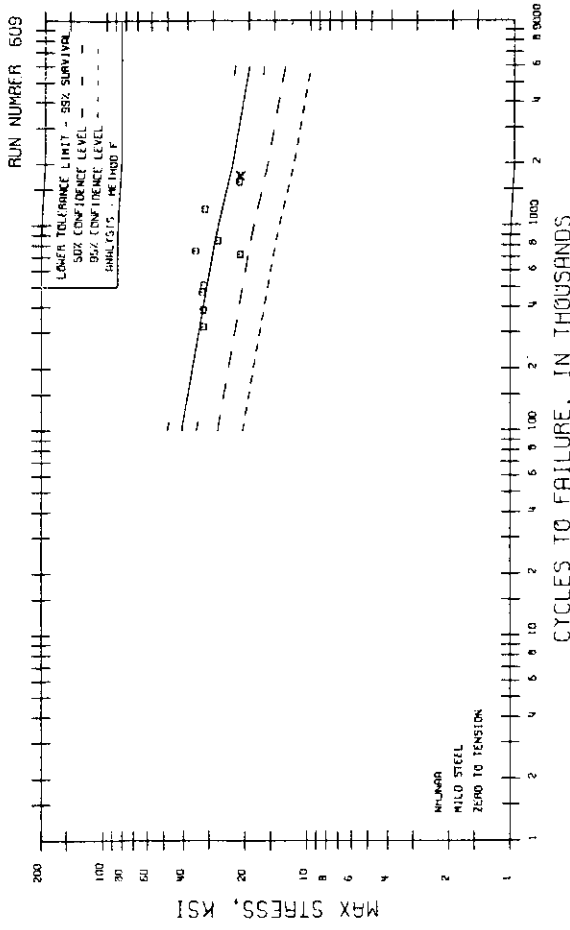


Detail No. 11

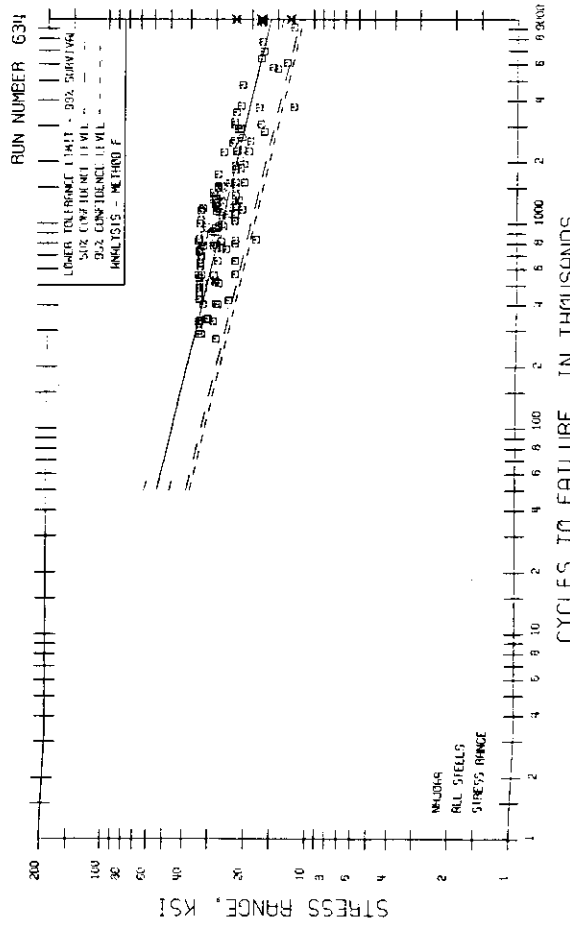


Detail No. 12

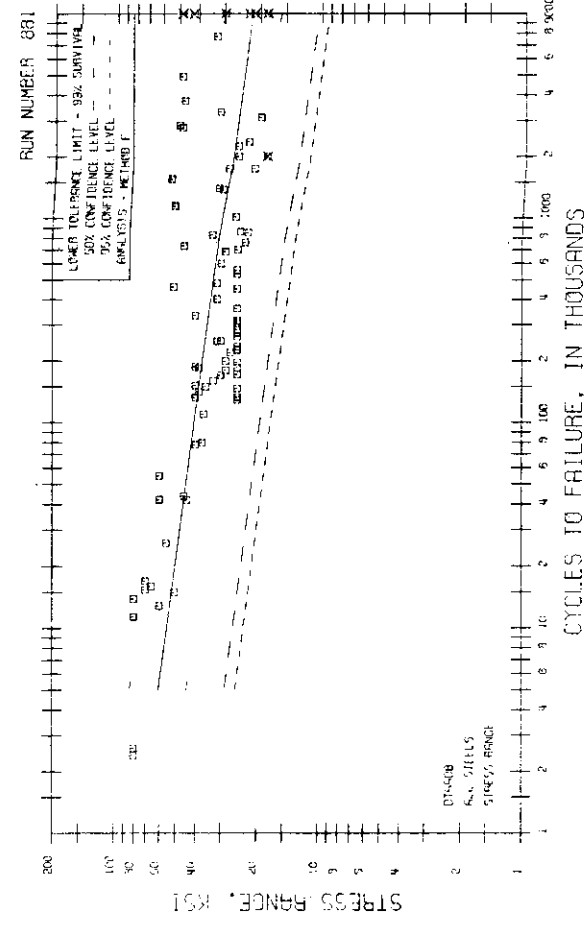
Fig. B.2 S-N Curves for Structural Details (Cont.).



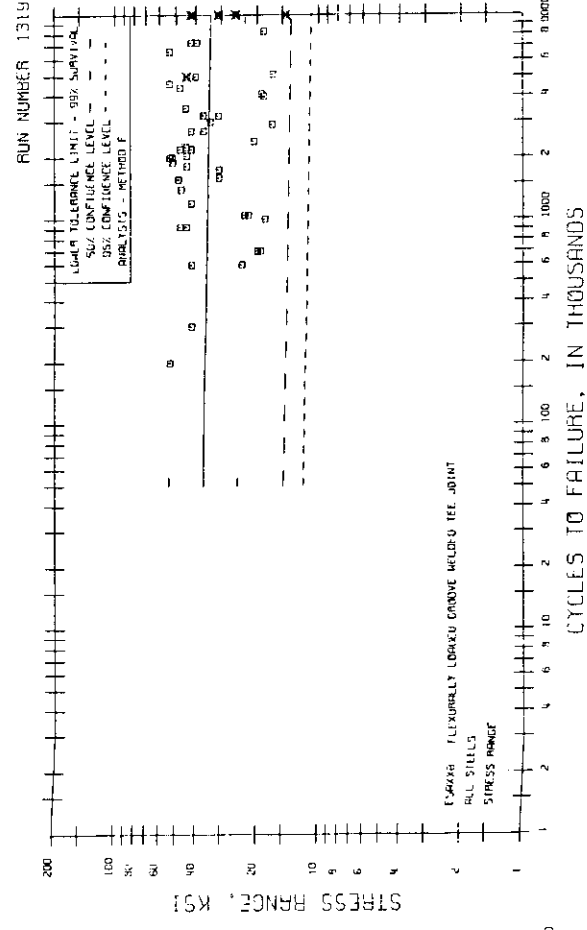
Detail No. 12(G)



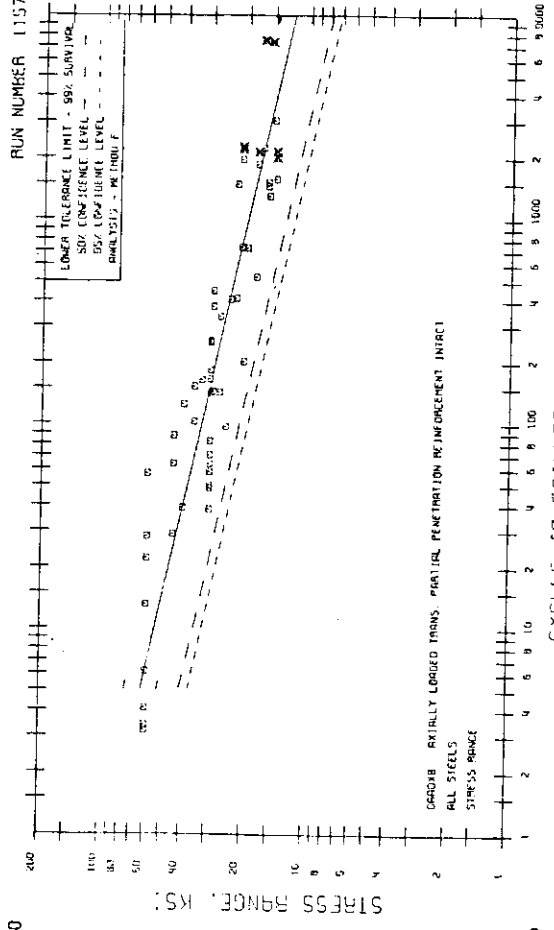
Detail No. 13



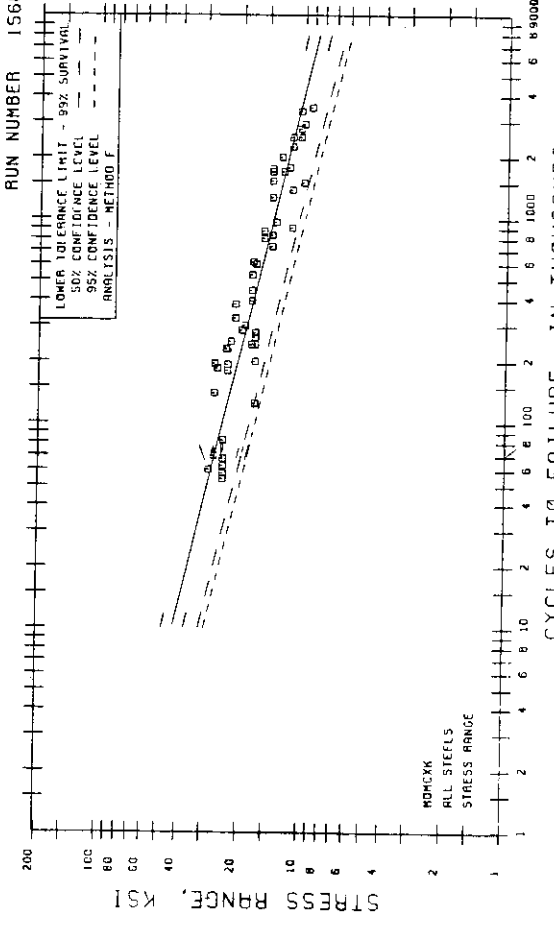
Detail No. 14



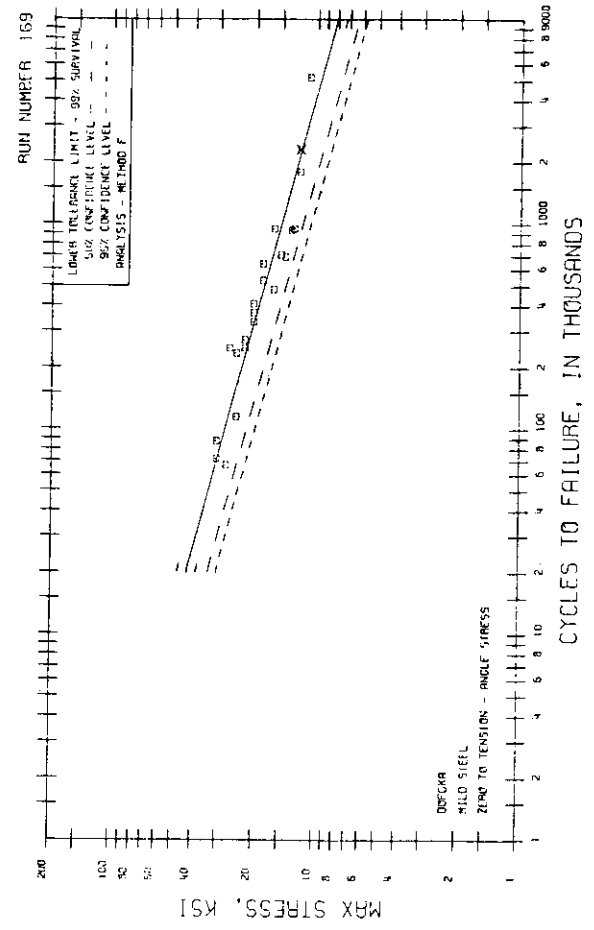
Detail No. 14A



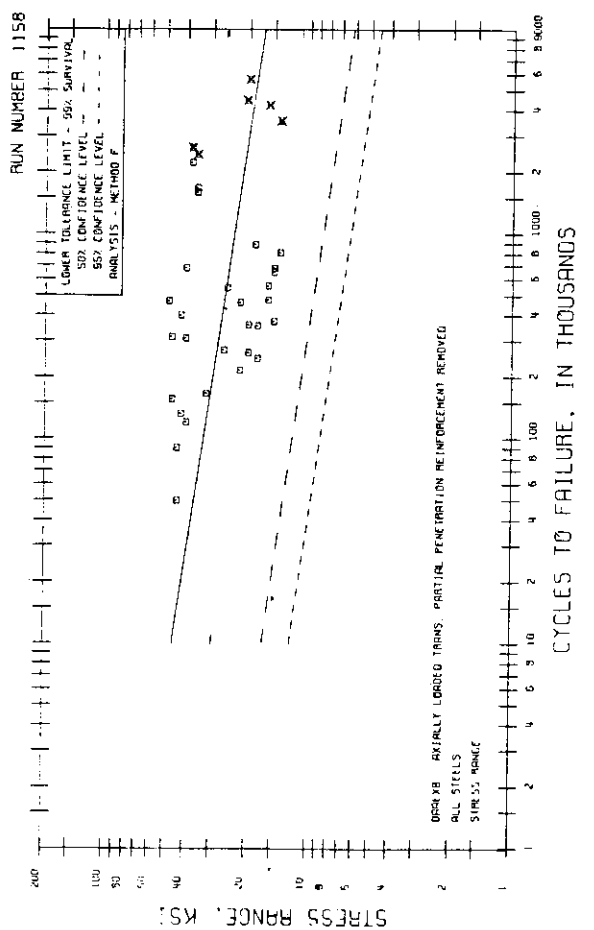
Detail No. 1560



Detail No. 1560

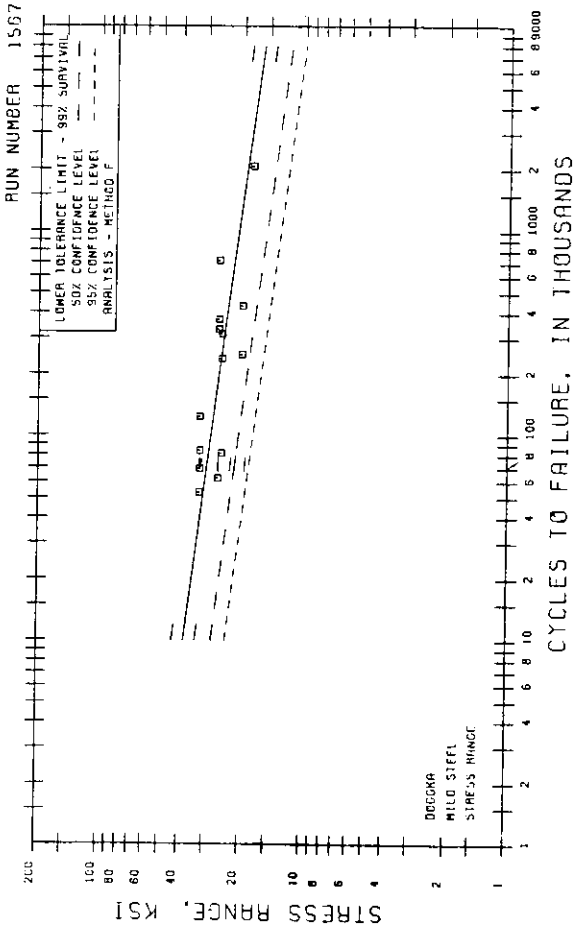


Detail No. 169

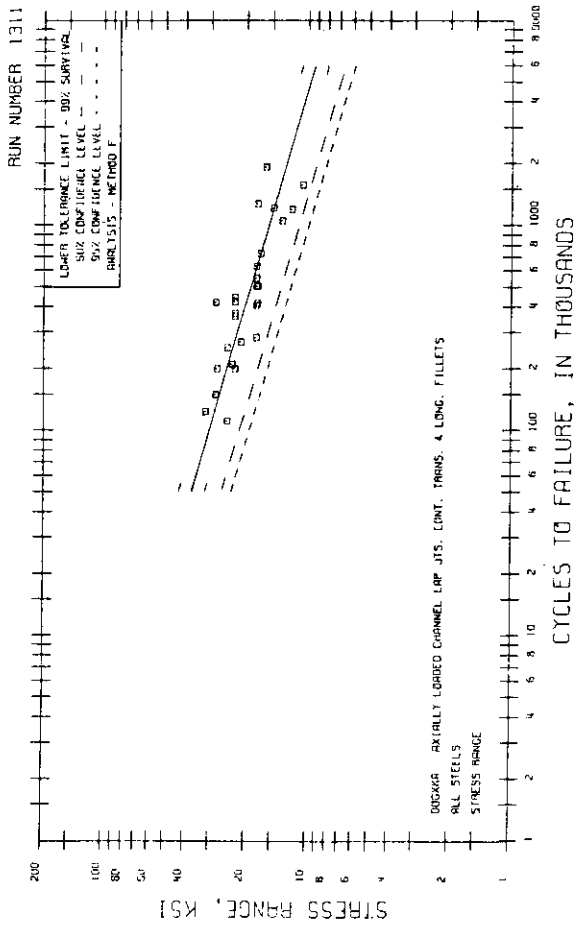


Detail No. 169(G)

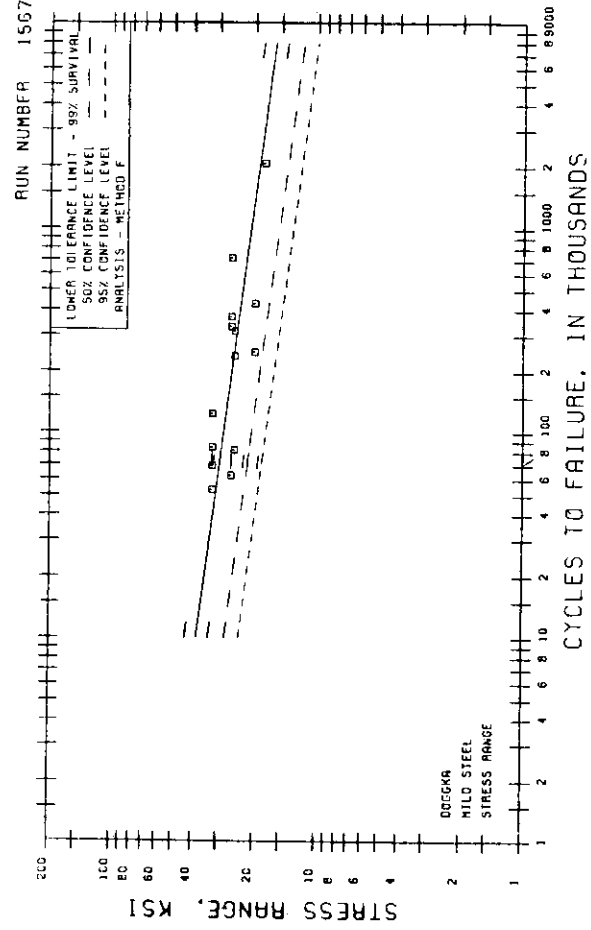
Fig. B.2 S-N Curves for Structural Details (Cont.).



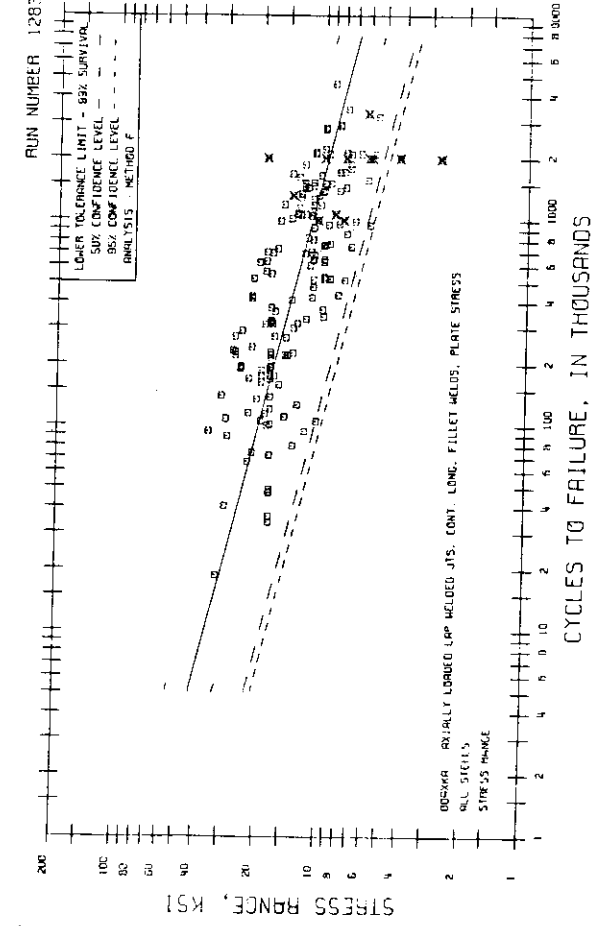
Detail No. 17(S)



Detail No. 17A

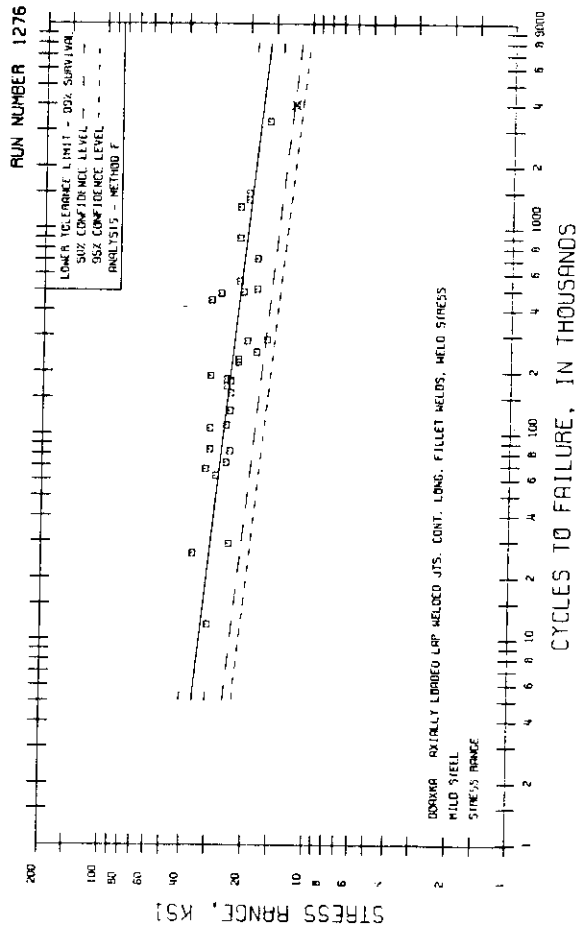


Detail No. 17A(S)

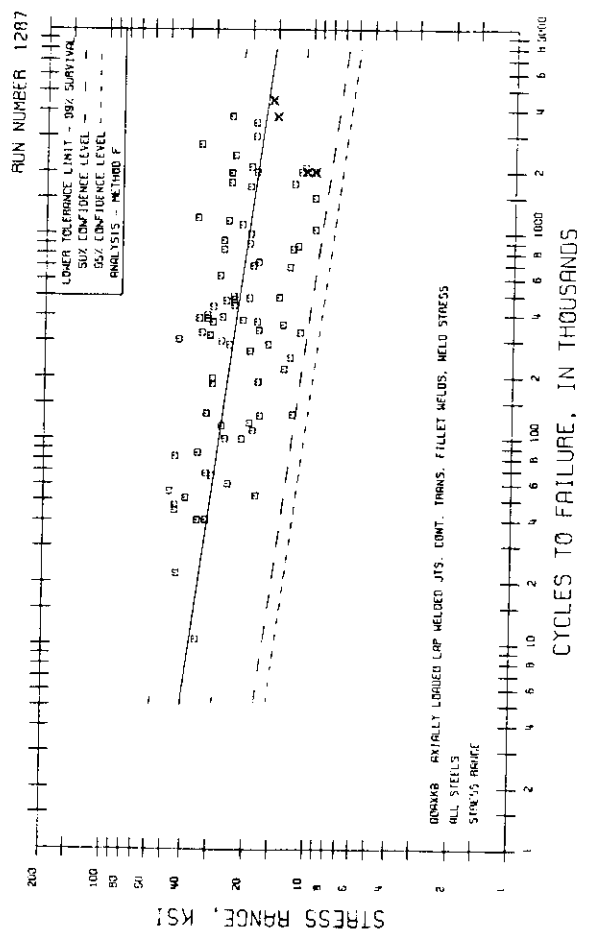


Detail No. 18

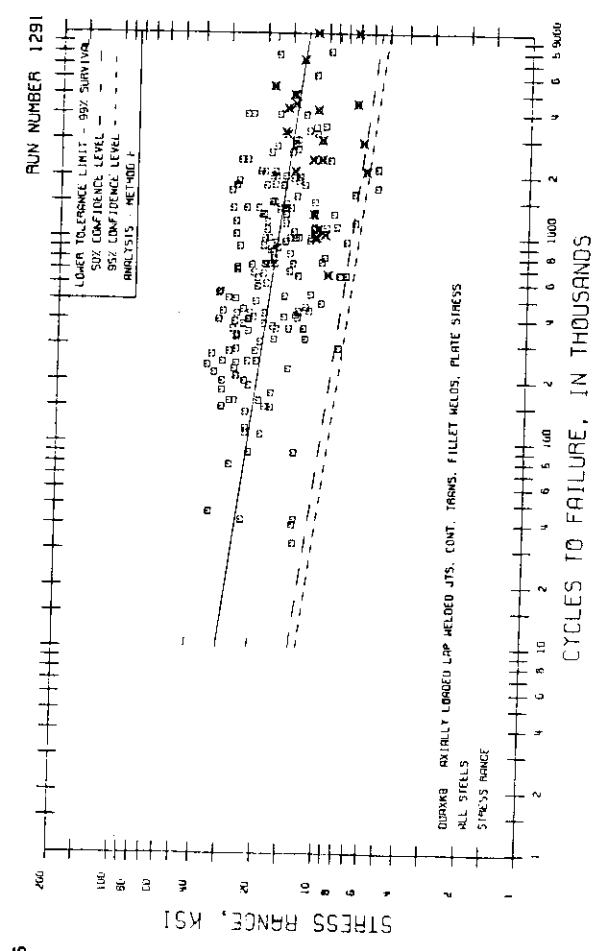
Fig. B.2 S-N Curves for Structural Details (Cont.).



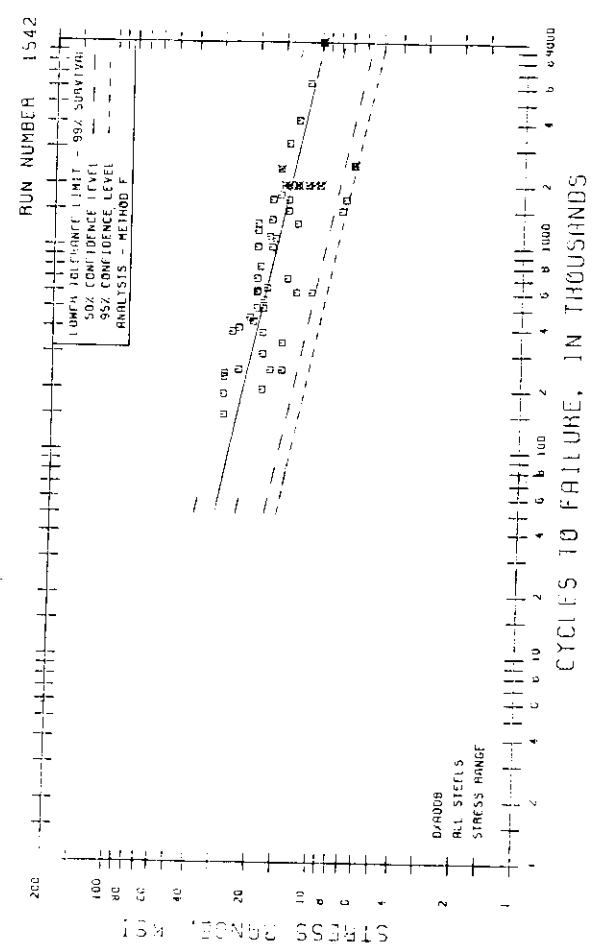
Detail No. 18(S)



Detail No. 19(S)

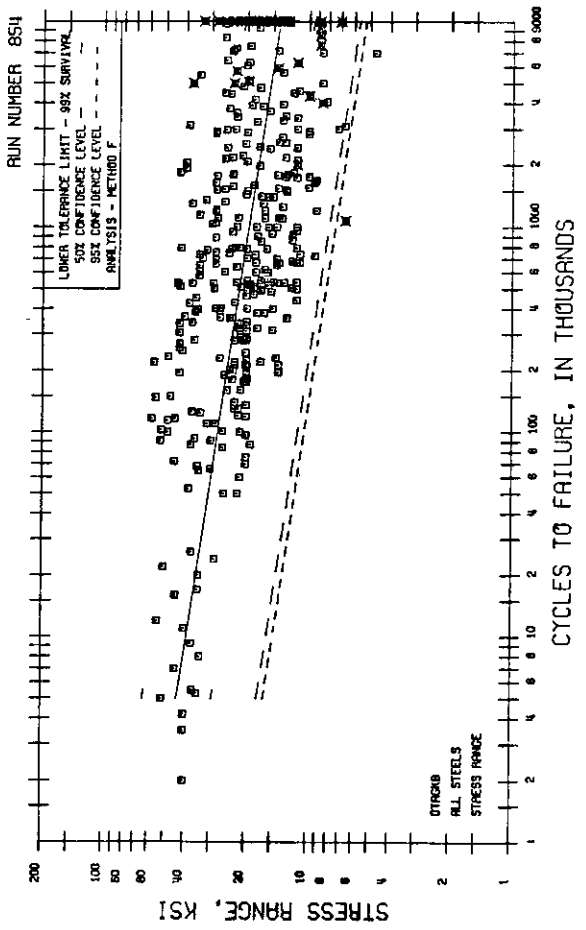


Detail No. 19

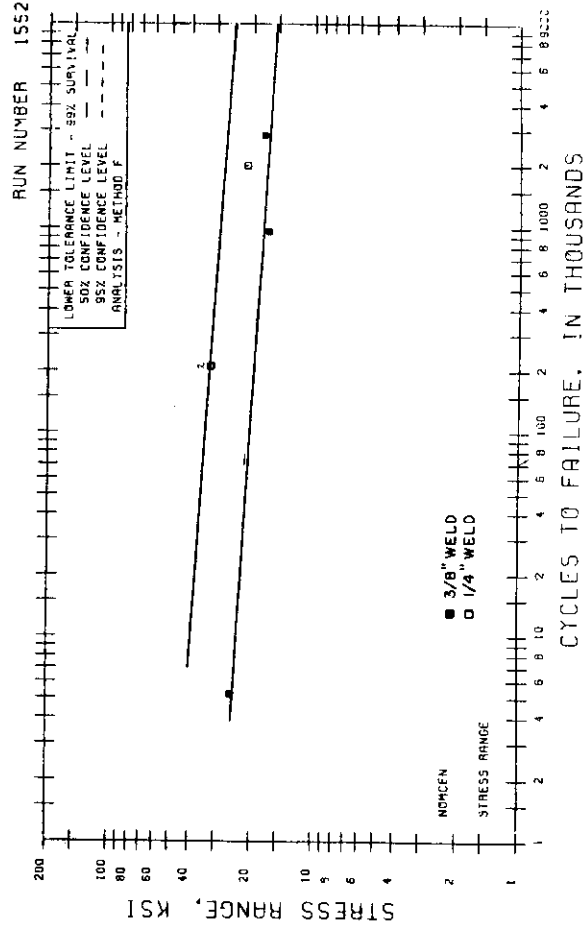


Detail No. 20

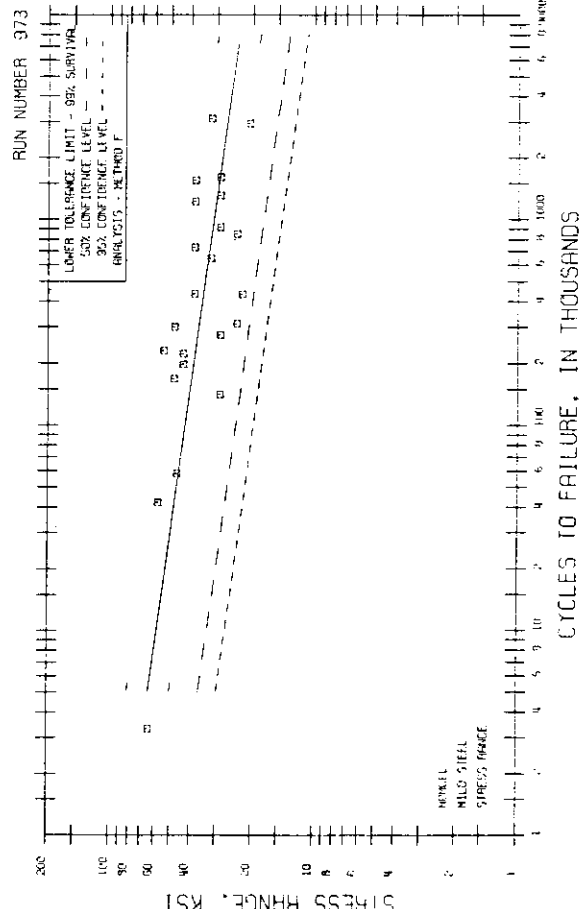
Fig. B.2 S-N Curves for Structural Details (Cont.).



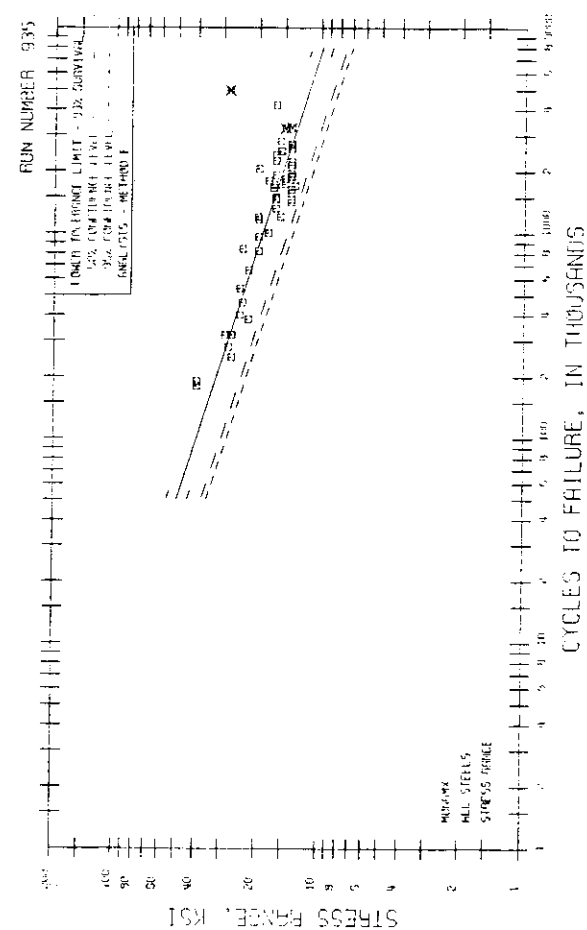
Detail No. 20(S)



Detail No. 21

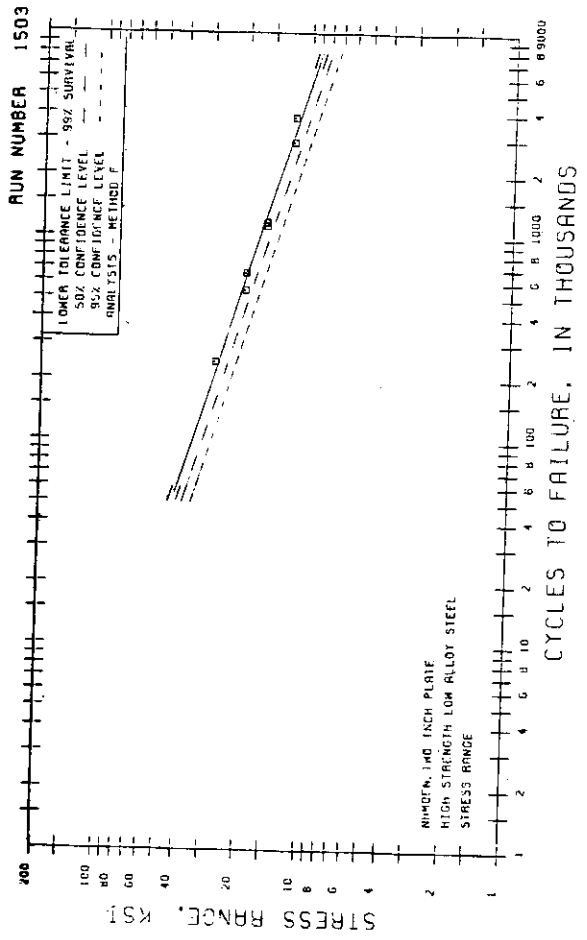


Detail No. 21(S)

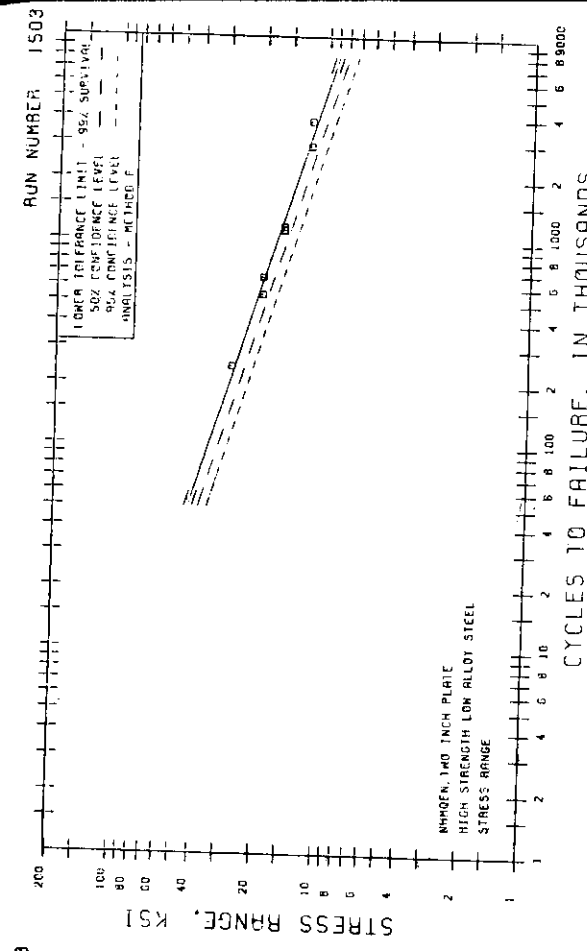


Detail No. 22

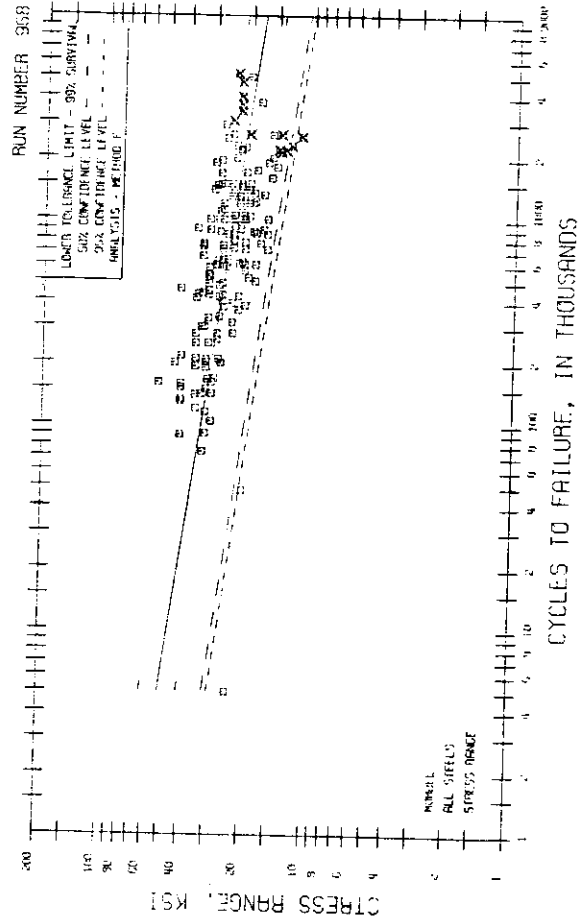
Fig. B.2 S-N Curves for Structural Details (Cont.).



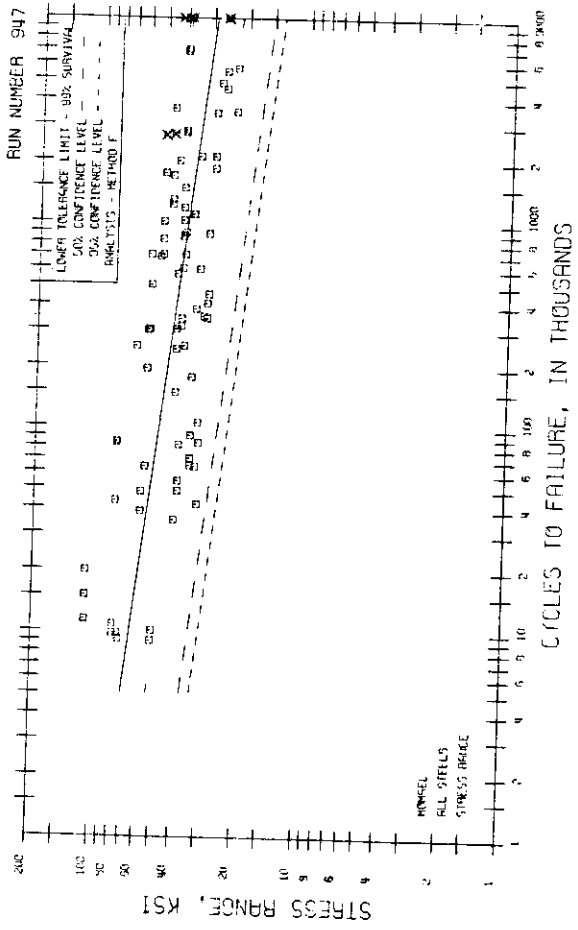
Detail No. 23



Detail No. 24

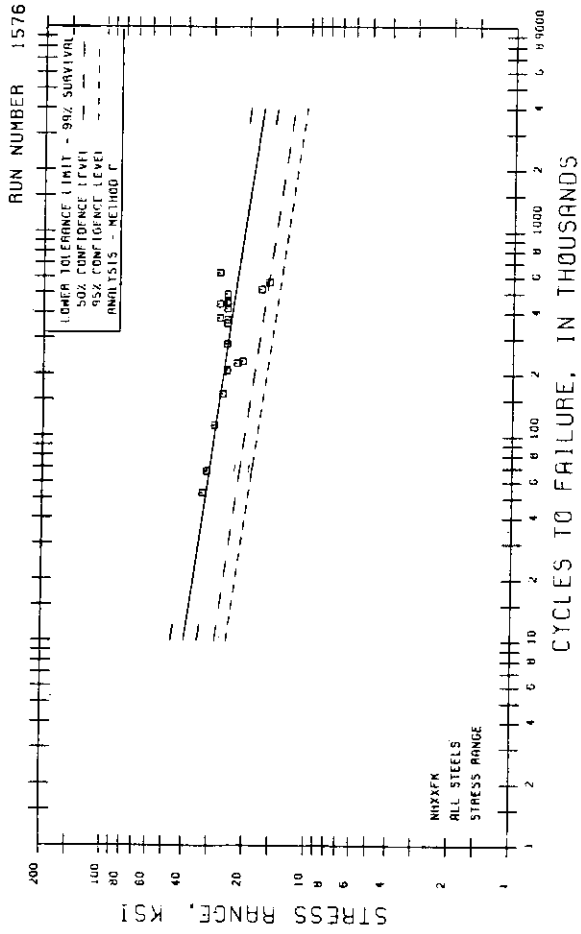


Detail No. 25

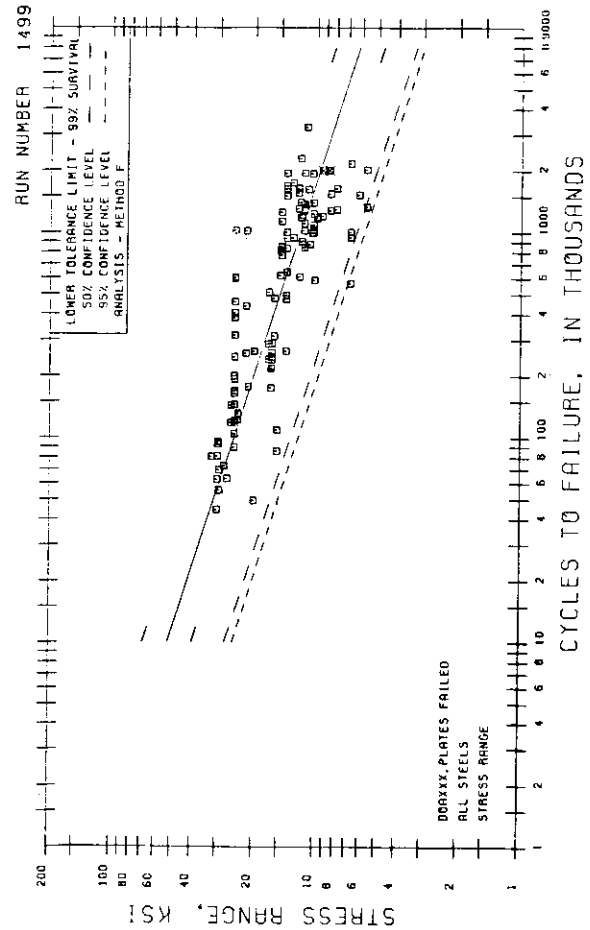


Detail No. 25A

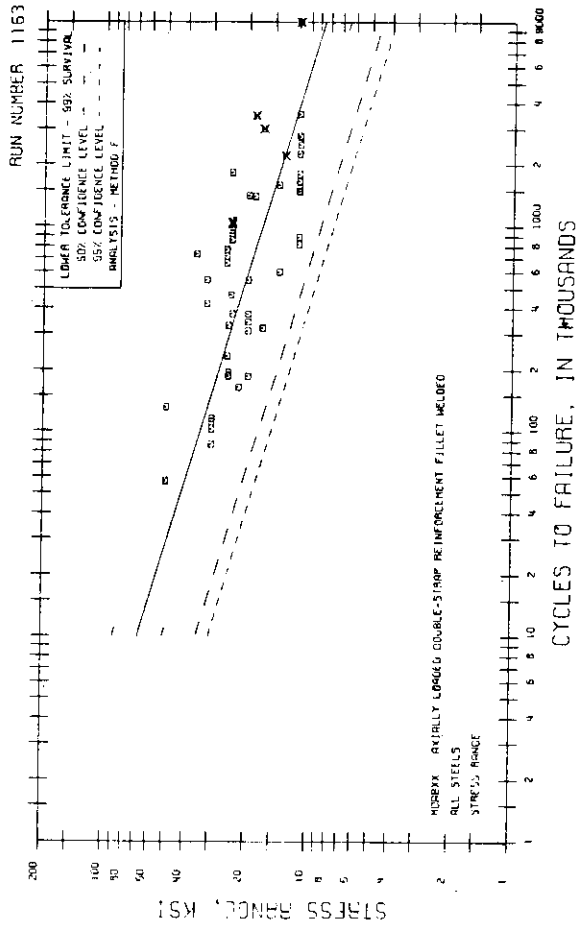
Fig. B.2 S-N Curves for Structural Details (Cont.).



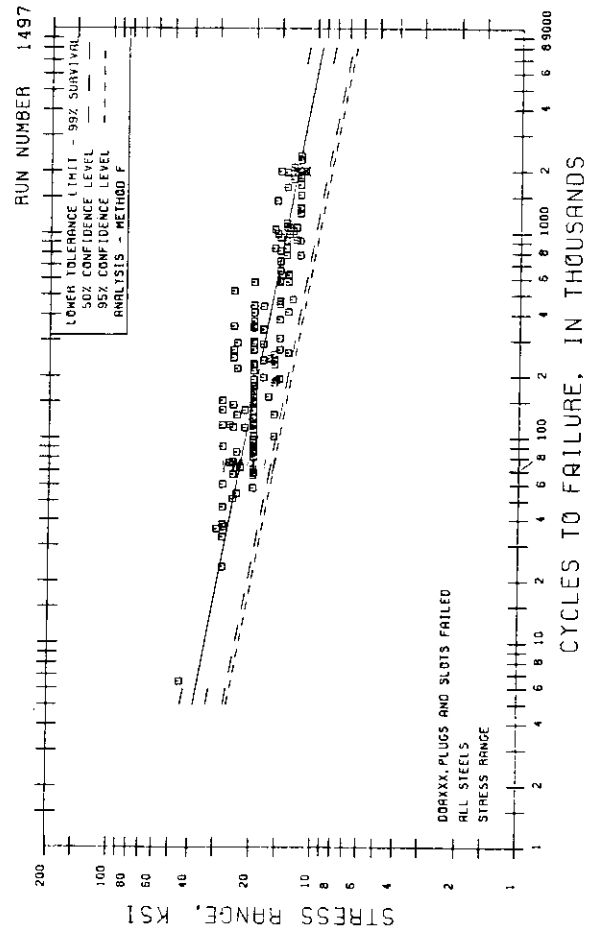
Detail No. 25B



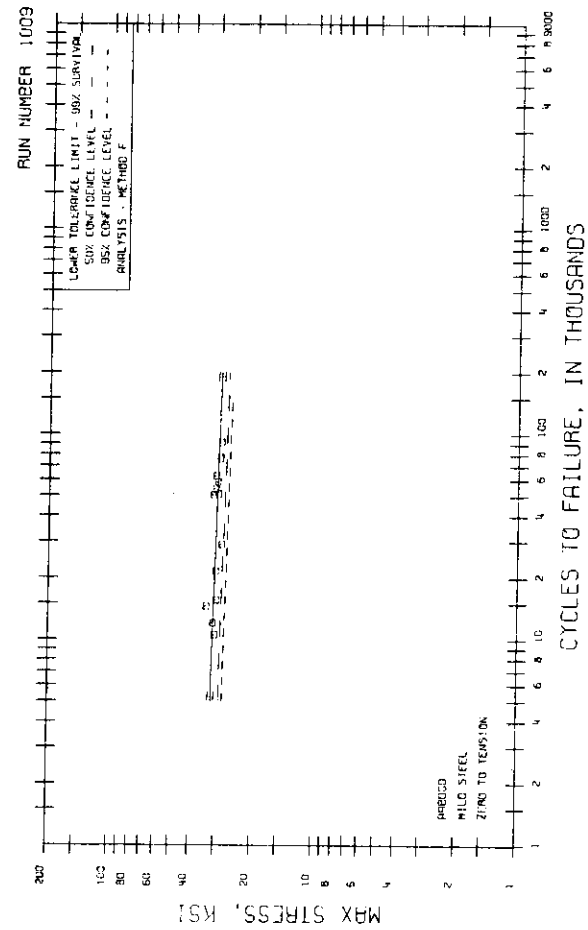
Detail No. 27



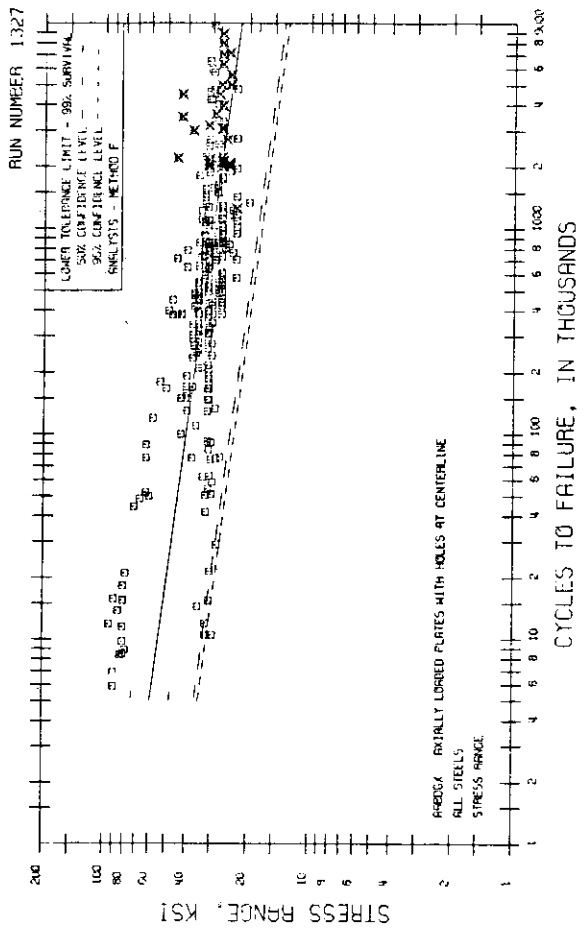
Detail No. 26



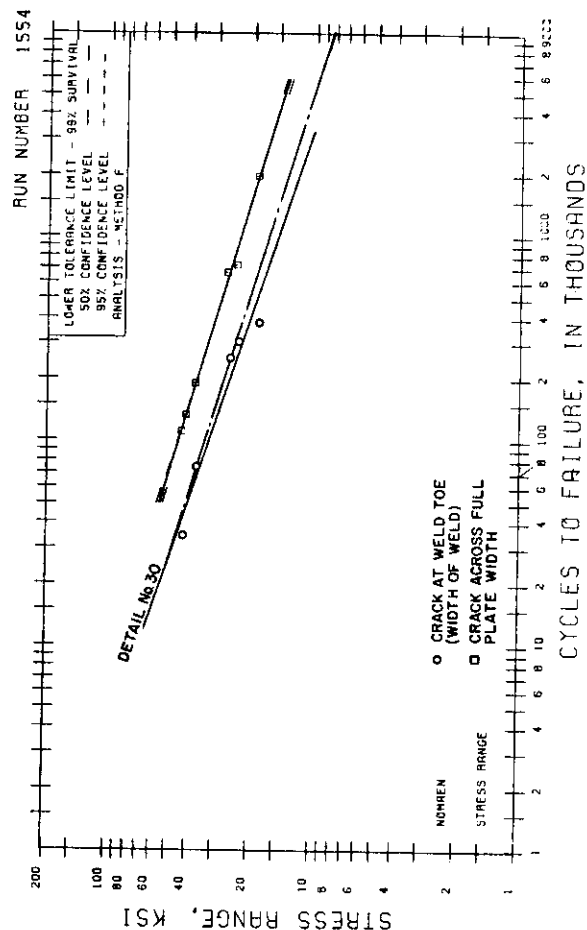
Detail No. 27(S)



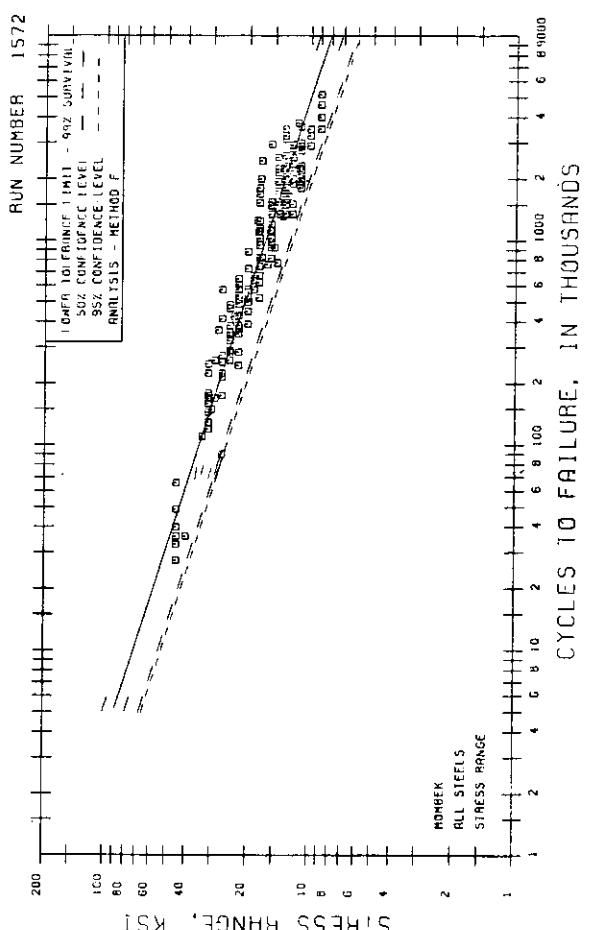
Detail No. 28(F)



Detail No. 28

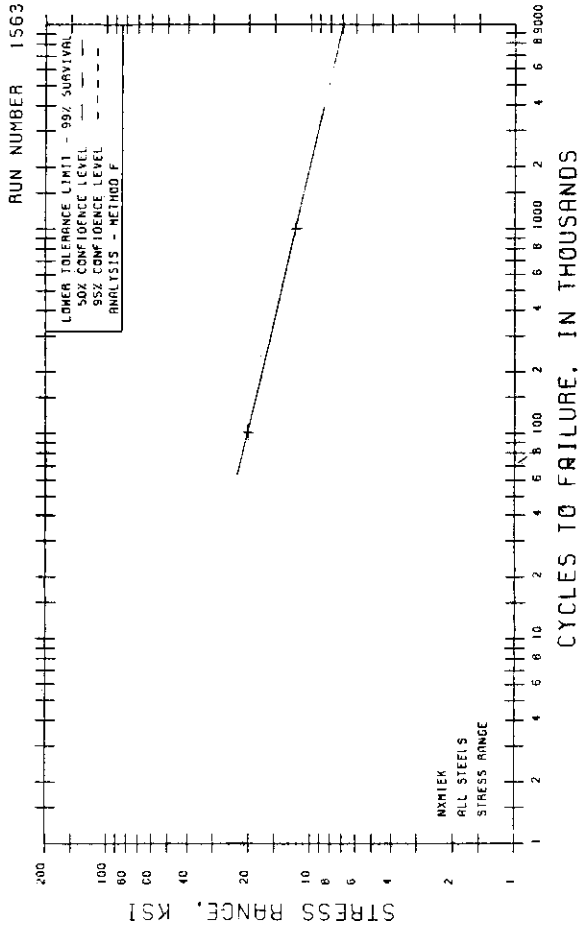


Detail No. 30A



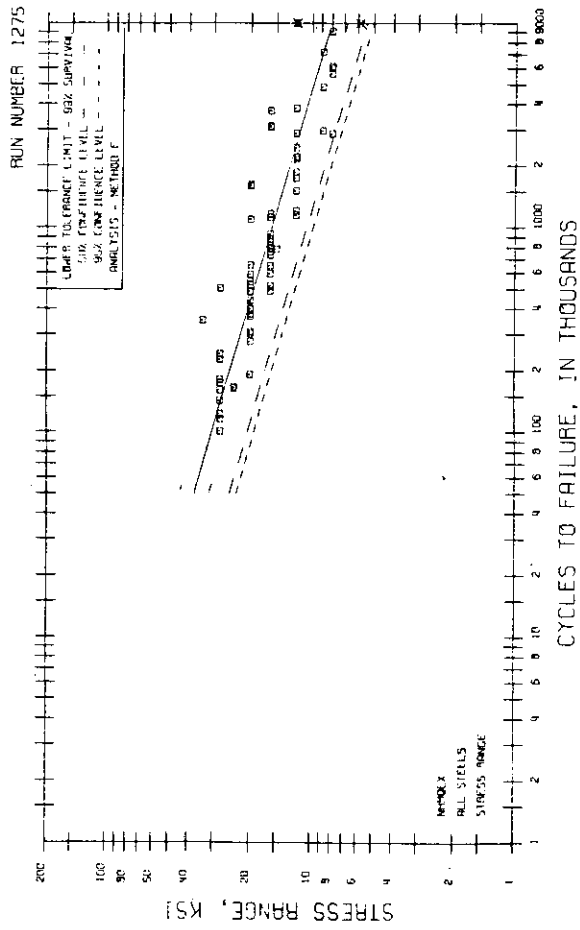
Detail No. 30

Fig. B.2 S-N Curves for Structural Details (Cont.).

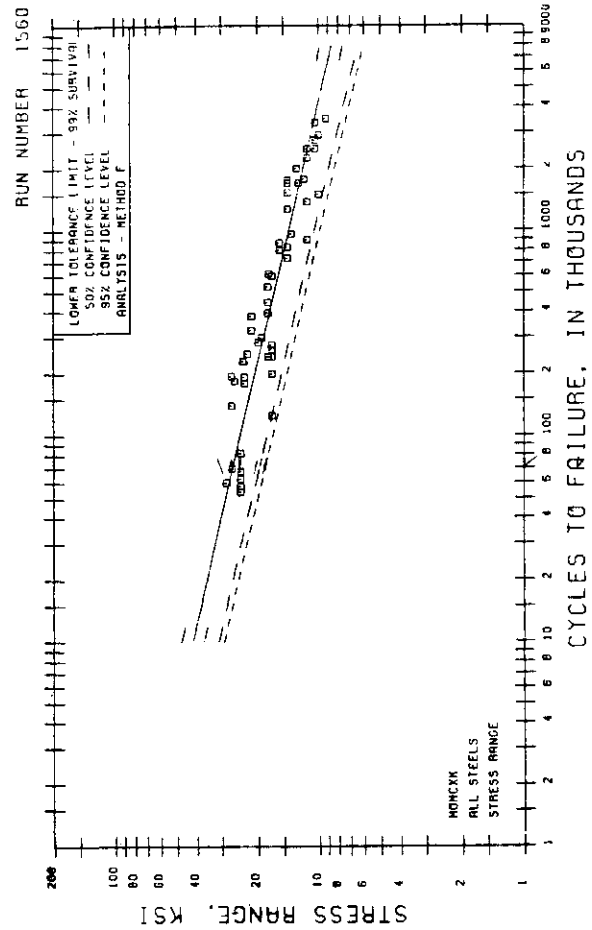


Detail No. 31

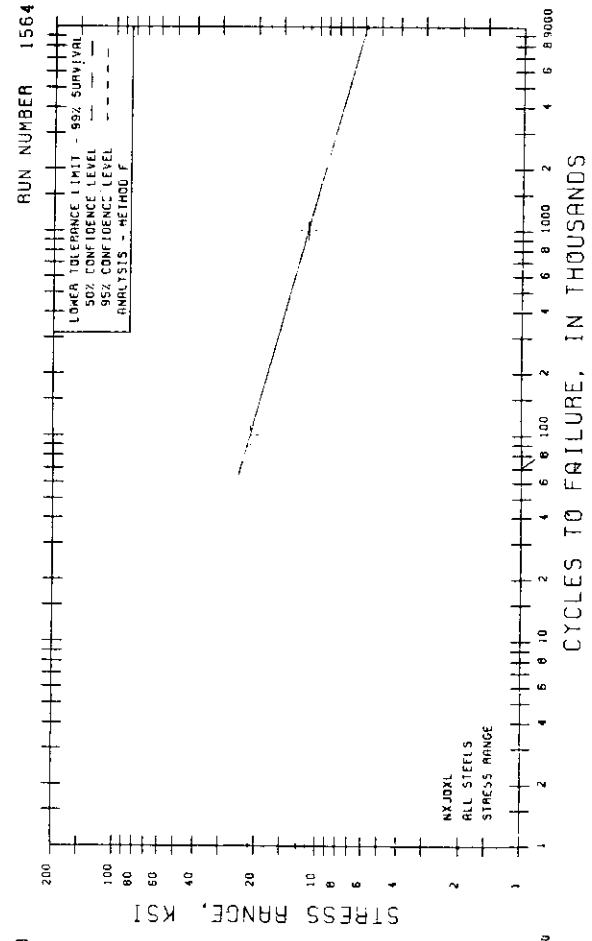
148



Detail No. 31A

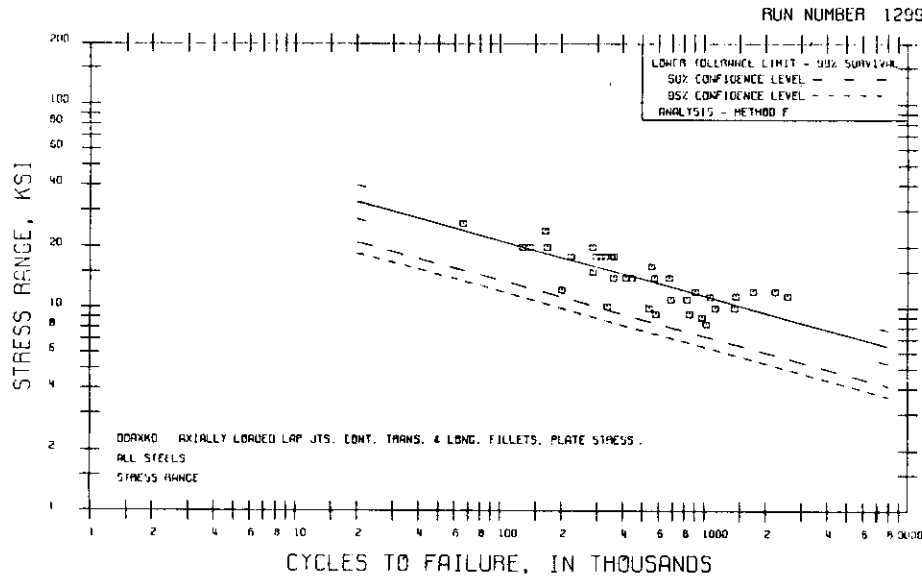


Detail No. 32A

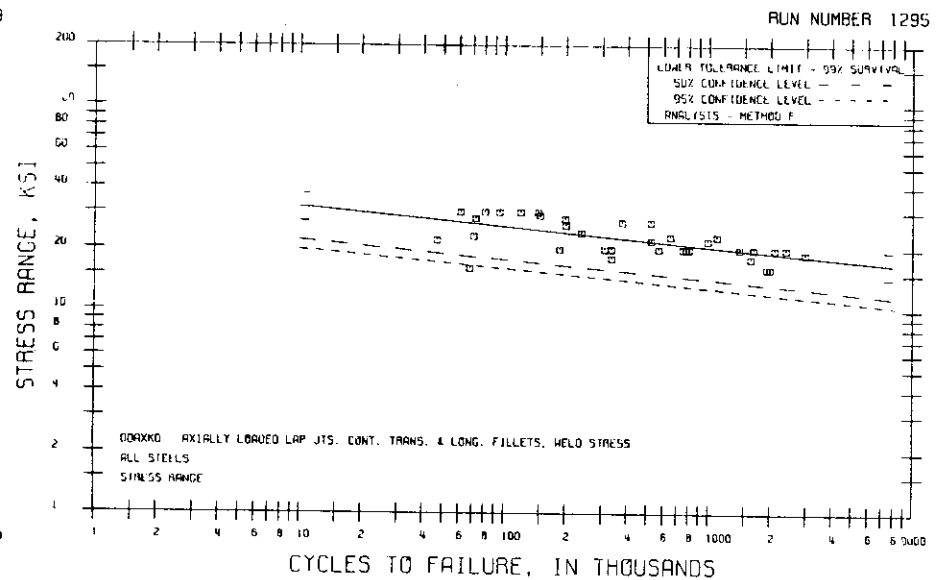


Detail No. 32B

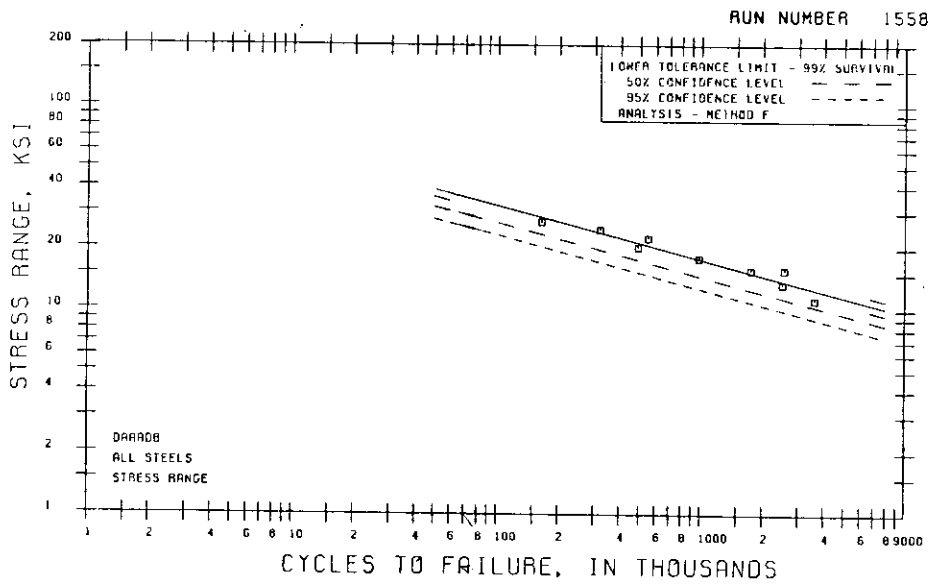
Fig. B.2 S-N Curves for Structural Details (Cont.)



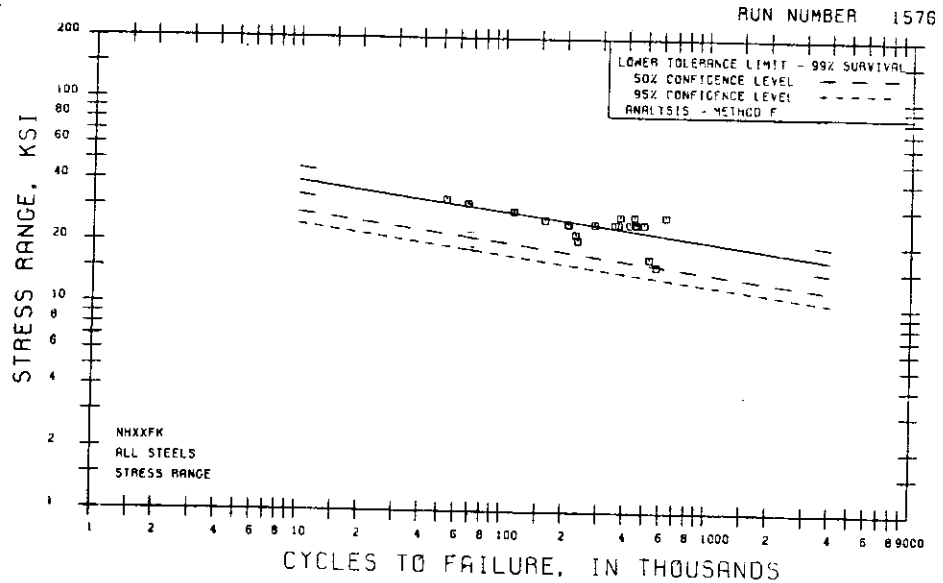
Detail No. 33



Detail No. 33(S)

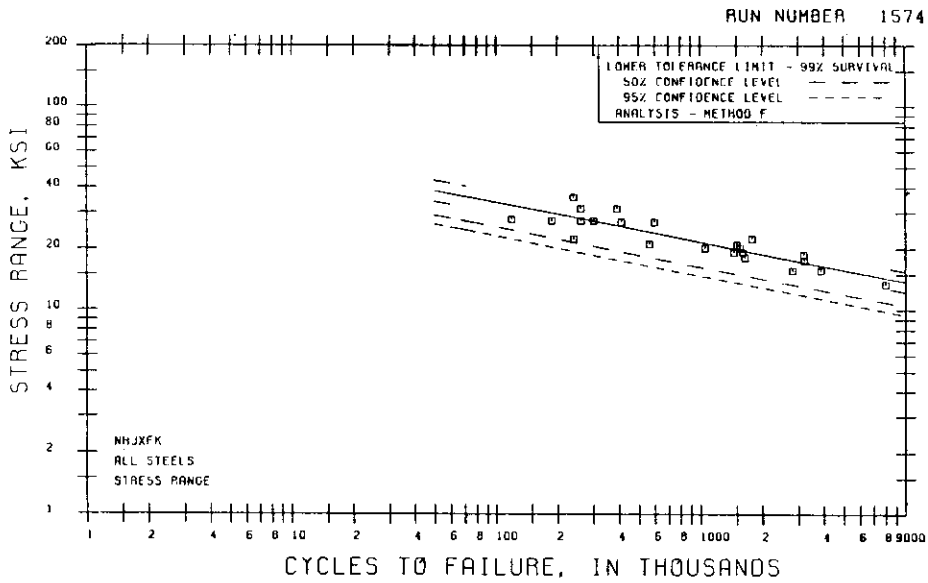


Detail No. 35

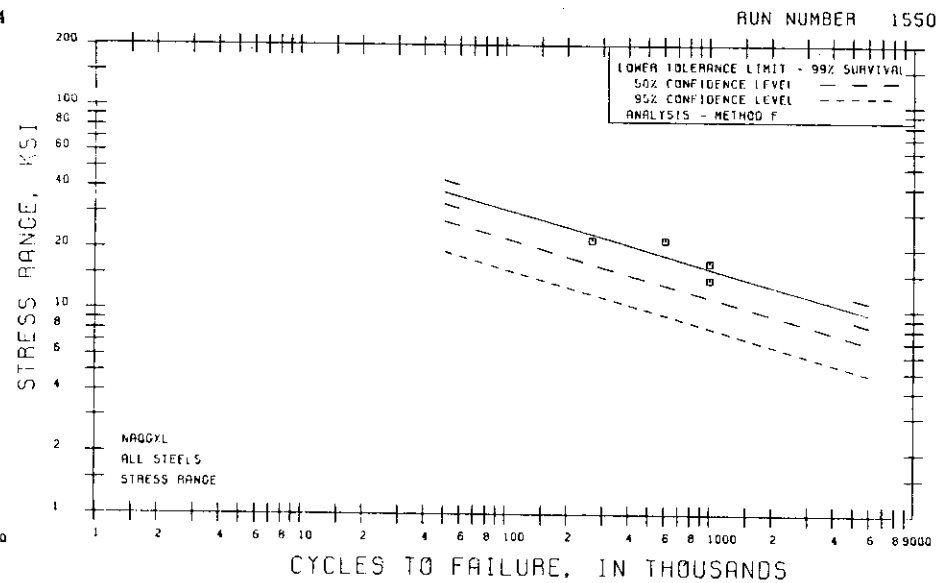


Detail No. 36

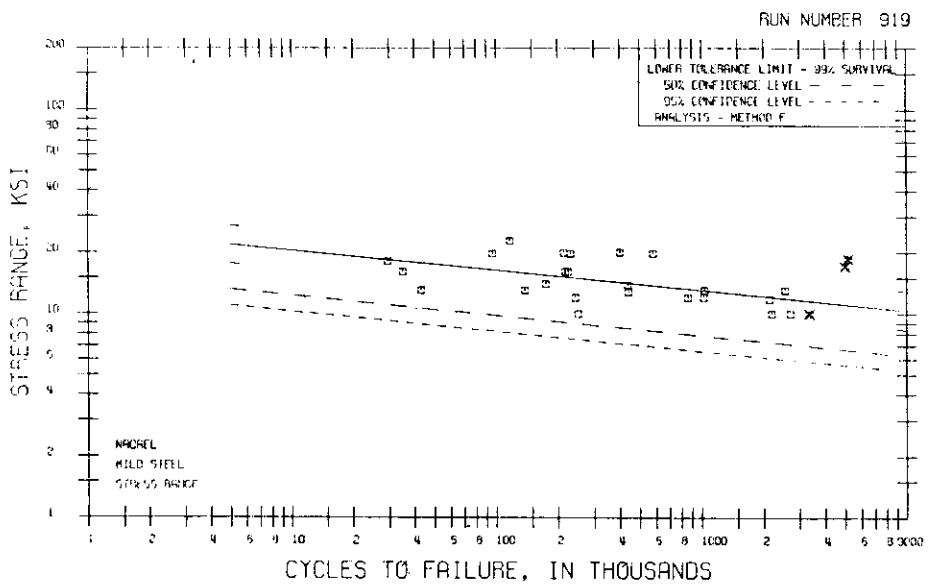
Fig. B.2 S-N Curves for Structural Details (Cont.).



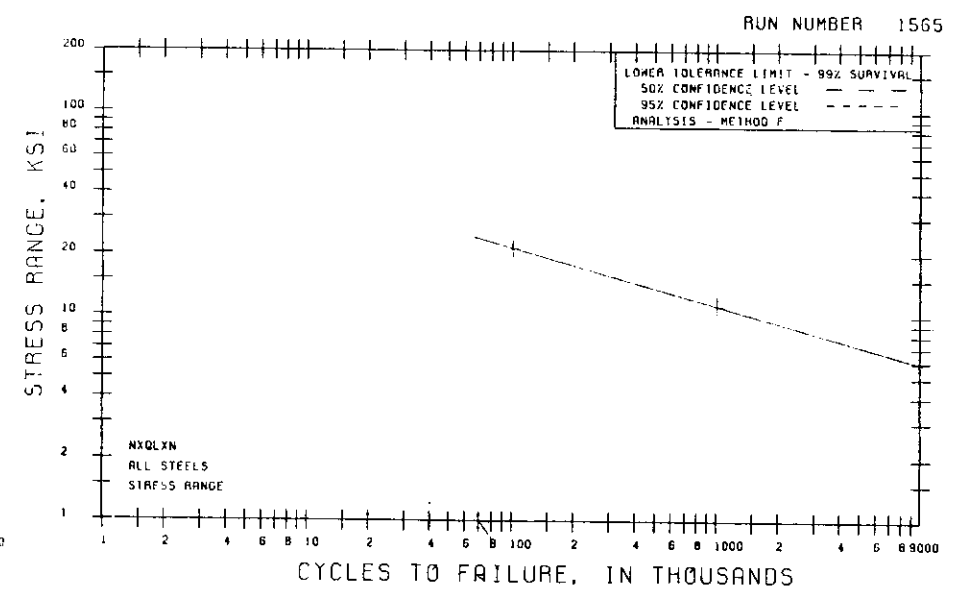
Detail No. 36A



Detail No. 38

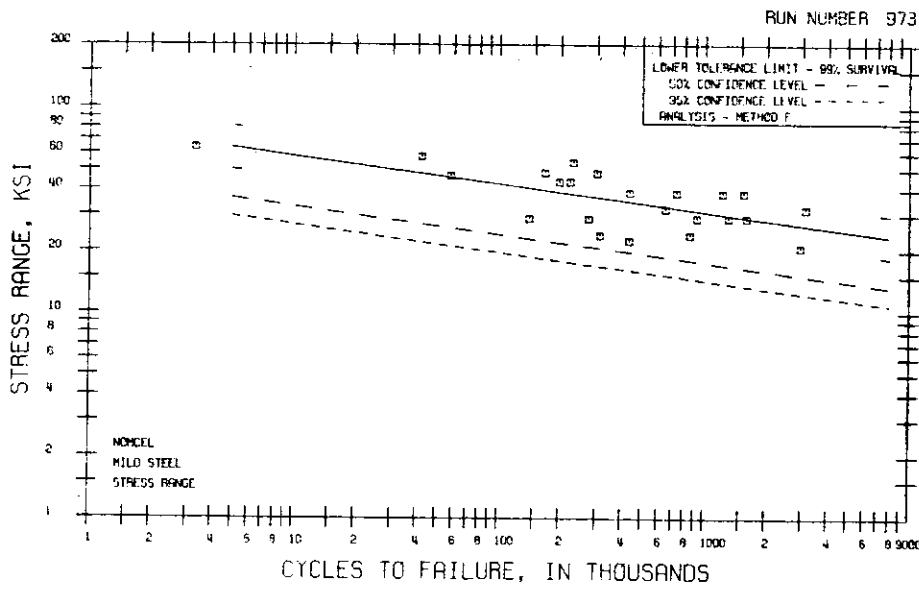


Detail No. 38(S)

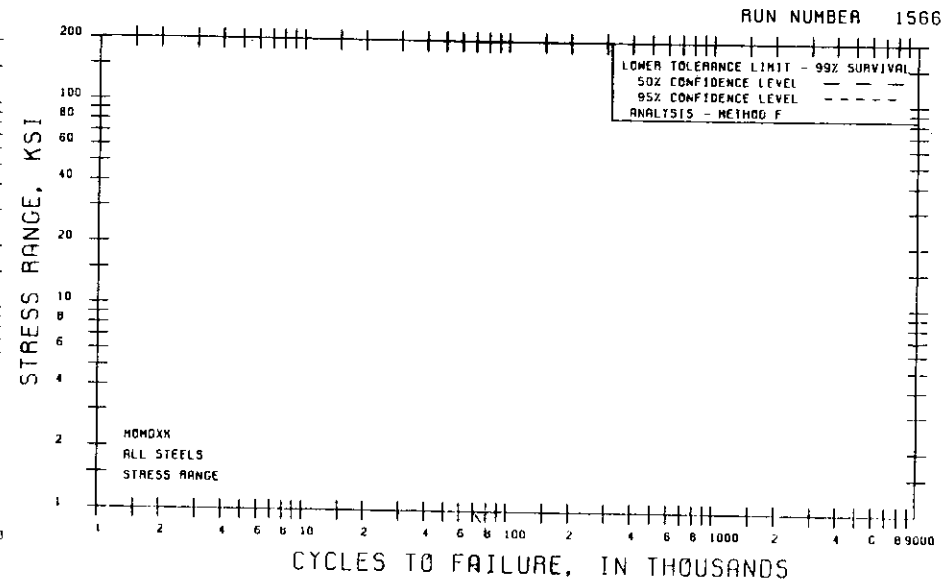


Detail No. 40

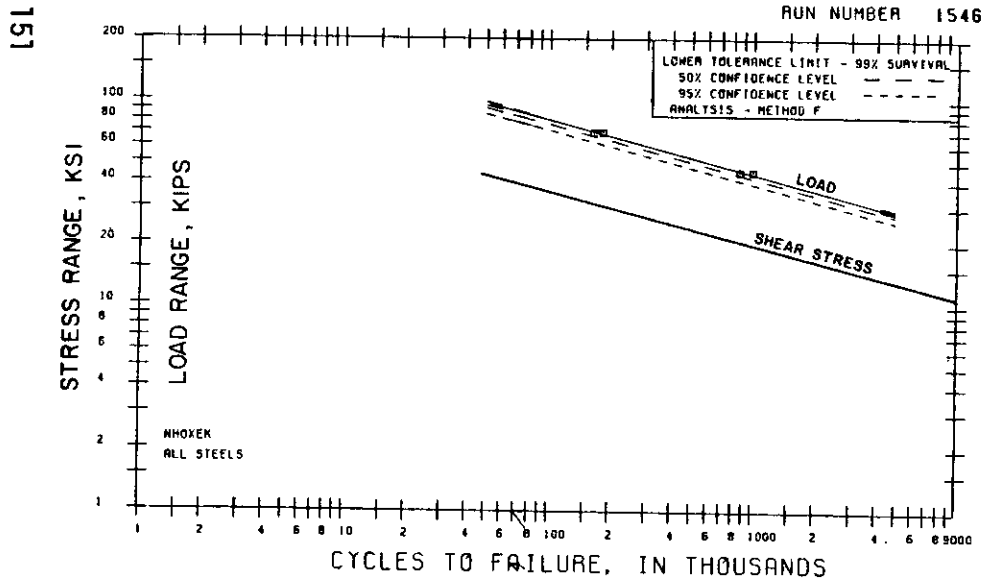
Fig. B.2 S-N Curves for Structural Details (Cont.).



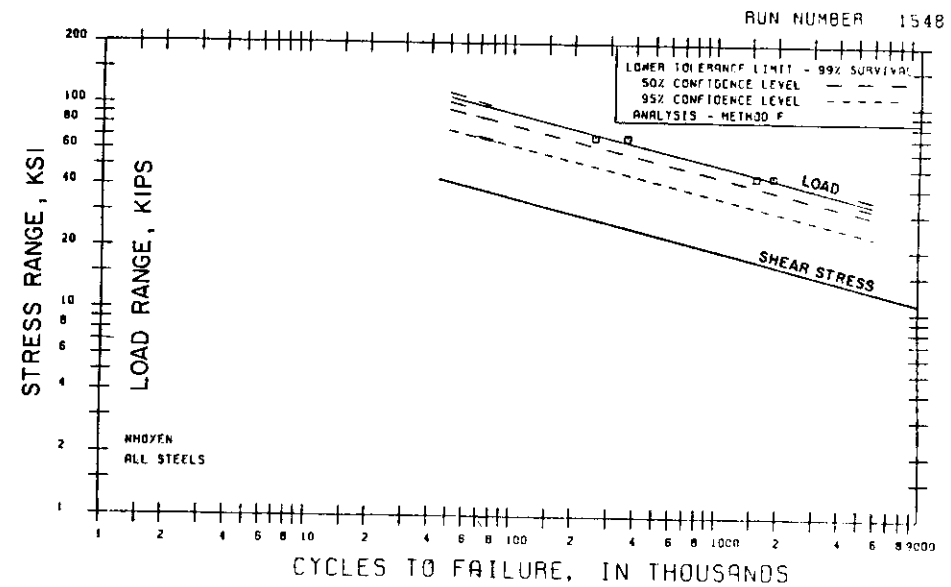
Detail No. 42



Detail No. 46



Detail No. 51



Detail No. 52

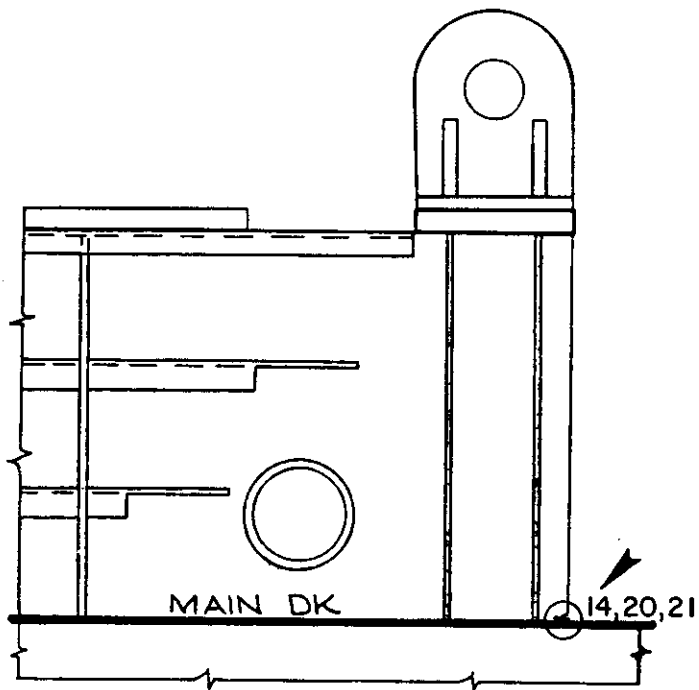
Fig. B.2 S-N Curves for Structural Details (Cont.).

Appendix C

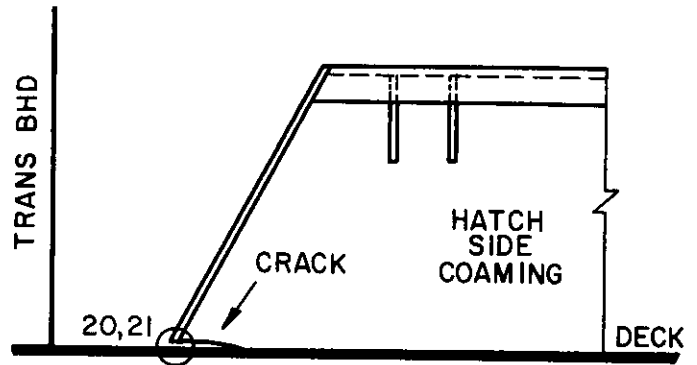
Examples of Cracking in Ship Structure Details

(Details from Ref's. C.1 and C.2)

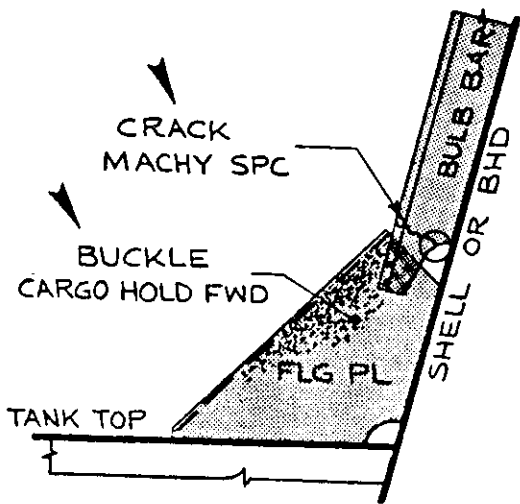
This appendix presents examples of cracks on various types of failures observed in ship structures. The locations at which the cracks initiated have been circled. Such information will help greatly in identifying those locations at which fatigue must be considered in design. Where possible, the local fatigue details at the crack locations have been identified.



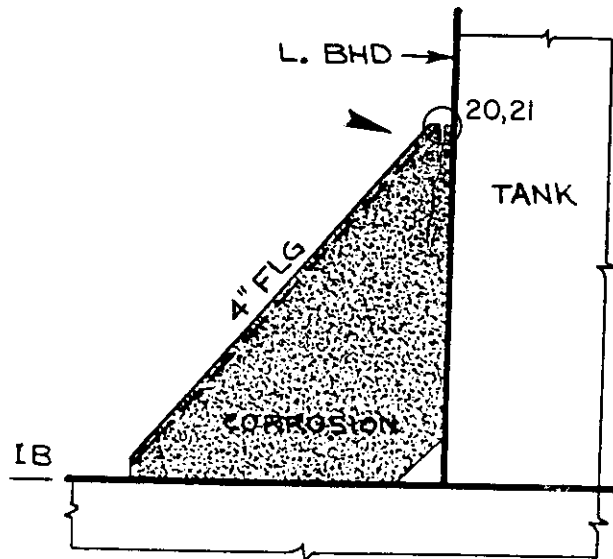
HATCH SIDE GIRDER
1J2
COMBINATION



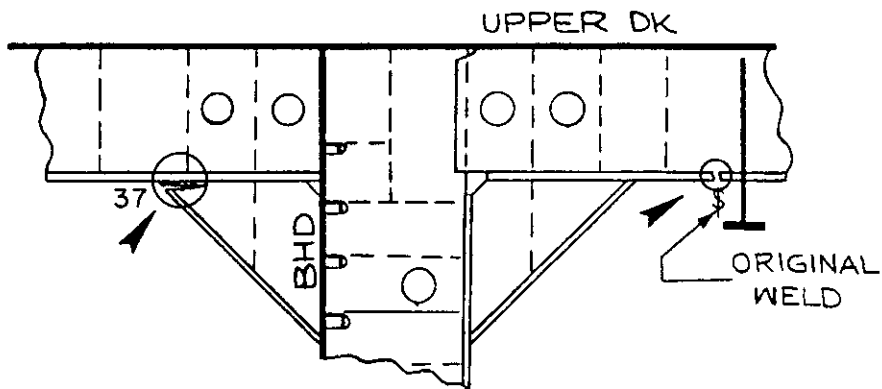
END OF HATCH SIDE COAMING
1J3



SHELL & TANK FRAMING
1M6
CONTAINERSHIP

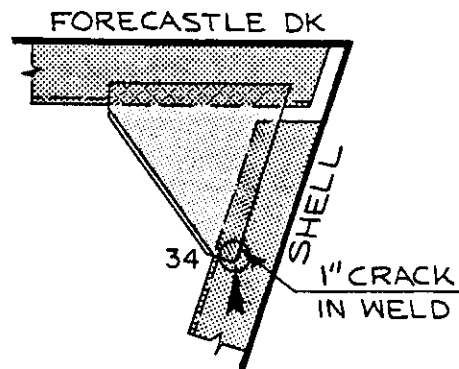


BRKT. IN MACHY SPACE
1M8
TANKER

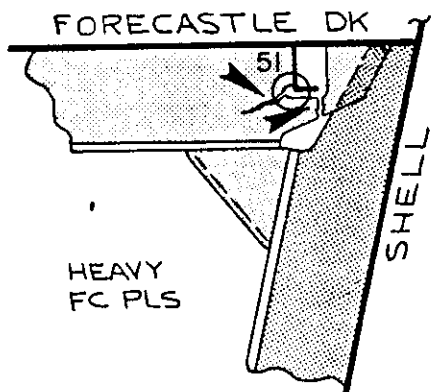


☐ GIRDER NEAR ☐

1G4
TANKER

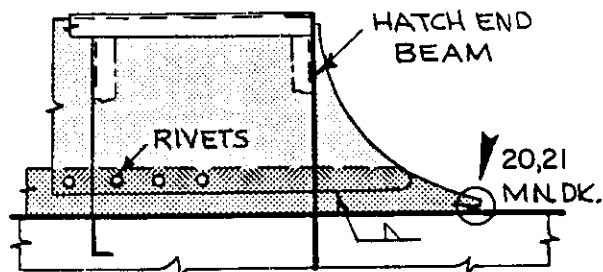


TRANS FRAMING
1E2
CONTAINERSHIP



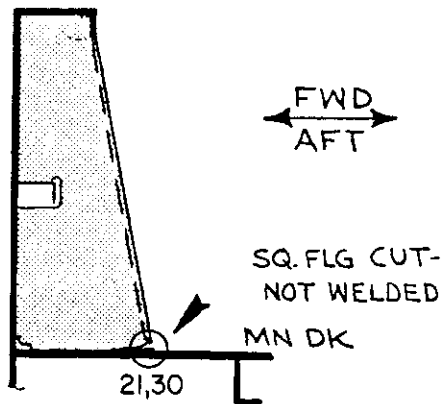
TRANS DK GIRDER

8E4
CONTAINERSHIP

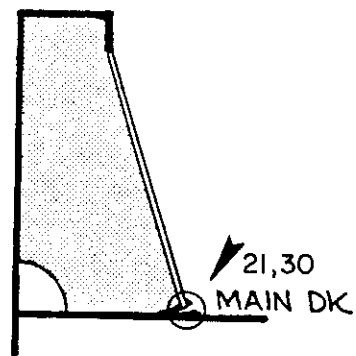


HATCH SIDE GIRDER ENDING
AT CORNER OF HATCH #1

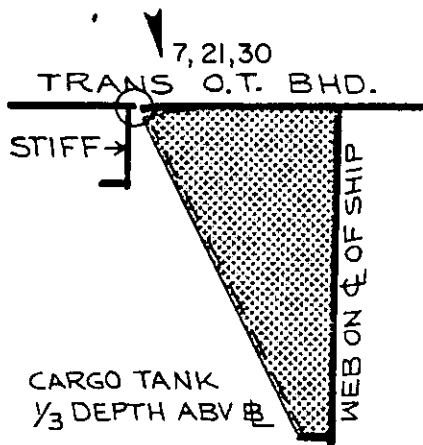
1J1
CONTAINERSHIP



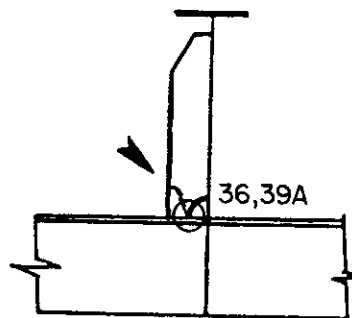
CARGO HATCH COAMING
2C6
ORE CARRIER



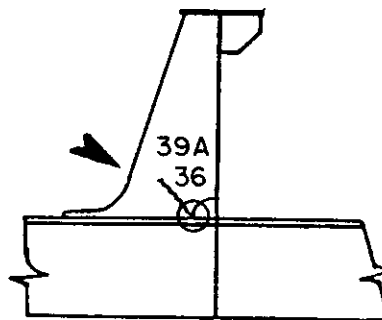
BKT ON HATCH END BEAM
2C7
CONTAINERSHIP



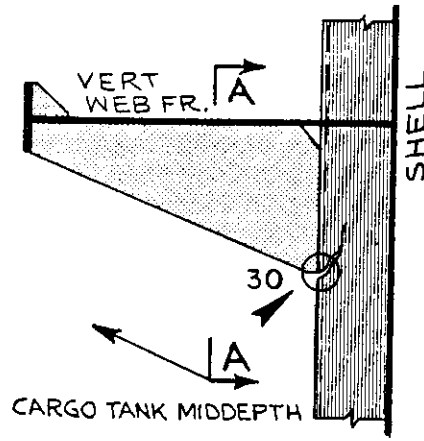
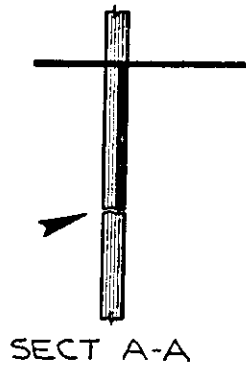
PLAN VIEW SECTION
2C2
TANKER



2A

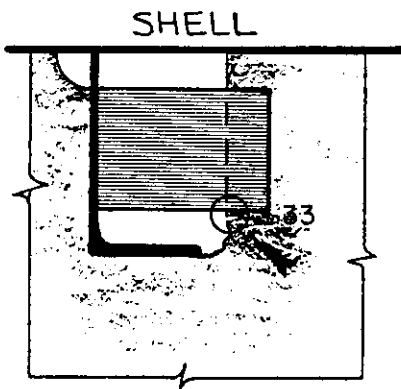


2B

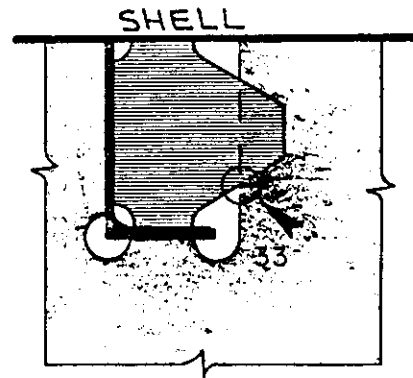


LONGL. AT A WEB FRAME

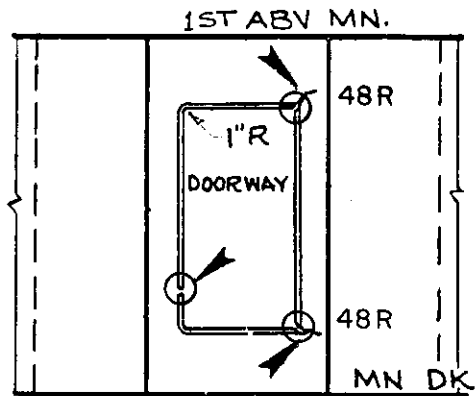
2B12
TANKER



SHELL FRAME ϕ
3A17
CONTAINERSHIP



WEB FRAME -AFT
3C3
BULK CARRIER



ELEV

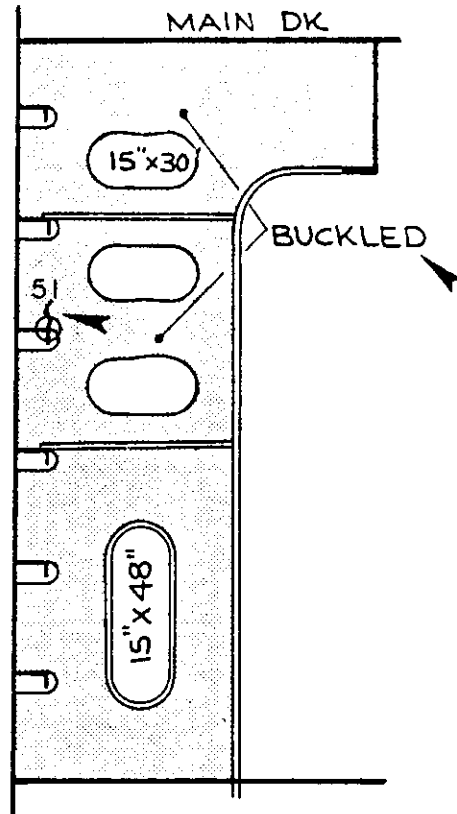


PLAN VIEW

LONGL ENCL. BHD Ø P&S

7A9

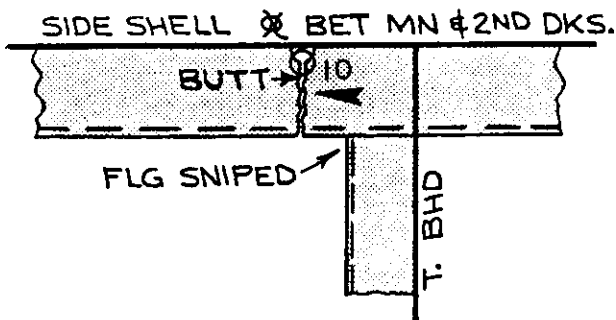
GENRL CARGO



TRANS WEB FR

8D5

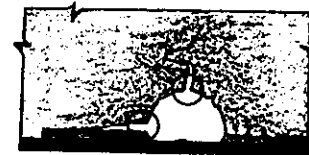
COMBINATION CARRIER



SHELL LONGL

7C1

COMBINATION CARRIER



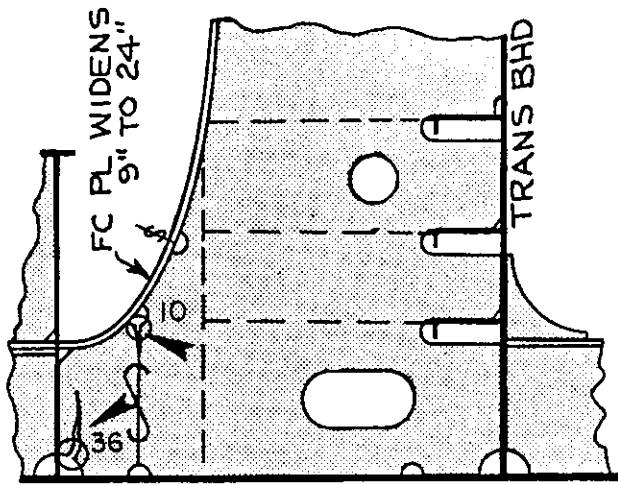
MIDSPAN



BOW SIDE SHELL
SHELL LONGL

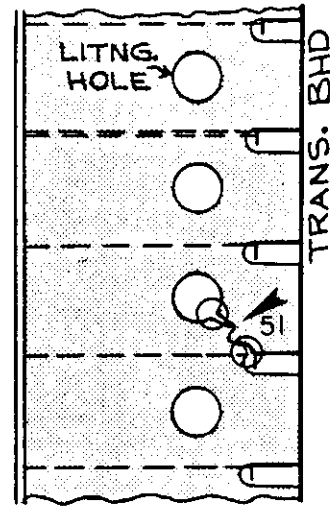
7C1

COMBINATION CARRIER



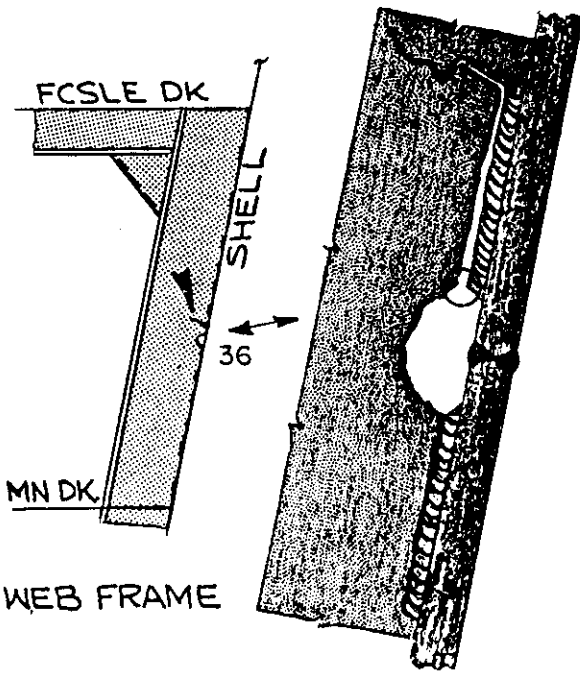
BOTT SHELL

O.T. BHD WEB
7C1
TANKER



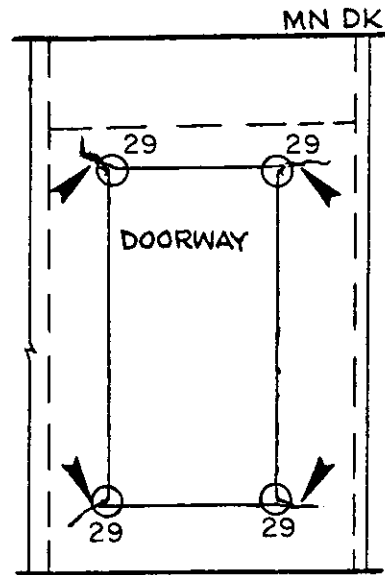
MIDLENGTH

O.T. BHD WEB
7E1, 8D1
TANKER



WEB FRAME

7H1
CONTAINERSHIP

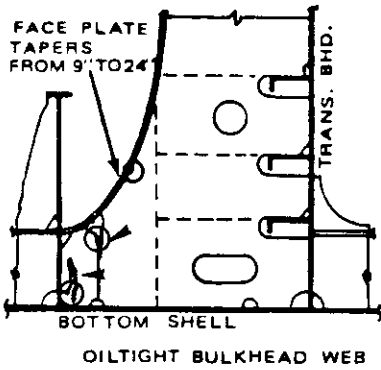


MISC NT BHD Ø

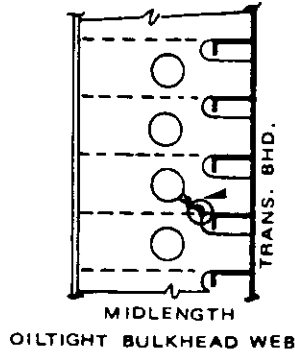
7A11
NAVY

(Cont'd next page)

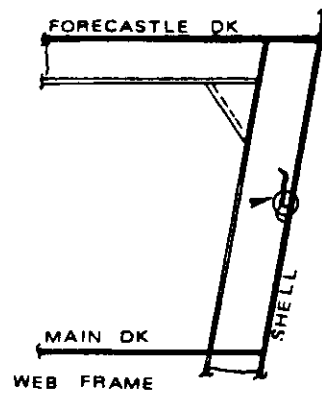
MISCELLANEOUS CUTOUT FAILURES



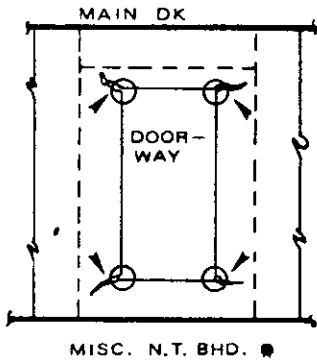
TANKER



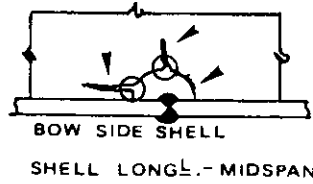
7E1
TANKER



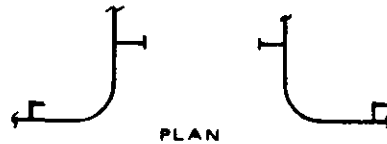
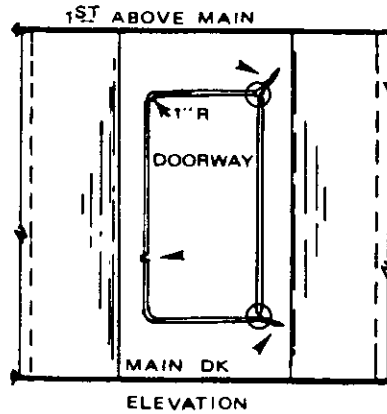
7C1
CONTAINERSHIP



7A11
NAVY

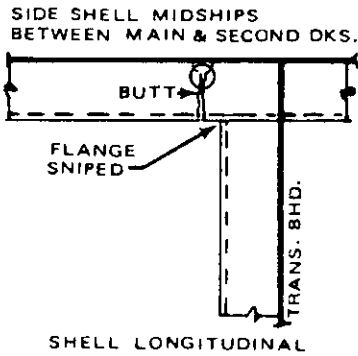


7G1
COMBINATION CARRIER

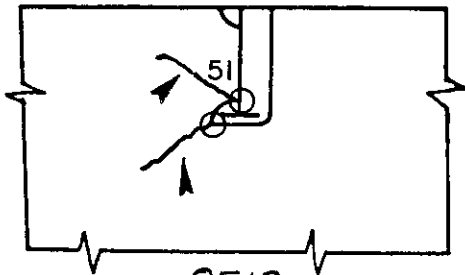


LONGITUDINAL ENCLOSURE
BULKHEAD @ P&S

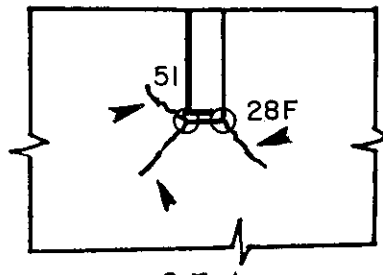
7A9
GENERAL CARGO



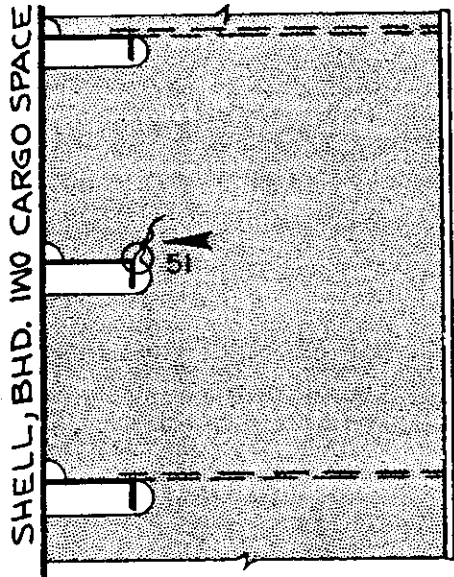
COMBINATION CARRIER



8E13



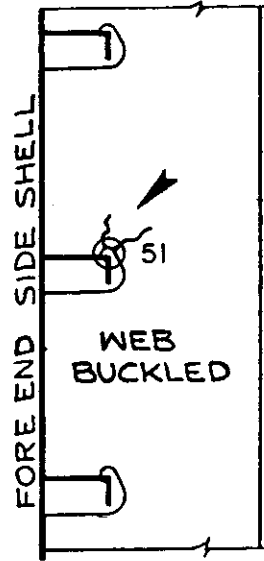
8E4



TRANS WEBS

8D6

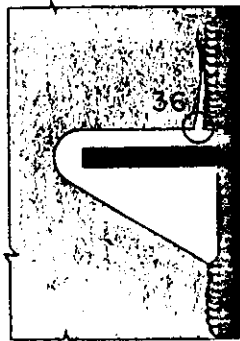
COMBINATION CARRIER,
TANKER



TRANS WEBS

8E7

COMBINATION CARRIER

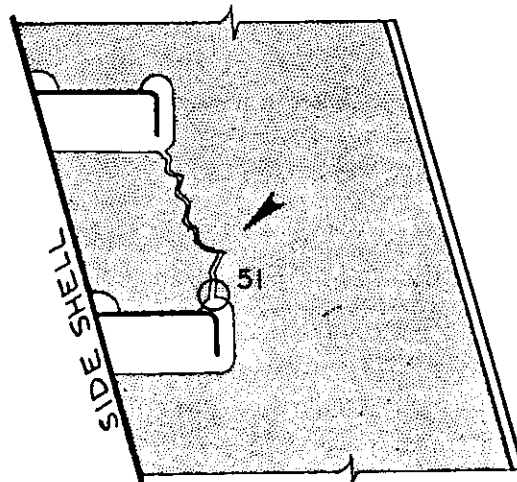


MN DK

BULWARK
AT MIDSHIP DKHSE

8A1

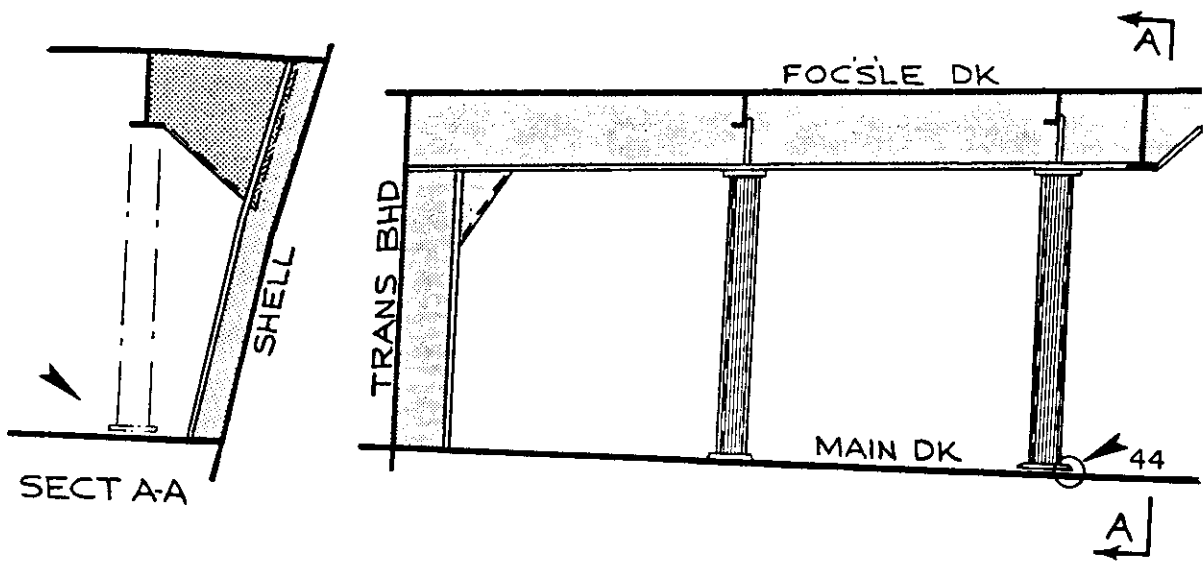
GENRL CARGO



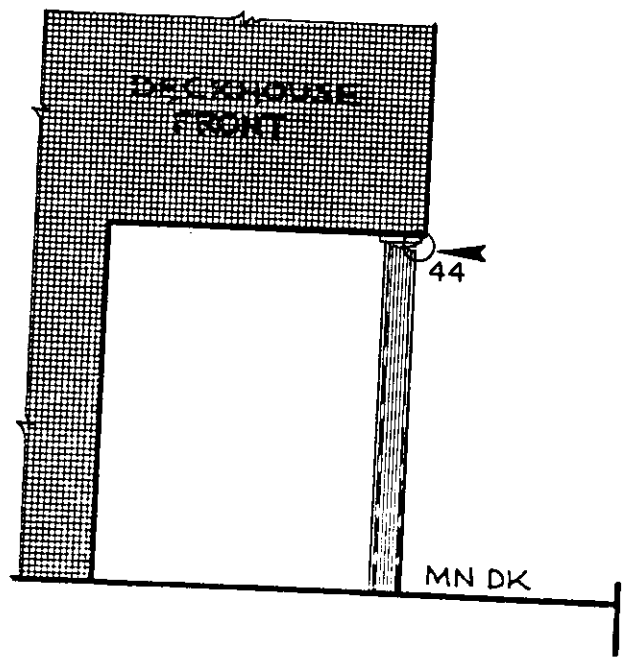
WEB FRAME
IN FWD DEEP TANK

8E2

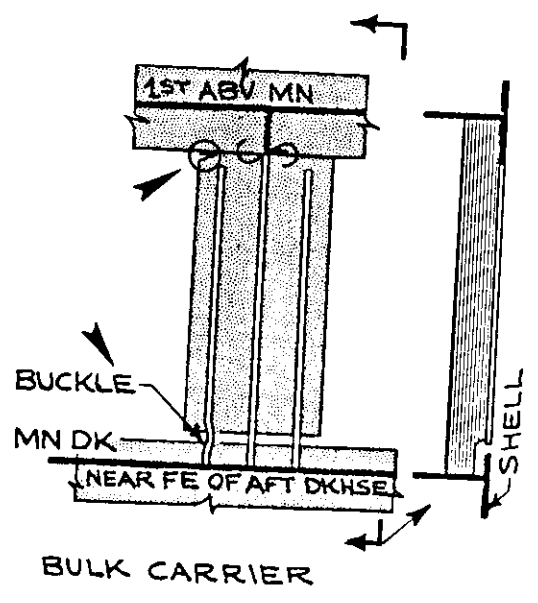
BULK CARRIER



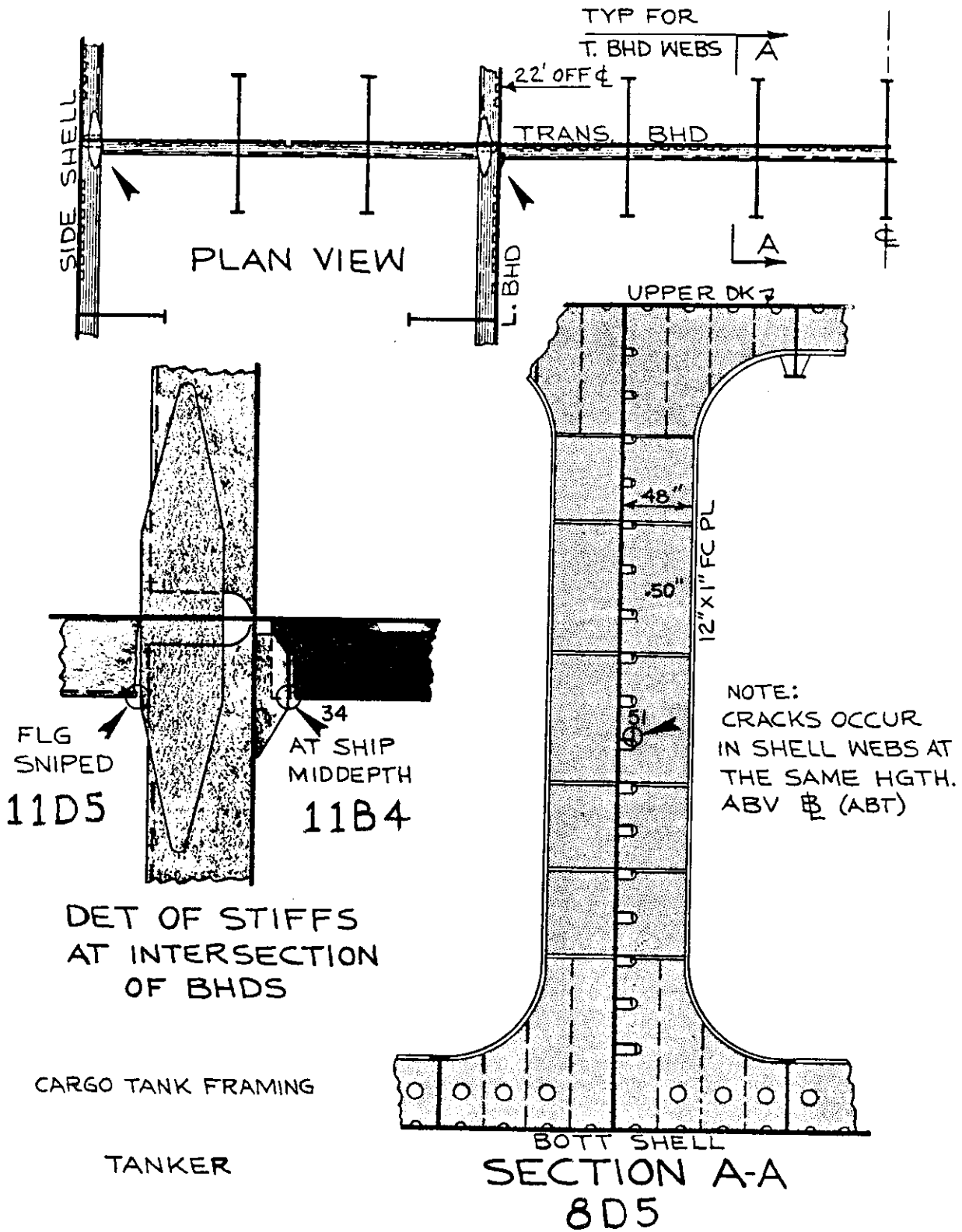
TANKER
10B2

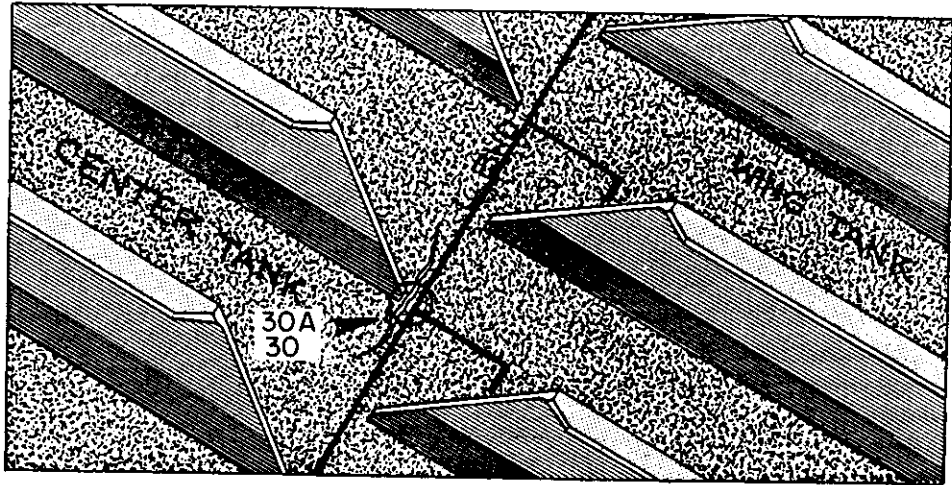


CONTAINERSHIPS
10B2

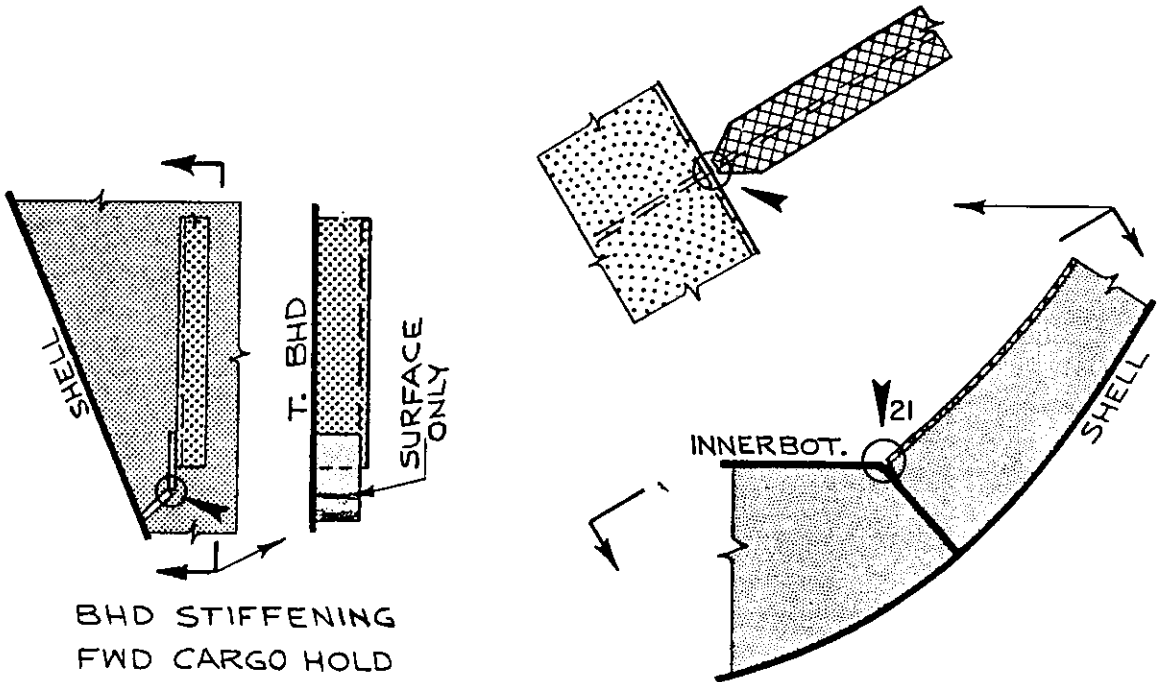


BULK CARRIER





TRANS. O.T. BHD.
11A1
 TANKER

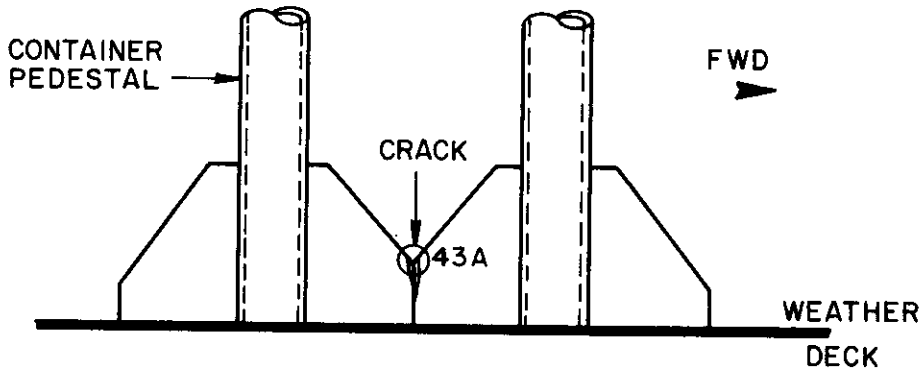


BHD STIFFENING
 FWD CARGO HOLD

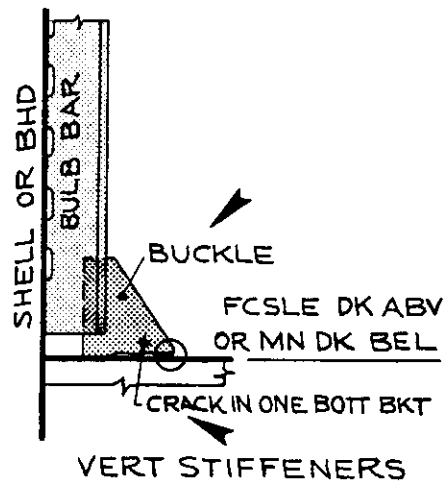
11B6
 CONTAINERSHIP

SHELL FRAMING

11A8
 NAVY

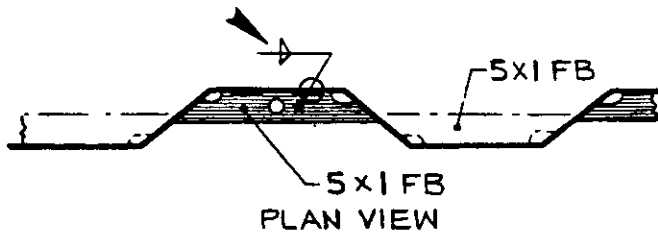


10B9



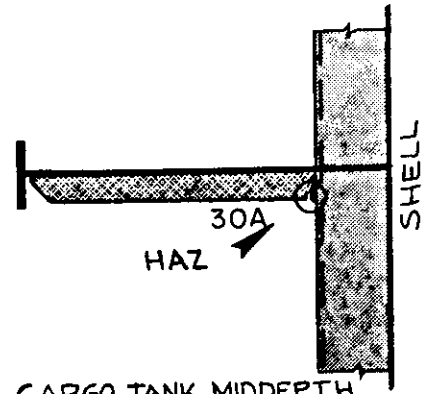
11B3

CONTAINERSHIP



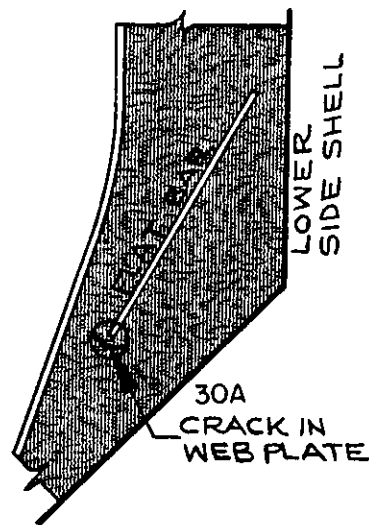
FBS. 0 CORRUGATED L.B.H.D
CARGO HOLD AMIDSHIP

12A10
COMBINATION CARRIER



CARGO TANK MIDDEPTH
LONGL AT WEB FR

12A5
TANKER



CARGO HOLD OUTBD
SHELL FRAME

12A1
BULK CARRIER

C. References

- C.1 Jordan, C. R. and Cochran, C. S. "In-Service Performance of Structural Details," SSC-272, 1978.
- C.2 Jordan, C. R. and Knight, L. T. "Further Survey of In-Service Performance of Structural Details," SSC-294, 1980.

APPENDIX D

Determination of Weibull Distribution to
Fit SL-7 Scratch Gage Data

D.1 Determination of Weibull Parameters k and w

The principal need is to find the Weibull distribution that has the same mean peak-to-peak stress value and coefficient of variation as the SL-7 stress histogram in Fig. D.1. (This histogram represents the maximum peak to minimum trough stress that occurred during more than 36,000 four-hour sampling periods in five data years of operation. It has been assumed that this distribution is representative of ship stress history during a life time of 10^8 cycles.)

The mean and standard deviation of the data in the loading histogram of Fig. D.1 were found to be 4.397 and 3.772, respectively. Thus, the coefficient of variation is

$$\delta = \frac{\sigma}{\mu} = \frac{3.772}{4.397} = 0.858$$

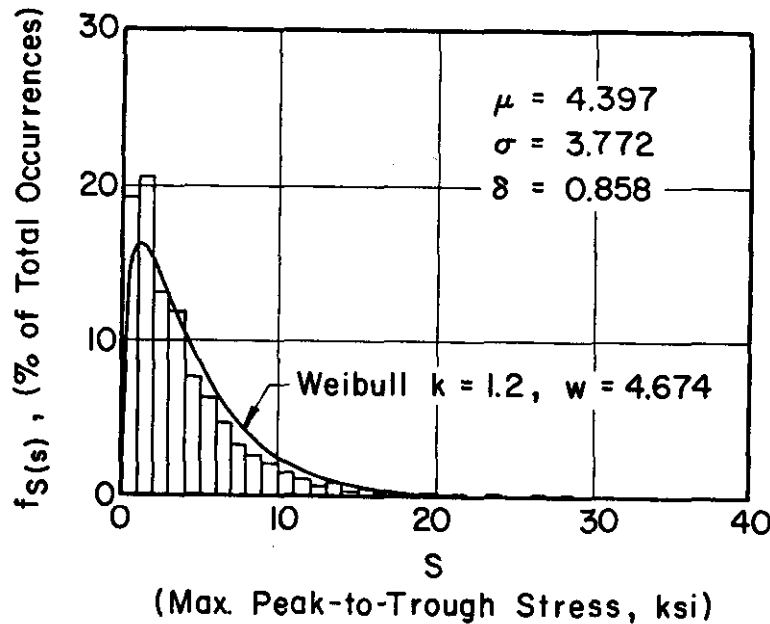


Fig. D.1 SL-7 Scratch Gage Data with Corresponding Weibull Distribution (6.10).

The expressions for the mean and standard deviation for the Weibull distribution are (from Table 6.4),

$$\mu_S = w\Gamma\left(1 + \frac{1}{k}\right) \quad (D.1)$$

$$\sigma_S = w\left[\Gamma\left(1 + \frac{2}{k}\right) - \Gamma^2\left(1 + \frac{1}{k}\right)\right]^{\frac{1}{2}} \quad (D.2)$$

It follows that the Weibull coefficient of variation is,

$$\delta_S = \frac{\sigma_S}{\mu_S} = \frac{[\Gamma(1 + \frac{2}{k}) - \Gamma^2(1 + \frac{1}{k})]^{\frac{1}{2}}}{\Gamma(1 + \frac{1}{k})} \quad (D.3)$$

It should be noted that the coefficient of variation is a function of the Weibull shape parameter k . Eqn. (D.3) is given in graphical form in Fig. D.2 and in tabular form in Table D.1 for values of k in the range of 0.5 to 4.0.

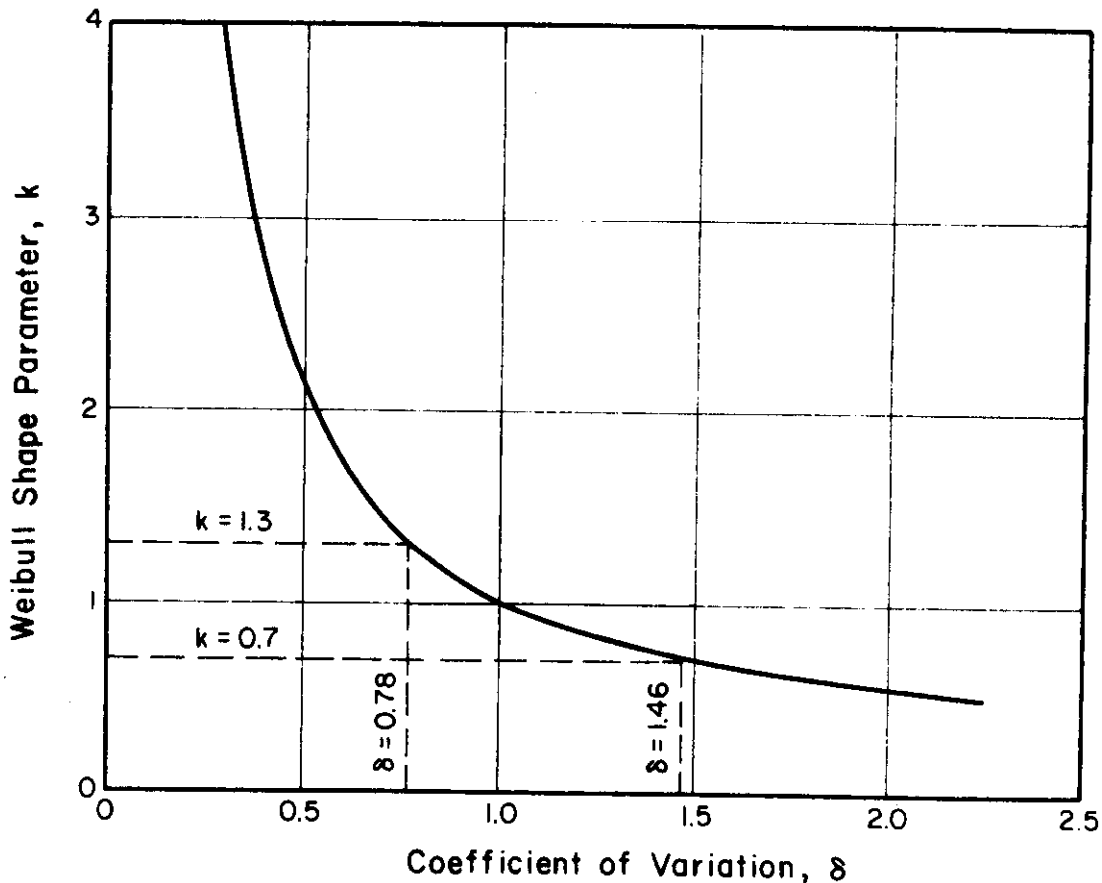


Fig. D.2 Coefficients of Variation for Weibull Shape Parameter, k .

The Weibull shape factor, k , which corresponds to the SL-7 coefficient of variation of 0.858 is found to be approximately 1.2 (from Fig. D.2 or Table D.1). The Weibull parameter, w , can be determined by substituting the shape parameter, $k = 1.2$, and the mean value of the load histogram, $\mu = 4.397$, into Eqn. D.1,

$$w = \frac{\mu}{\Gamma(1 + \frac{1}{k})} = 4.674 \quad (D.4)$$

TABLE D.1

Table of Weibull Shape Parameter
Values and Corresponding Coefficients
of Variation

Weibull Shape Parameter k	Coefficient of Variation δ
0.5	2.236
0.6	1.758
0.7	1.462
0.8	1.261
0.9	1.113
1.0	1.000
1.1	0.910
1.2	0.837
1.3	0.776
1.4	0.724
1.5	0.679
1.6	0.640
1.7	0.605
1.8	0.575
1.9	0.547
2.0	0.523
2.5	0.428
3.0	0.363
4.0	0.281

The frequency diagram corresponding to the SL-7 data is shown in Fig. D.1 along with the Weibull distribution determined above. The Weibull distribution shows excellent agreement with the actual data.

D.2 Estimation of S_{10-8} for Weibull Distribution

It should be noted that each stress range in the scratch gage data represents the maximum peak stress to the maximum trough stress which occurred during a four-hour sampling period and corresponds to one "occurrence."

If it is assumed that the average wave period is 7.5 seconds. The number of load cycles experienced by the ship in one occurrence is 1920. The number of occurrences corresponding to one ship lifetime of 10^8 cycles is approximately 52000. The maximum stress range expected in a ship lifetime of 10^8 cycles, designated as S_{10-8} , would correspond in this case to the stress range with the probability of exceeding $1/52000$ occurrences. Hence,

$$Q_S(S_{10-8}) = \frac{1}{52000}$$

$$1 - F_S(S_{10-8}) = (52000)^{-1}$$

$$1 - \{1 - \exp[-(\frac{S_{10-8}^k}{w})]\} = (52000)^{-1}$$

$$S_{10-8} = w[\ln(52000)]^{1/k} \quad (D.5)$$

Substituting $k = 1.2$ and $w = 4.674$ (from Section D.1) into the above equation yields,

$$S_{10-8} = 4.674 [\ln(52000)]^{1/1.2} = 34.11 \text{ ksi}$$

Thus, the maximum stress range to be expected during the life of the ship, based on the empirical data available and the assumed Weibull distribution, is approximately 34.1 ksi.

APPENDIX E

Derivation of $E(S^m)$ and ξ

The random load factor (ξ) approach for dealing with variable loading in fatigue design is developed in Section 7. This appendix presents the derivations of the relationships for the $E(S^m)$ and ξ expressions summarized in Table 7.4.

E.1 Weibull Distribution

The probability density function of the two-parameter Weibull distribution (E.1) is,

$$f_S(s) = \frac{k}{w} \left(\frac{s}{w}\right)^{k-1} \exp\left[-\left(\frac{s}{w}\right)^k\right]; s \geq 0 \quad (\text{E.1})$$

$$f_S(s) = 0 \quad ; s < 0$$

where,

k = shape parameter

w = characteristic value of S

The m^{th} moment of S is determined as,

$$\begin{aligned} E(S^m) &= \int_0^{\infty} s^m f_S(s) ds \\ &= \int_0^{\infty} s^m \left(\frac{k}{w}\right) \left(\frac{s}{w}\right)^{k-1} \exp\left[-\left(\frac{s}{w}\right)^k\right] ds \\ &= kw^m \int_0^{\infty} \left(\frac{s}{w}\right)^{m+k-1} \exp\left[-\left(\frac{s}{w}\right)^k\right] \frac{ds}{w} \end{aligned} \quad (\text{E.2})$$

Eqn. E.1 can be evaluated by employing the following integral form (E.2),

$$\int_0^{\infty} x^a \exp(-x^b) dx = \frac{1}{b} \Gamma\left(\frac{a+1}{b}\right) \quad (\text{E.3})$$

and substituting the following,

$$a = m + k - 1$$

$$b = k$$

$$x = s/w$$

$$dx = ds/w$$

into Eqn. E.2. This yields,

$$\begin{aligned} E(S^m) &= kw^m \left[\frac{1}{k} \Gamma\left(\frac{m+k-1+1}{k}\right) \right] \\ &= w^m \Gamma\left(\frac{m}{k} + 1\right) \end{aligned} \quad (\text{E.4})$$

The stress range $S_{10^{-8}}$ is, by definition, the stress range at which the probability of exceedance is 10^{-8} , i.e.,

$$Q_S(S_{10^{-8}}) = 10^{-8}$$

$$1 - F_S(S_{10^{-8}}) = 10^{-8} \quad (E.5)$$

Substituting the following expression for the Weibull cumulative distribution function (E.1),

$$F_S(s) = 1 - \exp\left[-\left(\frac{s}{w}\right)^k\right]$$

into Eqn. E.5 yields,

$$\exp\left[-\left(\frac{S_{10^{-8}}}{w}\right)^k\right] = 10^{-8}$$

$$\left(\frac{S_{10^{-8}}}{w}\right)^k = 18.42$$

$$w = (18.42)^{-1/k} S_{10^{-8}} \quad (E.6)$$

By substituting Eqn. E.6 into Eqn. E.4, the following expression for the m^{th} moment of S is obtained,

$$E(S^m) = (18.42)^{-m/k} S_{10^{-8}}^m \Gamma\left(\frac{m}{k} + 1\right) \quad (E.7)$$

The random load factor is obtained by substituting Eqn. E.7 into Eqn. 7.29 of the text (for Weibull distribution s_0 is replaced by $S_{10^{-8}}$),

$$\xi = \frac{S_{10^{-8}}}{\left[(18.42)^{-m/k} S_{10^{-8}}^m \Gamma\left(\frac{m}{k} + 1\right) \right]^{1/m}}$$

$$= (18.42)^{1/k} \left[\Gamma\left(1 + \frac{m}{k}\right) \right]^{-1/m} \quad (E.8)$$

E.2 Exponential Distribution

The probability density function of the exponential distribution is (E.3),

$$f_S(s) = \frac{1}{\lambda_e} \exp\left[-\left(\frac{s}{\lambda_e}\right)\right]; s \geq 0$$
$$f_S(s) = 0 \quad ; s < 0 \quad (E.9)$$

where,

$$\lambda_e = \text{mean value of } S$$

By inspection of Eqns. E.1 and E.9, it can be seen that the exponential distribution is a special case of the Weibull distribution where,

$$w = \lambda_e \quad (E.9a)$$

$$k = 1 \quad (E.9b)$$

Thus, the $E(S^m)$ and ξ expressions for the exponential distribution may be obtained by substituting Eqns. E.9 in the appropriate expressions for the Weibull distribution.

Hence, the $E(S^m)$ and ξ expressions for the exponential distribution are obtained from Eqns. E.7 and E.8, respectively.

$$E(S^m) = S_{10-8}^m (18.42)^{-m} \Gamma(1+m) \quad (E.10)$$

$$\xi = 18.42[\Gamma(1+m)]^{-1/m} \quad (E.11)$$

E.3 Rayleigh Distribution

The probability density function of the Rayleigh distribution is (E.3),

$$f_S(s) = \frac{2s}{s_{RMS}^2} \exp\left[-\left(\frac{s}{s_{RMS}}\right)^2\right]; s \geq 0$$
$$f_S(s) = 0 \quad ; s < 0 \quad (E.12)$$

where

s_{RMS} = root-mean-square value of s

By inspection of Eqns. E.1 and E.12, it can be seen that the Rayleigh distribution is a special case of the Weibull distribution where,

$$w = s_{\text{RMS}} \quad (\text{E.12a})$$

$$k = 2 \quad (\text{E.12b})$$

Hence, the $E(S^m)$ and ξ expressions for the Rayleigh distribution are obtained from Eqns. E.7 and E.8, respectively.

$$E(S^m) = S_{10}^m 0.8(18.42)^{-m/2} \Gamma(1 + \frac{m}{2}) \quad (\text{E.13})$$

$$\xi = \sqrt{18.42} [\Gamma(1 + \frac{m}{2})]^{-1/m} \quad (\text{E.14})$$

E.4 Shifted Exponential Distribution

The probability density function of the shifted exponential distribution is (E.3).

$$f_S(s) = \frac{1}{\lambda_e} \exp[-(\frac{s-a}{\lambda_e})]; s \geq a$$

$$f_S(s) = 0 \quad ; s < a \quad (\text{E.15})$$

where

λ_e = mean value of S

a = lower limit of S

The m^{th} moment of S is determined as follows:

$$\begin{aligned} E(S^m) &= \int_a^{\infty} s^m f_S(s) ds \\ &= \int_a^{\infty} s^m \frac{1}{\lambda_e} \exp[-(\frac{s-a}{\lambda_e})] ds \\ &= \frac{1}{\lambda_e} \exp(\frac{a}{\lambda_e}) \int_a^{\infty} s^m \exp(-\frac{s}{\lambda_e}) ds \end{aligned} \quad (\text{E.16})$$

Eqn. E.16 can be evaluated by employing the following integral form (E.4),

$$\int x^k e^{bx} dx = e^{bx} \sum_{n=0}^k (-1)^n \frac{k! x^{k-n}}{(k-n)! b^{n+1}} \quad (\text{E.17})$$

where k is an integer value. Substituting the following:

$$k = m \text{ (valid for integer values of } m)$$

$$b = -\frac{1}{\lambda_e}$$

$$x = s$$

$$dx = ds$$

into Eqn. E.16 and utilizing the integral form in Eqn. E.17 yields,

$$\begin{aligned} E(S^m) &= \frac{1}{\lambda_e} \exp\left(\frac{a}{\lambda_e}\right) \left| \exp\left(-\frac{s}{\lambda_e}\right) \sum_{n=0}^m (-1)^n \frac{m! s^{m-n}}{(m-n)! \left(-\frac{1}{\lambda_e}\right)^{n+1}} \right|_a^\infty \\ &= \frac{1}{\lambda_e} \exp\left(\frac{a}{\lambda_e}\right) \left| -\lambda_e \exp\left(-\frac{s}{\lambda_e}\right) \sum_{n=0}^m \frac{m! s^{m-n}}{(m-n)! \lambda_e^{-n}} \right|_a^\infty \\ &= -\frac{1}{\lambda_e} \exp\left(\frac{a}{\lambda_e}\right) \left\{ \lim_{s \rightarrow \infty} \lambda_e \exp\left(-\frac{s}{\lambda_e}\right) \sum_{n=0}^m \frac{m!}{(m-n)!} \lambda_e^n s^{m-n} \right. \\ &\quad \left. - \left[\lambda_e \exp\left(-\frac{a}{\lambda_e}\right) \sum_{n=0}^m \frac{m!}{(m-n)!} \lambda_e^n a^{m-n} \right] \right\} \quad (\text{E.18}) \end{aligned}$$

By *l'Hopital's* rule (E.5), the limit term in Eqn. E.18 vanishes. Thus,

$$E(S^m) = -\frac{1}{\lambda_e} \exp\left(\frac{a}{\lambda_e}\right) \left[-\lambda_e \exp\left(-\frac{a}{\lambda_e}\right) \sum_{n=0}^m \frac{m!}{(m-n)!} \lambda_e^n a^{m-n} \right]$$

$$= \sum_{n=0}^m \frac{m!}{(m-n)!} \lambda_e^n a^{m-n} \quad (E.19)$$

The stress range $S_{10^{-8}}$ is, by definition, the stress range at which the probability of exceedance is 10^{-8} , i.e.

$$Q_S(S_{10^{-8}}) = 10^{-8}$$

or $1 - F_S(s_{10^{-8}}) = 10^{-8}$ (E.20)

Substituting the following expression for the shifted exponential cumulative distribution function (E.3),

$$F_S(s) = 1 - \exp\left[-\left(\frac{s-a}{\lambda_e}\right)\right]$$

into Eqn. E.20 yields,

$$\exp\left[-\left(\frac{S_{10^{-8}-a}}{\lambda_e}\right)\right] = 10^{-8}$$

$$\frac{S_{10^{-8}-a}}{\lambda_e} = 18.42$$

$$\lambda_e = \frac{S_{10^{-8}-a}}{18.42} \quad (E.21)$$

By substituting Eqn. E.21 into Eqn. E.20, the following expression for the m^{th} moment of S is obtained,

$$E(S^m) = \sum_{n=0}^m \frac{m!}{(m-n)!} \left(\frac{S_{10^{-8}-a}}{18.42}\right)^n a^{m-n} \quad (E.22)$$

A closed form solution for the random stress factor may be developed by introducing a new parameter α such that,

$$a = \alpha S_{10-8}$$

and substituting this expression into Eqn. E.22,

$$\begin{aligned} E(S^m) &= \sum_{n=0}^m \frac{m!}{(m-n)!} \left(\frac{S_{10-8}^{-\alpha} S_{10-8}}{18.42} \right)^n (\alpha S_{10-8})^{m-n} \\ &= \sum_{n=0}^m \frac{m!}{(m-n)!} \left(\frac{1-\alpha}{18.42} \right)^n \alpha^{m-n} S_{10-8}^m \\ &= S_{10-8}^m \left[\sum_{n=0}^m \frac{m!}{(m-n)!} (18.42)^{-n} (1-\alpha)^n \alpha^{m-n} \right] \end{aligned} \quad (E.23)$$

The random stress factor is obtained by substituting Eqn. E.23 into Eqn. 7.29 of the text (for shifted exponential distribution s_0 is replaced by S_{10-8}),

$$\begin{aligned} \xi &= \frac{S_{10-8}}{\{S_{10-8}^m \left[\sum_{n=0}^m \frac{m!}{(m-n)!} (18.42)^{-n} (1-\alpha)^n \alpha^{m-n} \right]^{1/m}} \\ &= \left[\sum_{n=0}^m \frac{m!}{(m-n)!} (18.42)^{-n} (1-\alpha)^n \alpha^{m-n} \right]^{-1/m} \end{aligned} \quad (E.24)$$

where,

$$\alpha = \frac{a}{S_{10-8}}$$

$m = \text{integer}$

E.5 Lognormal Distribution (Ref. E.7)

A random variable Y may be introduced such that,

$$Y = \ln S \quad (E.25)$$

If S is lognormal with mean μ_S and coefficient of variation δ_S , then Y

is normal (E.3) with a mean of,

$$\lambda = \ln \mu_S - \frac{1}{2} \zeta^2 \quad (E.26)$$

and variance,

$$\zeta^2 = \ln(1 + \delta_S^2). \quad (E.27)$$

Eqn. E.25 may be transformed as,

$$S = e^Y$$

$$E(S^m) = E(e^{mY}) \quad (E.28)$$

Recognizing that $E(e^{mY})$ is the moment generating function of the normal variate Y (E.1), the m^{th} moment of S may be expressed as follows,

$$E(S^m) = \exp(m\lambda + \frac{1}{2}m^2 \zeta^2) \quad (E.29)$$

By substituting the expressions for λ and ζ , Eqns. E.26 and E.27, respectively, into Eqn. E.29, the m^{th} moment of S may be expressed in terms of the mean μ_S and coefficient of variation δ_S ,

$$\begin{aligned} E(S^m) &= \exp[m \ln \mu_S - \frac{m}{2} \ln(\delta_S^2 + 1) + \frac{m^2}{2} \ln(\delta_S^2 + 1)] \\ &= \exp[\ln \mu_S^m + \ln(\delta_S^2 + 1)^{-m/2} + \ln(\delta_S^2 + 1)^{m^2/2}] \\ &= \mu_S^m (\delta_S^2 + 1)^{-m/2} (\delta_S^2 + 1)^{m^2/2} \\ &= \mu_S^m (1 + \delta_S^2)^{\frac{1}{2}(m^2 - m)} \\ &= \mu_S^m (1 + \delta_S^2)^{\frac{1}{2}m(m-1)} \end{aligned} \quad (E.30)$$

The stress range $S_{10^{-8}}$ is, by definition, the stress range at which the probability of exceedance is 10^{-8} , i.e.,

$$P(S_{10^{-8}} < S < \infty) = 10^{-8}$$

For lognormal S, the $S_{10^{-8}}$ value may be determined as follows (E.3),

$$\Phi\left(\frac{\ln \infty - \lambda}{\zeta}\right) - \Phi\left(\frac{\ln S_{10^{-8}} - \lambda}{\zeta}\right) = 10^{-8}$$

$$1 - \Phi\left(\frac{\ln S_{10^{-8}} - \lambda}{\zeta}\right) = 10^{-8}$$

$$\frac{\ln S_{10^{-8}} - \lambda}{\zeta} = \Phi^{-1}(1 - 10^{-8})$$

$$\lambda = \ln S_{10^{-8}} - 5.60 \zeta \quad (E.31)$$

where $\Phi(x)$ is the standard normal probability function. Combining Eqns. E.31 and E.28 yields,

$$\ln S_{10^{-8}} - 5.60 \zeta = \ln \mu_S - \frac{1}{2} \zeta^2$$

$$\ln S_{10^{-8}} - \ln \mu_S = 5.60 \zeta - \frac{1}{2} \zeta^2$$

$$S_{10^{-8}} = \mu_S \exp\left[5.60 \zeta - \frac{1}{2} \zeta^2\right] \quad (E.32)$$

Substituting Eqn. E.29 into Eqn. E.32 yields,

$$S_{10^{-8}} = \mu_S \exp\left[5.60 \sqrt{\ln(1 + \delta_S^2)} - \frac{1}{2} \ln(1 + \delta_S^2)\right]$$

$$= \mu_S (1 + \delta_S^2)^{-\frac{1}{2}} \exp\left[5.60 \sqrt{\ln(1 + \delta_S^2)}\right]$$

or

$$\mu_S = \frac{S_{10^{-8}}}{(1 + \delta_S^2)^{-\frac{1}{2}} \exp\left[5.60 \sqrt{\ln(1 + \delta_S^2)}\right]} \quad (E.33)$$

By substituting Eqn. E.33 into Eqn. 30, the following expression for the m^{th} moment of S is obtained,

$$\begin{aligned}
E(S^m) &= S_{10-8}^m (1 + \delta_S^2)^{-\frac{1}{2}m + \frac{1}{2}(m-1)} \exp[-5.60m \sqrt{\ln(1 + \delta_S^2)}] \\
&= S_{10-8}^m (1 + \delta_S^2)^{m^2/2} \exp[-5.60m \sqrt{\ln(1 + \delta_S^2)}] \quad (E.34)
\end{aligned}$$

The random stress factor is obtained by substituting Eqn. E.34 into Eqn. 7.29 of the text (for lognormal distribution s_0 is replaced with S_{10-8}),

$$\begin{aligned}
\xi &= \frac{S_{10-8}}{\{S_{10-8}^m (1 + \delta_S^2)^{m^2/2} \exp[-5.60m \sqrt{\ln(1 + \delta_S^2)}]\}^{1/m}} \\
&= (1 + \delta_S^2)^{-m/2} \exp[5.60 \sqrt{\ln(1 + \delta_S^2)}] \quad (E.35)
\end{aligned}$$

E.6 Beta Distribution (Ref. E.6)

The probability function of the beta distribution with lower limit 0 and upper limit S_0 is (E.3),

$$\begin{aligned}
f_s(s) &= \frac{1}{B(q,r)} \frac{s^{q-1} (S_0 - s)^{r-1}}{S_0^{q+r-1}}; \quad 0 \leq s \leq S_0 \\
&= 0 \quad ; \text{ elsewhere} \quad (E.36)
\end{aligned}$$

where $B(q,r)$ is the beta function, and is related to the gamma function as (E.3),

$$B(q,r) = \frac{\Gamma(q) \Gamma(r)}{\Gamma(q+r)} \quad (E.37)$$

The m^{th} moment of S , therefore, is

$$E(S^m) = \frac{1}{B(q,r)} \int_0^{S_0} s^m \frac{s^{q-1} (S_0 - s)^{r-1}}{S_0^{q+r-1}} ds$$

$$= \frac{1}{B(q,r) S_0^{q+r-1}} \int_0^{S_0} s^{m+q-1} (S_0-s)^{r-1} ds \quad (E.38)$$

substituting $x = \frac{s}{S_0}$ and $dx = \frac{ds}{S_0}$ in the above equation, after algebraic simplification, results in the following,

$$E(S^m) = \frac{S_0^m}{B(q,r)} \int_0^1 x^{m+q-1} (1-x)^{r-1} dx \quad (E.39)$$

But the integral is $B(m+q, r)$ (E.3); hence,

$$E(S^m) = \frac{B(q+m,r)}{B(q,r)} S_0^m = S_0^m \left[\frac{\Gamma(m+q)\Gamma(q+r)}{\Gamma(q)\Gamma(m+q+r)} \right] \quad (E.40)$$

The random stress factor is obtained by transforming Eqn. E.40 into the form of Eqn. 7.29 of the text,

$$\begin{aligned} \xi &= \frac{S_0}{\left\{ S_0^m \left[\frac{\Gamma(m+q)\Gamma(q+r)}{\Gamma(q)\Gamma(m+q+r)} \right] \right\}^{1/m}} \\ &= \left[\frac{\Gamma(q)\Gamma(m+q+r)}{\Gamma(m+q)\Gamma(q+r)} \right]^{1/m} \end{aligned} \quad (E.41)$$

E.7 References

- E.1 Gumbel, D. E. "Statistics of Extremes," Columbia University Press, New York, 1958.
- E.2 Nolte, K. G. and Hansford, J. E. "Closed Form Expressions for Determining the Fatigue Damage of Structures Due to Ocean Waves," OTC-2606, 1976.
- E.3 Ang, A. H.-S. and Tang, W. H. Probability Concepts in Engineering Planning and Design, Volume I-Basic Principles, Wiley, 1975.
- E.4 CRC Standard Math Tables, 15th Edition.
- E.5 Thomas, G. B. Calculus and Analytic Geometry, 4th Edition, Addison-Wesley Publishing Company, December 1969.
- E.6 Ang, A. H.-S. and Munse, W. H. "Practical Reliability Basis for Structural Fatigue," Meeting Preprint 2492, American Society of Civil Engineers, 1975.
- E.7 Ang, A. H.-S. "Bases for Reliability Approach to Structural Fatigue," 2nd International Conference on Structural Safety and Reliability, Munich, September 1977.

Appendix F

Report of Fatigue Tests
Details 21, 30A, 51 and 52

A limited number of tests were performed on details for which the greatest number of failures were observed, but for which there was little or no fatigue data.

Four types of specimens were tested. These are local fatigue details No. 21, 30A, 51, and 52. Details of the specimens are shown in Figs. F.1, F.2 and F.3. A mild steel (yield \approx 36 to 40 ksi) was chosen for the specimens. Welding was done using the Shielded Metal Arc process and E7018 electrodes (see Fig. F.4). Weld size was selected on the basis of ABS design rules. The weld passes were continuous in regions where fatigue cracking was expected (wrapped around ends of bars).

The tests were conducted in 50^k, 100^k, and 600^k hydraulic testing machines. For ease of testing, a fixture similar to the specimen was used to provide for loading as shown in Figs. F.1, F.2 and F.3. Specimens were subjected to a stress cycle ranging from zero stress (small minimum stress to keep the fixture tight) to a maximum stress.

Test results are presented in Tables F.1, F.2 and F.3. Stress calculations for Detail 21 are based on the section modulus of the nominal weld throat area. Two S-N curves, one for details with 1/4" weld and one for 3/8" weld, are shown in Fig. F.5. In the fracture photographs of Figs. F.6 and F.7, the fatigue crack propagation from the root of the weld can be seen clearly. Figure F.8 shows the test setup for the specimen 21 detail.

Stress calculations for the detail 30A specimens were based on the section modulus of the plate at the toe of the weld. Table F.2 presents the test results for the 30A details. Two S-N curves are also shown for this detail. One is for the life of the crack across the weld toe. The other is for the crack across the full plate width (see Fig. F.9). Sketches of the cracks can be seen in Fig. F.10. Figure F.11 shows the location of the specimen 30A-2 fracture clearly, and Fig. F.12 shows the test setup.

The test setup for Detail 51 and 52 can be seen in Fig. F.13. The first test specimen was loaded to buckling of the web and tearing of a flangeweb weld ($P = 143.8^k$). Figure F.14 shows the web failure and the failure of welds in Detail 51 and the formation of shear lines on the web of Detail 52. The remaining specimens were tested to the appearance of a significant crack at Detail 51 (2-3 inches long), at which time this detail was reinforced. The fatigue test was then continued until a significant crack appeared at Detail 52. See Table F.3 for the test results. The various locations of the fractures are shown in Table F.3. The S-N curves for Details 51 and 52 are plotted as Load vs. Cycles to Failure (see Fig. F.15). Curves of the corresponding average shear stress on the net area of the web are also shown on the diagrams. It is evident from this figure that Detail 52 has a greater fatigue load resistance than Detail 51. However, the average shear stress capacities are not greatly different. Typical crack propagation in Detail 51 is shown in Fig. F.16.

Strain gages were used on Specimen 51-6 and 52-6 (see Fig. F.17). This specimen was tested as follows. Strains were recorded except in items (d), (f) and (h).

- (a) Load increased in 5k increments to 50k then reduced to 0k
- (b) Load increased in 5k increments to 75k then reduced to 0k
- (c) Load increased in 10k increments to 75k then reduced to 0k
- (d) Specimen cycled from 5k to 75k to 1000 cycles
- (e) Load increased in 10k increments to 75k then reduced to 0k
- (f) Specimen cycled from 5k to 75k to 10,000 cycles
- (g) Load increased in 10k increments to 75k then reduced to 0k
- (h) Specimen cycled from 5k to 75k to 50,000 cycles
- (i) Load to 5k, 75k, and 0k

A typical high-strain gage for a rosette (Gage #2) shows the strain behavior in the stages listed above (Fig. F.18). Figure F.19 shows the principal stresses calculated at the rosette locations for loading to 50k and 75k, after 1,000 cycles of loading (stage e above). Figure F.20 shows a plot of "Load vs. Deflection" obtained from the dial gage data. It is readily evident from these data that significant residual stresses existed in the test members as fabricated, but that these stresses are rapidly altered so that the material behaves in essentially an elastic manner under the repeated loadings.

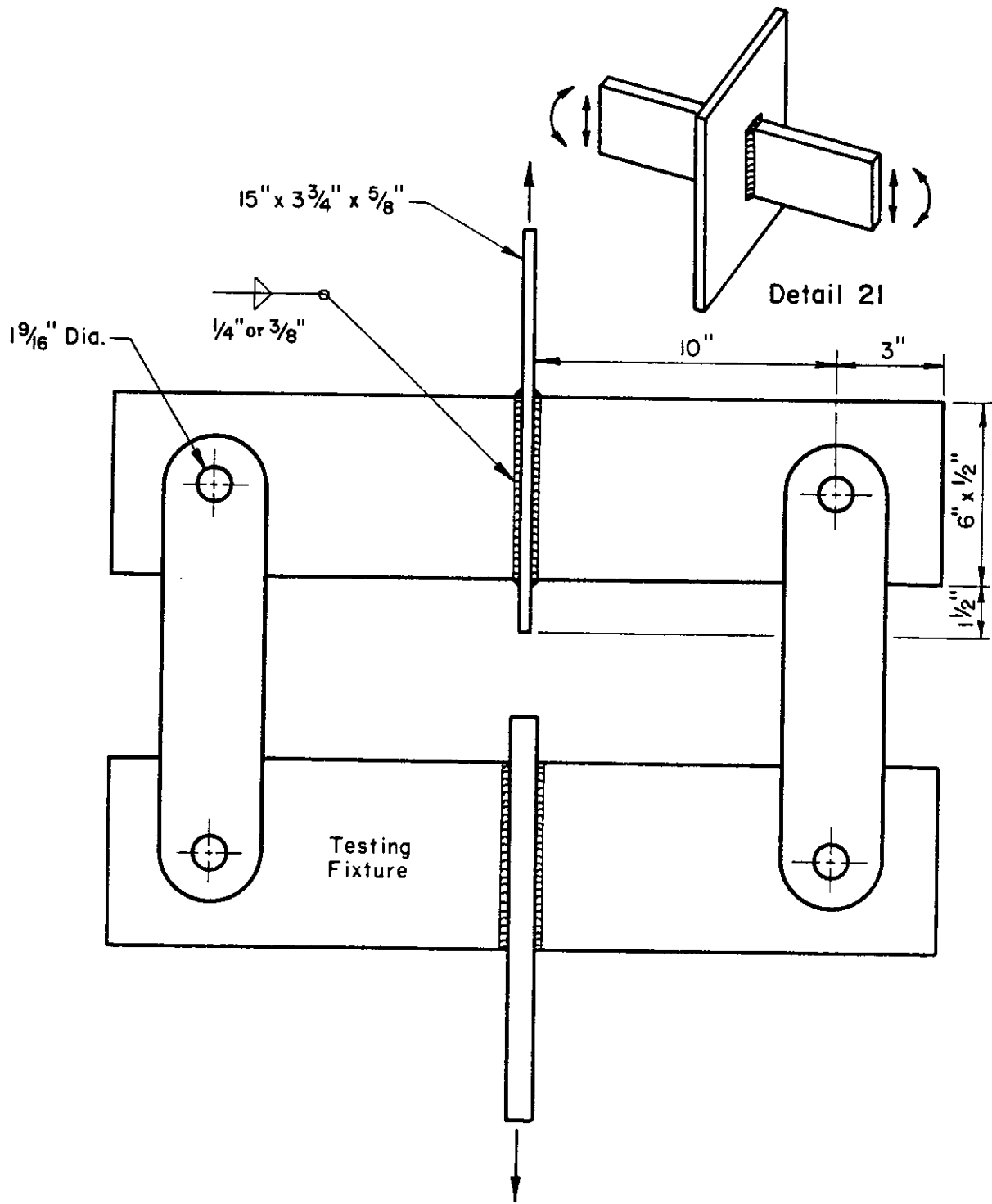


Fig. F.1 Detail 21 and Testing Fixture.

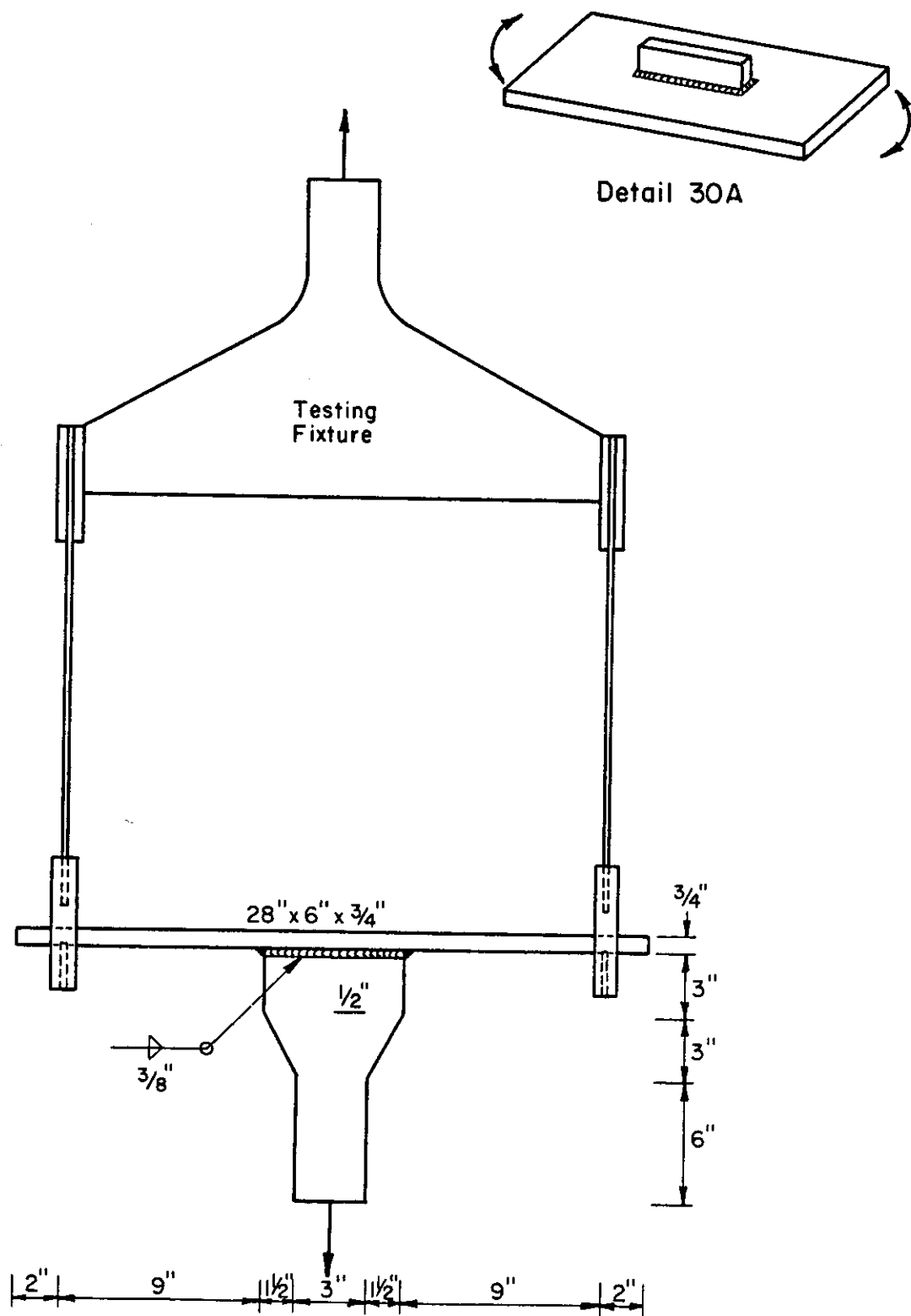
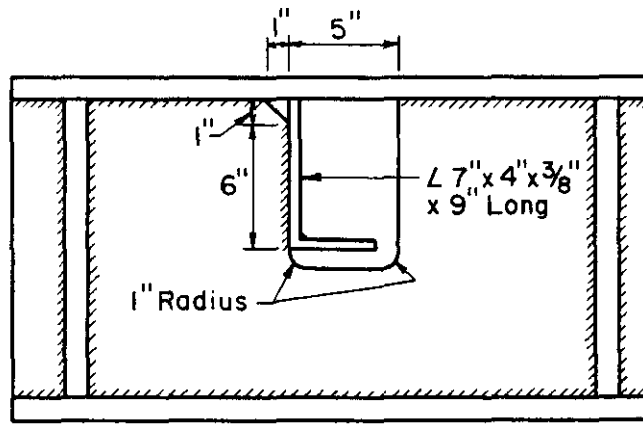
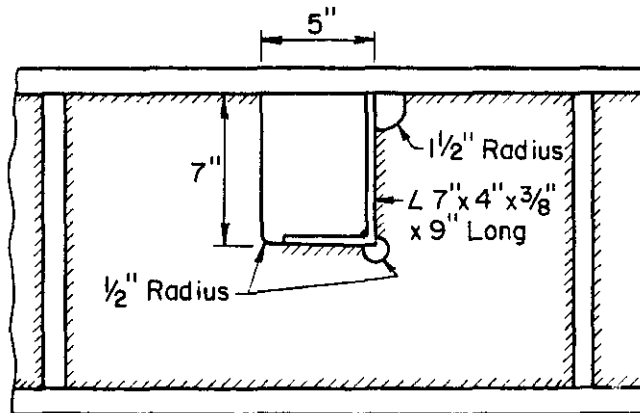
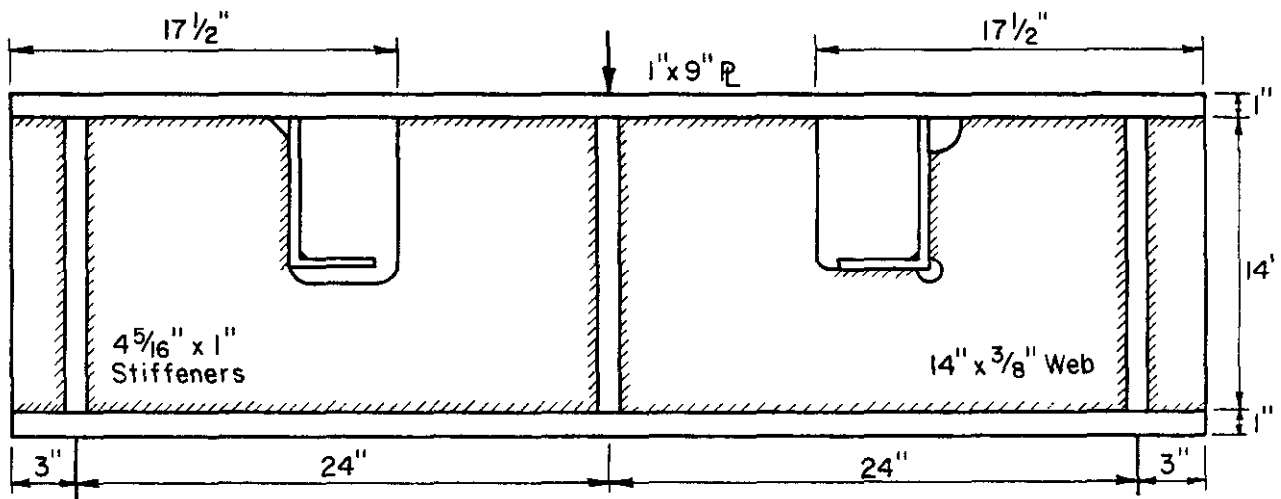


Fig. F.2 Detail 30A and Testing Fixture,



Detail 51



Detail 52

Fig. F.3 Detail 51 and Detail 52.

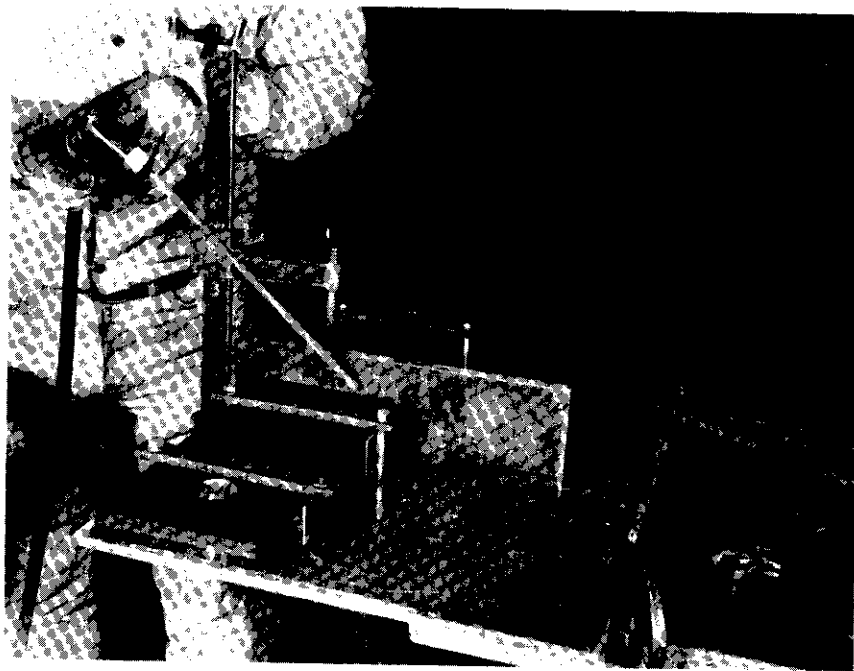


Fig. F.4 Welding of Detail 21, Specimen.

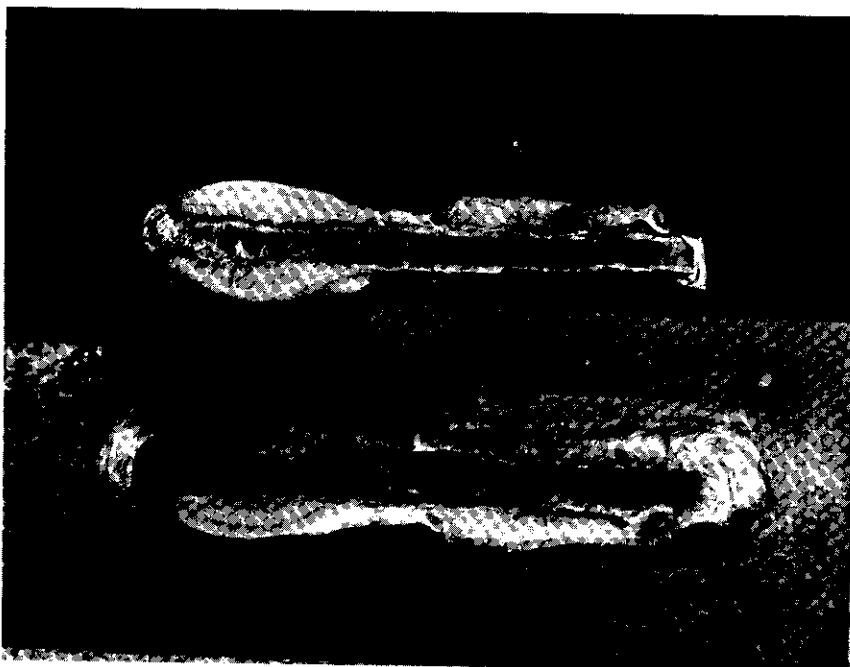


Fig. F.6 Fracture of Detail 21-5.

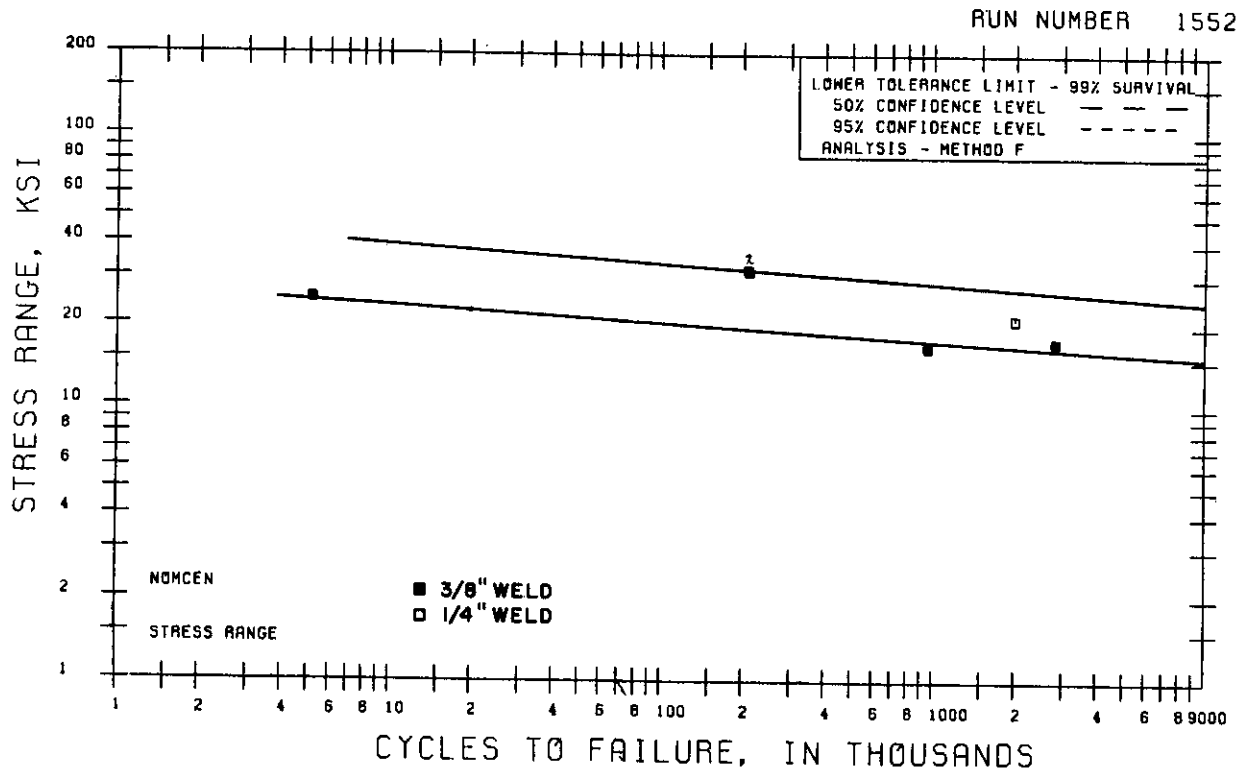
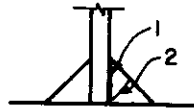


Fig. F.5 S-N Curve for Tests of Detail No. 21.

TABLE F.1

Results of Fatigue Tests on Detail 21

Spec. No.	Stress Cycle, ksi		Load Cycle, kips		Cycles to Failure	Failure Location
	min.	max.	min.	max.		
21-1	2.1	23.5	1.22	13.46	2,000,000 [†]	1,2
	2.1	44.9	1.22	25.72	2,800	
21-2	2.1	34.3	1.24	19.88	209,500	1,2
21-3	2.1	33.8	1.24	19.87	210,720	1,2
21-4	1.1	17.9	1.25	19.93	954,150	1,2
21-5	1.2	18.9	1.26	20.16	2,815,910	1,2
21-6	1.2	26.2	1.27	27.22	5,150	1,2



Failure Locations

Notes:

1. Specimens 21-1, 21-2 and 21-3 were fabricated with 1/4" welds.
2. Specimens 21-4, 21-5 and 21-6 were fabricated with 3/8" welds.
- † 3. 21-1 did not fail in 2,000,000 cycles at a 21.4 ksi stress range, so the stress range was increased to 42.8 ksi and carried to failure.
4. Stress calculations for Detail 21 are based on the section modulus of the weld throat. Load calculations are based on the plate section modulus.

TABLE F.2

Results of Fatigue Tests on Detail 30A

Spec. No.	Stress Cycle, ksi		Load Cycle, kips		Cycles to Failure	Failure Location
	min.	max.	min.	max.		
30A-1	1.9	28.7	0.25	3.69	665,770	See Fig. F.10
30A-2	2.0	21.0	0.25	2.70	1,986,660	See Fig. F.10
30A-3	2.0	40.0	0.25	5.08	190,360	See Fig. F.10
30A-4	2.0	26.0	0.26	3.34	722,070	See Fig. F.10
30A-5	2.0	44.0	0.26	5.62	133,420	See Fig. F.10

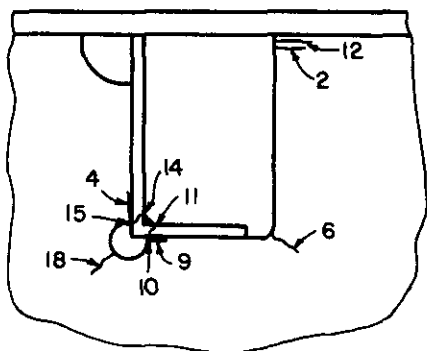
Stress calculations for Detail 30A are based on the section modulus of the plate and moment for the section at the toe of the fillet weld.

TABLE F.3

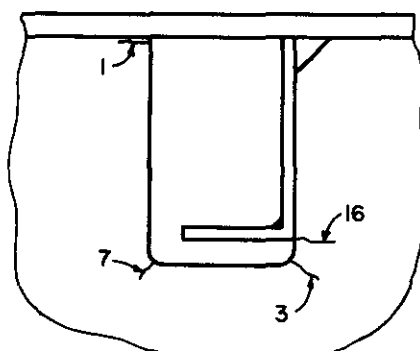
Results of Fatigue Tests on Details 51 & 52

Spec. No.	Load, kips	Cycles	Crack Location	Failure** Location	Crack Length, in.
51-1	Static-143.8 ^k	---	(See Fig. F.14)	---	---
51-2	5 ^k to 75 ^k	202,350	1, 3, 7	3	3 19/32
51-3	5 ^k to 50 ^k	1,007,100	1, 16	16	3 4/32
51-4	5 ^k to 75 ^k	203,110	1, 3	3	4 8/32
51-5	5 ^k to 50 ^k	910,510	1, 16	16	3 27/32
51-6	5 ^k to 75 ^k	241,800	1, 3, 7	3	8 24/32
52-1	Static-143.8 ^k ₊	---	(See Fig. F.14)	---	---
52-2	5 ^k to 75 ^k	202,350*	2, 4, 6, 12		18/32
52-3	5 ^k to 50 ^k	2,131,920	9, 10, 11	11	4 9/32
52-4	5 ^k to 75 ^k	500,750	2,4,6,14,15,18	14	4 23/32
52-5	5 ^k to 50 ^k	2,323,100	10, 11, 18	11	3 22/32
52-6	5 ^k to 75 ^k	461,510	2,6,10,11,18	11	5 20/32

Failure for Detail 51 and 52 was taken as a three-inch crack at the failure location.



Detail 52



Detail 51

Crack Locations

- * Detail 51-2 was not reinforced. Only short cracks existed in Detail 52-2 when test was discontinued.
- ** Crack 10 and crack 11 are essentially the same crack. Crack 10 appears on the bottom of the angle and crack 11 on the top. Crack 14 and 15 are also this way.

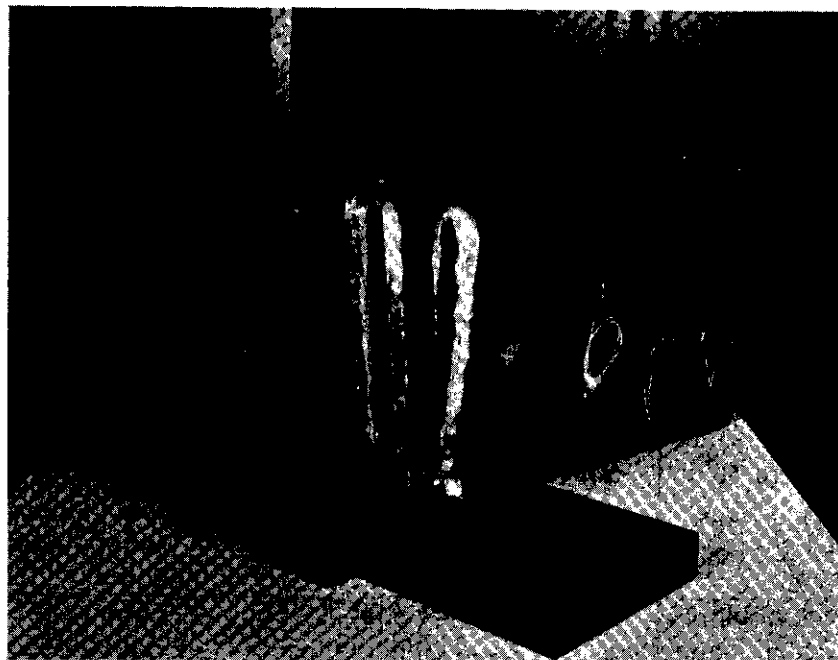


Fig. F.7 Fracture of Detail 21-6.



Fig. F.8 Detail 21 Test Setup.

RUN NUMBER 1554

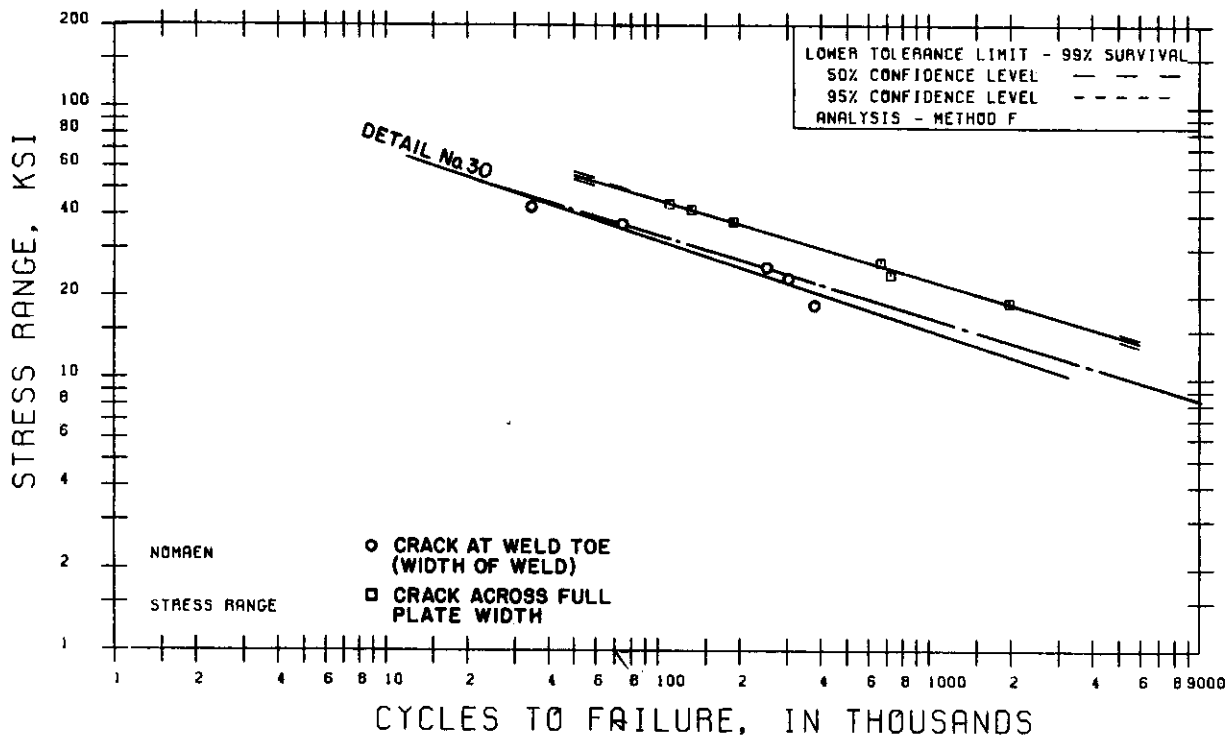
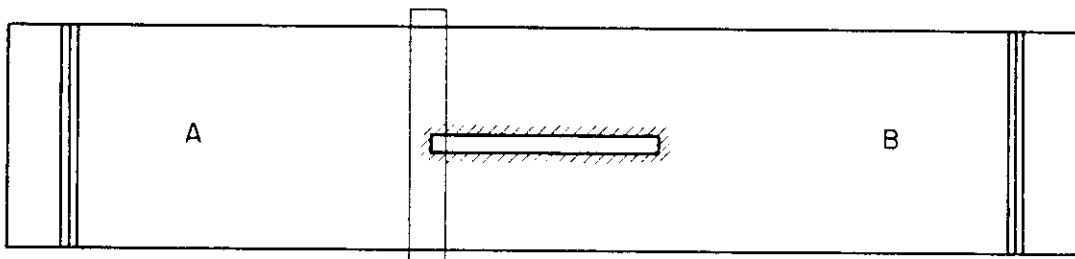
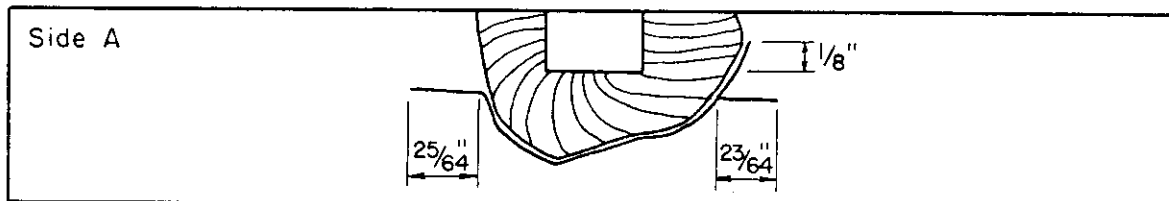


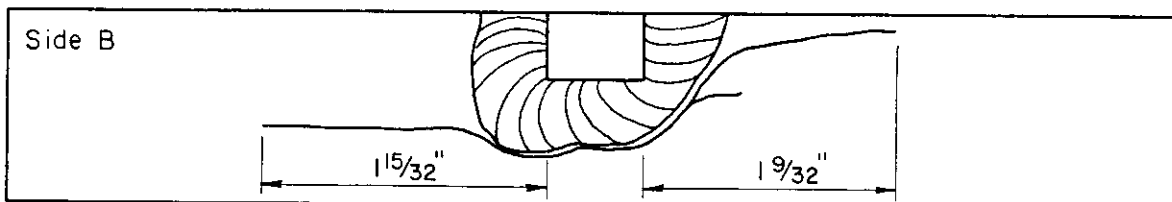
Fig. F.9 S-N Curve for Tests of Detail No. 30A.



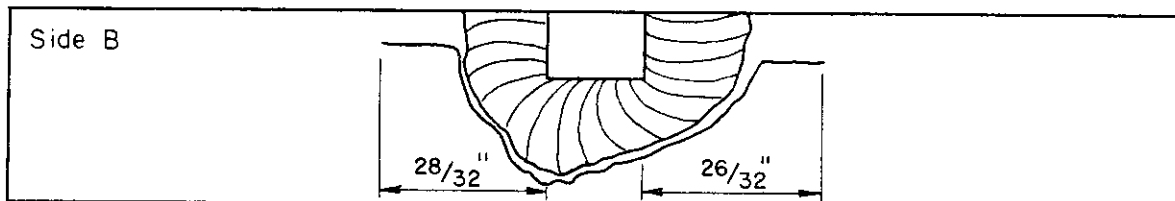
See Areas Sketched Below



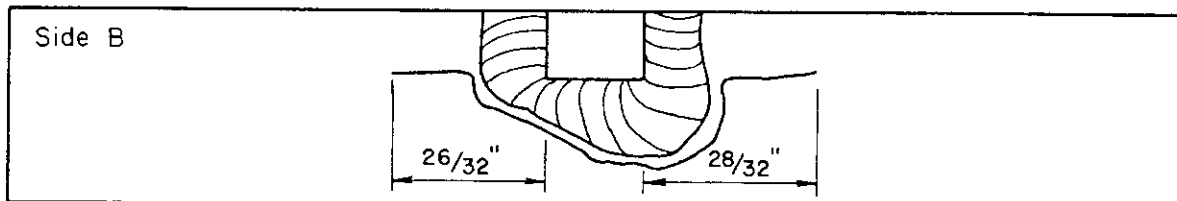
Specimen 30A-1



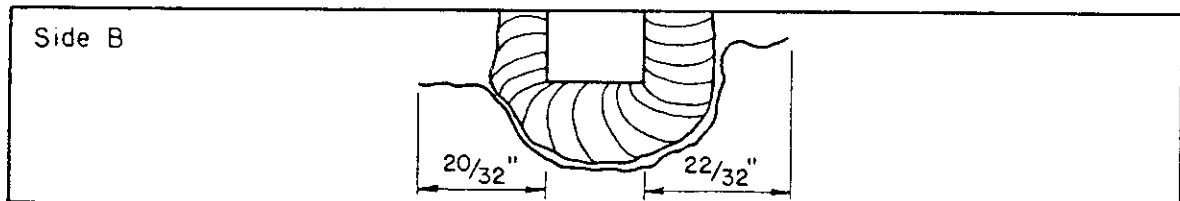
Specimen 30A-2



Specimen 30A-3



Specimen 30A-4



Specimen 30A-6

Fig. F.10 Failure Locations in 30A Specimens.

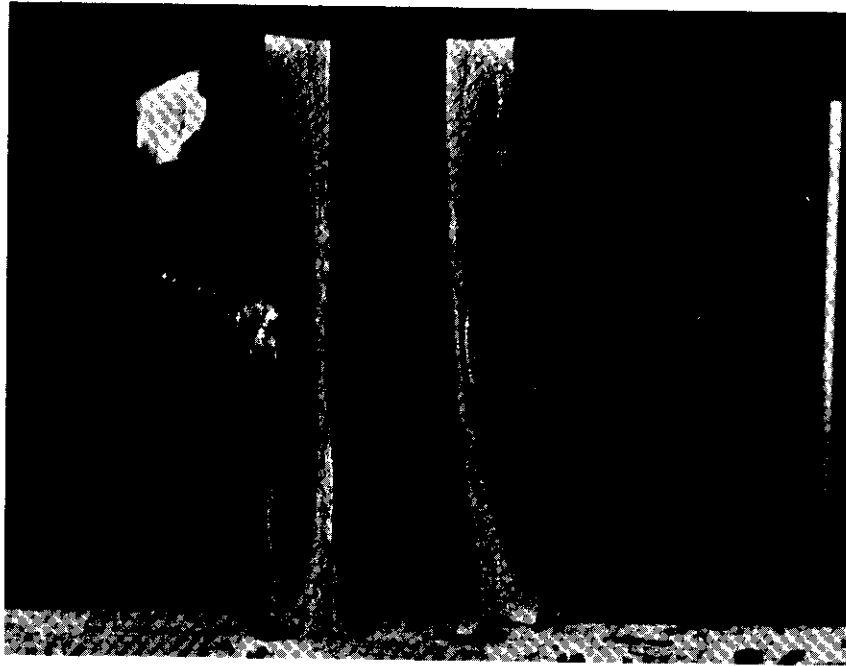


Fig. F.11 Fracture of Detail 30A-2



Fig. F.12 Detail 30A Testing Setup.

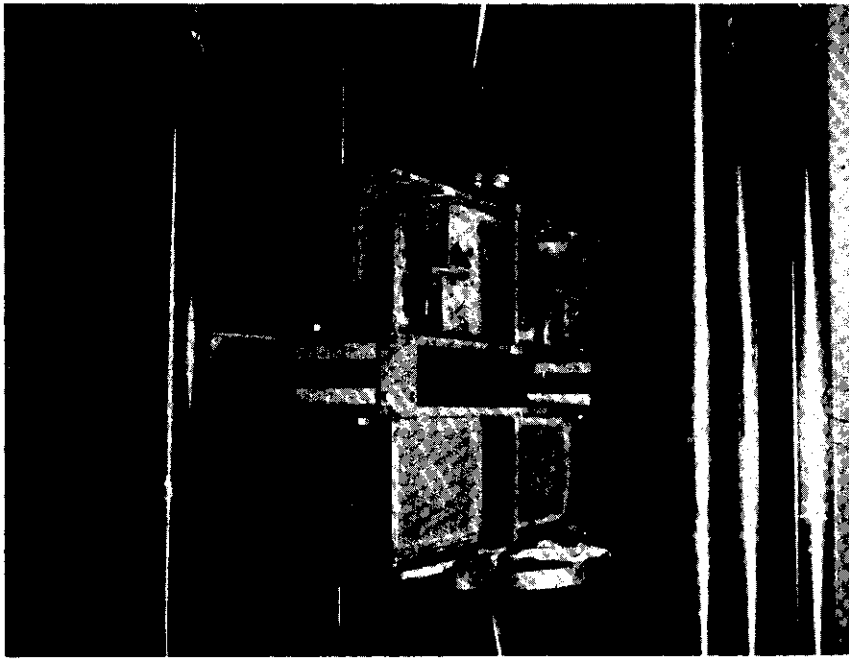


Fig. F.13 Detail 51 and 52, Testing in Progress

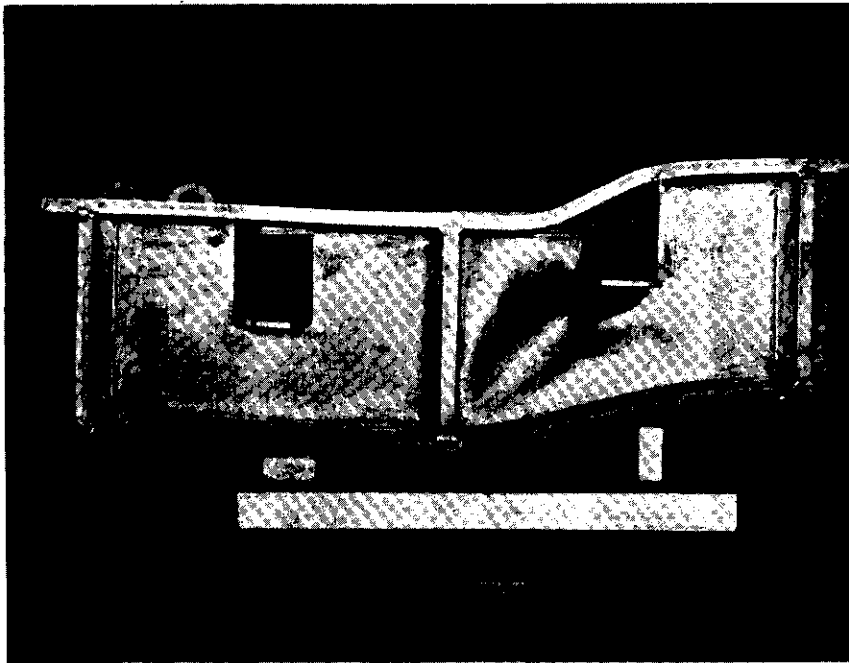
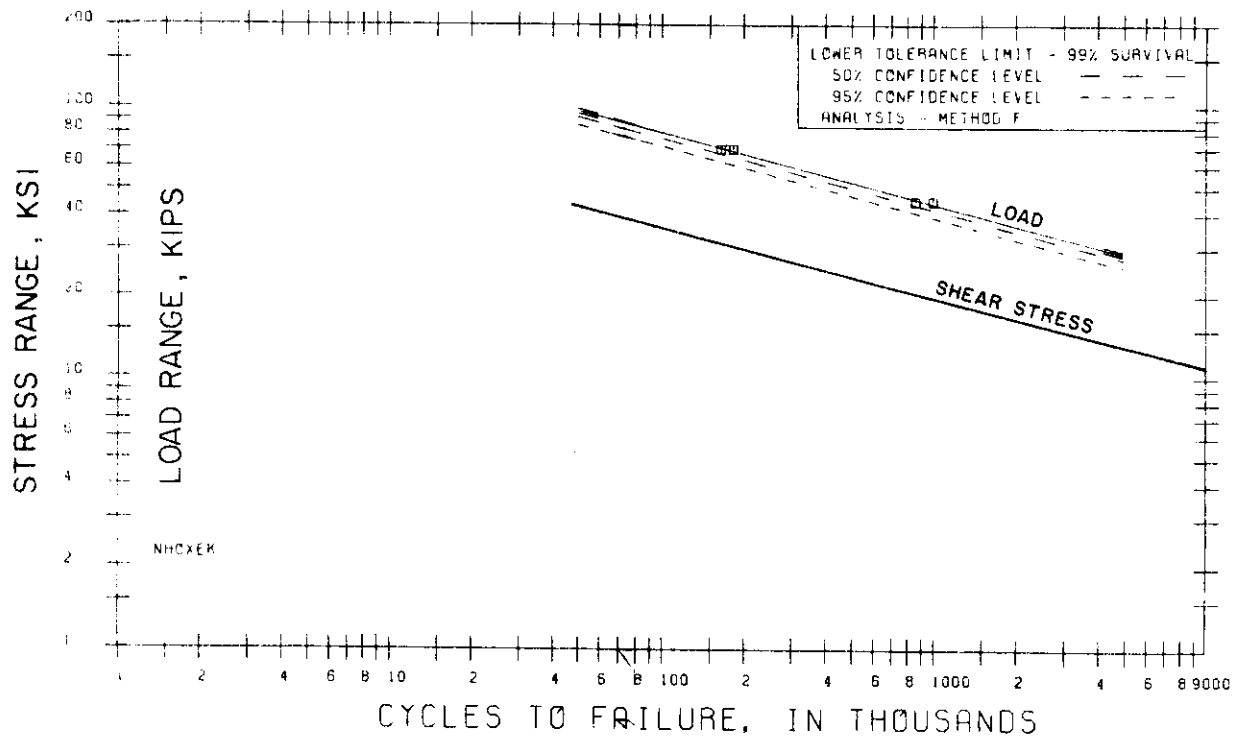


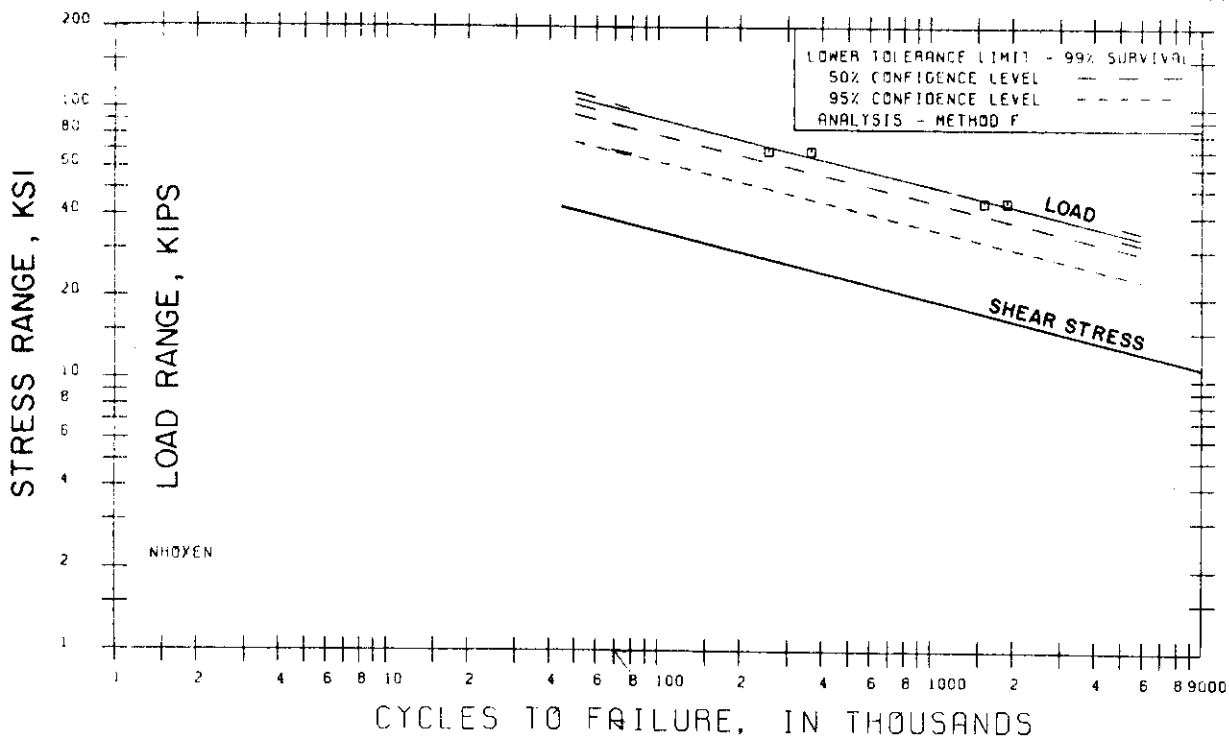
Fig. F.14 Detail 51 and 52-1, Static Test.

RUN NUMBER 1546



Detail 51

RUN NUMBER 1548



Detail 52

Fig. F.15 S-N Curve for Tests of Details 51 and 52.

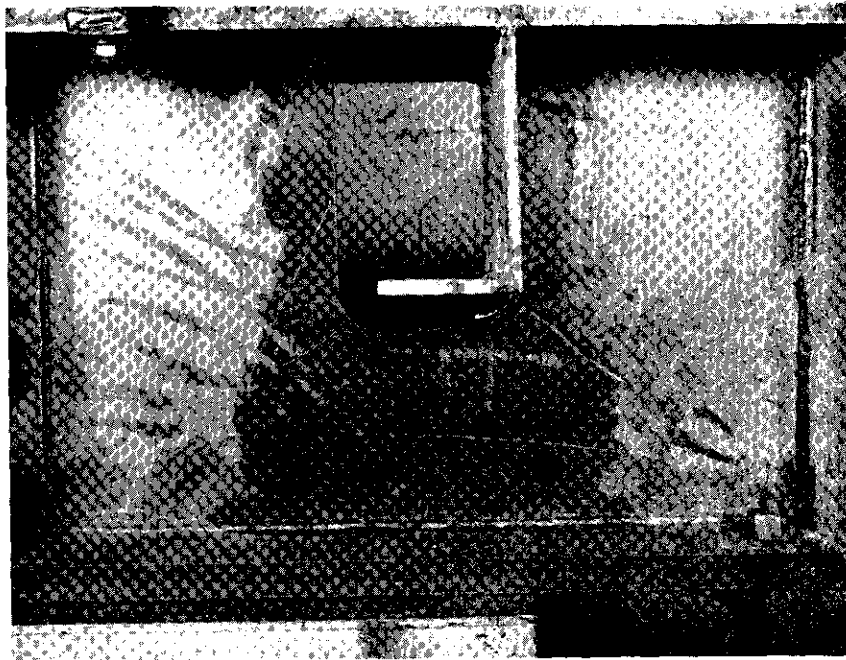


Fig. F.16 Fatigue Crack in Detail 51.

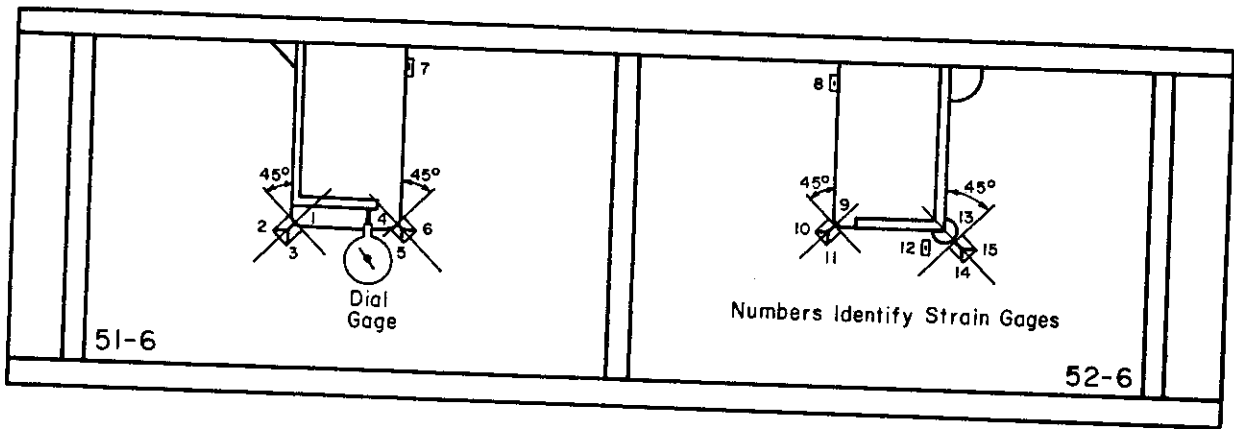


Fig. F.17 Strain Gage Locations, Specimen 51-6 and 52-6.

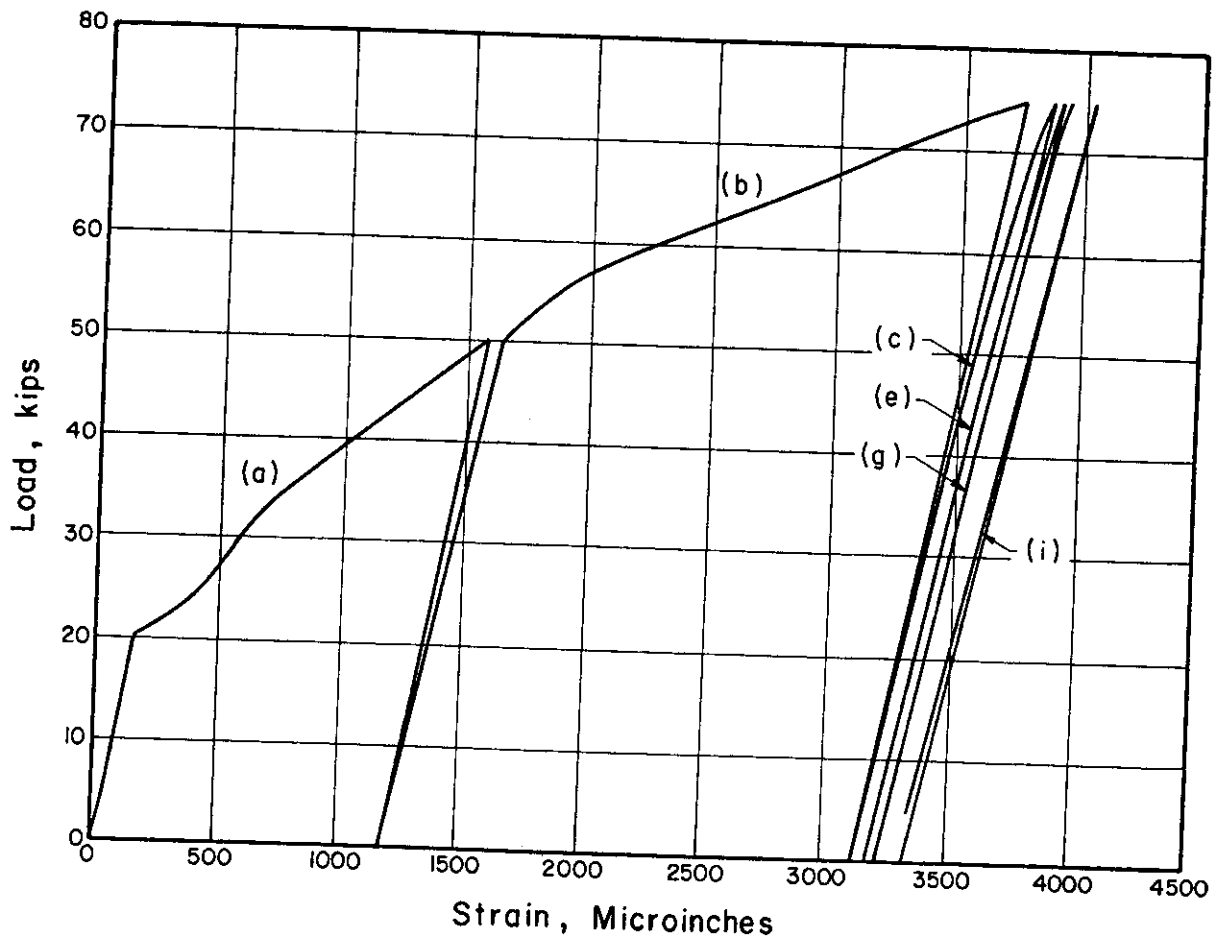
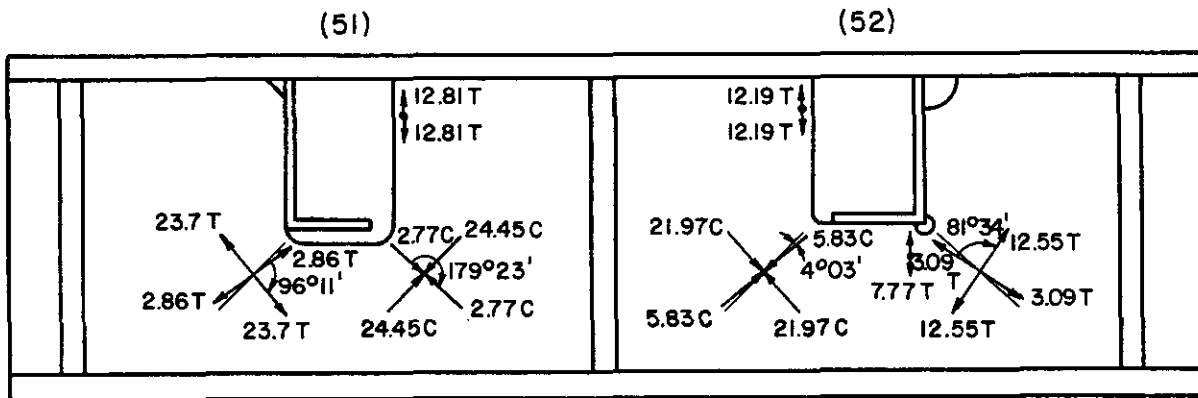
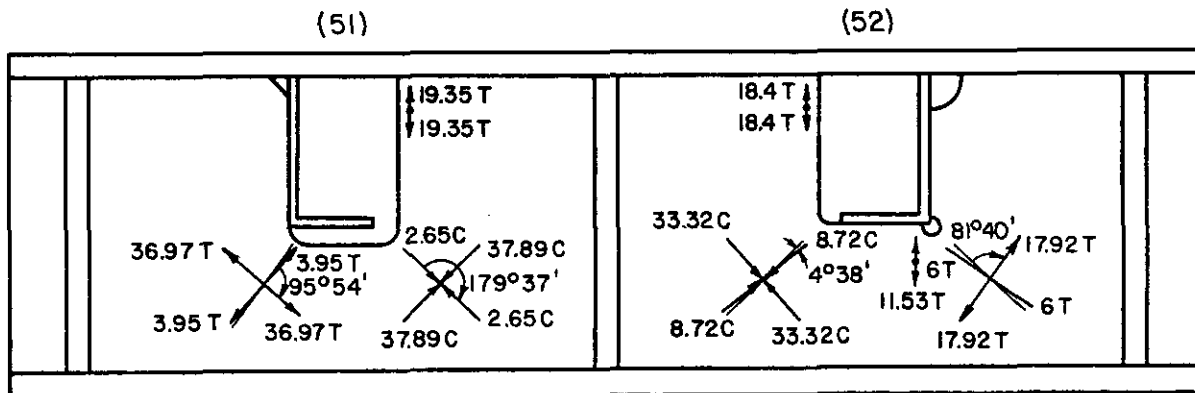


Fig. F.18 Strain Gage Data for Gage No. 2 on Specimen 51-6



(a) Stresses at Strain Gage Locations for 50^k Load (ksi)



(b) Stresses at Strain Gage Locations for 75^k Load (ksi)

Fig. F.19 Stresses at Strain Gage Locations.

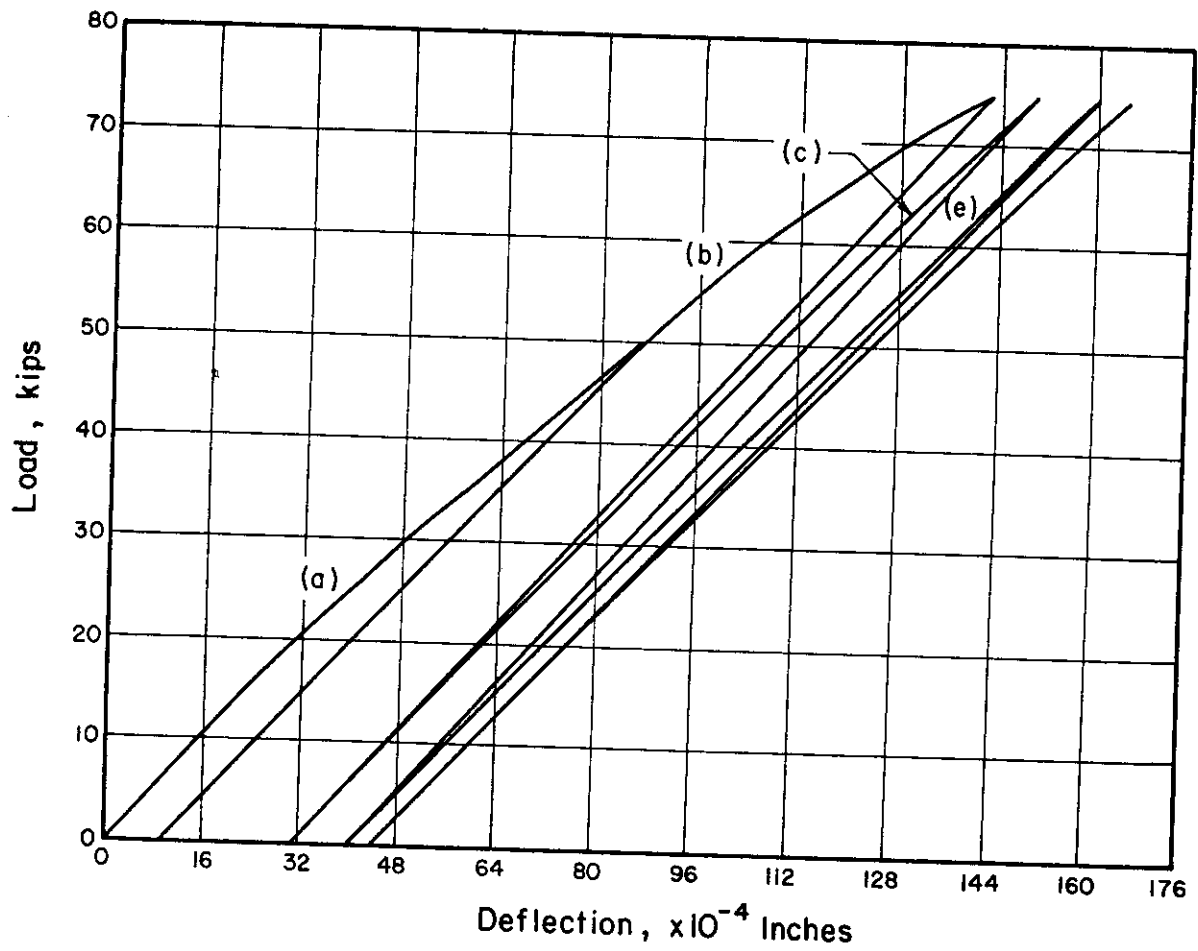


Fig. F.20 Dial Gage Data for Specimen 51-6.

* U.S. GOVERNMENT PRINTING OFFICE: 1984 0 - 421-428 (3559)

Committee on Marine Structures
Marine Board
National Academy of Sciences - National Research Council

The Committee on Marine Structures (Formerly Ship Research Committee) has provided guidance of the Interagency Ship Structure Committee's research program.

Mr. A. D. Hare, Chairman, Annapolis, MD
Mr. A. B. S. Ang, University of Illinois, Champaign, IL
Mr. K. A. Blank, Amoco Production Company, Tulsa, OK
Mrs. Margaret Ochi, Gainesville, PA
Mr. D. Bruce, National Oceanic and Atmospheric Administration, Rockville, MD
Mr. J. A. Sarno, ARMO Inc., Middletown, OH
Mr. J. B. Steele, Naval Architect, Quakertown, PA
Mr. R. W. Runke, Executive Secretary, Committee on Marine Structures

DEPARTMENTAL ADVISORY GROUP

The Materials Advisory Group reviewed the project proposals and advised the project on technical and administrative matters.

Mr. G. C. Galloway, ARMO Inc., Middletown, OH
Mr. J. B. Sarno, ARMO Inc., Middletown, OH
Mr. J. A. Sarno, ARMO Inc., Middletown, OH
Mr. J. B. Steele, Naval Architect, Quakertown, PA
Mr. R. W. Runke, Executive Secretary, Committee on Marine Structures

PROJECT ADVISORY COMMITTEE

The Project Advisory Committee provided the liaison technical guidance and reviewed the project with the investigators.

Mr. J. B. Sarno, Chairman, ARMO Inc., Middletown, OH
Mr. J. A. Sarno, ARMO Inc., Middletown, OH
Mr. R. W. Runke, Executive Secretary, Committee on Marine Structures

SHIP STRUCTURE COMMITTEE PUBLICATIONS

These documents are distributed by the National Technical Information Service, Springfield, VA 22314. These documents have been announced in the Greenhouse Journal, U. S. Government Research & Development Reports (USGRDR) under the indicated AD numbers.

- SSC-308. Criteria for Hull-Machinery Rigidity Compatibility by W. E. H. Budd, S. V. Karve, J. G. de Oliveira, and P. G. Xanthopoulos. 1981. AD-A117056
- SSC-309. A Rationale Basis for the Selection of Ice Strengthening Criteria for Ships - Vol. I by J. L. Coburn, F. W. DeBord, J. B. Montgomery, A. M. Nawwar, and K. E. Dane. 1981. AD-A120601
- SSC-310. A Rational Basis for the Selection of Ice Strengthening Criteria for Ships - Vol. II - Appendices by J. L. Coburn, F. W. DeBord, J. B. Montgomery, A. M. Nawwar, and K. E. Dane. 1981. AD-A120602
- SSC-311. Evaluation of SL-7 Scratch-Gauge Data by J. G. de Oliveira. 1981. AD-A120598
- SSC-312. Control of Internal Corrosion and its Effect on the Control of Commercial Tankships by J. G. de Oliveira and A. N. S. 1981. AD-A120600
- SSC-313. Ship Structure Program Summary, Conclusions and Recommendations by R. D. Stout and W. A. Wood. 1981. AD-A120603
- SSC-314. Contribution on Models of the Ship and Great Lakes Bulk Carrier S.I. CORT in Waves by J. G. de Oliveira and S. Stochastic. 1982.
- SSC-315. Fatigue Considerations in View of Measured Load Spectrum by W. G. Dobson, R. F. Broderick, J. W. Wheaton, J. C. Giannotti, and K. A. Stambaugh. 1982.
- SSC-316. Ship Structure Committee Long-Range Research Plan - Guidelines for Program Development by E. M. MacCurcheon, G. H. Oakley, and R. D. Stout. 1982.
- SSC-317. Determination of Strain Rates in Ship Hull Structures - A Feasibility Study by J. C. Giannotti and K. A. Stambaugh. 1982.
- SSC-318. Fatigue Characterization of Fabricated Ship Details for Design by W. H. Munse, T. W. Wilbur, M. L. Tellalian, K. Nicoll and K. Wilson. 1982.
- SSC-319. Development of a Plan to Obtain In-Service Still-Water Bending Moment Information for Statistical Characterization by J. W. Boylston and K. A. Stambaugh. 1982.